

ERASMUS MUNDUS MSc PROGRAMME

COASTAL AND MARINE ENGINEERING AND MANAGEMENT
CoMEM

MORPHOLOGICAL VARIABILITY OF EMBAYED BEACHES ALONG THE CATALAN COAST

Universitat Politècnica de Catalunya

{June 16, 2011}

Cinthyà Gomez Castro

{4053419}

The Erasmus Mundus MSc Coastal and Marine Engineering and Management is an integrated programme organized by five European partner institutions, coordinated by Delft University of Technology (TU Delft).

The joint study programme of 120 ECTS credits (two years full-time) has been obtained at three of the five CoMEM partner institutions:

- Norges Teknisk- Naturvitenskapelige Universitet (NTNU) Trondheim, Norway
- Technische Universiteit (TU) Delft, The Netherlands
- City University London, Great Britain
- Universitat Politècnica de Catalunya (UPC), Barcelona, Spain
- University of Southampton, Southampton, Great Britain

The first year consists of the first and second semesters of 30 ECTS each, spent at NTNU, Trondheim and Delft University of Technology respectively.

The second year allows for specialization in three subjects and during the third semester courses are taken with a focus on advanced topics in the selected area of specialization:

- Engineering
- Management
- Environment

In the fourth and final semester an MSc project and thesis have to be completed.

The two year CoMEM programme leads to three officially recognized MSc diploma certificates. These will be issued by the three universities which have been attended by the student. The transcripts issued with the MSc Diploma Certificate of each university include grades/marks for each subject. A complete overview of subjects and ECTS credits is included in the Diploma Supplement, as received from the CoMEM coordinating university, Delft University of Technology (TU Delft).

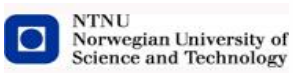
Information regarding the CoMEM programme can be obtained from the programme coordinator and director

Prof. Dr. Ir. Marcel J.F. Stive
Delft University of Technology
Faculty of Civil Engineering and geosciences
P.O. Box 5048
2600 GA Delft
The Netherlands



Thesis Director:

Jose A. Jiménez



Summary and Keywords

Embayed Beach, Shoreline Position, Beach Mobility, Beach Rotation

Natural and man made embayment beaches are a common feature along the Catalan coast. Many of these embayment beaches have experienced changes in shoreline position jeopardizing the protective and recreational functions of the beach. Therefore, an understanding of the morphological variability of this system is needed in order to facilitate an effective and sustainable coastal zone management.

The present study was undertaken with the objectives of: 1) study the shoreline evolution of the Catalan coast, 2) determine medium term oscillation and the forcing mechanisms governing this process by means of a theoretical model and 3) evaluate the frequency of the theoretical model using the last 7 years of wave data. Data from nine sandy beaches along the Catalan coast consisted of previously defined digitalized coastlines from the Environmental Ministry, the Cartographic Institute of Catalonia and satellite images from Google Earth.

Results from the shoreline evolution showed that the embayed beaches of Catalonia presented a stable behavior, beaches with the same morphology followed a same trend in the stability test proposed by Hsu, 1989. The results of beach mobility showed a non-uniform behavior of the sub-aerial beach width within a beach and along the Catalan coast. The major difference between beaches was due to the orientation of the shoreline, the beach type and the exposure to wave conditions. Embayed beaches also exhibited a wide degree of beach rotation. Beaches with similar morphology show similar degrees of rotation.

A theoretical model of the main configurations observed during the study period has been developed for each beach. Results showed that exposed beaches presented an anticlockwise, quasi-uniform and clockwise configuration, while semi-exposed beaches only show a higher anticlockwise and a lower anticlockwise configuration. In the analysis of wave forces on the embayment, it has been observed that wave direction was the primary forcing mechanism that generated changes in beach configuration (e.g. beach rotation), however the combination of wave height, period and direction were responsible for the response time of the beach to a new configuration. The percentage of occurrence of the wave climate during 2001 to 2007 suggested that some beaches have a tendency towards one configuration, in most cases to a higher anticlockwise rotation. Differences between beaches can be attributed to the shelter nature of the beach, the orientation and the effect of the natural or man made headland.

Preface

A thesis/dissertation presented in partial fulfillment of the requirements for the degree of MSc in Civil Engineering Coastal and Marine Engineering and Management (CoMEM).

Universitat Politècnica de Catalunya, June 16, 2011.

Acknowledgments

I would like to thank first of all to Prof. Jose Jimenez, for his supervision and guidance with this master thesis. I would also like to thank the staff and members of the three host universities; Norwegian University of Science and Technology, Delft University of Technology and the Universitat Politècnica de Catalunya for their hospitality and guidance through the study program.

I would also like to thank my family and my companion Mauricio for their support and love through these past years. To my CoMEM friends this would not be the same without you guys.

Table of Contents

Summary and Keywords.....	4
Preface.....	5
Acknowledgments	5
Table of Contents	6
List of Figures.....	9
List of Tables	14
1. Introduction.....	17
1.1 Problem Definition	18
1.2 Objectives.....	19
1.3 Scope and limitations of the work	19
1.4 Thesis outline	20
2. Literature Study.....	21
2.1 Embayed beaches	21
2.1.1 Sediment Transport within an Embayed Beach	22
2.1.2 Parabolic Bay Shape.....	24
2.1.3 Beach Rotation and Oscillation.....	26
2.1.4 Related Studies	27
3. Study Area and Data.....	33
3.1 Description of the Catalan Coast.....	33
3.2 Shoreline Data.....	36
3.3 Wave Data.....	40
3.3.1 Data Type	40
3.3.1.1 Simulated Data (1958- 2001): HIPOCAS-SIMAR-44 data set	40
3.3.1.2 Instrumental Information (2001 to 2007): XIOM Wave Buoy	41

3.4 Beach site description	43
3.4.1 Beach geomorphology	44
3.4.2 Wave climate description	50
3.4.3 Wave Data Selection	52
4. Shoreline Evolution.....	54
4.1 Methodology	55
4.1.1 Beach Platform Analysis	55
4.1.2 Beach Mobility	57
4.1.3 Sub-Aerial Beach Area	63
4.2. Results	63
4.2.1 Beach Platform Analysis	63
4.2.2 Beach Mobility	67
4.2.3 Beach Area	73
4.2.4 Beach Mobility as a Function of Different Beach Type.....	77
4.3 Discussion.....	80
4.4 Summary	81
5. Beach Rotation and Oscillation: Rotation Coefficient	83
5.1 Methodology.....	83
5.1.1 Rotation Coefficient (RO).....	83
5.1.2 Theoretical Rotation Coefficient (RO _T)	85
5.1.3 Waves Forcing on the Theoretical Model.....	86
5.2 Results	90
5.2.1 Sant Pol Beach	90
5.2.2 Canyelles Beach	95
5.2.3 Lloret del Mar Beach.....	99
5.2.4 Fenals Beach	106
5.2.5 Bogatell Beach	114
5.2.6 Nova Icaria Beach	121

5.2.7 Barceloneta Beach	127
5.2.8 Playa Larga Beach	144
5.2.9 Salou Beach.....	149
5.3 Discussion.....	155
5.4 Summary	157
6. Wave Condition and the Theoretical Model Respond: 2001- 2007	158
6.1 Methodology.....	159
6.2 Results	160
6.2.1 Tordera Buoy	160
6.2.2 Llobregat Buoy	168
6.2.3 Tortosa Buoy.....	176
6.3 Discussion.....	179
6.4 Summary	181
7. Conclusions and Recommendation	182
8. References	185
Appendix A: General Classification of the Embayed Beaches along the Catalan Coast.....	188

List of Figures

Figure 1 A) Aro Beach. B) La Fosca and Castel Beach, Costa Brava, Spain.....	21
Figure 2 Identification zones Tossa de Mar, Costa Brava, Spain.....	22
Figure 3 Definition sketch of α and coefficient used in the parabolic equation (Hsu and Evans, 1989).	25
Figure 4 Representative diagram of beach rotation process (Short and Masselink, 1999).....	27
Figure 5 Catalan coastline.....	34
Figure 6 Location of the studied beaches.....	35
Figure 7 Location of wave data nodes and wave buoys.	43
Figure 8 Schematic of the beach classification parameters used.	44
Figure 9 Aerial photographs from Google Earth 2007.	45
Figure 10 Aerial photographs from Google Earth 2006 and 2010.	47
Figure 11 Aerial photographs from Google Earth 2006.	48
Figure 12 Average beach length (blue triangles) and beach orientation (red dots) for all beaches. The x-labels are discussed in section 3.1.	49
Figure 13 Wave rose with direction from the nodes 1 and 2 from 1957-2001.	51
Figure 14 Wave rose with direction from the nodes 3 and 4 from 1957-2001.	52
Figure 15 Schematization of the used parameters, Fenals beach.	55
Figure 16 Indentation ratio a/R_o and β , Hsu 1989.	56
Figure 17 Distance along the Gerona beaches, as define by the length of the southern end along the embayment platform. (Photo: Ortophotos 2008, ICC).	59
Figure 18 Distance along the Barcelona City beaches, as define by the length of the southern end along the embayment platform. (Photo: Ortophotos 2006 and 2008, ICC).	61
Figure 19 Distance along the Tarragona beaches, as define by the length of the southern end along the embayment platform. (Photo: Ortophotos 2008, ICC).	62
Figure 20 Stability test Girona beaches.	64
Figure 21 Stability test Barcelona City beaches.	66
Figure 22 Stability test Tarragona beaches.....	67
Figure 23 Beach width variation Girona beaches.	69
Figure 24 Beach width variation Barcelona City beaches.	72
Figure 25 Beach width variation Tarragona beaches.....	73

Figure 26 Emerged beach area Girona beaches. 74

Figure 27 Emerged beach area: Bogatell and Nova Icaria. 75

Figure 28 Emerged beach area: Barceloneta. 76

Figure 29 Emerged beach area Tarragona beaches. 77

Figure 30 Distance and the correspondent beach width along the Salou beach as defined by the length from the southern end along the shoreline of the embayment platform (top). Definition of rotation coefficient (bottom). (Photo: Ortophotos Salou 1 June 2008). 84

Figure 31 Parameters use to define beach rotation (Ojeda and Guillen, 2008). 85

Figure 32 Theoretical Model: Typical Configurations (e.g. Fenals, Configuration 1, shoreline of June 1st, 1994 (dotted blue line), Configuration 2, shoreline of May 1st, 2006 (dotted black line) and Configuration3, June 30, 2004 (dotted red line)). 86

Figure 33 Definition of the angle of breaking. 88

Figure 34 Evolution of the rotation coefficient, Sant Pol. 90

Figure 35 Theoretical Model of Sant Pol (Photo: Ortophotos 2008, ICC). Configuration 1, shoreline of November 11, 2007 (solid blue line) and Configuration 2, shoreline of June 1st, 2004 (solid red line). 91

Figure 36 Wave condition during and shoreline effects at Sant Pol (Configuration 1) November 11, 2007. 93

Figure 37 Wave condition during and shoreline effect at Sant Pol (Configuration 2), 1 June 2004. 94

Figure 38 Evolution of the rotation coefficient, Canyelles. 95

Figure 39 Theoretical Model of Canyelles (Photo: Ortophotos 2008, ICC). Configuration 1, shoreline of June 1st, 2004 (solid blue line) and Configuration 2, shoreline of June 30, 2004 (solid red line). 96

Figure 40 Wave condition during and shoreline effect at Canyelles, June 2004. 99

Figure 41 Evolution of the rotation coefficient, Lloret del Mar. 100

Figure 42 Theoretical Model of Lloret del Mar (Photo: Ortophotos 2008, ICC). Configuration 1, shoreline of April 27, 2004 (solid blue line), Configuration 2, shoreline of July 1st, 1986 (solid black line) and Configuration 3, shoreline May 1st, 2001 (solid red line). 101

Figure 43 Wave condition during and shoreline effect at Lloret del Mar (Configuration 1), 1 April 2005. 103

Figure 44 Wave condition during and shoreline effect at Lloret del Mar (Configuration 2), 1 July 1986. 105

Figure 45 Wave condition and shoreline effect at Lloret del Mar (Configuration 3), 1May 2001. 106

Figure 46 Evolution of the rotation coefficient, Fenals. 107

Figure 47 Theoretical Model of Fenals (Photo: Ortophotos 2008, ICC). Configuration 1, shoreline of June 30, 2008 (solid blue line), Configuration 2, shoreline of June 1st, 1995 (solid black line) and Configuration 3, shoreline July 1st, 1994 (solid red line).109

Figure 48 Wave condition and shoreline effect at Fenals (Configuration 1), 30 June 2004.111

Figure 49 Wave condition and shoreline effect at Fenals (Configuration 2), 1 July 1995.113

Figure 50 Wave condition and shoreline effect at Fenals (Configuration 3), 1 June 1994.114

Figure 51 Evolution of the rotation coefficient, Bogatell. The rotation coefficient is illustrated in degrees. A positive slope indicates clockwise rotation.115

Figure 52 Theoretical Model of Bogatell (Photo: Ortophotos 2008, ICC). Configuration 1, shoreline of June 8, 2007 (solid blue line), Configuration 2, shoreline of November 15, 2007 (solid black line) and Configuration 3, shoreline February, 1995 (solid red line).116

Figure 53 Wave condition and shoreline effect at Bogatell (Configuration 1), 8 June 2007.118

Figure 54 Wave condition and shoreline effect at Bogatell (Configuration 2), 15 November 2007.119

Figure 55 Wave condition and shoreline effect at Bogatell (Configuration 3), 1 February 1995.121

Figure 56 Evolution of the rotation coefficient, Nova Icaria. The rotation coefficient is illustrated in degrees. A positive slope indicates clockwise rotation.122

Figure 57 Theoretical Model of Bogatell (Photo: Ortophotos 2008, ICC) Configuration 1, shoreline of November 15, 2007 (solid blue line) and Configuration 2, shoreline of March 1st, 2008 (solid red line).123

Figure 58 Wave condition and shoreline effect (Configuration 1) at Nova Icaria, 15 November 2007.125

Figure 59 Wave condition and shoreline effect (Configuration 2) at Nova Icaria, 1 June 2004.126

Figure 60 Evolution of the rotation coefficient, Barceloneta Before 2006. The rotation coefficient is illustrated in degrees. A positive slope indicates clockwise rotation.128

Figure 61 Theoretical Model of Barceloneta before 2006 (Photo: Ortophotos 2006, ICC) Configuration 1, shoreline of June 1st, 2004 (solid blue line), Configuration 2, shoreline of September 1st, 2000 (solid black line) and Configuration 3, shoreline February 1st, 1995 (solid red line).129

Figure 62 Wave condition and shoreline effect (Configuration 1) at Barceloneta before 2006, 1 June 2004.131

Figure 63 Wave condition and shoreline effect (Configuration 2) at Barceloneta before 2006, 1 September 2000.133

Figure 64 Wave condition and shoreline effect (Configuration 3) at Barceloneta before 2006, 1 February 1995.134

Figure 65 Evolution of the rotation coefficient, Barceloneta After 2006, north section (solid black line) and south section (solid blue line). The rotation coefficient is illustrated in degrees. A positive slope indicates clockwise rotation.135

Figure 66 Theoretical Model of Barceloneta after 2006 (Photo: Ortophotos 2008, ICC) North Section: Configuration 1, shoreline of December 30, 2008 (solid blue line), Configuration 2, shoreline of December 31, 2009 (solid black line) and Configuration 3, shoreline June 23, 2009 (solid red line). South Section: Configuration 1, shoreline of November 15, 2007 (solid blue line), Configuration 2, shoreline of June 23, 2009 (solid black line) and Configuration 3, shoreline April 14, 2009 (solid red line).137

Figure 67 Wave condition and shoreline effect (Configuration 1) at Barceloneta after 2006 North Section, 15 November 2007.....139

Figure 68 Wave condition and shoreline effect (Configuration 2) at Barceloneta after 2006 North Section, June 8, 2007. ..141

Figure 69 Wave condition and shoreline effect (Configuration 1) at Barceloneta after 2006 South Section, June 8, 2007. ..142

Figure 70 Wave condition and shoreline effect (Configuration 2) at Barceloneta after 2006 South Section, April 25, 2007. 143

Figure 71 Wave condition and shoreline effect (Configuration 3) at Barceloneta after 2006 South Section, November 15, 2007.....144

Figure 72 Evolution of the rotation coefficient, Playa Larga. The rotation coefficient is illustrated in degrees. A positive slope indicates clockwise rotation.....145

Figure 73 Theoretical Model of Playa Larga (Photo: Ortophotos 2008, ICC) Configuration 1, shoreline of November 11, 2007 (solid blue line), Configuration 2, shoreline of March 1^{rst}, 1995(solid red line).146

Figure 74 Wave condition and shoreline effect (Configuration 1) at Playa Larga, November 11, 2007.148

Figure 75 Wave condition and shoreline effect (Configuration 2) at Playa Larga, March 1^{rst}, 1995.149

Figure 76 Evolution of the rotation coefficient, Salou. The rotation coefficient is illustrated in degrees. A positive slope indicates clockwise rotation.....150

Figure 77 Theoretical Model of Playa Larga (Photo: Ortophotos 2008, ICC) Configuration 1, shoreline of March 1^{rst}, 1977 (solid blue line), Configuration 2, shoreline of March 1^{rst}, 1995(solid red line).151

Figure 78 Wave condition and shoreline effect (Configuration 1) at Salou, March 1^{rst}, 1977.....153

Figure 79 Wave condition and shoreline effect (Configuration 2) at Salou, March 1^{rst}, 1995.....154

Figure 80 Sectors of wave conditions.159

Figure 81 Frequency of occurrence per year, Tordera Buoy.161

Figure 82 Join Frequency Distribution Significant Wave Height and Peak Period a) E Directions, b) ESE Directions, c) SE Directions and d) SSE Direction. The color bars illustrate the frequency of the data. The wave direction is the direction the waves come from.....162

Figure 83 Join Frequency Distribution Significant Wave Height and Peak Period e) S Directions, f) SSW Directions, g) SW Directions and h) WSW Direction. The color bars illustrate the frequency of the data. The wave direction is the direction the waves come from.163

Figure 84 Frequency of occurrence per year, Tordera Buoy.168

Figure 85 Join Frequency Distribution Significant Wave Height and Peak Period a) NE Directions, b) ENE Directions, c) E Directions and d) ESE Direction. The color bars illustrate the frequency of the data. The wave direction is the direction the waves come from.....169

Figure 86 Join Frequency Distribution Significant Wave Height and Peak Period e) SE Directions, f) SSE Directions, g) S Directions and h) SSW Direction. The color bars illustrate the frequency of the data. The wave direction is the direction the waves come from.170

Figure 87 Join Frequency Distribution Significant Wave Height and Peak Period i) SW Directions and j) WSW Direction. The color bars illustrate the frequency of the data. The wave direction is the direction the waves come from.171

Figure 88 Frequency of occurrence per year; Tortosa Buoy.....176

Figure 89 Join Frequency Distribution Significant Wave Height and Peak Period a) SE Directions, b) SSE Directions, c) S Directions and d) SSW Direction. The color bars illustrate the frequency of the data. The wave direction is the direction the waves come from.177

Figure 90 Join Frequency Distribution Significant Wave Height and Peak Period e) SW Directions and f) WSW Direction. The color bars illustrate the frequency of the data. The wave direction is the direction the waves come from.178

List of Tables

Table 1. Description of beaches.....	35
Table 2. Number of study coastlines per beach	36
Table 3. Number of study coastlines per beach	37
Table 4 Coastlines by date	38
Table 5. Description of nodes and the beach affected by the wave data	41
Table 6. Description of wave buoys and the beach affected by the wave data	42
Table 7 Wave data selection.....	53
Table 8 Mean values of a/R_o , Girona	63
Table 9. Mean values of a/R_o , Barcelona	65
Table 10 Mean values of a/R_o , Tarragona	66
Table 11 Grouping Catalan beaches according with the beach type.....	78
Table 12 Values of berm height and depth of closure per beach.....	87
Table 13 Theoretical Rotation Coefficient Sant Pol	92
Table 14 Measured Volume between configurations Sant Pol.....	92
Table 15 Wave condition that generates configuration 1, Sant Pol	93
Table 16 Wave condition that generates Configuration 2, Sant Pol.....	94
Table 17 Theoretical Rotation Coefficient Canyelles	97
Table 18 Measured volume between configurations Canyelles.....	97
Table 19 Wave condition that generates configuration 1, Canyelles	98
Table 20 Wave condition that generates configuration 2, Canyelles	98
Table 21 Theoretical Rotation Coefficient Lloret del Mar	101
Table 22 Measured volume between configurations Lloret del Mar	102
Table 23 Wave condition that generates configuration 1, Lloret del Mar	103
Table 24 Wave condition that generates configuration 2, Lloret del Mar.....	104
Table 25 Wave condition that generates configuration 3, Lloret del Mar	105
Table 26 Theoretical Rotation Coefficient Fenals	109
Table 27 Measured volume between configurations Fenals.....	110
Table 28 Wave condition that generates configuration 1, Fenals.....	110

Table 29 Wave condition that generates configuration 2, Fenals	112
Table 30 Wave condition that generates configuration 3, Fenals	113
Table 31 Theoretical Rotation Coefficient Bogatell	116
Table 32 Measured volume between configurations Bogatell	117
Table 33 Wave condition that generates configuration 1, Bogatell	117
Table 34 Wave condition that generates configuration 2, Bogatell	119
Table 35 Wave condition that generates configuration 3, Bogatell	120
Table 36 Theoretical Rotation Coefficient Nova Icaria	123
Table 37 Measured volume between configurations Nova Icaria	124
Table 38 Wave condition that generates configuration 1, Nova Icaria	124
Table 39 Wave condition that generates configuration 2, Nova Icaria	126
Table 40 Theoretical rotation coefficient Barceloneta Before 2006	130
Table 41 Measured volume between configurations Barceloneta Before 2006	130
Table 42 Wave condition that generates configuration1, Barceloneta Before 2006	131
Table 43 Wave condition that generates Configuration 2, Barceloneta Before 2006	132
Table 44 Wave condition that generates configuration 3, Barceloneta Before 2006	134
Table 45 Theoretical rotation coefficient Barceloneta After 2006	138
Table 46 Measured volume between configurations Barceloneta Before 2006	138
Table 47 Wave condition that generates configuration 1, Barceloneta Before 2006 North Section	139
Table 48 Wave condition that generates configuration 2, Barceloneta Before 2006 North Section	140
Table 49 Wave condition that generates configuration 1, Barceloneta Before 2006 South Section	142
Table 50 Wave condition that generates configuration 2, Barceloneta Before 2006 South Section	143
Table 51 Wave condition that generates configuration 3, Barceloneta Before 2006 South Section	144
Table 52 Theoretical Rotation Coefficient Playa Larga	147
Table 53 Measured volume between configurations Playa Larga	147
Table 54 Wave condition that generates configuration 1, Playa Larga	148
Table 55 Wave condition that generates configuration 2, Playa Larga	149
Table 56 Theoretical Rotation Coefficient Salou	151
Table 57 Measured volume between configurations Salou	152
Table 58 Wave condition that generates configuration 1, Salou	152
Table 59 Wave condition that generates configuration 2, Salou	153

Table 60 Table Buoy description and beach associated to it..... 159

Table 61 Frequency of Occurrence of the Specific Wave Condition Sant Pol..... 164

Table 62 Frequency of Occurrence of the Specific Wave Condition Canyelles 165

Table 63 Frequency of Occurrence of the Specific Wave Condition Lloret del Mar 166

Table 64 Frequency of Occurrence of the Specific Wave Condition Fenals 167

Table 65 Frequency of Occurrence of the Specific Wave Condition Bogatell..... 172

Table 66 Frequency of Occurrence of the Specific Wave Condition Nova Icaria..... 173

Table 67 Frequency of Occurrence of the Specific Wave Condition Barceloneta Before 2006..... 174

Table 68 Frequency of Occurrence of the Specific Wave Condition Barceloneta After 2006 North Section 174

Table 69 Frequency of Occurrence of the Specific Wave Condition Barceloneta After 2006 South Section 175

Table 70 Frequency of Occurrence of the Specific Wave Condition Playa Larga..... 176

Table 71 Frequency of Occurrence of the Specific Wave Condition Salou 179

1. Introduction

The largest part (75%) of the world's continental and islands margins consist of rocks. Along rocky coasts, nearshore wave energy is often high because the size of the waves is related to the nearshore bathymetry and refraction patterns. The wave energy focused on the headlands and dispersed in to the bays, so the headlands erode while the intervening bays fill up (Bosboom and Stive, 2010). Beaches bounded by rocky outcrop or headland where the shoreline take some form of curvature are known as curved, embayed, hooked, pocket and headland-bay beaches (Guillen, 2008).

Embayed bay beaches differ from the long sandy beaches in the limited alongshore sediment transport, which varies according to the beach boundaries (Guillen, 2008). Most of the studies of the embayed beaches have been focus on the static equilibrium configuration; when the tangential section down coast the beach tend to be parallel to the wave crest approaching the coast from offshore. During this condition, the longshore component of breaking waves energy does not longer exist and hence littoral drift within the embayed. Three main models have been use to fit this static configuration, the logarithmic-spiral propose by Silvester in 1960, the parabolic bay shape propose by Hsu in 1989 and the hyperbolic tangent propose by Moreno and Kraus in 1999. This configuration is useful to determine the mean shoreline position associated with some specific wave climate (e.g. wave direction). The approach of static equilibrium configuration has been apply on several beaches around the world in order to validate it with different wave environments; we can mention the studies done by Klein in Brazil, Pinto in Portugal and Guillen in the Spanish coast.

However, embayed beaches are dynamic environments that respond to different time scales and processes. Beaches are typically affected by headland by passing around it boundaries, by the formation of rips and by beach rotation. A beach is experience headland bypassing if the predicted curve of static equilibrium is located landward or seaward of the existing beach, this means that a continuous supply of sediment has prevailed to maintain its stability over a longer period. If the supply of sand in the beach decrease or increase, the shoreline will response to it in terms of erosion or accretion (Klein, 2009).

Beach rotation can be define as a longitudinal sediment transport that alternates towards opposite ends of a beach delimited by headlands (Vintem, 2009) and beach oscillation refers to longitudinal sediment transport across the entire embayment (Ranashinge et. al, 2004). The difference is that these processes do not lead to long-term loss of sediment since the beach often returns to the original location, in response to a new change in wave direction.

Variations in beach morphology (rotation and oscillation) have long been documented as a respond to equilibrium wave condition as opposite to an instantaneous wave conditions (Wright and Short, 1984). Short from 1995 to 2007 and Ranashinge in 2004 have performed an extensive study, on the southern and central

coastline of New South Wales, Australia. The objective of the study was to determine a link between the Southern Oscillation Index, the wave climate and beach rotation in Narrabeen and Palm Beach. As expected, there appears to be an inverse correlation between a significant wave height and beach oscillation, and a direct correlation between wave directions and beach rotation.

The consequences of the fluctuation in the shoreline due to a specific wave conditions can be significantly high, since within this region a large portion of the world's population reside. Recent estimates suggest that 23% of the global population live within 100km and 100m elevation of the coast (Small and Nicholls, 2003). These zones also support significant touristic activities and represent a primary resource on regional economies. In this context, Spain is a typical case, as it is one of the world's major tourist destinations within this sector (Ariza, 2008). The Catalan coast of Spain, correspond to a very well known tourist destination. At the north is characterize by it highly intended coast, where bayed and pocket beaches are common features, at the center consisted in artificial pocket beaches and at the south is characterized by long curved beaches. Changes in the future shoreline position of the beach can damage beachfront property, generate a loss in recreational areas and can affect the stability of structures along the coast.

1.1 Problem Definition

Coastal environment has been extensively used for activities as fishing, tourism, transport of good, water treatment and housing. In this regard, Spain is a typical case; also is it is one of the world's mayor touristic destinations within this sector. Tourism accounted for 11.4% of Spanish GDP in 2003. Much of the tourism industry is based on the sun and san model. Therefore, beaches are considered to be one of the country's major resources (Ariza et.al. 2007).

Beach variation (rotation and oscillation) are of greater importance when the functions of the beach are considered. The assessment of 38 municipalities along the Catalan coast of Ariza et al, 2007, has show that two thirds of these local authorities (20 municipalities) reported erosion problems on some of the beaches. The main concern in these areas was related to sediment management. The loss of sub-aerial beach area is a critical issue in the recreational use of the beach and in the protective function of the system. Since a reduction of the beach width also decrease the available surface for dissipating wave energy during storm.

A good comprehension of morphodynamics of embayed beaches is necessary in order to facilitate effective and sustainable coastal zone management.

1.2 Objectives

The main objective of this study was to analyze the behavior of the embayed beaches along the Catalan Coast in order to quantify the morphological variability of these bounded systems. This analysis can provide sufficient information to understand how beach morphology changes may impact the natural state of beaches and the potential impacts on development and infrastructure. The study works in a medium scale, where the static configuration and the fluctuations of the shoreline are studied.

From this main objective, three specific objectives were defined:

1. *Study of the shoreline evolution based on the analysis of historical aerial photographs of embayed beaches in the Catalan coast:*

Measure the variation of the shoreline position from aerial photographs and orthophotos of nine sandy embayed beaches of the Catalan coast. The shoreline data set vary in time and space along the coast, but consist in information from 1986 to 2009 of previously defined coastlines of the Environmental Ministry, the Cartographic Institute of Catalonia and digitalize shorelines of satellite images from Google Earth .

2. *Determine the presence of medium term oscillation and variation of the embayed beaches along the Catalan Coast and identify the conditions required that accomplish a change in the shoreline position using a theoretical model.*

From the shoreline data set we would determine the most typical configurations that a beach would experience within the data set. Based on this theoretical model we will determine the conditions required to move an amount of sediment from one configuration to the other. The quantity of volume moved will be defined by the wave height, wave period, wave direction and the duration of the event.

3. *Determine the frequency of occurrence of the wave conditions that produce a change in the theoretical model over 2001 to 2007.*

Once we define the necessary conditions to develop a future configuration we will be able to determine the frequency of occurrence of this condition over the last 7 years of available wave data of the Catalan coast.

1.3 Scope and limitations of the work

The study was based on the shoreline data from aerial photographs, orthophotos and previously defined coastlines. The study does not use any information from profile surveys. The distribution of the shoreline through the years was uneven, therefore seasonal and inter-annual variations couldn't be studied.

The available wave data consist in simulated data from 1958 to 2001 and instrumental data from 2001 to 2007. Only the wave conditions that affected the morphology of the beaches have been study, by means of an effective range of direction. Direction coming from land and parallel to the coast has been eliminated.

The study is base on the longshore sediment transport behavior of the beach, the main assumption is that the profile (e.g. slope) of the beach does not change; the only exchange of volume will occur in alongshore direction.

1.4 Thesis outline

Following on from this chapter, the thesis is separated into chapters depending on the sub-objectives that are treated, each chapter present the methodology used to asses the result, a discussion and summary of the conclusions. Firstly, **Chapter 2** presents the theory of embayed beaches and the related studies within this subject. **Chapter 3**, consist of a description of the Catalan coast and the beaches sites. A description of the shoreline and wave data used in this thesis is also given.

Chapter 4: Shoreline Evolution

Chapter 4 presents the result of the equilibrium behavior of the shoreline and the variation of the beach width and beach area (e.g. beach mobility variations) through the data set. In this section also a distinction has been made in the beach type and the beach mobility variations.

Chapter 5: Beach rotation and oscillation: Rotation Coefficient

In Chapter 5, the results of beach rotation and oscillation by means of a theoretical model are presented. An analysis of the forcing mechanism (wave conditions) responsible of the change in the shoreline configuration is also presented.

Chapter 6: Wave condition and the theoretical model respond: 2001-2007

Chapter 6 presented the frequency of occurrence of the wave conditions previously obtain in chapter 5 during the last 7 years of available wave data.

Chapter 7: Conclusion and Recommendations

A summary of all the results and the key findings of the morphological variation of the embayment beaches of the Catalan coast were provided in chapter 6. This chapter also presents some suggestions from future research in the subject.

2. Literature Study

The aim of this chapter is to present theory of the process observed within the embayed beaches for example equilibrium parabolic shape (static equilibrium) and beach rotation and oscillation (dynamic process), followed by a review of several studies related with the subject.

Two large scales will be described, the larger scale corresponded to the static equilibrium configuration propose by Hsu, 1989 and a medium scale that correspond to the fluctuations of the shoreline from the mean platform configuration (e.g. beach rotation and oscillation).

2.1 Embayed beaches

The shape of an embayed beach between headlands is influence by the location of the headlands. Where the headlands are closely spaced and a limited volume of sand is present, small pocket beaches formed. Where the headlands are far apart and an adequate sediment supply exists, long and wide beaches formed (F.J.H. Olijslagers, 2003). Between these two extreme, most of the beaches within headlands tend to built up transverse to the direction of approach of the most important constructive waves, in the down coast sector we obtain a long and straight beach while on the up coast end the beach is curve. See figure 1.



Figure 1 A) Aro Beach. B) La Fosca and Castel Beach, Costa Brava, Spain.

2.1.1 Sediment Transport within an Embayed Beach

In the following paragraphs, we present an explanation of the process of sediment transport within an embayed beach. The sediment balance in the embayed beach is determined by the effectiveness of the headlands in terms of the disruption of the longshore sediment transport (J. Jimenez, 2007).

In an embayed beach two zones can be identify, zone I (protective zone) where the sediment transport is generated by the longitudinal current (oblique incident) and by the gradient currents (wave height gradients). In this zone, the wave climate is affected by diffraction cause by an obstacle located up coast.

Zone II (expose zone) where the sediment transport is induce by the longitudinal current, created by the oblique wave direction, and where the wave climate is not affected by an obstacle up coast.



Figure 2 Identification zones Tossa de Mar, Costa Brava, Spain.

The configuration of the beach has been study in a long-term equilibrium situation. Where the beach adopts a form due to the mean wave climate conditions, call the equilibrium bay condition. Depending of the sediment balance in the bay, we could have a static equilibrium or a dynamic equilibrium. We would focus in the static equilibrium.

Static equilibrium Condition

In a static equilibrium, the sediment balance is zero, no sediment coming in or out. This condition can be explain by the continuity equation, since the change in the coastline of the beach is produce by the longshore sediment gradient along the beach, in the continuity equation (Equation 1) this longshore gradient has to be zero in order to have a static equilibrium. Therefore, the rate of sediment transport has to be constant (J. Jimenez, 2007).

$$\frac{\delta x}{\delta t} + \frac{1}{(B+dc)} \cdot \frac{\delta S_l}{\delta y} = 0$$

(Eq. 1)

$$\frac{\delta x}{\delta t} = 0 \rightarrow \frac{\delta S_l}{\delta y} = 0$$

Where $\frac{\delta S_l}{\delta y}$ is the longshore sediment transport.

In order to analyze the equilibrium condition, we need to consider that the sediment transport is composed by two components:

- Longitudinal current generated by the oblique wave climate (direction)
- Currents created by the wave height gradients

$$S_l = H_b^2 \cdot C_{gb} \cdot (\varepsilon_1 \cdot \text{sen}(2 \cdot \alpha_{bs}) - \varepsilon_2 \cdot \cos(\alpha_{bs})) \cdot \frac{\delta H_b}{\delta y}$$

(Eq. 2)

If we apply the equilibrium criteria in a beach with barriers at either extremity, we obtain that the sediment transport has to be zero.

$$\frac{\delta S_l}{\delta y} = 0 \rightarrow S_l = 0$$

For the zone II, the equilibrium condition is given by the cancelation of the sediment transport induce by the obliquity of the wave incidence, in this condition the coastline (α_w) is parallel to the wave breaking angle (α_s).

$$S_l = 0 \rightarrow S_l \propto H_b^{2.5} \cdot \text{sen}(2\alpha_{bs}) = 0 \rightarrow \text{sen}(2\alpha_{bs}) = 0 \rightarrow \alpha_s \parallel \alpha_w$$

For the zone I, the equilibrium configuration is achieved when the configuration of the sediment transport along the coastline (both components) is annulled. This means that equation 2 tends to zero.

$$S_l = 0 \rightarrow (\varepsilon_1 \cdot \text{sen}(2 \cdot \alpha_{bs}) - \varepsilon_2 \cdot \cos(\alpha_{bs}) \cdot \frac{\delta H_b}{\delta y}) = 0 \rightarrow \frac{\delta H_b}{\delta y} = 2 \frac{\varepsilon_1}{\varepsilon_2} \cdot \text{sen}(\alpha_{bs})$$

In the zone I, this static configuration is difficult to generated, since the diffraction is the one that generate its typical equilibrium form. Several models have been created in order to develop the configuration of the beach. The parabolic bay shape proposes by Hsu in 1989, the logarithmic spiral proposes by Silvester in 1960 and the hyperbolic tangent by Moreno and Kraus in 1999. We would focus in the parabolic bay shape.

2.1.2 Parabolic Bay Shape

The term parabolic was first mentioned by Mashima (1961) to describe the geometric configuration of the bow-shaped stable coast found on the coastal margin of Tokyo Bay, Sagami Bay and Boso Peninsula in Japan. He found a close relationship between the wave energy ellipse and the bay shape; from this relationship, he derives the parabola equation.

$$y = p \cdot x^2 - b$$

(Eq.3)

However, there were complications centering the parabola for any particular bay, not taking diffraction into account, or the wave obliquity.

In 1989, Hsu suggested a new approach. He derives a parabolic beach profile by:

$$\frac{R}{R_0} = C_0 + C_1 \cdot \frac{\beta}{\theta} + C_2 \cdot \left(\frac{\beta}{\theta}\right)^2$$

(Eq. 4)

From fitting the platform of 27 mixed cases of prototype and model bays believed to be in static equilibrium, where the radio (Ro) or the control line are draw from the point of diffraction to the beach at angle β to the wave crest line. The radii (R) define the location of the shoreline at angle θ measured from the predominant wave crest.

The coefficient C_0 , C_1 and C_2 are empirically derived, vary uniformly with β as figure 3. These C values are bounded within 2.5 and -1.0 for the usual range of angle β from 10° to 80° applicable in most field conditions.

For a bay with a given set of β and R_0 locations for pairs of R_n and θ_n can be marked and a curve can be sketched for the static bay shape prediction.

The static equilibrium configuration is reached when the angle β is the same between R_0 and the tangent to the down coast beach line. The wave ray is orthogonal to the shoreline position, therefore the longshore component of breaking waves energy does not longer exist and hence littoral drift within the embayed.

Wave heights and periods are not included in expressions of equilibrium bay shape, although they were once investigated but found to be insignificant for bayed beaches in static equilibrium (Hsu and Evans, 1989)

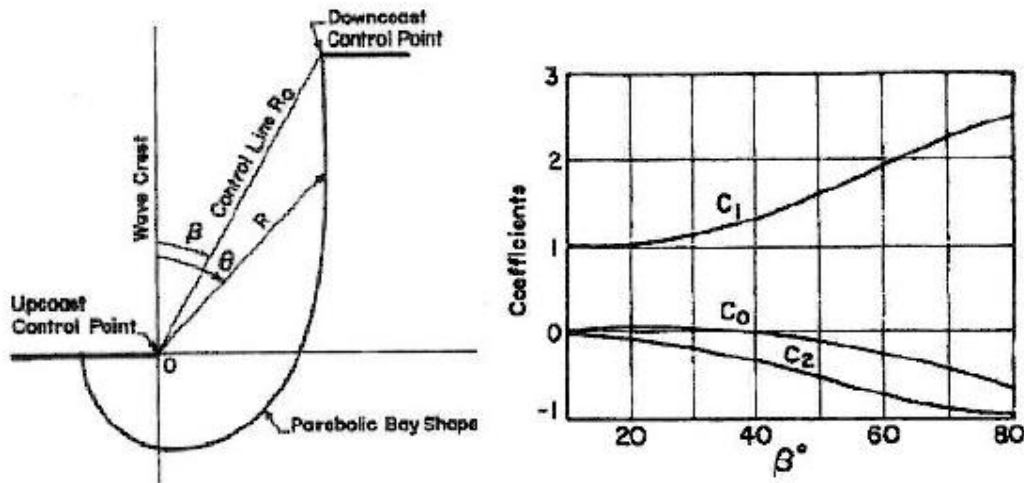


Figure 3 Definition sketch of and coefficient used in the parabolic equation (Hsu and Evans, 1989).

Upcoast control point

The upcoast control point is defined as the point of diffraction. It can be a mainland point, a small island, another rock outcrop or even a reef offshore. Once the wave orthogonal normal to the downcoast tangent is transferred across to the upcoast headland, it is the intercept with any of the above features that determine the control point (Silvester, R., Hsu, J.R.C., 1997).

Downcoast control point

The down coast control point is defined as the point when the tangential section downcoast the beach tend to be parallel to the wave crest. In some cases, the downcoast headlands protruded into the bays, where diffraction take place behind it, causing a deviation in the mild curvature of the down coast end of the bay. In this situation a transition point between this two curves have to be determined to which the accepted orthogonal is normal. Then the limit of the bay becomes this transitions point.

2.1.3 Beach Rotation and Oscillation

Within an embayed beach we can observe two important dynamic process, beach rotation and beach oscillation. Beach rotation refers to the longitudinal sediment transport that alternates towards opposite ends of a beach delimited by headlands; we would observe a maxima displacement at the limits of the beach and minimum displacements at the central section represented by the pivotal point. And beach oscillation refers to the erosion or accretion across the entire embayment.

The inverse relationship between the opposite ends of a beach is most often identified when comparing beach width or beach volume data (e.g. Klein 2002, Ranasinghe et. al 2004 and Short 2000). It has been suggested that this process results from a change in the longshore sediment transport direction between headlands extremities on the embayed beaches (Short and Masselink, 1999). However, Ranashinge et.al 2004 speculate that the different cross-shore responses at either end of the embayment might also been important.

Beach rotation has been often related to periodic or long term changes in the wave climate, particularly the wave direction (Short and Masselink, 1999, Klein 2002). Though, it has been observed that beach rotation can occur on a range of timescales without any net gain or loss of sediment (Klein, 2002).

This process has been observed in Southeast Australia (Short from 1995 to 2007 and Ranashinge in 2004), Brazil (Klein, et.al, 2009) and Spain (Ojeda and Guillen, 2008).

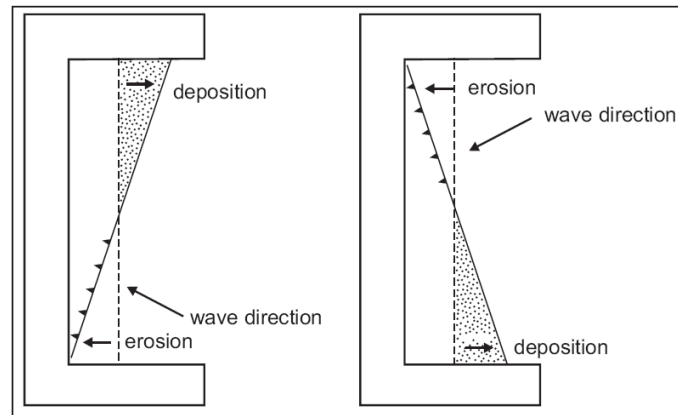


Figure 4 Representative diagram of beach rotation process (Short and Masselink, 1999).

2.1.4 Related Studies

In this section a review of similar studies will be presented. The studies deal with shoreline variability in short, medium and long scales; they will be treated in accordance with the location.

- Southeast, Brazil;
- New South Wales, Australia;
- West coast of Algarve, Portugal;
- Barcelona, Spain;

Southeastern, Brazil

Several studies have been performed in the Southeastern coast of Brazil related with a large scale morphodynamics processes, most specifically in Santa Catarina state. The studies cover a period between 1990s and early 2000s and had been develop by Klein and co-workers.

The following topics are specifically set forward: a) analyze the platform of headland-bay beaches using the empirical parabolic model; b) identify the beach morphodynamics and sequence profile for bay-headland coast; c) investigate the small-scale beach rotation in different headland-bay beach.

The Santa Catarina coast line is a micro-tidal east swell coast environment with headland and bay geomorphologies.

In order to investigate historical scale the morphodynamics process, they use satellite images from Google Earth and evaluate the parabolic bay shape propose by Hsu (1989). They also study detail morphological field investigation (beach profiles) from 1993 to 1996 in an effort to determine alongshore sediment mobility. Then the morphological changes were correlated with forecasting wave information, it does not include offshore wave records, field experiments to define wave refraction and diffraction/attenuation, and wave crest pattern behind headlands.

Base on the study material, they found the following conclusion:

- The parabolic bay shape has proved to be an adequate tool to study the stability of the headland-beaches in Santa Catarina, Brazil.
- The longshore beach profile monitoring program exhibited different patterns of sediment removal as a function of the degree of curvature.
- Short term beach rotation processes were evident in exposed reflective and dissipative beach.

New South Wale, Australia

Short (1995, 2000) and Ranashinge (1999, 2004) have performed an extensive study along the south-east Australian coastline. Over the last few decades, many of the beaches along this coastline have intermittently undergone erosion, resulting in significant damage to dunes and beachfront property. It appears that erosion is related to a periodic medium term process (period of 2-8 years). Two mayor studies have been perform in order to understand the dominant forcing mechanisms driving this shoreline behavior, 1) a study relating beach rotation, wave climate and the Southern Oscillation Index (Ranashinge, 2004) and 2) a study of rotation and oscillation of embayed beaches (Harley, 2008). Both study will be summarize in the following paragraphs.

The Southern Oscillation Index, wave climate and beach rotation (Ranashinge, 2004)

The objectives of the study were to establish the links between the Southern Oscillation Index (SOI), wave climate and beach rotation and to determine the physical process governing beach rotation. Data from two similar beaches were analyze, Narrabeen Beach and Palm Beach. The first set of data comprise 24 years of monthly beach profile of Narrabeen Beach, these data were subjected to time series analysis to investigate possible link between the SOI, wave climate and beach rotation. Second set of data, consist on daily time exposure video images obtained at Palm Beach, during 1997-1999 El Niño/La Niña event, this set of data were used to investigate the morphodynamics processes governing beach rotation.

The wave data consisted of measured hourly directional wave data from 1992, measured non-directional wave data from 1987 to 1992, and hindcasted daily wave direction from 1987 to 1992. All measured data were

obtained from wave rider at long Reef Point at depth of 80m. The time of monthly averaged Troup SOI data over the last 50 years was obtained from the Australian Bureau of Meteorology.

From the material describe above, the following conclusion were presented:

- During El Niño phases, the northern end of the beach accretes while the southern end erodes resulting in a net clockwise rotation of the beach around the center. The opposite occurs during La Niña phases resulting in a net anti-clockwise rotation of the beach.
- The northern end of the beach respond to trend shifts in SOI about 3 months after the trend shift occurs, while the southern end of the beach lags the SOI trend shift by up to 1.5 years. The mean shoreline fluctuation during El Niño phases appear to be about 10m greater than La Niña phases.
- Waves are predominant incident from the southeast during both El Niño and La Niña phases. Nevertheless, wave height increase/decrease with increasing/decreasing SOI.
- Incident waves become more southerly with decreasing SOI, while become more northerly with increasing SOI. On average, the number of storms per year doubles from El Niño to La Niña.
- A conceptual model of beach rotation is presented, the model describe a combination of cross-shore and long-shore sediment transport and hydrodynamics process (wave direction), that are expected to result in the observed clockwise and anti-clockwise beach rotation during El Niño and La Niña phases respectively.

Rotation and Oscillation of Embayed Beaches (Harley, 2008)

In order to understand the dominant forcing mechanism driving the observed beach rotation/oscillation cycles in the Collaroy-Narrabeen embayed; the author investigated the inter-annual wave climate and their implications on the coastal zone. In the past studies, this could not be performed since the 16 years of the multi-decadal beach survey data set was not accompanied by directional wave data.

Using the wave data from the European Center for Medium-range Weather Forecasts (ECMWF) they address these limitation, known as the ERA-40 data set, it has a sufficient length (45 years) to investigate both inter-annual wave climate variations and their effect in coastal zone.

The three aims of the study are 1) present the result of the multi-decadal beach surveys updated to August 2008, 2) evaluate the applicability of ERA-40 wave data to south-east Australian region and 3) observe how inter-annual variability in the wave climate may affect the observed beach rotation/oscillation cycles.

In order to accomplish the objective the use five representative cross-shore profile lines along the beach, the survey consisted in monthly interval between April 1996 and August 2006. Each profile was measured using the Emery method, since May 2005 the five profiles lines have continued measured using high accuracy Real-Time Kinematic GPS (RTK-GPS).

The following results were obtained:

Sub aerial beach variability: 1976-2006

From the analysis of the time-series of the beach width, they determine that the beach variability present three different time scales: inter-annual variations with frequency of months, bi-annual variations with cycles of 2-3 years; and longer-term cycles of up to 10 years.

Inter-annual wave variability and beach response

An EOF analysis was performed in order to separate the dominant modes of beach variability. The first EOF mode represents the non-stationary mean beach width, which can be interpreted as the beach oscillations time series. Since beach oscillation correspond to cycles of accretion and erosion across the entire embayment, it is likely to be controlled by inter-annual changes in wave energy. Comparing this time series with annually average values of H_{sig} , they observe an inverse relationship between beach oscillations and wave height.

The second EOF mode represents the beach rotation signal and represents the remaining 60% of the beach variability. Since it has been suggested that beach rotation is a result of reversal longshore currents, these rotation cycle were compared to inter-annual changes in the offshore wave direction. However, direct correlation between wave direction variability and beach rotation, was not clear.

West Coast of Algarve, Portugal;

The west coast of Algarve is dominated by relative short embayment beaches. These beaches intermittently undergo erosion, resulting in an occasional loss of recreational area and damage of dune and beachfront property. In order to understand this process, regional management authorities develop a beach monitoring program. This program has been effective since allow to analyze the beach morphodynamics in different time scale. In the study of Pinto in 2009, the author use this information to evaluate the seasonal and meso-scale variation of Armação de Pera located in the southern Algarve coast of Portugal and compared with offshore wave data record in order to understand the changes in shoreline position.

For the study the author uses the following methodology:

- Offshore wave data were classified according to prevailing directional wave climate. Wave frequency and energy for each directional class were computed for the period elapsed between beach surveys. Empirical relations between longshore energy flux and sediment transport rate stated in the CERC formula (SPM, 1984) were used to estimate longshore transport rates.
- Six beach profiles were monthly and bimonthly monitored during 2.3 years (May 2002-August 2004). Beach width was defined as the horizontal distance between MSL and landward fixed point, and beach volume was calculated as the cross sectional area within those limits per unit length of shoreline.
- The study of shoreline evolution between 1965 and 2001 was based on the analysis of documentary records, like aerial photographs. GIS software was used to geo-referencing and to calculate shoreline evolution.

Finally the author concludes that variations in beach platform were found to be more complex than predicted by simple rotation models. In-phase responses emerged in relation with the dominance of cross-shore process, where out of phase beach behavior essentially relates with longshore process. The results indicate that process may coexist at different sector of the beach; smaller time scales are dominated by cross-shore component, and larger time scales is conditioned by longshore process.

Barcelona City, Spain

The objective of the study propose by Ojeda and Guillen in 2008, was to achieve a better understanding of artificial embayed beach morphodynamics using shoreline position an beach area data from three beaches (Barceloneta, Nova Icaria and Bogatell) in Barcelona City during a three years period. In order to accomplish these objective the define three specific objectives, 1) examine the dynamics of the shoreline and their changes in the emerged beach are, 2) compare the temporal evolution of the beach area with the temporal evolution of the beach orientation to establish which changes in beach orientation are related to episodes of beach rotation and 3) examine the response of the beaches to storm events and try to find a relation between the alongshore component of the radiation stress and changes in beach orientation.

The shoreline position of the beaches was obtained from November 2001 to December 2004 by an Argus video system located a top of a building at a height of around 142m. The images are in the visible range of light and the sampling is done every daylight hour during a ten-minute period (1 picture per second). Shoreline was measure with a time gap between images varying from one to fifteen days, depending on the changes occurring at the coastline. A reference shoreline was defined for each beach as the result of the averaged position from all available shoreline fitted to a polynomial curve. Beach mobility was defined for each alongshore location as the standard deviation of the shoreline position throughout the study period. The emerged beach area is defined as the area bounded by the shoreline and the hard structures in the rear and lateral part of the beaches. Beach orientation during the study period was defined through linear regression.

Wave data were characterized using information from the WANA model data set, computed by the Spanish National Institute of Meteorology using HIRLAM and WAM numerical models. Mean values of alongshore component of the radiation stress were computed for the storms events, Hs higher than 1.5m.

The following conclusions were derived:

- Over the three-year study period the artificial embayed beaches of Barcelona display a beach mobility of similar magnitude to that of natural embayment beaches. Maximum beach mobility occurs at the ends of the beaches and it is associated to beach rotation.
- Changes in beach orientation were caused by beach rotation related to storm events and by local erosion or accretion due to storms action.
- The advance or retreat of each beach segment associated with beach rotation were not alongshore constant due to the influence of the morphodynamics (sediment exchange with the submerge profile and formation of sedimentary structures).

3. Study Area and Data

3.1 Description of the Catalan Coast

The present study was carried out along the Catalan coast of northeast Spain; respectively the province of Girona in the north, the province of Barcelona in the center and the province of Tarragona in the south. The Catalan coast of northeast Spain stretches over 580 km, from the French border to the south of the Ebro Delta. The configuration of the Catalan coast largely depends on its geological and structural background. The northern coast corresponds to the eastern Pyrenees and to coastal transversal ranges, consisting in metamorphic and granite rocks. This highly resistant lithology forms the most characteristic rocky coast of Costa Brava (J. Guillen, 2008).

To the south the coast follows a NE-SW orientation in accordance with the coastal ranges. The Maresme coast runs parallel to the Coastal Range, and is only interrupted by several commercial and fishing ports. Next, the Barcelona city area is characterized by artificial beaches and a big harbor that extends along more than 15 km. Its southern part developed over the delta plain of the Llobregat River, which creates a sandy coastline over 18 km long. Additionally in the south, the Garraf coast is characterized by the low calcareous cliffs. From this point and after Sitges the coast is no longer straight and is oriented toward the South, up off the port of Tarragona. This is the second biggest port of Catalonia and extends along more than 5 km, before the entrance of Cabo de Salou.

The next coastal unit to the south is Costa Daurada with open beaches, sometimes bonded by groins and harbors with small calcareous coastal relief. The southern segments are the Ebro Delta with sandy delta plain of 320km². Natural embayment beaches are especially abundant along the rocky coast of Costa Brava and Garraf, where artificial beaches are most frequent in the Barcelona city area and along Costa Daurada. The sediment grain size also varies along the Catalan coast, with a tendency to be coarser in the north and finer toward the south.

The Catalan coast is micro tidal, with a range of less than 0.2m and it has a seasonal wave climate. Summer corresponds to the low energy period while during fall and winter we will experience the high energy conditions. Mean wave periods are 4-6s and the mean significant wave height is 0.7m. The most severe storms come from the east, and during extreme storms, the period increases to 13 s and the maximum measured significant wave height can be up to 7 m (J. Guillen, 2008).



Figure 5 Catalan coastline

The study consisted of 9 sandy beaches from Girona in the north to Tarragona in the south. In order to study the shoreline evolution of the embayed beaches, we analyze the shoreline position from historical aerial photograph, 1:5000 and 1:2500 ortophotos and previously define coastlines. The parameters use to determine the evolution of the embayment beaches correspond to the parameters define by the equilibrium configuration propose by Hsu in 1989. Most of the parameters employed have been use in earlier studies (e.g. Silvester and Hsu, 1993; Short, 1999; Klein and Menezes, 2000).

Below is a list of beaches from north to south that will be used in the thesis, see figure 6:

- Sant Pol (a)
- Canyelles (b)
- Lloret del Mar (c)
- Fenals (d)
- Bogatell (e)
- Nueva Icaria (f)

- Barceloneta (g)
- Playa Larga (h)
- Salou (i)



Figure 6 Location of the studied beaches

Table 1. Description of beaches			
Province	Beach	Latitude (N)	Longitude (E)
Girona	Sant Pol	41°47'27.90"	3° 2'57.51"
Girona	Canyelles	41°42'16.12"	2°53'1.52"
Girona	Lloret de Mar	41°41'57.18"	2°51'3.26"
Girona	Fenals	41°41'39.93"	2°49'57.08"
Barcelona	Bogatell	41°23'40.99"	2°12'25.46"
Barcelona	Nueva Icaria	41°23'27.08"	2°12'9.48"
Barcelona	Barceloneta	41°22'58.60"	2°11'42.61"
Tarragona	Playa Larga	41° 3'53.87"	1° 9'22.52"
Tarragona	Salou	41° 4'27.08"	1° 8'15.49"

3.2 Shoreline Data

The shoreline data set consist on information from the Cartographic Institute of Catalonia (ICC), the Ministry of Environment (MMA) in addition with the aerial photograph from Google Earth (G).

This data set is not continuous in time or space; therefore some beaches have more shoreline position than others. The shorelines from 1947, 1957, 1965, 1973, 1977, 1983, 1995 and 1998 corresponded to coastlines previously define by the Ministry of Environment.

The shorelines from 1986, 1994, 1997, 2000, 2001 and 2004 corresponded to coastlines define by Cartographic Institute of Catalonia; also the digitalized coastlines from the Ortophotos from 2006, 2008 and 2009. Finally the shorelines from 2004, 2005, 2006, 2007, 2008 and 2009 corresponded to digitalized coastlines from aerial photographs from Google Earth.

The following table shows a detail of the number of shoreline per year that has been study, the coastline does not represent a yearly average; correspond to a specific date of the year.

Table 2. Number of study coastlines per beach

Beach	Year									
	1947 (MMA)	1957 (MMA)	1965 (MMA)	1973 (MMA)	1977 (MMA)	1983 (MMA)	1986 (icc)	1994 (icc)	1995 (MMA)	
Sant Pol										1
Canyelles							1	1	1	
Lloret de Mar							1	1	1	
Fenals							1	1	1	
Bogatell	1	1	1	1	1	1		1	1	
Nueva Icaria	1	1	1	1	1	1		1	1	
Barceloneta	1	1	1	1	1	1		1	1	
Playa Larga									1	
Salou	1	1	1	1	1	1			1	

Table 3. Number of study coastlines per beach

Beach \ Year										
	1997 (icc)	1998 (MMA)	2000 (icc)	2001 (icc, MMA)	2004 (icc, G)	2005 (G)	2006 (icc, G)	2007 (G)	2008 (icc, G)	2009 (icc, G)
Sant Pol			1		2		2	1	2	2
Canyelles			1		2		2	1	2	2
Lloret de Mar	1		1	2	2	1	2	1	2	2
Fenals	1		1	1	2	1	2	1	2	2
Bogatell			1		2		2	4	2	5
Nueva Icaria			1		2		2	4	2	5
Barceloneta			1		2		2	4	2	5
Playa Larga		1	1		2	1	4	1	2	2
Salou		1	1		1	1	4	1	2	2

Next table show the dates of each coastline for the study. Before 1992 the coastline of Bogatell, Nova Icaria and Barcelona was the same, therefore this shoreline data was not used in the study of the embayment beaches. By knowing the exact date of the coastline we will be able to know which was the wave condition needed to accomplish a specific configuration and in what time was achieved.

Table 4 Coastlines by date									
Date	Sant Pol	Canyelles	Lloret de Mar	Fenals	Bogatell	Nueva Icaria	Barceloneta	Playa Larga	Salou
1-Feb-47									*
1-Jun-47					*	*	*		
2-Jun-57					*	*	*		*
1-Jun-65					*	*	*		*
1-Jul-73					*	*	*		*
1-Mar-77									*
1-Nov-77					*	*	*		
1-Jun-83					*	*	*		
1-Dec-83									*
1-Jul-86		*	*	*					
1-Jun-94		*	*	*					
1-Sep-94					*	*	*		
1-Feb-95					*	*	*		
1-Mar-95								*	*
1-Jul-95	*	*	*	*					
1-Aug-97			*	*					
1-Jan-98								*	*
1-Jul-00		*						*	*
1-Sep-00	*		*	*	*	*	*		
1-May-01			*						
1-Dec-01			*	*					

1-May-04								*	*
1-Jun-04	*	*	*	*	*	*	*		
30-Jun-04	*	*	*	*	*	*	*	*	*
27-Apr-05			*	*					
7-Jun-05								*	*
12-Feb-06									*
12-Mar-06								*	
1-May-06	*	*	*	*					
1-Jun-06					*	*	*	*	*
14-Nov-06								*	*
31-Dec-06	*	*	*	*	*	*	*	*	*
25-Apr-07					*	*	*		
8-Jun-07					*	*	*		
11-Sep-07					*	*	*		
11-Nov-07	*	*	*	*				*	*
15-Nov-07					*	*	*		
1-Mar-08					*	*	*		
1-Jun-08	*	*	*	*				*	*
31-Dec-08	*	*	*	*	*	*	*	*	*
7-Feb-09					*	*	*		
1-Apr-09								*	*
14-Apr-09					*	*	*		
1-Jun-09	*		*	*					
23-Jun-09					*	*	*		
1-Aug-09		*			*	*	*		
31-Dec-09	*	*	*	*	*	*	*	*	*

3.3 Wave Data

Within the wave characteristic, the available information for the Catalan marine region can be divided in two categories: 1) simulated data and 2) instrumental information.

In our study, the effects of refraction were considered. Unpublished shallow submarine maps to 1: 5 000 scale with 1 m contours interval from the Instituto de Ciencias del Mar, Barcelona, have demonstrate that the hilly headland relief surrounding pocket beaches may not persist underwater i.e. no submarine embaymentization may be demonstrated in front of some pocket beaches (J.Guillen 2009). Base in this assumption that the contour lines were parallel to the coastline; we determine the nearshore wave condition using the Snell's law to propagate the offshore wave data across the shelf and over the shallow water.

Four wave data nodes have been selected from the hindcast data set and three wave buoys from the instrumental information. This data provide sufficient spatial and temporal variation along the study beaches; this information can help us to characterize the forcing factors that control the morphodynamics processes in a specific area.

3.3.1 Data Type

3.3.1.1 Simulated Data (1958- 2001): HIPOCAS-SIMAR-44 data set

The SIMAR-44 data set was generating by a temporal series of atmospheric and oceanographic parameters from a numerical simulations from 1958 to 2001.

This data set was created from a high-numerical model resolution of atmospheric, sea level and waves climate that covers the entire Spanish coastal environment. The Spanish Port Authorities under the supervision of the European Project HIPOCAS performed the simulation of the Mediterranean coast (3 hourly-simulated data). The objective of this project was to obtain a 44-year hindcast of wind, wave, sea level and current climatology for European waters and coastal seas for application in coastal and environmental decision processes.

Wave parameters were generating using a wave spectral model WAM. Two types of spacing mesh resolution were use, 15x15 for the eastern edge of the mesh and 7.5x7.5 (approx 12.5kmx 12.5km) for the rest of the domain. There has been a decomposition of wind waves and swell waves, in order to describe situations were both seas state take place. The WAN model includes refraction and shoaling effects but because of the resolution of the grid, these effects are only considered in a large scale.

As mention before only four nodes from the SIMAR-44 data set will be use, the location of the wave data nodes are show in the figure 7, the description of the nodes and the corresponding beach to which data applied are presented in table 5.

Table 5. Description of nodes and the beach affected by the wave data				
Node	SIMAR-44 Description	Longitude E	Latitude N	Beach affected
1	2073054	41.750	3.125	Sant Pol
2	2071053	41.625	2.875	Canyelles Lloret del Mar Fenals
3	2067051	41.375	2.375	Bogatell Nova Icaria Barceloneta
4	2056048	41.000	1.000	Playa Larga Salou

3.3.1.2 Instrumental Information (2001 to 2007): XIOM Wave Buoy

The buoys are part of the Xarxa d' Instrumentacio Oceanografica I Meteorologica (XIOM) that belongs to the Generalitat de Catalunya.

The scalar buoys have a spherical form with a diameter of 70 cm. The buoys measure the vertical acceleration of the ocean surface along the wave. These accelerations are two times integrated in order to obtain the elevation of the ocean surface.

Then data are transmitted to a coastal station. The analogical signal then is converted to a digital signal and analyze. Normally, the scalar buoys determine the wave frequency spectrum associated to a certain time interval (e.g. 20 to 30 min), then is reproduced to a certain number of hours (e.g. 2 or 3 hours). The scalar buoys only manage real time data.

In the case of the directional buoys, these produce two types of information: real time and spectral data. The real time data consists in measurements taken 1/1.28s. From these data the receptor builds the time series of wave height and period that are used to make the statistical analysis. The spectral data are fast Fourier transformations (FFT) of 8 series of 256 consecutive measurements (Mendoza Ponce, 2008).

Table 6. Description of wave buoys and the beach affected by the wave data

Name	Type	Depth (m)	Longitude E	Latitude N	Beach affected
Tordera	Scalar	74	2 48.93	41 38.81	Sant Pol Canyelles Lloret del Mar Fenals
Llobregat	Scalar Directional from 2004	45	2 08.48	41 16.69	Bogatell Nova Icaria Barceloneta Playa Larga
Tortosa	Directional	60	00 58.89	40 43.29	Salou



Figure 7 Location of wave data nodes and wave buoys.

3.4 Beach site description

Due to the spatial and temporal variation of the study site, a method of beach classification was required to identify geomorphologic characteristics of the study beaches. The following characteristics were used to initially classify beach systems, each parameter correspond to an average value.

- Beach length (L)
- Beach orientation (θ)
- Headland characteristics (Hdl)

The parameters were calculated from the historical shorelines. The Autodesk Land Development 2004, were use to geo-referencing and digitalize the coastline. The beach length corresponds to an average value of the length of the embayment beach, the beach orientation correspond to the orientation of the linear distance between the edges of the embayment beach relative to the north. The headland characteristics correspond to the length of both of the headland of beach and other features that can affect the wave climate approaching the beach.

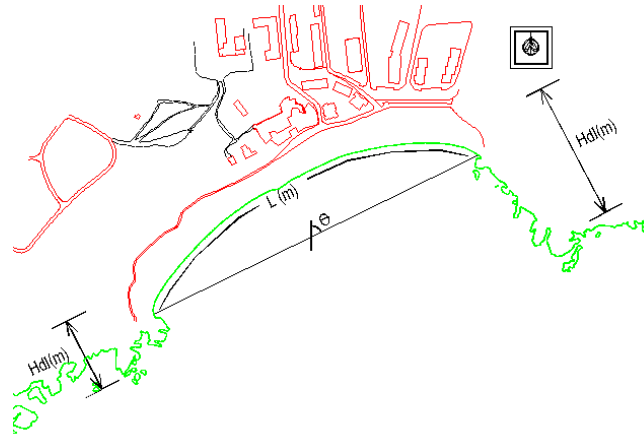


Figure 8 Schematic of the beach classification parameters used.

In this subsection a characterization of the wave climate affecting the study area is presented. For the analysis the SIMAR-44 data base has been used, since some of the buoys are scalar and lack the information of wave direction which is one of the main components when characterizing the waves and its morphodynamics effects. Finally a description of the wave data that will be used in each beach is presented.

3.4.1 Beach geomorphology

The following section provides a summary of the geomorphologic characteristics of each beach. Figure 12 illustrate the respective average beach length and beach orientation of each beach from north to south. The location of each beach is show in figure 6.

I- Girona Province: Sant Pol, Canyelles, Lloret del Mar and Fenals

The following beaches are located in the north part of the Catalan coast in the province of Girona which corresponds to the Costa Brava. This region is characterized by a rocky coast not that steep as the cliff coasts and normally lowers than 20m. Therefore, the beaches are relative short and limited by headland in a form of bay-beaches usually compose by coarse material.

The northern beach of the study is Sant Pol, which corresponded to a medium pocket beach (869 m) with headlands barriers at each end. Approximately the north headland has a length of 500 meters and the south headland of about 630 meters, both headlands extended perpendicular to the shoreline into the sea. The orientation of the beach is 73° relative to the north.

About 17 kilometers to the south is located Canyelles. Canyelles is a small beach with a length of 434 meters, with headland at each ends. This beach is confine between the north headland and a marina located in the

south part of the beach. Both headlands have a length of approximately 300 meters and there are not oriented perpendiculars to the shoreline. Due to this, the beach is oriented 102° relative to the north.

Situated 2 kilometers from Canyelles, we have Lloret del Mar. This beach is different from the previous ones because the headland in the north part is very small almost insignificant, so there is no obstacle that can cause a diffraction pattern and create a well define curvature shape in the north part, in the other hand the headland in the south part has a length of 400 meters and help to maintain the sand inside this area. Therefore, Lloret del Mar will be treated as a linear configuration. The beach as a length of 1110 meters and is oriented 64° relative to the north.

Next to Lloret del Mar we found Fenals, with headlands at the each end of the beach. Fenals is a medium pocket beach with a length 731 meters. The north headlands, that corresponded to the south headland of Lloret del Mar has a length of approximately 400 meters. The beach is also oriented 64° relative to the north. The medium grain size ranges between 0.38 mm at Sant Pol, 1.16mm at Canyelles, 1.46mm at Lloret del Mar and 1.41mm at Fenals.

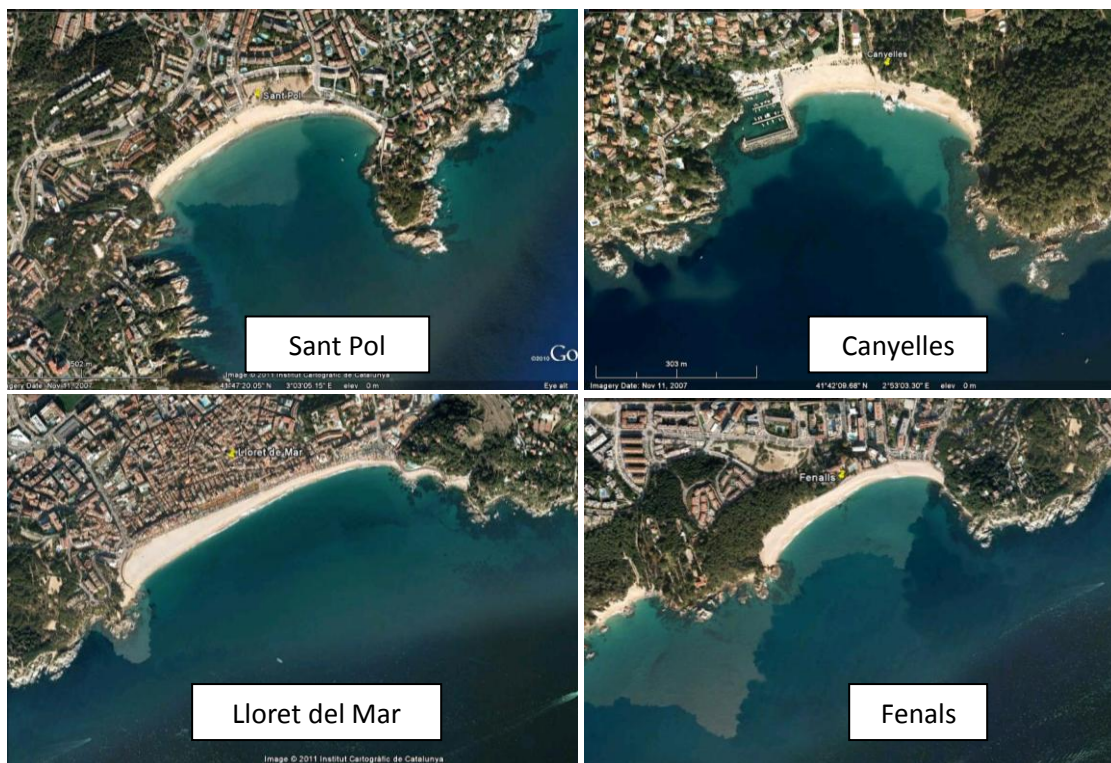


Figure 9 Aerial photographs from Google Earth 2007.

II- Barcelona Province: Bogatell, Nova Icaria and Barceloneta

These three beaches are located in the center part of the Catalonian coast in the Barcelona province, in the Barcelona city area. The beaches were created as part of the renewal plan that took place in the zone for the 1992 Olympic Games. Before this time the beach was a long beach without any disturbance. Now days, the beaches correspond to a symbol of the city (J. Guillen, 2008). The medium grain size ranges between 0.47 mm at Bogatell, 0.46mm at Nova Icaria and 0.27mm at the north section and 0.66mm at the south section of Barceloneta.

The northern beach correspond to Bogatell, this is a medium barred beach with a length of about 600 meters. This beach is enclosed by two double dikes that extend perpendicular to the shoreline. The beach has an orientation of 40° relative to the north. Next to this beach, we found Nova Icaria this is a small beach with a length of approximately 400 meters, is separated in the north from Bogatell by a double dike and also protected by two submerge breakwaters, the longest of which extend at the tip of the dike; in the south neighbor with the Olympic Marina. Nova Icaria is oriented 46° relative to the north.

Moving south of the Olympic Marina is Barceloneta beach; this is bounded by the Barcelona Harbor in the south and the Somorrostro dyke in the north. The beach has a length of 1.3 kilometers and has an orientation of 19° relative to the north. It was considered a barred beach before 2006, where the construction of the submerge breakwater took place.

After 2006 the beach change it configuration and instead of one long beach, two beaches appear. The northern section has a length of 465m with an orientation of 22° relative to the north. The southern section was a length of 924 m with an orientation of 14° relative to the north.



Figure 10 Aerial photographs from Google Earth 2006 and 2010.

III- Tarragona Province: Playa Larga and Salou.

This two last study beaches are located in the south part of the Catalan coast in the Tarragona province, known as Costa Daurada. These areas are basically composed by long open beaches characterized by having an almost straight coastline being usually associated to low-lying coast. The dominant beach is mild slopes one with fine material. In this specific area the shoreline is NW-SE oriented.

The northeastern beach corresponded to Playa Larga, is a medium beach with a length of 640 meters. With headlands at both ends of the beach, the east headland corresponded to a last part of the Cape Salou; so is a small headland of about 100 meters. The west headland corresponded to a small outcrop of rock of about 300m. The beach is oriented 116° relative to the north.

Around 700 meters southeast is located Salou; this beach is a long beach of about 1.2 kilometers. It has one headland in the east part of about 150 meters, and in the west side neighbor with the Port of Salou. The beach is oriented 109° relative to the north. The medium grain size ranges between 0.21mm at Playa Larga and 0.22mm at Salou.



Figure 11 Aerial photographs from Google Earth 2006.

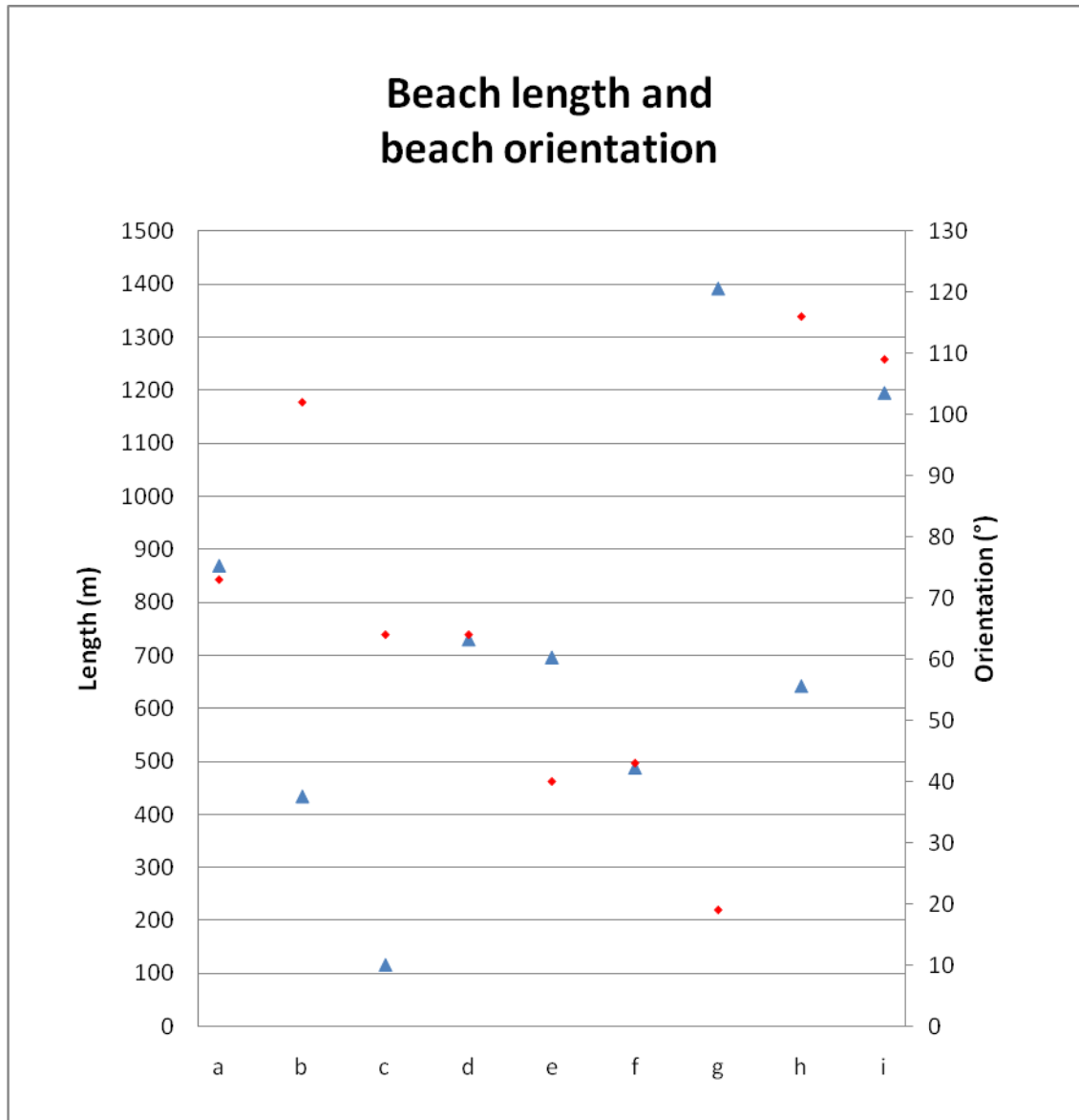


Figure 12 Average beach length (blue triangles) and beach orientation (red dots) for all beaches. The x-labels are discussed in section 3.1.

3.4.2 Wave climate description

In this subsection we characterize the wave climate that affects each beach. For the analysis we will use the HIPOCAS SIMAR-44 data base, four nodes have been used for the analysis. Table 5 shows the description of the nodes and the corresponding beach to which data applied. Node 1 represent the wave condition for the Sant Pol beach; node 2 represent the condition for Canyelles, Fenals and Lloret del Mar; node 3 correspond to the wave condition for the Barcelona city beaches and node 4 correspond to the beaches of Playa Larga and Salou.

Directional Distribution

Wave direction is one of the principal variables when characterizing the forcing factors that act in the coast in terms of morphodynamics. The following rose diagrams illustrate the wave height and the directional distribution for the entire data set of the four nodes used in our study. The numbers on the circumference of each panel represented a percentage of waves with a certain height identified by the color of the label; the rose diagram is divided into 16 directions centered in the north. The WindrosePro of Enviroware was use to generate the rose diagrams.

From the figures it is clear that there is high variation in the directional distribution of the waves from north to south. The first node is characterized by a bidirectional configuration, since is clearly dominated by the NNE component and SSW component.

This bidirectional distribution become less significant in the second and third nodes, we observed that for these two nodes the dominant component is the SSW, and the second dominant component change from NE to ENE. So we obtain a more homogenous distribution.

For the fourth node we observed that the waves coming from NE practically disappear, due to the orientation of the coastline. In this distribution the dominant component is the S, and the second dominant component is the ESE. But we also observed waves emerging from the NW component this is due to the action of the local Mistral which is created inland (Mendoza Ponce, 2008).

In terms of Hs for the all the nodes the highest values come from the E, only the node 1 experience also highest values from the ENE.

Wave Height and Peak Period

From the available data we determine the maximum value of wave height and wave period for the study nodes. From this we observe that the maximum value of wave height correspond to the node 1 with a value of 8.15m, moving south to the nodes 2 and 3 the wave height decreases about 7.57 m and 7.64m correspondently. Finally the node 4 presents the lowest value of about 5.62m.

Differently from the H_s , the period (T_p) is lower at the northern part and higher in the southern part of the study area. Nodes 1 and 2 present a T_p of 13.5s, the node 3 of 14.9 s and node 4 16.3s. However, if the average values are of T_p are analyze instead of the maximum values the northern node is the one with the longest period (5.2s) while moving to the south the average period decrease until reach 4.5s in the node 4.

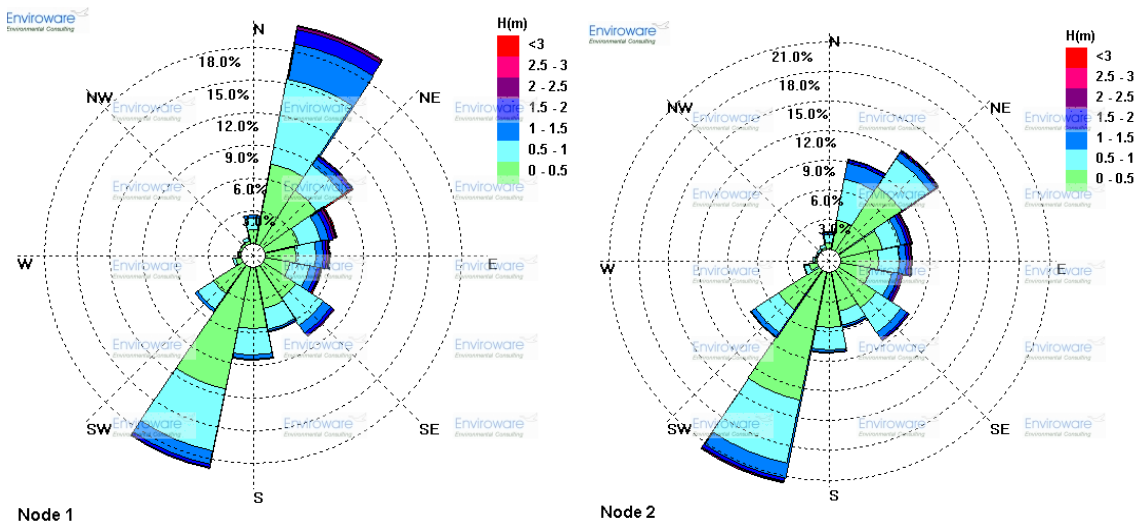


Figure 13 Wave rose with direction from the nodes 1 and 2 from 1957-2001.

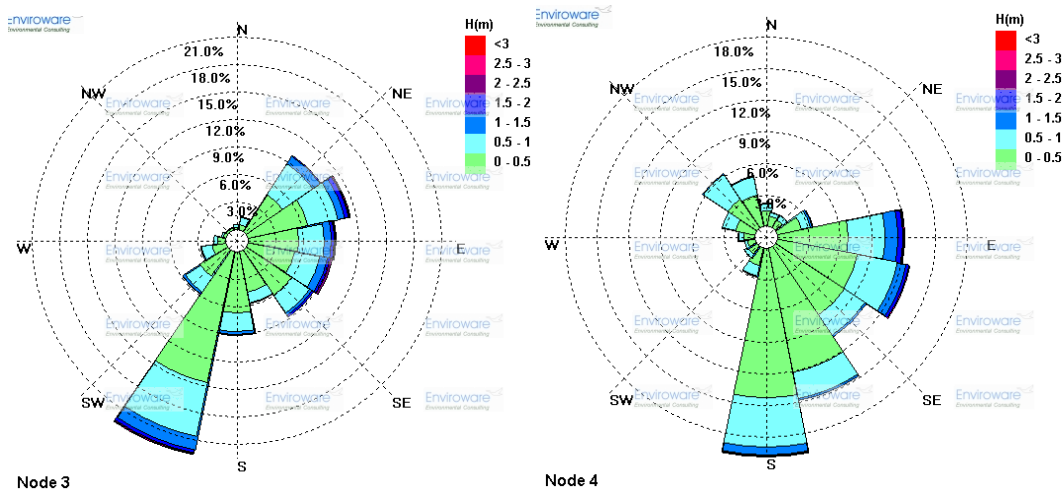


Figure 14 Wave rose with direction from the nodes 3 and 4 from 1957-2001.

3.4.3 Wave Data Selection

As we mention before the influence of the wave climate on open coastlines is an important parameter that can affect the behavior of the coastline. In order, to determine the factors that contribute the shoreline evolution we need to determine which data we will use, since the effect of the headlands along the coast provide sheltering to embayed beaches, as a result, inshore wave condition can be less energetic and the directional characteristic can change significantly from the offshore wave.

Base on the hypothesis of the static equilibrium configuration propose by Hsu 1989 (parabolic bay shape), we need to determine a window with the maximum un-diffracted energy, based on the directional distribution. Due to this, we need to eliminate the directions that would not affect the morphodynamics of the beach. For example the direction parallel to the coastline, and the ones that are attenuated by a costal feature.

Therefore, for each data set a window of direction as been established. The best approach is to evaluate the direction by the angle of the incoming wave. This way only the real direction that affects the embayed beach will be taking into account in the analysis. The next table shows the established region of direction for each beach.

Table 7 Wave data selection	
Beach	Effective Range of Direction *
Sant Pol	E-SW
Canyelles	SSE-WSW
Lloret del Mar Fenals	E-SW
Bogatell Nova Icaria Barceloneta	NE-SSW
Playa Larga Salou	SE-WSW

*Relative to the north.

From the table, the effective range of direction for Sant Pol corresponded to waves approaching the coastline from an angle between E to SW sector (78.75° and 236.25° relative to the north). This range has been chosen because the coastline is oriented NE-SW.

Due to the orientation of Canyelles, the range of direction that could affect the beach corresponded to the SSE to the WSW sector (146.25° to 258.75°). For Lloret del Mar and Fenals, the range that will be evaluated corresponded to the E to the SW sectors (78.75° and 236.25° relative to the north), since in this area the coastline is again oriented NE-SW.

For the Barcelona City Beaches the window with maxima un-diffracted energy, will be define between the NE and the SSW sectors (22.5° and 213.75° relative to the north). And finally, for Playa Larga and Salou range that will be evaluated is between SE and the WSW sectors (123.75° to 258.75°), in this area the coastline is NW-SE orientated.

4. Shoreline Evolution

An embayed beach is defined as a coastal feature that has one or two natural or artificial barriers at either extremity (headlands), which cast a degree of curvature on the beach platform (Harley, M. 2009). Most of the studies of embayed beaches have been focused on the determination of the equilibrium curve (e.g. Silvester, 1970; Hsu 1989) but only a few of the studies have investigated the short to medium-term morphodynamics of these coastal features (e.g. Ojeda and Guillen, 2008).

The embayed beaches differ from straight open coast beach in the limited alongshore sediment that is confined inside the boundaries of the embayment. The varying amount of wave exposure within the embayment can also lead to a highly alongshore non-uniform beach response (Harley, M. 2009). For example, in a highly curved beach, there is a well-developed shadow zone and a range of morphodynamics conditions, from sheltered low-energy beach adjacent to the diffraction point to a high-energy exposed beach on the straight end of the beach. However, in a less curved beach we observe a more uniform behavior since they are directly exposed to incident waves (Klein, A.H.F., Menezes, J.T., 2001).

The micro-tidal environment of the Catalan Coast is characterized by a series of embayed beaches; the moderate to high energy easterly wave condition will dominate the wave climate of the NE-SW facing coast, resulting in a nearshore wave gradient along the beach, ranging from sheltering conditions at the northern end and exposed conditions at the southern end.

Few survey programs have been conducted on the embayment beaches of Catalonia, the most important one has been located in the Barcelona city beaches, this survey program consisted in obtaining the shoreline position of three beaches (Bogatell, Nova Icaria and Barceloneta) by means of an Argus video system from November 2001 to December 2004. The study was based on storm conditions, and over this period they found that the artificial beaches of Barcelona present a beach mobility of similar magnitude to that of natural embayed beaches (Ojeda and Guillen, 2008), and that the maximum beach mobility occurs at the ends of the beach.

Studying the shoreline evolution of the embayed beaches is important since coastal zone managers are always targeted with the problem of quantifying the erosion for sandy beach environments to determine setback lines for developing future infrastructure (Wood, 2010). Knowing how the shoreline adapts to different conditions is required in order to avoid jeopardizing the safety of the existing structures or the new ones that would be implemented (Hsu, 2009).

The aim of this chapter is to analyze the shoreline evolution of nine sandy beaches along the Catalan coast. In order to determine the variations from coastal section to coastal section, as mentioned before (Chapter 3) we will work in a middle term scale (time scale: year to decades, space scale: 1 to 5 km) based on historical coastline

from existing chart and orthophotos maps. This chapter is divided into 4 sections. Following this introduction is a description of the data processing and the applied methods. Section 4.2 shows the results of beach platform analysis, beach mobility and beach area over the study period of each beach. And the final sections present the discussion and the summary.

4.1 Methodology

4.1.1 Beach Platform Analysis

In order to study the beach platform variation of the Catalan coast, several parameters have been defined. The beach platform analysis consisted in study the stability state of the beaches through the study period, the parameters used follow the parabolic bay shape propose by Hsu in 1989. It has been prove that this approach is a good representation of the morphological process within an embayment.

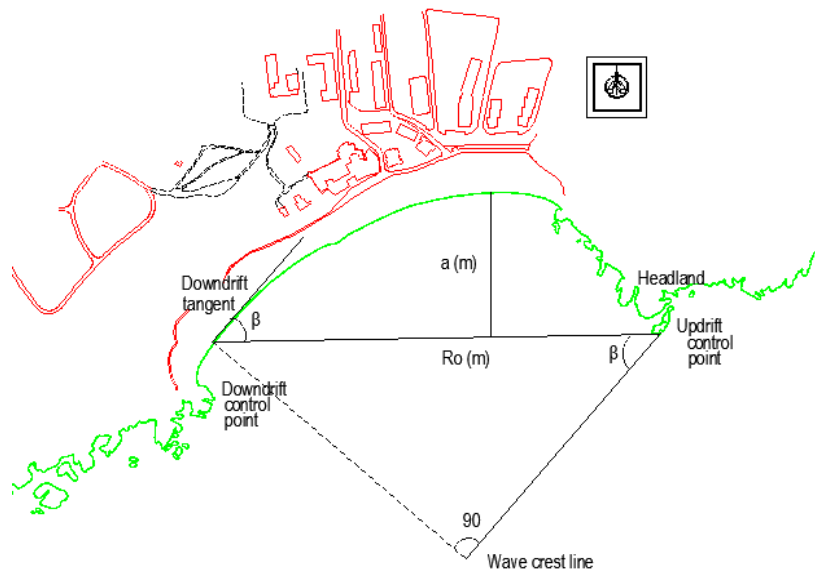


Figure 15 Schematization of the used parameters, Fenals beach.

In the definition sketch are two main parameters, β and R_o . The first is known as wave obliquity, or the angle between the incident wave crest (assumed linear) at the wave diffraction point and the control line, joining the updrift diffraction point to the near straight downdrift beach.

The second parameter is the control line (R_o) which is also angle β to the tangent at the same downdrift beach point. Other parameter that we would use to identify the stability of the beach is the indentation value (a) this is the perpendicular distance between the control line and the shoreline.

By using the equation in the form of second order polynomial (See section 2.1.2) we would obtain the static equilibrium platform of a beach, and determine if the shoreline is in static condition or not, however this manual application can be repetitive and laborious. So an alternative method to determine if a beach platform is in a dynamic, stable or unstable condition is applied.

This method is know as the indentation ratio a/R_o . This ratio has been correlated with β by Hsu 1989 for model test and prototype bays. If the point fall below the line the bay is unstable, indicating that could indented back to the values so presented. If fall above the line the beach is in dynamic condition, which means that there is a continuous supply of sediment and if this supply is reduce the embayment could degrade.

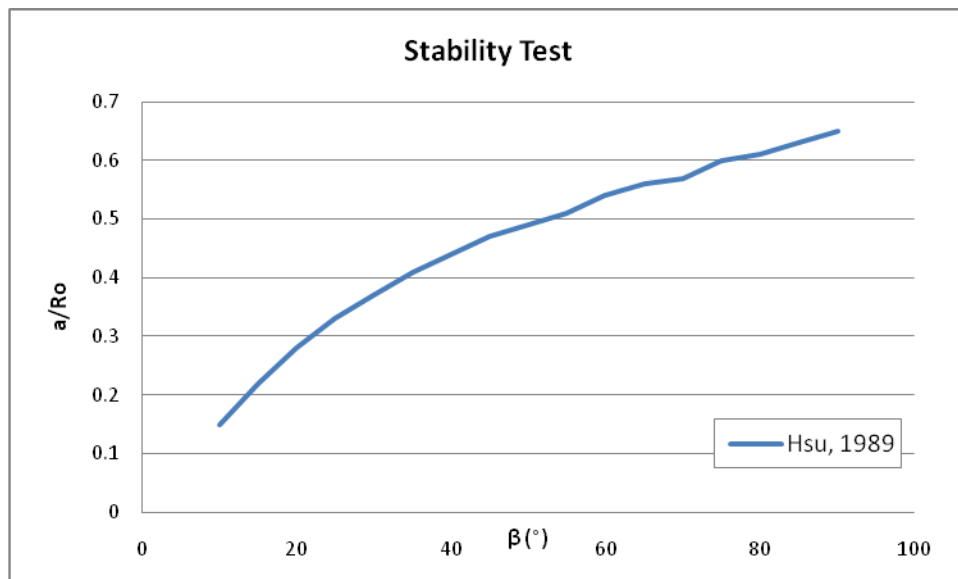


Figure 16 Indentation ratio a/R_o and β , Hsu 1989.

This parameter can also be associated with the curved platform of the embayment and the effects of headland impact on it. In the study of Santa Caterina beaches in Brazil, Klein et al.,2009 has suggest that beaches with indentation ratio (a/R_o around 0.20) have less curvature, therefore they experienced less headland impact on profile beach mobility, they had a small poorly define shadow zone, and the beach volume changes along the

beach will be more uniform. On the other hand, beaches with values of indentation in the order of 0.39 to 0.40 are highly curve, and experience greater headland influence on profile mobility and had a well define shadow zone.

4.1.2 Beach Mobility

To quantify shoreline variability of the study areas, we would study a particular form know as “beach mobility”, which was defined as a standard deviation of the shoreline relative to its linear trend (Dolan et. al, 1978 cited by M.J.F. Stive et. al,2002). It has been suggested that this is a function of the morphodynamics state of a beach (Short and Hesp, 1982 cited by M.J.F. Stive et. al, 2002): dissipative, intermediate and reflective and correspond to low-moderate, moderate-high and low beach mobility, respectively.

The shoreline was studied using a number of control lines along each beach, the number will depend on the length of the beach, with a minimum of five to a maximum of nine control lines. The control lines corresponded to perpendicular lines to the reference shoreline, in order to avoid the error induce by the curvature. The distance between controls locations vary from each beach.

Within this control lines we measure the sub-aerial beach width. Beach width was defined as the distance between the MSL and a landward point (i.e. line of building, promenade or line of vegetation). Beach erosion and accretion was described in terms of normalized sub-aerial beach width (measured width subtracted of the respective mean width of the data set). For the present study beach mobility is defined as the standard deviation of beach width at different control points.

The following figures show the control lines for the study beaches.

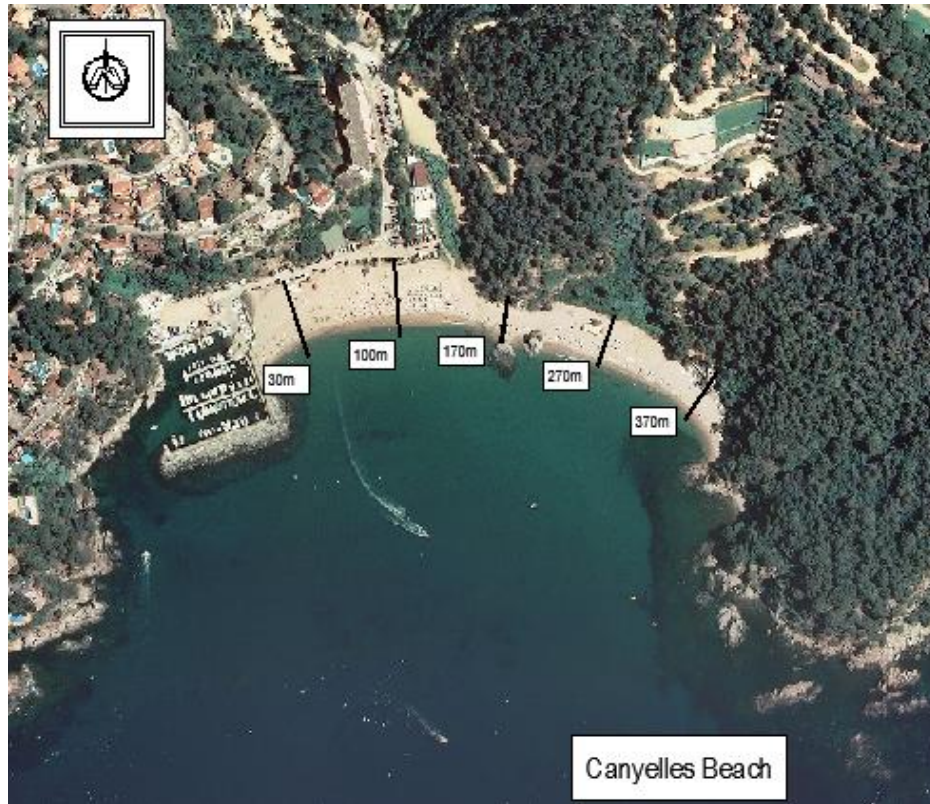




Figure 17 Distance along the Girona beaches, as define by the length of the southern end along the embayment platform. (Photo: Ortophotos 2008, ICC).





Figure 18 Distance along the Barcelona City beaches, as define by the length of the southern end along the embayment platform. (Photo: Ortophotos 2006 and 2008, ICC).

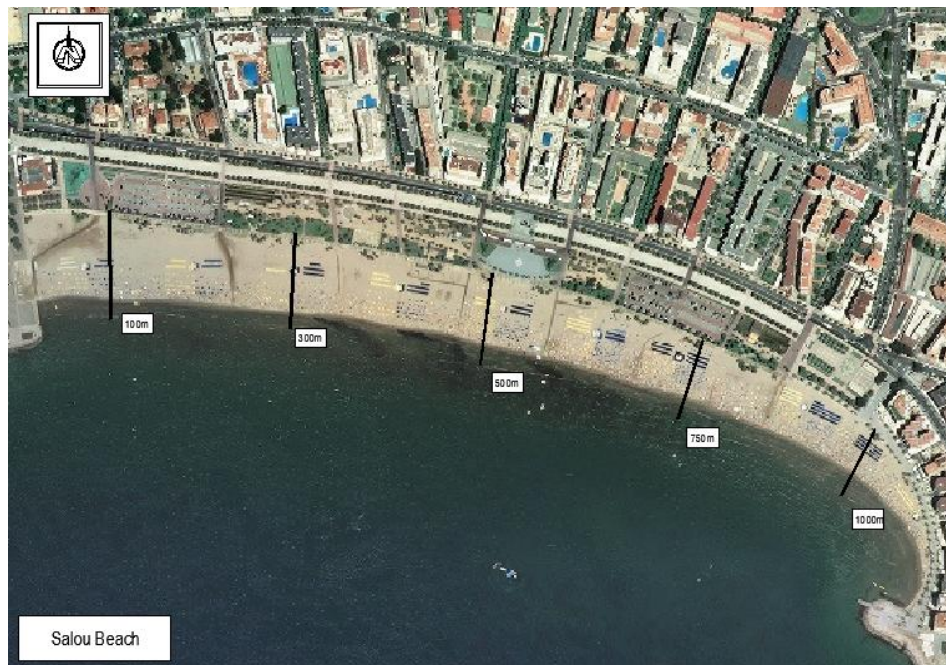
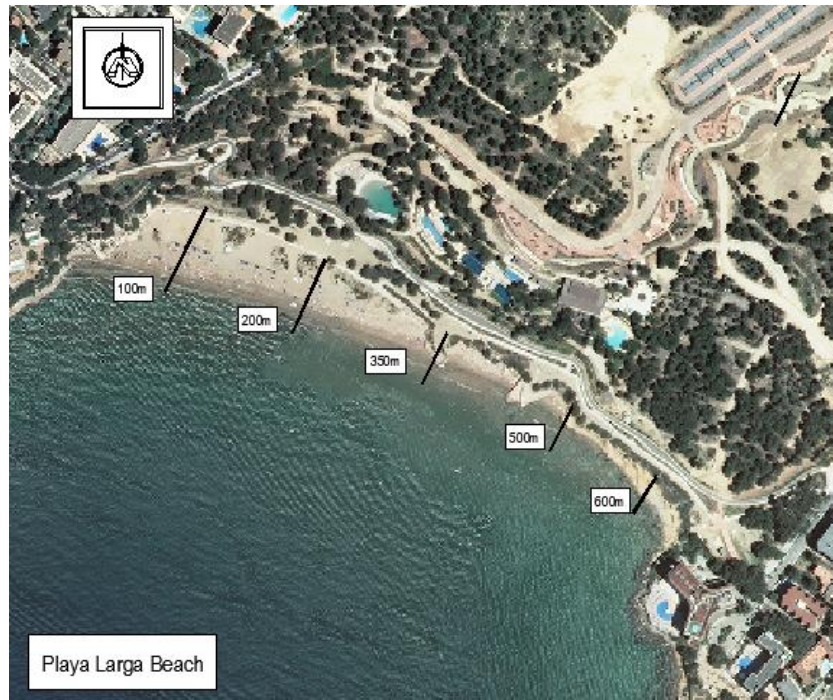


Figure 19 Distance along the Tarragona beaches, as define by the length of the southern end along the embayment platform. (Photo: Ortophotos 2008, ICC).

4.1.3 Sub-Aerial Beach Area

The total sub-aerial beach area for the entire embayment was calculated for each shoreline. Beach area was defined as the area bounded by the MWL and the hard structures in the back and lateral part of the beaches. Time series of the beach area give an initial estimation of the trends of each beach during the study period.

4.2. Results

4.2.1 Beach Platform Analysis

The data used is organized from north to south, divided by provinces: Girona, Barcelona and Tarragona. The following tables show the results of the indentation ratio for the different beaches through the study period. The figures presented show the behavior of the beach in term of stability following the criteria of Hsu, 1989.

Since Lloret del Mar have a liner configuration the following analysis could not be apply to the beach platform.

Girona Beaches

The Girona beaches presented a wide range of indentation (see table 8). The beaches are considered moderate to highly indented with values around 0.3 to 0.70. The more indented beaches are San Pol and Fenals with a value of 0.42 and 0.70 correspondently; this implies that the beach could be characterized by a moderate to highly curved platform. On the other hand, Canyelles is considered moderate indented beach ($a/R_o = 0.30$). This value corresponds to beaches that experience less to moderate headland impact on beach mobility, therefore have a less curve platform.

Table 8 Mean values of a/R_o , Girona	
Beach	a/R_o
Sant Pol	0.42
Canyelles	0.30
Fenals	0.71

The result from the stability test suggest that the a/R_o criteria of Sant Pol and Canyelles fall below the stability curved of Hsu, indicated that they are in unstable condition. However, Fenals fall above the stability curve showed in figure 20; the beach shoreline is seaward of its static equilibrium criteria of Hsu.

From the figure 20 it is clear that Sant Pol and Canyelles presented a similar trend, while Fenalls presented a different behavior. Since the curve of Hsu has been determine for a specific set on data, it is possible that for the Girona beaches the stability curve do not follow the same behavior that the stability curve of Hsu and presented a different trend. Therefore, it is possible that the beaches are in a stable condition.

Base on these results and the observation of the aerial photographs, Sant Pol and Fenalls are moderate to highly curve beaches. While Canyelles corresponded to a less curve beach, since is a well protected beach due to its orientation. The beach does not experience the impact of waves coming from highly energetic direction (E) and only the waves from less energetic direction affect it(SE and S). For the highly curve beaches greater difference along the beach width is expected, since the expose strait part of the beach presented larger breaker height than the shelter part.

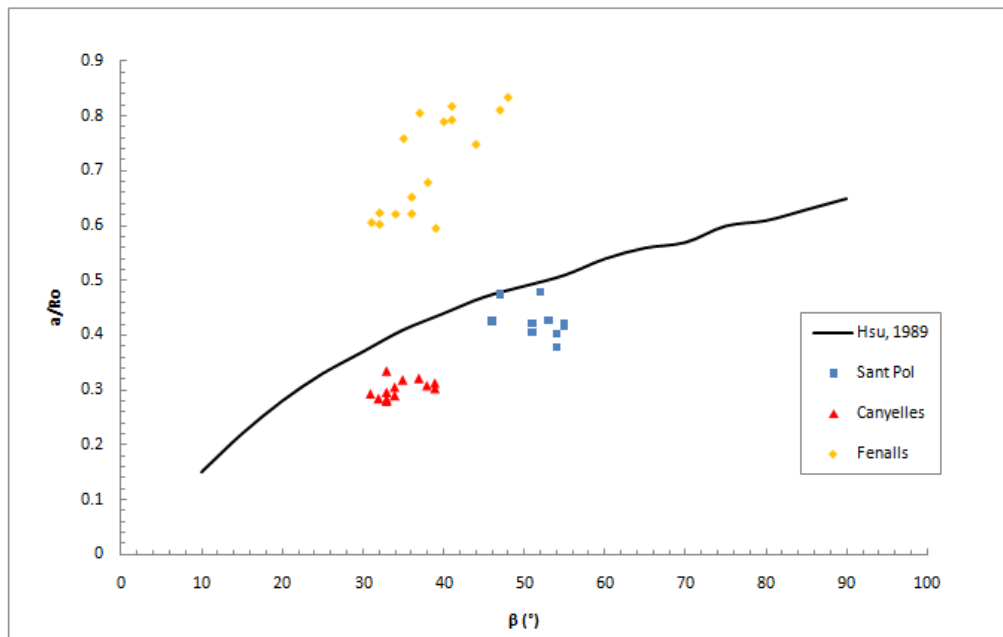


Figure 20 Stability test Girona beaches.

Barcelona City Beaches

Barcelona city beaches, also present a wide range of variation. Bogatell and Nova Icaria are considered the more indented with values of 0.40 and 0.53.

Barceloneta will be evaluated before and after the construction of the offshore breakwater (2006), because the shoreline has a different behavior due to the new structure. Table 9 shows the result of the analysis. Before the construction of the offshore breakwater the beach was considered a less indented with a value of 0.26. After the construction of the offshore breakwater the beach was divided in two sections; a northern section and a southern section. Both sections are considered moderate indented with a value of 0.38 and 0.30, correspondently.

Table 9. Mean values of a/Ro, Barcelona	
Beach	a/Ro
Bogatell	0.40
Nova Icaria	0.53
Barceloneta: Before Offshore Breakwater	0.26
Barceloneta: After Offshore Breakwater North Section	0.38
Barceloneta: After Offshore Breakwater South Section	0.30

In the stability test, all the beaches presented a similar trend. Some of the points of the beaches coincide with the curve described by Hsu (see figure 21). The points of Barceloneta located far away from the curve correspond to the periods where nourishment campaigns were undertaken (e.g. June 2004, Ojeda and Guillen 2008). The behavior of the beaches showed that for this specific area the stability curve corresponded to the trend that the beaches presented, rather than the curve trend that Hsu propose. The coefficients of the parabolic bay shape are not universal and different considerations need to be undertaken in order to fit the curve to the specific conditions of the beach.

We observe that Bogatell and Nova Icaria are consider a highly curve beaches with a well define shadow zone. For Barceloneta we observed that before the construction of the offshore breakwater, the beach was less curve; and after the construction of the breakwater the north section have develop a more curve bay shape, while the south section remain less curve.

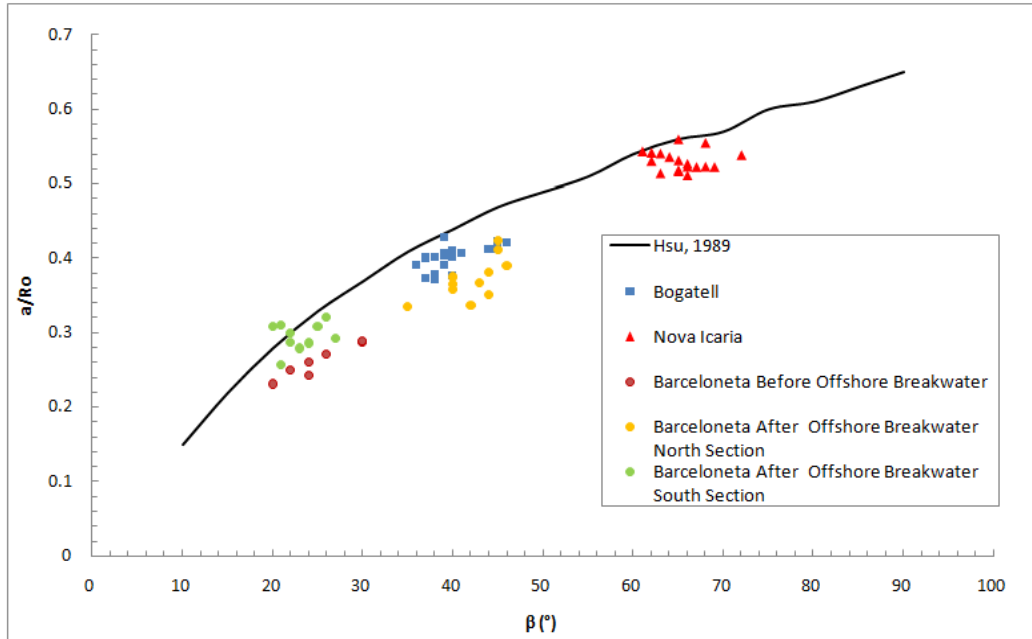


Figure 21 Stability test Barcelona City beaches.

Tarragona's Beaches

Tarragona beaches corresponded to the less indented beaches of the study. Playa Larga presented an indentation ratio of 0.32 (see table 10). The stability test cannot be performed in Salou, since the beach don't follow the requirements proposed by Hsu, in this beach an input of sediment has been observed with the construction of the port, the beach has accumulated sediment at the southern end.

Table 10 Mean values of a/R_o , Tarragona	
Beach	a/R_o
Playa Larga	0.32

Similar to the rest of the study beaches we observed that the values of a/R_o of Playa Larga fall below the stability curve of Hsu (see figure 22). This same behavior has been observed in the previous six beaches. It is possible that the stability curve of the beach is different that the one presented by Hsu, since as mention before the coefficients of the parabolic bay shape are not universal.

Based on the characterization proposed by Klein et al., 2009, the beaches were considered less curved shape, with a small shadow zone, therefore the volume changes along the beach are expected to be more uniform.

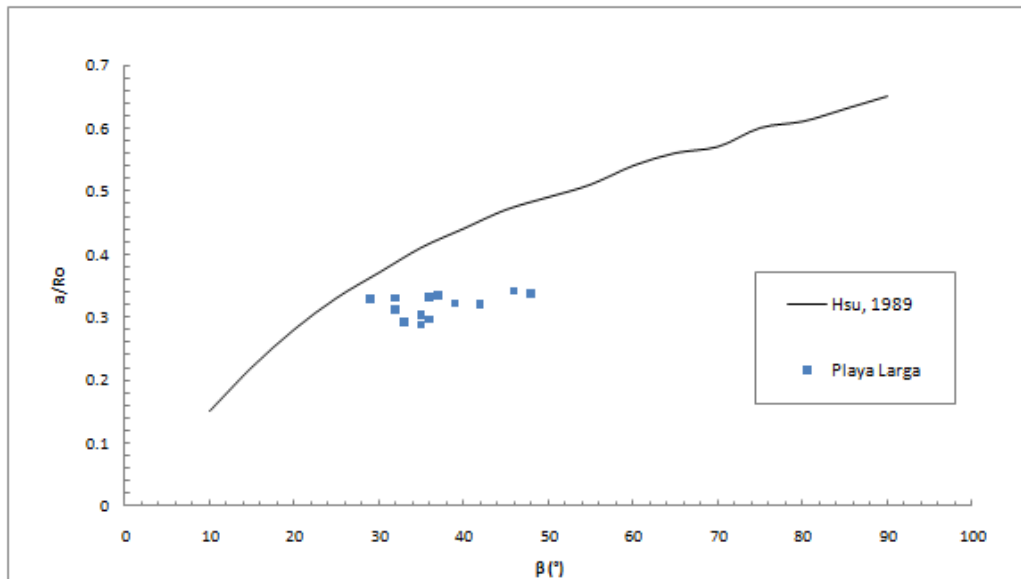


Figure 22 Stability test Tarragona beaches.

4.2.2 Beach Mobility

The following figures show the normalized beach width variation of the three control points considered representative of the different beach sectors. The blue lines (P1) correspond to the location at the southern end, the red lines (P5) correspond to the location at the northern ends and the green lines (P3) correspond to a location in the middle of the embayment. The data has also been divided by provinces.

Girona Beaches

During the study period the beaches of Girona suffered relative large width variations. An out of phase behavior in beach width was observed between the southern and northern end of the beaches; which is logical in a conservative environment where the longshore sediment transport is the primary process.

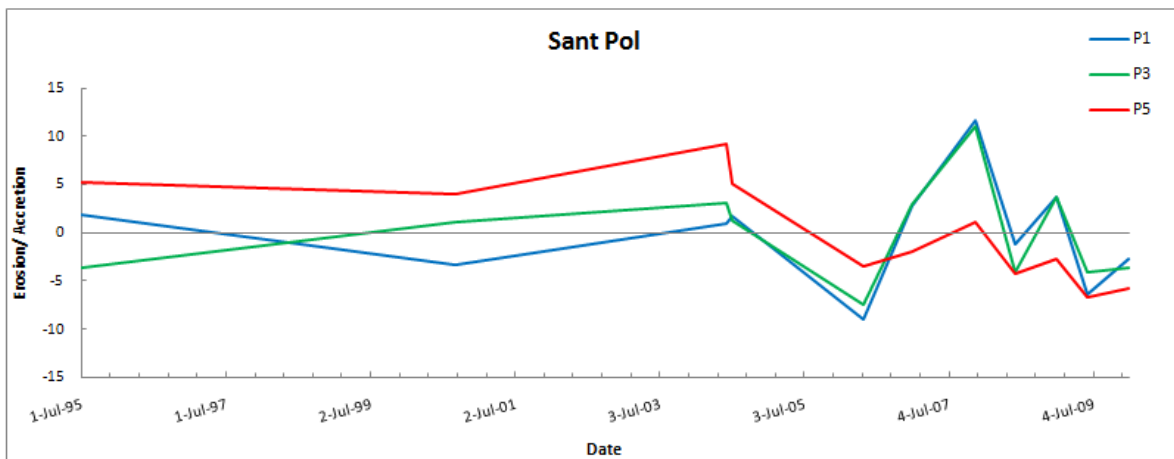
In Sant Pol we observed that the southern end (P1) and the central part (P3) exhibit the largest beach width variation, with changes larger than 12 meters. The northern end (P5) presented a less beach width variation, with changes on the order of 9 meters. The evolution rate of the locations P1, P3 and P5 are 0.1m/yr ($r^2=0.1$), 0.24m/yr ($r^2=0.1$), and -0.74m/yr ($r^2=0.5$), correspondently.

At Canyelles, the variability of the beach width along the shoreline was more homogeneous, the three sectors of the beach presented changes of about 5 meter. In terms of evolution rate; the southern end (P1) shows a rate of -0.36m/yr ($r^2=0.6$), the center part (P3) of -0.55m/yr ($r^2=0.7$) and the northern end (P5) of -0.13m/yr ($r^2=0.1$).

At Lloret del Mar, both ends of the embayment presented high beach mobility, with maximum changes around ± 60 meters. However, the center part also presented significant changes of 20 meter, but they were more uniform along the study period. The evolution rate of the shoreline in the southern end was 1.5m/yr ($r^2=0.2$); the center area presented a lower rate of 0.04 m/yr ($r^2=0.1$) and the northern end of -0.9m/yr ($r^2=0.1$).

In Fenals, the differences in beach mobility are similar in the extremities of the beach. Both ends presented the maximum changes of ± 30 meters. The center part presented a more uniform behavior with changes lower than 10 meters. The evolution rate of the locations P1, P3 and P5 were 0.24m/yr ($r^2=0.1$), -0.16 m/yr ($r^2=0.1$) and -0.64m/yr ($r^2=0.1$), respectively.

From the analysis we have observed that the most frequent exposed areas (southern end) presented higher beach variability that those that are less exposed (northern end). This is evident at Sant Pol, the very well define shadow zone at the northern end have less change in beach width. For Lloret del Mar and Fenals, this cannot be assured since the length of the headland does not generate a defined curved platform. Both areas are exposed to wave climate from the South and the East directions; the variability is higher at both ends. For the four beaches, the shoreline evolution rate of the northern part was negative; this implies that a persistent erosion pattern is occurring at these areas.



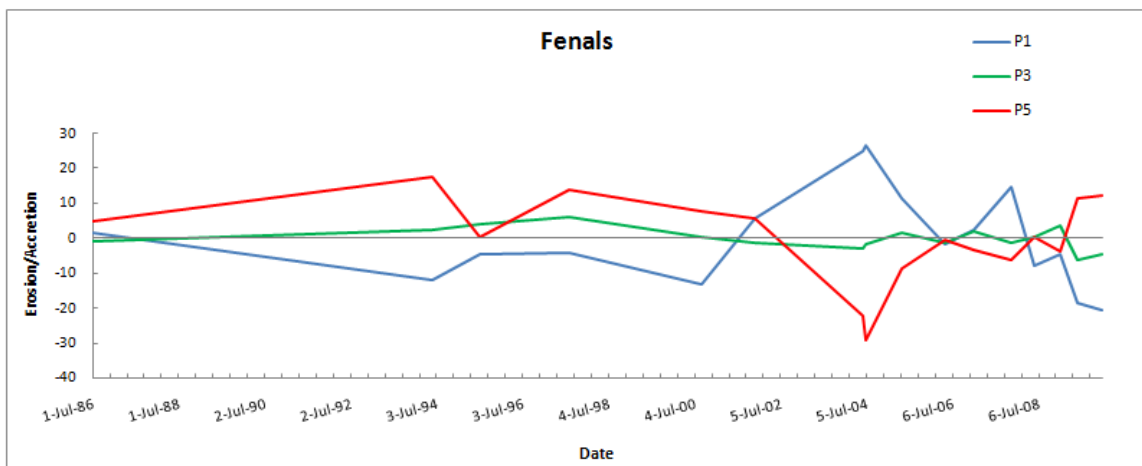
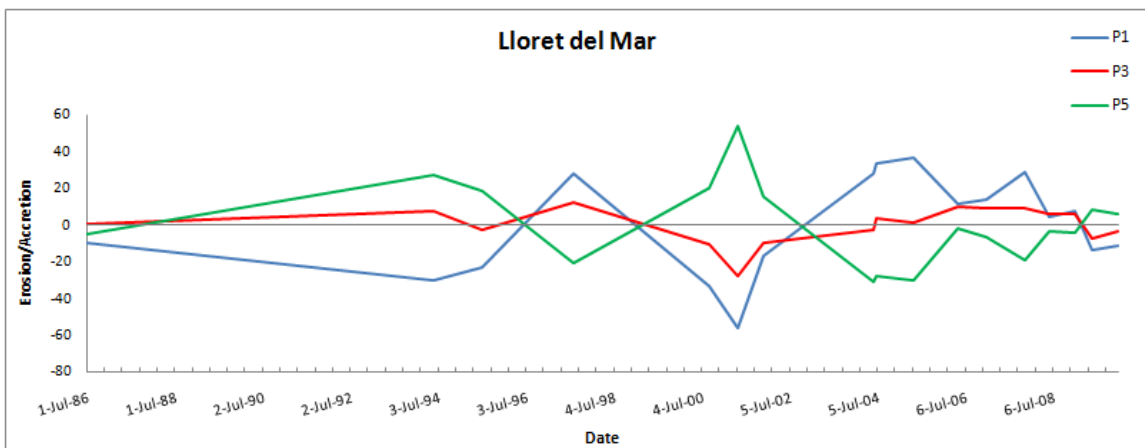
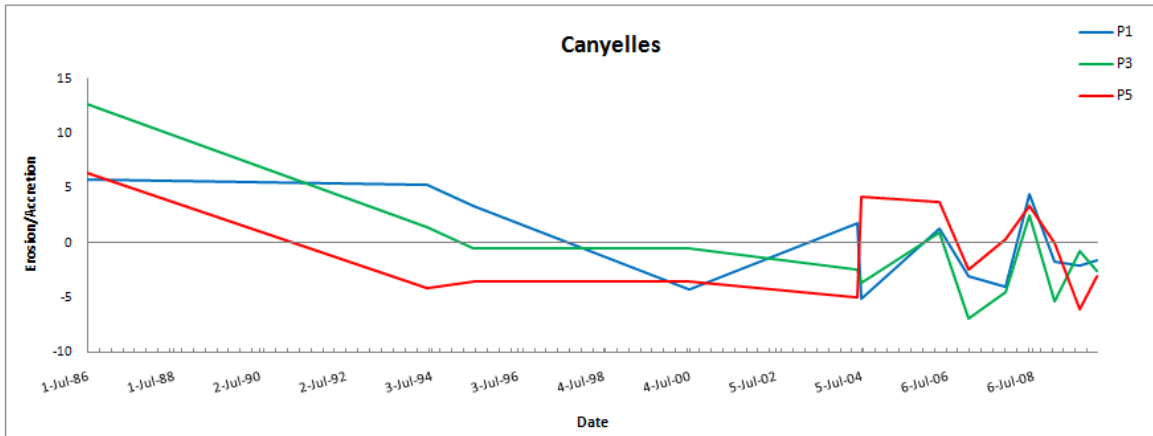


Figure 23 Beach width variation Girona beaches.

Barcelona City Beaches

The largest beach mobility values were found at both ends of la Barceloneta (before 2006), at the northern end of Bogatell and at the southern end of Nova Icaria.

At Bogatell, the northern part (P5) presented a maximum change of 18 m. The southern and central part (P1 and P3) presented values around 10 meters. The evolution rate of the representative sectors were 0.3 m/yr ($r^2=0.1$), -0.42 m/yr ($r^2=0.4$) and -1.14 m/yr ($r^2=0.5$).

Nova Icaria, presented the lower values of beach mobility of the three beaches. The maximum mobility occurs at the southern end (P1) with a seaward displacement of 9 meters. The northern end (P5) presented the lower value of beach mobility around 6 meters. The evolution rate of the beach at the southern end was -0.19 m/yr ($r^2=0.1$), the value at the center was about -0.24 m/yr ($r^2=0.5$) and at the northern end was 0.21 m/yr ($r^2=0.2$). The lower beach mobility at the northern end of Nova Icaria can be associated to the higher protection caused by the defense structures on that side of the beach. This aspect also affected the evolution rate of the beach; the values suggested that the southern and central parts are the ones that experience an erosion trend, while the northern part experienced an accretion trend. This behavior is different from the others, since only a few waves coming from a narrow range of angles can cause a significant retreat.

At Barceloneta, the analysis of beach mobility has been separated in two parts, the first one correspond to the beach before the construction of the offshore breakwater (before 2006) and the second one after its construction (after 2006), where the beach is divided in a northern section and a south section.

Barceloneta before the offshore breakwater presented maximum changes at both ends of 30 meters, while the northern part (P9) advances the southern part retreats (P1). The evolution rates of the beach from 1994 to 2006 were 5.4 m/yr ($r^2=0.9$) for the southern part, -0.6 m/yr ($r^2=0.5$) for the center part (P5) and -2.2 m/yr ($r^2=0.5$) for the northern part.

After the construction of the offshore breakwater, the beach changes its configuration. The shadow effects of the breakwater divided the beach in a small northern section and a medium southern section. In the north section we observed that the width variation were very homogeneous along the beach. The three representative sections (P1, P3 and P5) have a maximum displacement in a seaward direction of about 20 meters.

At the southern section we observed that the south end (P1) presented a maximum retreat of 30 meters. The lower beach mobility occurs at the northern end (P6) with an advance in the shoreline of 20 meter. Since we only have three years of information from this new configuration of the Barceloneta beach, a value of evolution rate could not be generated.

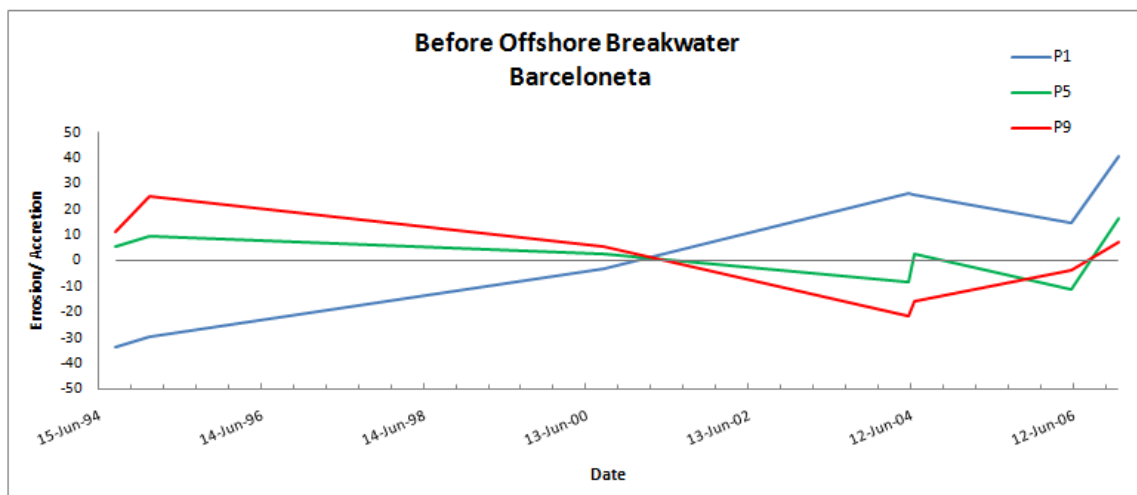
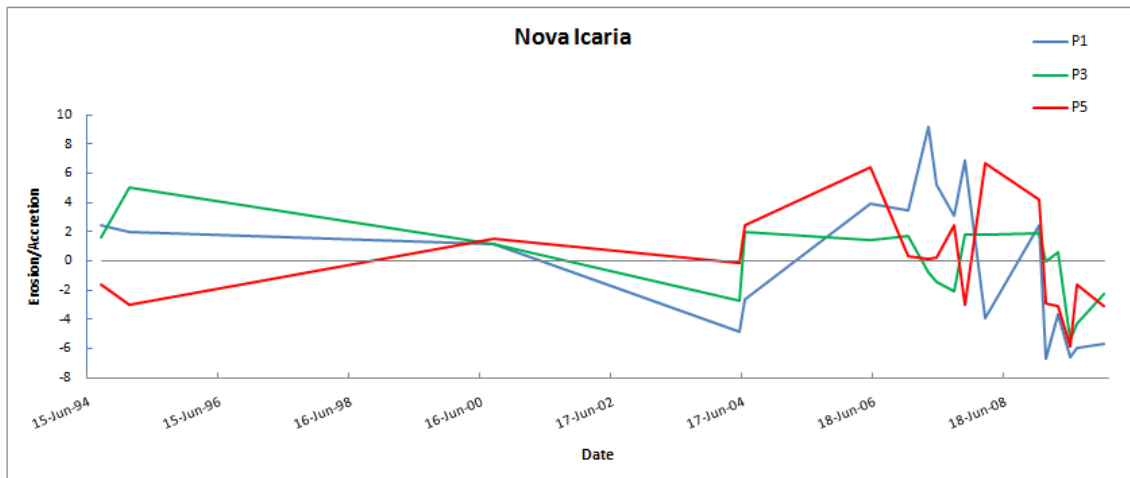
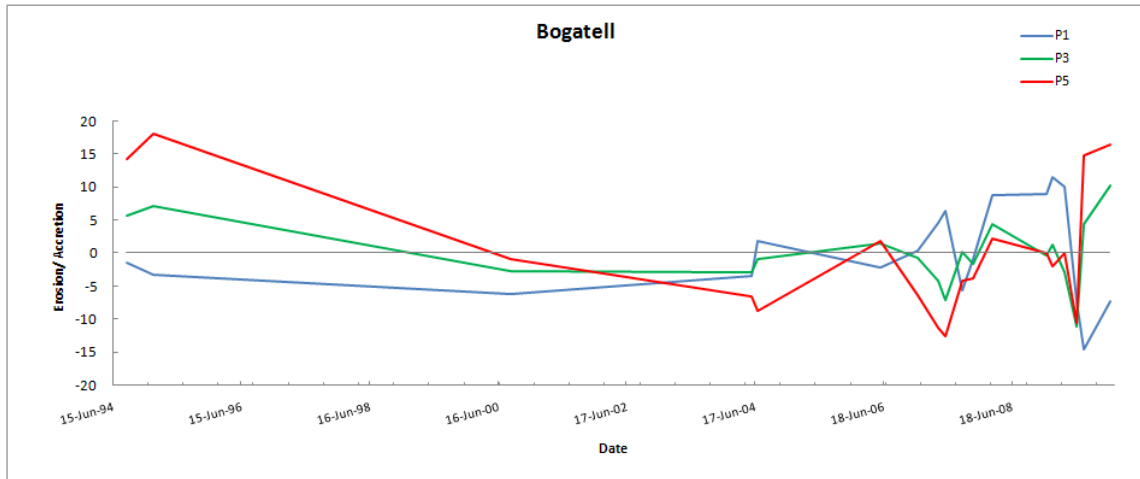




Figure 24 Beach width variation Barcelona City beaches.

Tarragona Beaches

Tarragona beaches presented also high beach mobility. At Playa Larga the southern end (P1) presented the largest variation, with changes larger than 45 meters in a seaward direction. The center (P3) and northern part (P5) display a lower variation, with changes on the order of 10 meters. The rate of change for the control sections were -0.11 m/yr ($r^2=0.1$) at the southern end, -0.9 m/yr ($r^2=0.3$) at the center part, and -1 m/yr ($r^2=0.6$) at the northern part.

At Salou, the southern ends experience a maximum beach width variation on the order of 25 meters. The center and northern end presented a lower variation on the order of 18 meters. The evolution rate for the sections of the beach corresponds to 0.14 m/yr ($r^2=0.1$) at the southern end, 0.33 m/yr ($r^2=0.3$) at the central part and 0.27 m/yr ($r^2=0.2$) at the northern end.

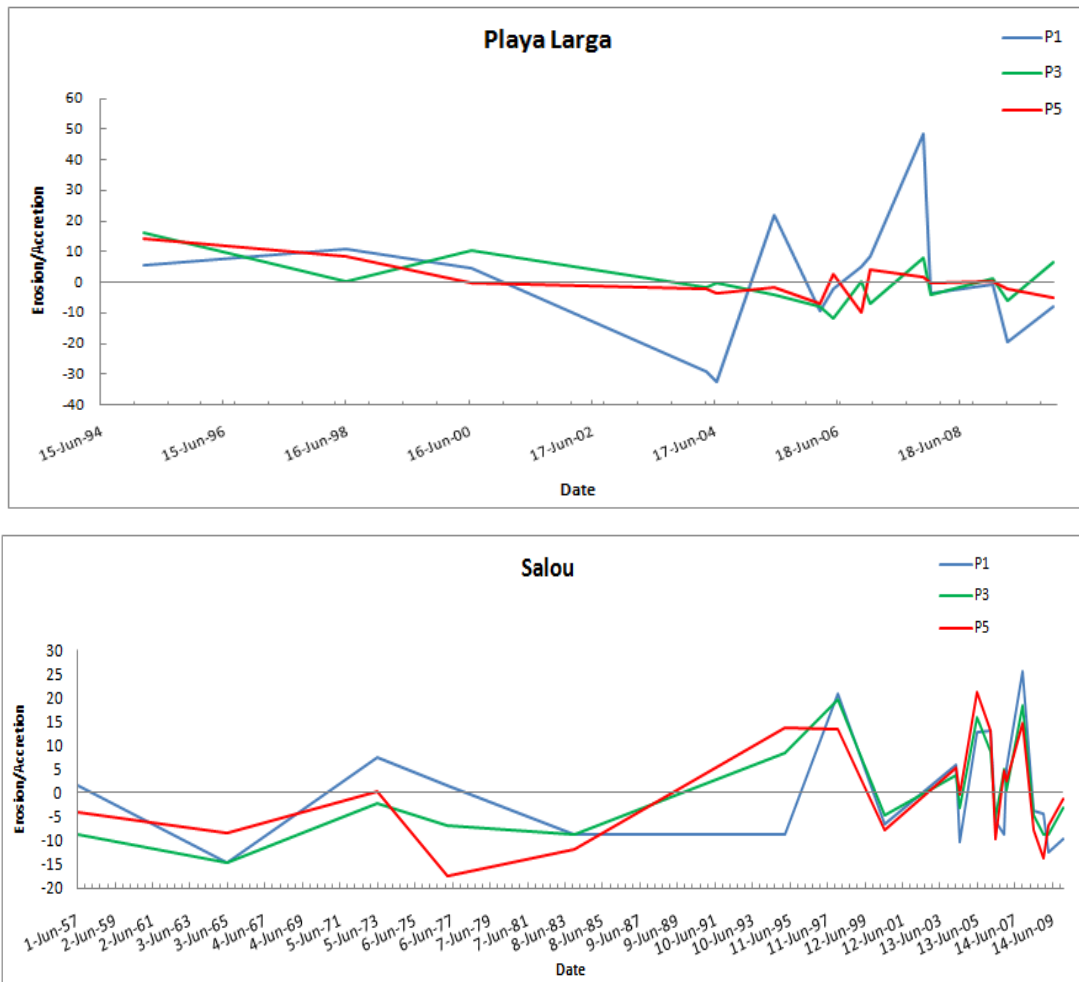


Figure 25 Beach width variation Tarragona beaches.

4.2.3 Beach Area

Figure 26 to 28 shows the temporal evolution of the sub-aerial beach area of all nine beaches. The result has also been grouped by provinces.

Girona Beaches

The result showed that Girona beaches don't present any trend in the sub-aerial beach area. This is logical for a conservative environment.

Sant Pol presented a maximum value of 40800m² in November 2007 followed by a progressive lost of beach area until reach a normal value of 25000-26000 m². At Canyelles, the mean beach area is approximately 16000 m², the data analysis suggest that the beach don't experience any progressive lost of beach area.

At Lloret del Mar, the beach area does not varied as much as Sant Pol with an average value of 53000 m², two accretive periods has been observed followed by a erosion period. These accretive periods took place from July 1986 to August 1997 and from September 2000 to December 2006 the result of these periods were an increase in beach area of 8000 m² and 13000 m², followed by an erosive period from December 2006 to December 2009, with a loss in beach area of 8800 m².

The mean beach area at Fenalls corresponds to 39300 m²; through the study period the beach doesn't experience any loss of beach area. The maximum value of beach area was presented in August 1997 with an increase in beach area of about 44920 m².

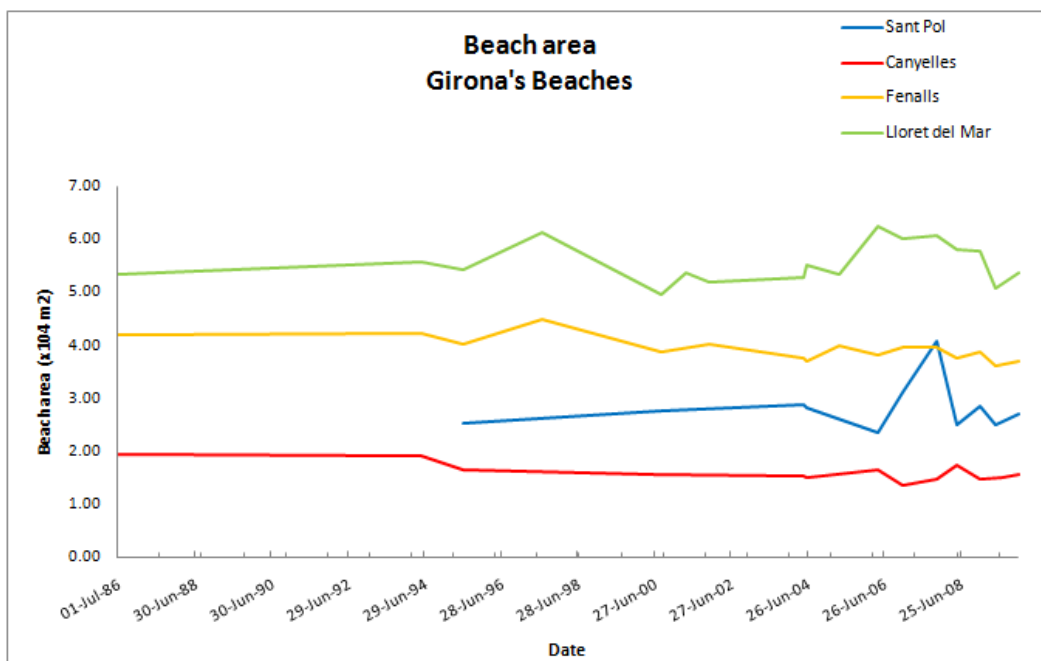


Figure 26 Emerged beach area Girona beaches.

Barcelona City Beaches

The sub aerial beach area at Bogatell and Nova Icaria doesn't display any trend during the study period. The mean beach area for Bogatell was 21760 m² and for Nova Icaria was 21960 m². The maximum value for both beaches correspond to February of 1995 (31800 m² and 25 400 m²). Bogatell experienced a loss in beach area in June of 2009 (14400 m²).

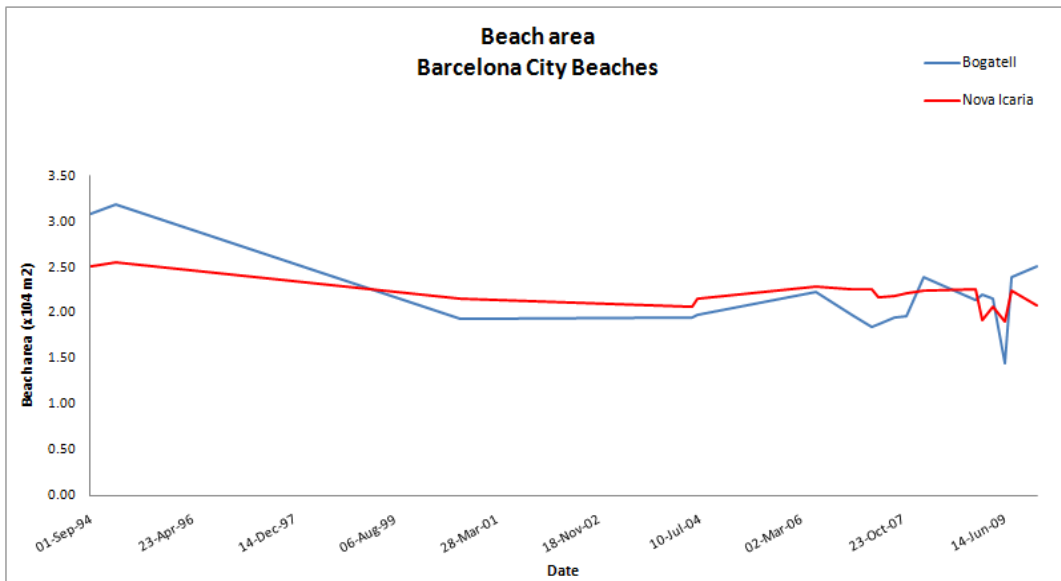


Figure 27 Emerged beach area: Bogatell and Nova Icaria.

During the study period Barceloneta beach does not experience any trends. Before 2006, the mean beach area of Barceloneta was 45000 m². During this period the maximum value of beach area occurred in December of 2006 (65800 m²), the increase in beach area can be caused by nourished campaigns along the beach.

From 2006, we observed that both sections presented a high variation of beach area. The maximum values correspond to April 2007, with an area of 33700 m² at the Northern end and 53300 m² at the Southern end. The mean emerged areas of the sections are 25000 m² and 44000 m², respectively. The minimum emerged area corresponds to 15000 m² and 24300 m² in February of 2009 and December of 2009.

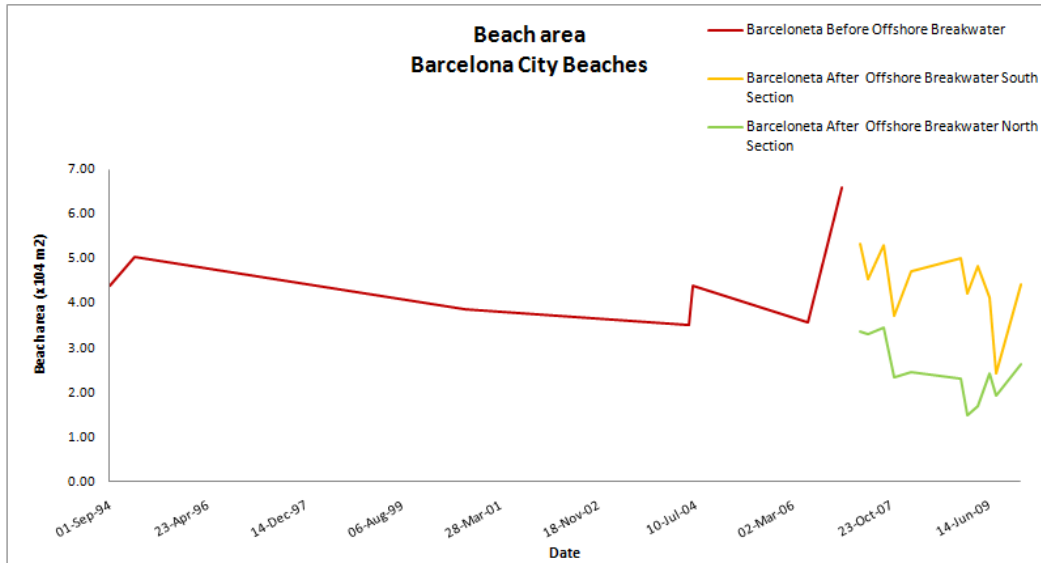


Figure 28 Emerged beach area: Barceloneta.

Tarragona Beaches

At Tarragona beaches, we observed that Playa Larga does not present any trend. However, Salou showed an accretionary trend generated by the accumulation of sediment at the southern end. The mean value of beach area at Playa Larga correspond to 17300 m^2 , the maximum value is presented on November 2007 of about 31600 m^2 . The minimum value is presented on June 2004 with an area of 7400 m^2 .

At Salou, the mean value correspond to an area of 82888 m^2 . The accretive trend leads to a high value of 100900 m^2 on January of 1998, followed by an erosive period. In June of 2005 the beach recovered again a maximum value of 100100 m^2 . This same process is observed in November 2007 when the beach achieved the maximum value of beach area of about 103600 m^2 . The minimum value observed at Salou, occurs in June 1965 (67900 m^2).

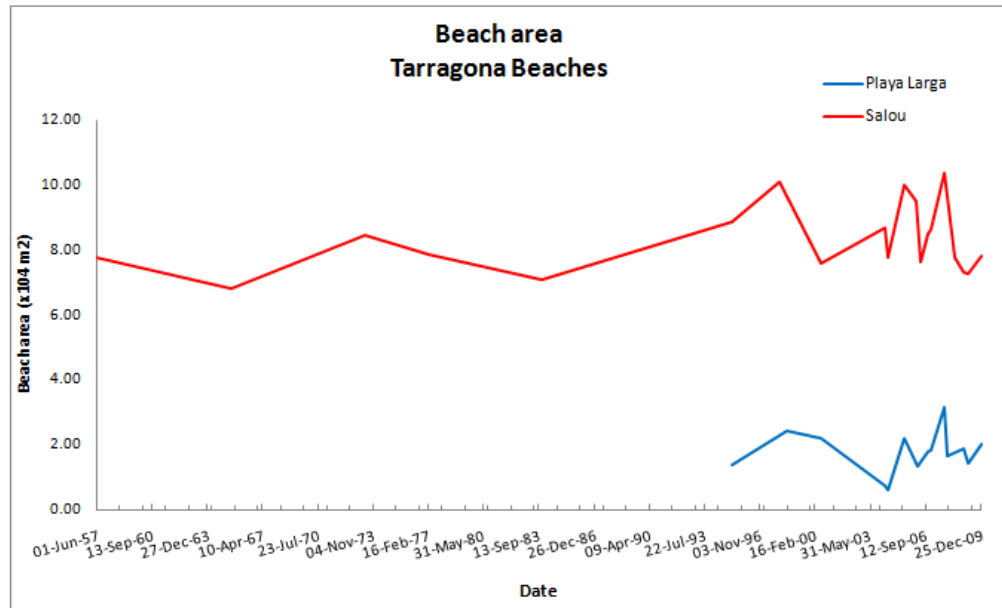


Figure 29 Emerged beach area Tarragona beaches.

4.2.4 Beach Mobility as a Function of Different Beach Type

As mention before in section 4.2.2, beach variability (mobility) is a function of the morphodynamics state of a beach (dissipative, intermediate and reflective).

The beaches in this study have been separated following the classification given by Wright and Short, 1984. By using the mean value of beach face slope (m) and mean grain size (D_{50}), we determine the sediment fall velocity for each beach (ω_s).

A typical reflective beach is characterized by a coarse sand ($D_{50} > 0.6\text{mm}$), with a relative high berm and a steep slope ($m = 0.1$), a dissipative beach is composed by fine sand ($D_{50} < 0.25\text{mm}$), and a very mild slope ($m = 0.01$) (Mendoza, 2008). An intermediate beach will relay between this two extremes.

Table 11 Grouping Catalan beaches according with the beach type

Beach	m	D ₅₀ (mm)	ω_s (m/s)	Degree of Exposure	Beach Type
Canyelles	0.10	1.16	0.21	Semi-exposed	Reflective
Lloret del Mar	0.15	1.46	0.24	Exposed	
Fenals	0.34	1.41	0.23	Exposed	
Barceloneta Before 2006	0.12	0.66	0.16	Exposed	
Barceloneta After 2006: South Section	0.12	0.66	0.16	Exposed	
Bogatell	0.13	0.47	0.14	Exposed	Intermediate
Nova Icaria	0.15	0.46	0.13	Semi-exposed	
Sant Pol	0.12	0.38	0.12	Semi-exposed	
Barceloneta After 2006: North Section	0.09	0.27	0.10	Exposed	
Playa Larga	0.05	0.21	0.09	Semi-exposed	Dissipative
Salou	0.02	0.22	0.09	Semi-exposed	

From the previous result the beaches has been classified in relation of the degree of exposure to the easterly wave condition, since this is one of the predominant directions.

The reflective beaches have been divided in two categories exposed and semi-exposed. Canyelles is the only reflective semi-exposed beach, due to its orientation (102°) is well protected by east wave condition and is only affected by southern wave condition. It is for our interest, knowing that these exposed reflective beaches experience less headland impact. The exposed reflective beaches are characterized by a small shadow zone, so changes at both ends can be very similar. From the previous analysis we had observed that this type of beach presented high sub-aerial beach width mobility at both ends; on reflective beaches waves can reach the beach face without breaking and surge strongly up to the beach, resulting in a removal of larger amounts of sediment. Also the steep slope reduced the effects of refraction and the waves can reach the shore at more angles, generating an alongshore sediment transport exchange between both ends. The present of megacusps at La Barceloneta before 2006 (Ojeda and Guillen, 2008) and at the South section after 2006 change the

characterization from reflective beach to an intermediate beach, since this submerged bar affect the configuration of the shoreline.

The intermediate beaches have also been divided in exposed and semi-exposed. Nova Icaria and Sant Pol are considered semi-exposed, the first one is due to the hard structures that protected by east wave condition and the second one is due to its orientation and the protection of the headland features that bounded the beach.

Based on the results the exposed-intermediate beaches are characterized by high beach mobility. These beaches present a well define shadow zone at the northern end (e.g. Barceloneta North Section) and a more exposed zone at the southern end. Therefore, the maximum beach displacements were presented at the southern end and the lower displacements occur at the northern end. However, the displacements in the shoreline were less compared with the reflective beaches. These differ in Bogatell where the maximum displacement occurs at the northern end.

Finally, Playa Larga and Salou were considered semi-exposed dissipative beaches. They are considered semi-exposed due to it orientation 116° and 109° , respectively. In these two beaches we observed that beach mobility was in smaller magnitude than the rest of the study beaches, with only one episode during the study period with a maximum value of displacement. However, for Playa Larga the maximum displacement always occur at the southern end while Salou present a more homogeneous beach width in accord with the morphodynamics of the lower degree of curvature.

4.3 Discussion

The result from this study indicates that the embayed beaches along the Catalan coast display a wide range of indentation index values. The beaches of Girona and Barcelona fall into the category of moderato to high indented, while the beaches of Tarragona exhibit a less indent behavior.

By applying the indentation criteria, we observed that moderate to highly indented beaches presented a moderate to a higher degree of curvature (e.g. Nova Icaria). While, the less indented beaches present less degree of curvature (e.g. Salou and Lloret del Mar). As a result the curved beaches will experience greater variation (e.g. beach width) in the exposed straight end compared with the shelter areas. The beach that presents a smaller shadow zone or even a straight platform will have a constant variation of beach mobility along the beach.

The stability test applied to the nine beaches of the study, reveal that most of the beaches are experiencing a similar behavior, the stability criteria of most of the beaches fall below the stability curve of Hsu. With the difference of Fenals that fall above the stability curve of Hsu. Since the stability curve has been propose for a specific set of data and the coefficient of the parabolic shape are not universal, it appears that the beaches of the Catalonian coast present a different trend. Beaches with the same exposed conditions and similar morphological characteristics presented similar stability criteria, therefore the stability curve for the Catalonian coast could be shifted from the stability curve of Hsu.

On the analysis of beach mobility, we have observed that all the beaches presented a non- uniform behavior of the sub-aerial beach width within a beach and along the Catalonian coast. The mayor difference between beaches was the orientation of the shoreline and the exposure to wave conditions (e.g. headland feature or hard structure).

Girona beaches, in particular Lloret del Mar and Fenals had experienced the higher degree of variation along the beach. At Barcelona city beaches; Barceloneta show the higher beach mobility compared with Bogatell and Nova Icaria, this behavior can be result of the nourishment campaigns in the area (e.g. June 2004). At Tarragona, Playa Larga is the one that presented the maximum displacement at the southern end, while Salou presented a more uniform behavior along the beach.

The analysis of beach area, suggested that the study beaches doesn't presented any erosive trend. However, Salou presented and accretive trend due to the existence of the port at the southern end. The beaches presented a moderate to high variation of emerged beach area.

Other major difference along the nine study beaches were the beach slope and main grain size. So in order to analyze what is the influence of these two parameters on the beach mobility, we have applied the Wright and Short classification on the study beaches. This classification does not mean that the beaches are subjective to any beach state but for the purpose of this thesis we have grouped according to those parameters (beach slope, mean grain size and fall velocity), we will relate the beach state with the sub-aerial behavior of the beach.

The majority of the reflective beaches correspond to exposed beaches (e.g. Lloret del Mar, Fenals) with a small shadow zone (northern end) and a straight exposed area (southern end). These systems presented the higher beach mobility of all the study beaches, on the order of 30 meters and 60 meters. This variability was evident at both ends of the beach.

On the other hand, the intermediate beach were characterized by a well define shadow zone (e.g. Sant Pol, Bogatell, Nova Icaria and Barceloneta). Due to this aspect the protected area (northern end) presented the lower degree of variation and the exposed area presented the higher displacements, with the exception of Bogatell that present a different behavior. This intermediate beaches, can experience different beach state, therefore a specific behavior cannot be establish.

Finally, the dissipative beaches were found at Tarragona. The morphodynamics behavior of the two beaches differs from each other. Both beaches present a less degree of curvature, which implies that the beach variability will be more uniform in along the shore, but this only occurs in Sant Pol. At Playa Larga the greatest displacement occurs at the southern end while the northern end present a low variation.

4.4 Summary

From the study of shoreline evolution of nine sandy embayed beaches along the Catalan coast, the following conclusion can be draw:

- The stability tests have revealed that the stability curve of the study beaches is shifted from the curve proposed by Hsu, 1989. Therefore, the beaches are experiencing a stable mode.
- The study beaches presented a wide range of indentation. Girona and Barcelona presented the moderate to high indented beaches, while Tarragona presented the less indented beaches.
- The beaches presented a non- uniform behavior of the sub-aerial beach width within a beach and along the Catalonian coast. However, some beaches had a large degree of similarity.

- Beach mobility (e.g. beach width) along the beaches presented a high degree of variability and is function of the degree of curvature of the beach and their exposure to wave conditions.
- Most of the beaches do not present any trends in the emerged beach area, characteristic of the conservative environments.
- Reflective beaches had the greatest variation on the sub-aerial beach, and were characterized by beaches with moderate to less curvature.
- Intermediate beaches had the smaller variation on the sub-aerial beach, and were characterized by beaches with a moderate curvature.
- The dissipative beaches of the study presented a different behavior with each other.

Since only the sub-aerial beach behavior has been study, it is logical to observe that the reflective beaches are the one that presented a higher variability. But, intermediate beaches has been known to exist in a grater range of beach state, therefore an specific study of beach profile should be perform in order to observe what is the behavior of this specific beach types.

5. Beach Rotation and Oscillation: Rotation Coefficient

Coastlines are highly vulnerable to wave variability at different time scales (Nicholls et. al, 2007 cited by Harley M, 2009). Variations in beach morphology (rotation and oscillation) have long been documented as a respond to equilibrium wave condition as opposite to an instantaneous wave conditions (Wright and Short, 1984). While studying the shoreline evolution was significant in the analysis of beach variation, determine medium term oscillation may also be fundamental.

Beach rotation is an oscillatory medium scale process which is characteristic in short embayment beaches. This process has been shown to occur in large scales where wave direction is critical, hence an analysis of this process through our shoreline dataset is important, in order to determine if the beaches along the Catalan coast are experience beach rotation.

The aim of this chapter is to obtain more definitive links between mean wave climate and the embayment beach response (beach rotation and oscillation). This is undertaken by using a theoretical model defined by the typical configurations observed in each beach. The chapter is divided into four sections. Following this introduction, section 5.1 presents the methodology used in the analysis; the results per beach are presented at section 5.2. The final two sections 5.3 and 5.4 present the discussion and summary.

5.1 Methodology

The following methodology has been applied, in order to determine if the beaches are experienced the process of beach rotation and in what degree.

5.1.1 Rotation Coefficient (RO)

In order to quantify the degree of beach rotation or oscillation a method known as rotation coefficient has been implemented. This method has been proposed by Wood, 2010. It has been considered an accurate tool when the data set has a high spatial and temporal variability, and also when there is an unstable or poor relationship between the control lines along the beach that will give a low rotation coefficient.

The rotation coefficient consist in relate each control point from its origins to it's alongshore location. The degree of rotation was quantify by evaluating the beach width with respect the alongshore location of the control point. For each shoreline position the beach width (e.g. w_1 , w_2 , w_3 , w_4 and w_5) has been plotted against the alongshore location of each control point (e.g. x_1 , x_2 , x_3 , x_4 and x_5). By using linear regression, a best fit line was fitted to each shoreline. The rotation coefficient (RO) corresponds to the slope component of the resulting linear equation which was been converted to degrees.

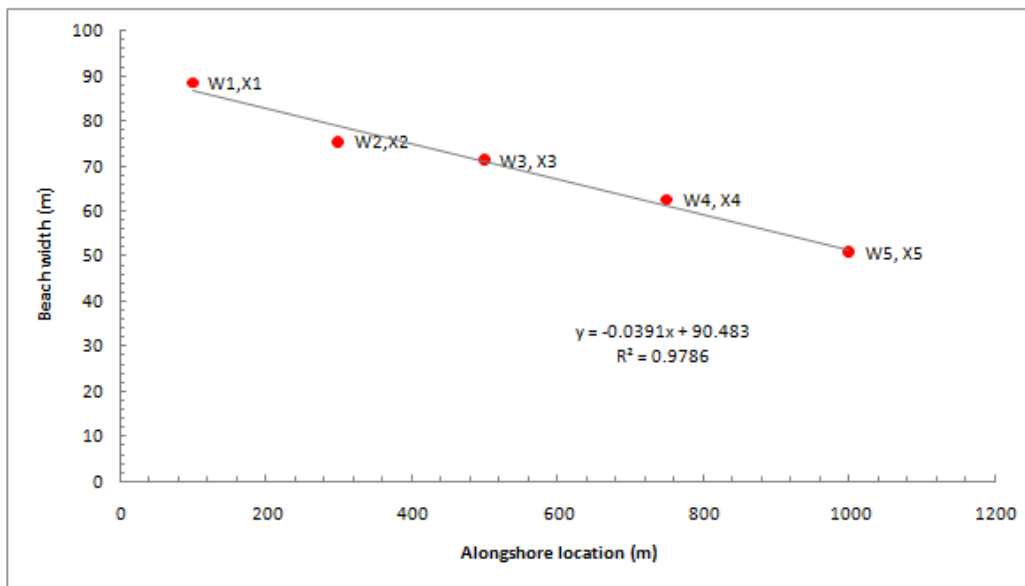
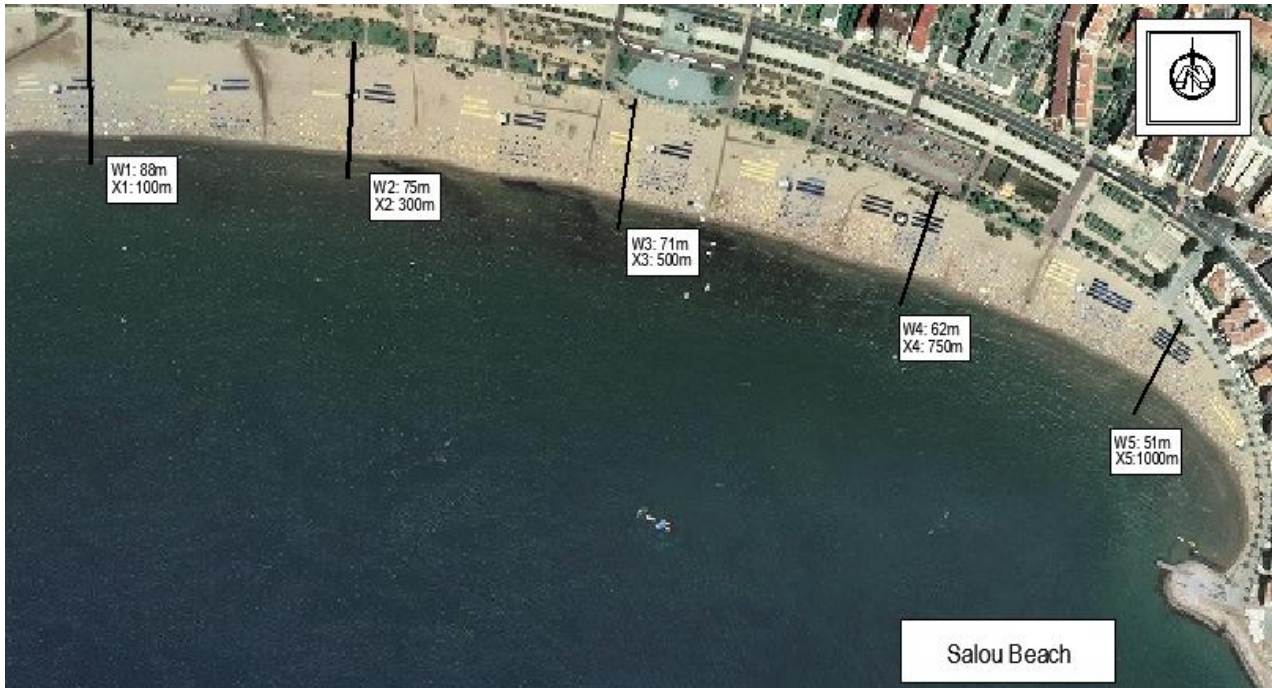


Figure 30 Distance and the correspondent beach width along the Salou beach as defined by the length from the southern end along the shoreline of the embayment platform (top). Definition of rotation coefficient (bottom). (Photo: Ortophotos Salou 1 June 2008).

If there is a large degree of variation between the beach widths at each end, we would obtain a strong rotation coefficient. A positive rotation coefficient implies a greater beach width at the northern end of the beach (right hand side looking landward), and clockwise rotation (Figure 31). The opposite applies for a negative coefficient and an anticlockwise rotation. If the rotation coefficient presents a low degree of variation indicate that beach oscillation is the predominant process. A time series of the rotation coefficient was generated for each beach.

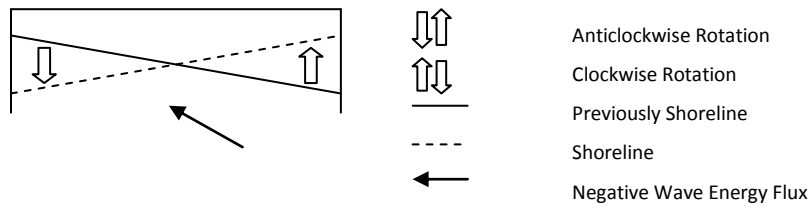


Figure 31 Parameters use to define beach rotation (Ojeda and Guillen, 2008).

5.1.2 Theoretical Rotation Coefficient (RO_T)

In order to obtain the theoretical rotation coefficient, first we need to determine the theoretical model of each beach. This model consist in establish which were the typical configuration of the beach during the study period. From the data set of the coastlines two or three typical configurations per beach has been determined. The envelope of the shorelines shows a moderate to highly fluctuation beaches.

Once the theoretical model of the beach (e.g. C1, C2, C3) has been defined, the rotation coefficient for each configuration is determined as described above, this will be known has the theoretical rotation coefficient (e.g. RO_{TC1} , RO_{TC2} , RO_{TC3}). This parameter is important since it can be related with the wave direction and the longshore sediment transport. The following figure shows an example of the theoretical model for a specific beach.



Figure 32 Theoretical Model: Typical Configurations (e.g. Fenals, Configuration 1, shoreline of June 1st, 1994 (dotted blue line), Configuration 2, shoreline of May 1st, 2006 (dotted black line) and Configuration3, June 30, 2004 (dotted red line)).

5.1.3 Waves Forcing on the Theoretical Model

A study of the driving forces on the theoretical configuration for each beach has been developed. The objective of this section is to establish which conditions (wave height, period, direction and duration) are needed to accomplish each configuration of the theoretical model. The mean wave climate is the one that is study.

This will be done by comparing the volume of sand that moves between configurations, known as measured volume (ΔV_m) with an estimated volume, that consisted in the cumulative volume generate by the immediately wave action (ΔV_s) prior the date of the shoreline configuration. When the estimated value tends to the measured value, we would obtain the conditions required to pass from one configuration to another. The group of data that correspond to the estimated volume will be considered the specific wave conditions (wave height, period, direction).

Wave data used in this analysis have been previously explained in chapter 3. The analysis has been performed to the shoreline that represent the typical configuration and also to the shoreline that have a similar theoretical rotation coefficient, this with the objective to have more combination of wave height, period and direction and

achieve a better understanding of the behavior within the embayment. A distinction will be made in the number of times that the same rotation coefficient has been observed within the shoreline data set.

The main assumption to apply this method was that the profile (e.g. slope) of the beach does not change; the only exchange of volume will occur in alongshore direction.

Measured Volume (ΔV_m)

The measured volume consists in the sub aerial area that accretes between consecutives configurations (e.g. From C1 to C2, C2 to C3 and C1 to C3) multiplied by the corresponded value of the berm height and depth of closure of each beach.

Table 12 shows the values of the berm height and depth of closure per beach.

Table 12 Values of berm height and depth of closure per beach		
Beach	Berm height (m)	Depth of closure (m)
Sant Pol	1.65	8.7
Canyelles	2.54	7.7
Lloret de Mar	2.12	7.7
Fenals	2.33	7.7
Bogatell	2.50	6.5
Nova Icaria	1.70	6.5
Barceloneta (Before 2006)	1.65	6.5
Barceloneta (After 2006): North Section	2.65	6.5
Barceloneta (After 2006): South Section	1.65	6.5
Playa Larga	1.00	7.0
Salou	0.50	8.1

Estimated Volume (ΔV_s)

Mean wave climate (1958 to 2007) were used to calculate the estimated volume. The estimated volume consisted in a cumulative sum of the volume obtained by the longshore sediment transport rate (Q (m³/s)) multiplied by the 3 hourly interval of each wave data.

The Kamphuis formula will be used to obtain the sediment transport rate (Q (m^3/s)). This formula is based on the grain size, beach slope and the breaking condition.

In order to apply the formula, we need to transform our offshore wave data to breaking conditions. This has been done by using the dispersion relation, the breaker index ($\gamma=0.88$ for H_{max}) and the Snell's Law.

The following condition will be applied to define the angle of breaking, and the direction of the longshore sediment transport. Negative values correspond to a longshore sediment transport directed to the south, positive values correspond to a transport directed to the north. The sign of the breaking angle will depend on the orientation of the shoreline.

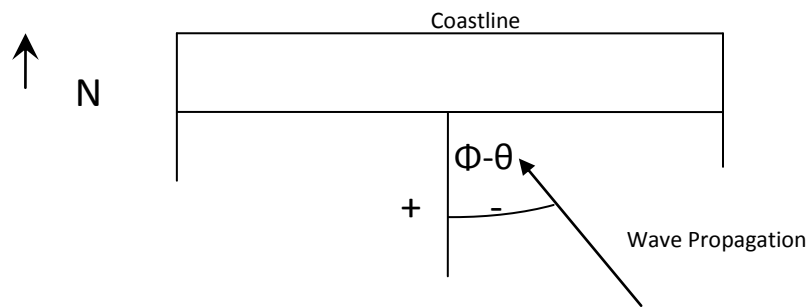


Figure 33 Definition of the angle of breaking.

After this step a new wave breaking data set will be obtained. This data set (breaking wave height H_b , period T , wave direction φ and orientation of the shoreline θ) will be used to obtain the sediment transport rate, which will be transformed into a volume quantity, by multiplying it by the interval (Δt) between data points.

$$[H_b, T, (\varphi - \theta)]_i \rightarrow Q_i$$

(Eq.5)

$$V_i = Q_i \cdot \Delta t$$

(Eq. 6)

Finally by a cumulative sum of the volume obtained from the wave data we would determine the estimated value (ΔV_s). $N(D)$ is the number of data point between 1 and D days prior to the date of the shoreline that is study.

$$\sum_{i=1}^{N(D)} V_i(t) = \Delta V_s$$

(Eq. 7)

When the estimated value (ΔV_s) tends to the measured value (ΔV_m), we would obtain the conditions required to pass from one configuration to another. The results of the wave height and period are presented as an arithmetic average; the wave direction is presented as a weighted average and the longshore sediment transport rate as a cumulative average, as presented below:

$$\frac{\sum_{i=1}^{N(D)} H_{si}(t)}{N(D)} = \langle H_s \rangle_D$$

(Eq. 8)

$$\frac{\sum_{i=1}^{N(D)} T_i(t)}{N(D)} = \langle T \rangle_D$$

(Eq. 9)

$$\frac{\sum_{i=1}^{N(D)} \varphi_i(t) \cdot Q_i(t)}{\sum_{i=1}^{N(D)} Q_i(t)} = \langle \varphi \rangle_D$$

(Eq. 10)

$$\frac{\sum_{i=1}^{N(D)} Q_i(t)}{N(D)} = \langle Q \rangle_D$$

(Eq. 11)

The average of the longshore sediment transport is independent of the wave height and period, since inside the cumulative sum there will be positive and negative values.

5.2 Results

The result will be presented individually. In the previous chapter we observed that each beach follow a different behavior, therefore for each beach the results of the rotation coefficient, the theoretical model and the results from the waves forcing on the embayment are presented.

5.2.1 Sant Pol Beach

Sant Pol was considered an intermediate curved beach; with a very well define shadow zone at the northern end and a straight zone at the southern end. The beach is oriented towards the SSE (163°) except to the northern end that is oriented toward the SSW. The length of the beach is 630 meters.

Rotation Coefficient (RO)

Figure 34 shows the evolution of the rotational coefficient of the 11 shorelines that described the beach through the study period. The rotation coefficient was display in degrees, with a negative slope indicating anticlockwise rotation. The figure showed that Sant Pol appear to be rotated to the south, with a minimum value of rotation coefficient of -1.83° and a maximum of -0.48° .

The values between these two extremes indicate that the beach is oscillating instead of rotating; this means that there is an overall erosion/accretion at the entire embayment. The beach does not experience a clockwise rotation, since all the values are negative.

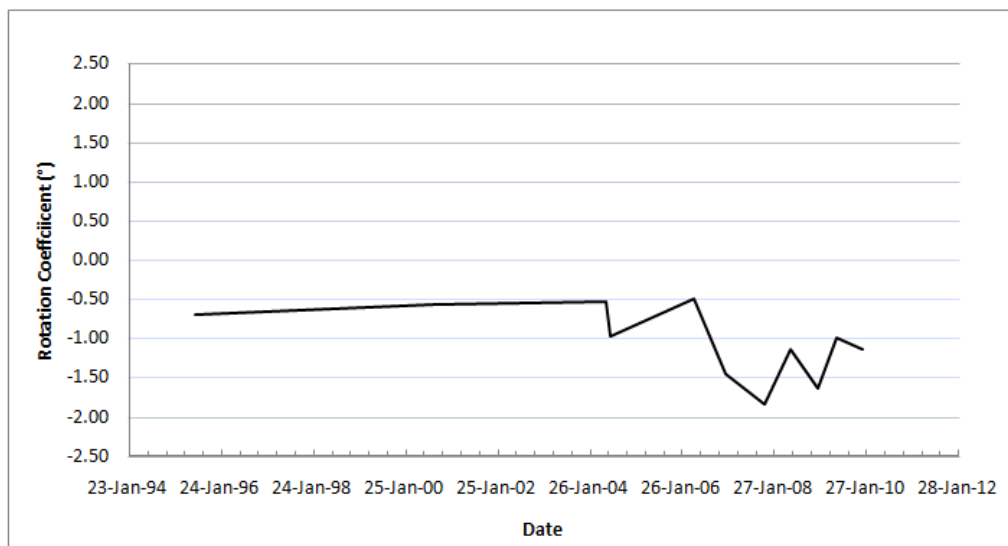


Figure 34 Evolution of the rotation coefficient, Sant Pol.

Theoretical Rotation Coefficient (RO_T)

A data set of 11 coastlines from July 1995 to December 2009 has been used to analyze the theoretical rotation coefficient. Two major configurations can be distinguished, the first one correspond to the beach leaning to the south ($RO_T=-1.8^\circ$), with a maximum width of 55 m at the center, at the southern end a beach width of 47 m and the northern end a minimum value of 18 m. This configuration is represented by the shoreline of November 11, 2007.

The second configuration ($RO_T=-0.5^\circ$) correspond to the beach tilted to the north, with a maximum value at the center of 47m, at the southern end of 36 m and at the northern end of 26 m. This configuration is represented by the shoreline of June 1, 2004.



Figure 35 Theoretical Model of Sant Pol (Photo: Ortophotos 2008, ICC). Configuration 1, shoreline of November 11, 2007 (solid blue line) and Configuration 2, shoreline of June 1st, 2004 (solid red line).

Table 13 shows the correspondent RO_T value for the two typical configurations and the number of times that the same RO_T has been observed within the shoreline data set. The first configuration has been observed only one time during the eleven study shorelines; the correlation coefficient of this configuration was 0.4. The second configuration has been observed 3 times and presented a correlation coefficient of 0.2.

Configuration	Theoretical rotation coefficient	Number of observations
C1	-1.8 ($r^2=0.4$)	1
C2	-0.5 ($r^2=0.2$)	3

Waves Forcing on the Theoretical Model

Once the theoretical model of Sant Pol was been identified, the wave conditions that generate this rotation can be determined. The analysis has been performed to the shoreline that represent the typical configuration and also to the shoreline that have a similar rotation coefficient. Bold values correspond to the representative shoreline configuration.

Table 14 shows the volume exchange from one configuration to the other. Negative value corresponds to a deposition at the southern end (See figure 35), the converse applied for positive volume. This was consistent with the curved platform of the beach, the northern end (shadow zone) will experience a less volume exchange since the sediment movement in this area is defined by the gradient currents, while the sediment movement at the southern end (exposed area) is defined by the longshore current.

From To	ΔV_m [C1]	ΔV_m [C2]
ΔV_m [C1]	-----	-40271
ΔV_m [C2]	17367	-----

Configuration C1

From the analysis of the shorelines with a similar configuration (e.g. theoretical rotation coefficient), we obtain the conditions required to move a volume of sand from the configuration C2 to C1 (e.g. $RO_T = -1.8$). Since only one shoreline had presented the theoretical pattern, only one wave condition has been established.

Table 15 show the wave information, the information corresponds to a cumulative average values. Figure 36 show the wave condition during the past six months before the date of the shoreline study.

We observed that to achieve an anticlockwise rotation we need to have a wave condition coming from a South-East direction (range between 123° to 146°). The mean wave height is 0.58 m and the period corresponds to 7.7s. This condition generate a cumulative mean sediment rate of 4204m³/yr south directed.

Table 15 Wave condition that generates configuration 1, Sant Pol					
From	Time (Days)	H _s Mean (m)	T _p Mean (s)	Φ Mean (°)	Q Cumulative Mean (m ³ /yr)
C2	2	0.58	8	136	-4204

From the figure we observed that between July to November of 2007, only one storm occur with significant wave height of approximately 3 meters, with a direction that generate sediment transport directed to the south (E storm). The wave distribution of 2007 showed that southern movements of sediment are more frequent that those that generate a northern movement.

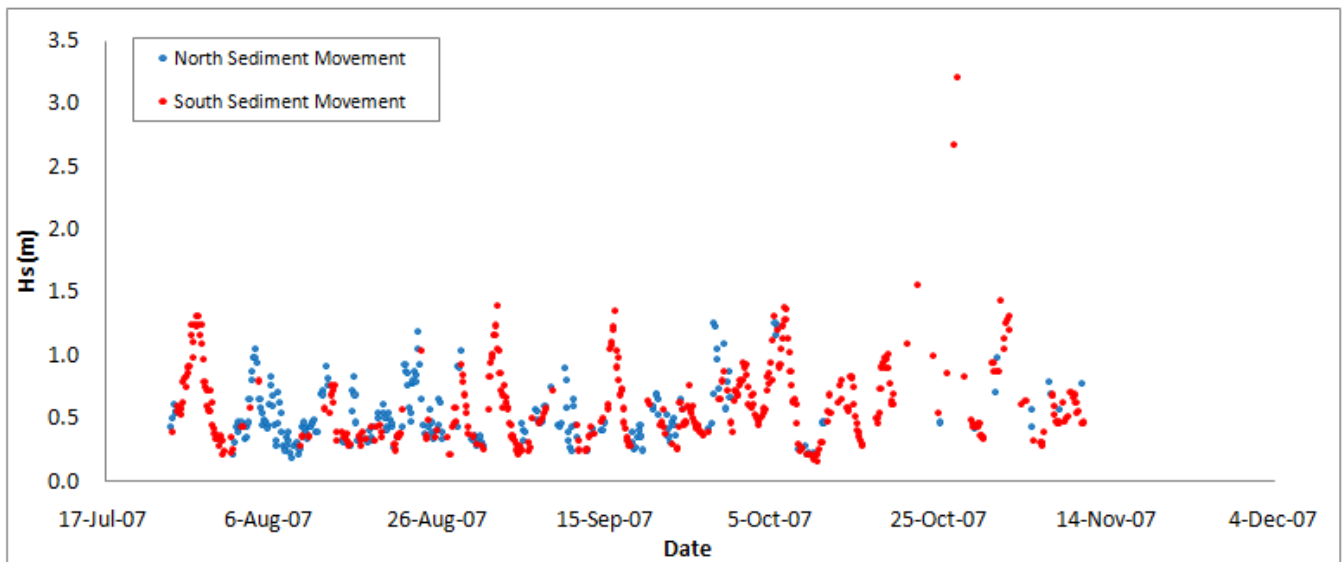


Figure 36 Wave condition during and shoreline effects at Sant Pol (Configuration 1) November 11, 2007.

Configuration C2

For the second configuration we obtain three different combinations. Results showed that to generate this platform distribution ($RO_T = -0.5$) it required a wave condition coming from South direction (ranges from 168° to 191°). The mean wave height is very similar in the three combinations (range between 0.34 to 0.40m), while the period differ from 3 s to 5s. The mean cumulative sediment budget was around 2563 to 4949 m^3/yr , the value is lower than the one generated by configuration 1.

However, this longshore sediment rate was consistent with the lower wave height and period. Figure 37 showed that before June 1st, 2004 there was one storm event with a wave height around 3 meters ($\phi = 94^\circ$), which generate south directed sediment transport. But most of the wave condition during this period generates north sediment transport.

Table 16 Wave condition that generates Configuration 2, Sant Pol

From	Time (Days)	Hs _{Mean} (m)	T _{Mean} (s)	Φ _{Mean} (°)	Q _{Cumulative Mean} (m ³ /yr)
C1	2	0.34	3.07	187	4949
	2.75	0.39	3.58	172	3095
	7.75	0.40	5.63	168	2563

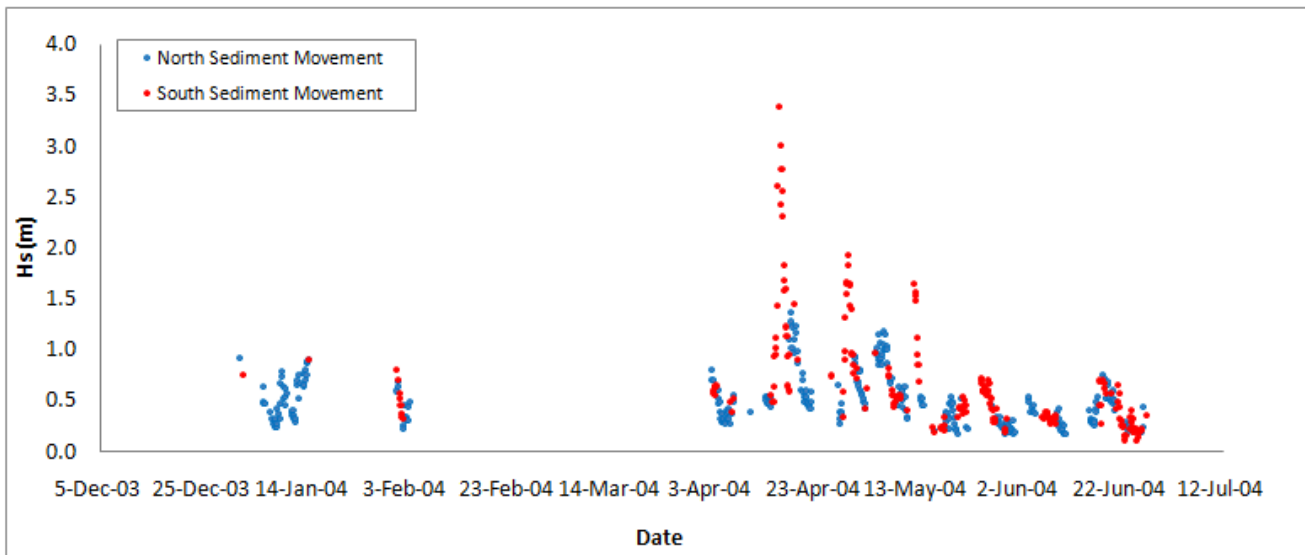


Figure 37 Wave condition during and shoreline effect at Sant Pol (Configuration 2), 1 June 2004.

5.2.2 Canyelles Beach

Canyelles was considered a reflected moderate curved beach with a beach length of 434 m, the headland at the northern end protected from easterly waves, and the beach is oriented towards the SSW (192°). The result from the analysis of beach rotation and oscillation are presented below.

Rotation Coefficient (RO)

Figure 38 shows the evolution of the rotation coefficient for the 13 shorelines from July 1986 to December 2009. It is clear from this figure that the beach only experiences an anticlockwise rotation, with a maximum value of -3.5° and a minimum value of -5.8°.

The anticlockwise rotation occurs two times during the study period, on July 1st 1995 and on June 1st 2004. The minimum anticlockwise rotation only occurs one time during the end of June 2004. The rest of the values corresponds to oscillations, the beach width data show that the entire embayment was moving in a landward or seaward direction.

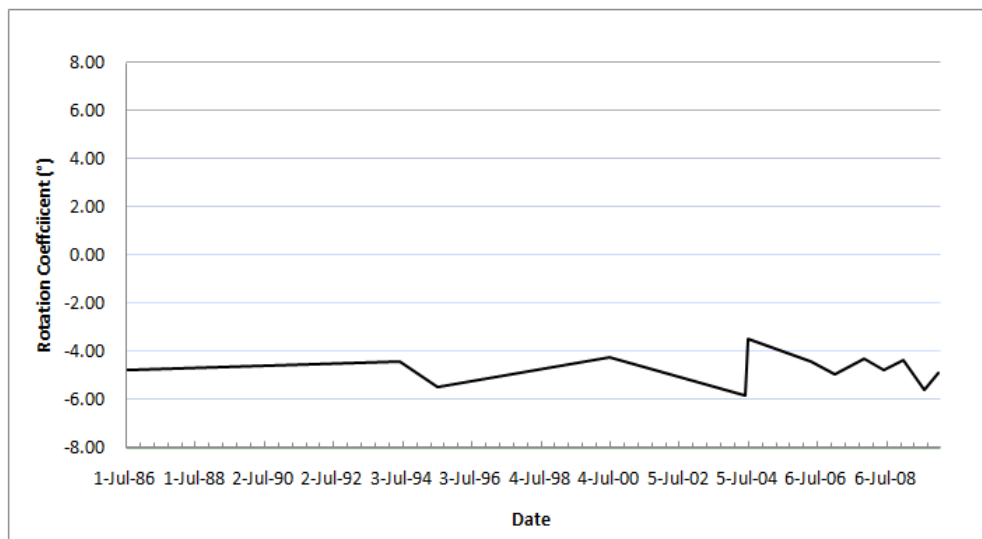


Figure 38 Evolution of the rotation coefficient, Canyelles.

Theoretical Rotation Coefficient (RO_T)

The theoretical model of Canyelles consisted in two platform distribution. The first one corresponded to the beach tilted to the south, with a maximum width of 53 m at the southern end which progressively decrease at the center and northern part to achieve a beach width of 20 m and 15 m correspondently. The shoreline of June 1, 2004 will be considered a good representation of this configuration.

The second configuration was represented by the beach leaning to the north, with a maximum value at the southern end of 46 m, at the center of 19 m and at the northern end of 26 m. This configuration is represented by the shoreline of June 30, 2004.



Figure 39 Theoretical Model of Canyelles (Photo: Ortophotos 2008, ICC). Configuration 1, shoreline of June 1st, 2004 (solid blue line) and Configuration 2, shoreline of June 30, 2004 (solid red line).

Table 17 present the theoretical rotation coefficient (RO_T) for each configuration. The RO_T of configuration 1 corresponded to values between -5.5 and -5.8, and presented a value of $r^2= 0.7$. For the second configuration the value corresponded to -3.5 with an $r^2=0.4$. The first configuration has been observed two times within the shoreline data, while the second configuration was observed only one time.

Table 17 Theoretical Rotation Coefficient Canyelles		
Configuration	Theoretical rotation coefficient	Number of observations
C1	-5.5 to -5.8 ($r^2=0.7$)	2
C2	-3.5 ($r^2=0.4$)	1

Waves Forcing on the Theoretical Model

The exchange volume between the two configurations was on the same order; figure 39 indicated that only the two end of the beach accrete or erode, while the rest of the embayment maintain the same beach width. This differ from the previous beach since this beach have a less curved platform, therefore the sediment transport is more define by the angle of the wave approach.

Table 18 Measured volume between configurations Canyelles		
From To	ΔV_m [C1]	ΔV_m [C2]
ΔV_m [C1]	-----	-7380
ΔV_m [C2]	7870	-----

The results of the analysis of wave forcing on the theoretical model are presented below.

Configuration C1

Two different combination of wave condition has been obtained from the analysis of driving forces. Table 19 shows that a wave condition coming from S direction (range 168° to 191°) was needed to accomplish a sediment movement towards the southern end ($RO_T=-5.5$ to -5.8). The mean wave height was around 0.30 m with a period between 4 and 5 s. The time needed to achieve the response on the beach generated a cumulative sediment rate around -388 and $-118 \text{ m}^3/\text{yr}$ respectively.

Table 19 Wave condition that generates configuration 1, Canyelles

From	Time (Days)	Hs _{Mean} (m)	T _{Mean} (s)	Φ _{Mean} (°)	Q _{Cumulative Mean} (m ³ /yr)
C2	2.63	0.31	4.57	188	-388
	3.13	0.28	5.47	190	-118

Configuration C2

Only one combination could be obtained from the analysis for this configuration ($RO_T = -3.5$). The mean direction of the wave condition is 199° , so directions from SSW could generate an exchange of sediment between the ends of the embayment. The cumulative mean rate of longshore sediment transport was low with only $515 \text{ m}^3/\text{yr}$. The time of respond of the beach was 8 days.

Table 20 Wave condition that generates configuration 2, Canyelles

From	Time (Days)	Hs _{Mean} (m)	T _{Mean} (s)	Φ _{Mean} (°)	Q _{Cumulative Mean} (m ³ /yr)
C1	8.00	0.40	5.53	199	515

It has been observed that the range of direction that generates both configurations were very small, with a difference of about 10 degrees. Due to the shelter nature of the beach only a small range of direction could affect the behaviour of the beach.

Figure 40 presented the wave condition during the previous months, based on the result of wave height there is no evidence of storms during this period. The maximum wave height occurred at April with a value of 1.4 m and generated a sediment transport to the north ($\phi = 194^\circ$).

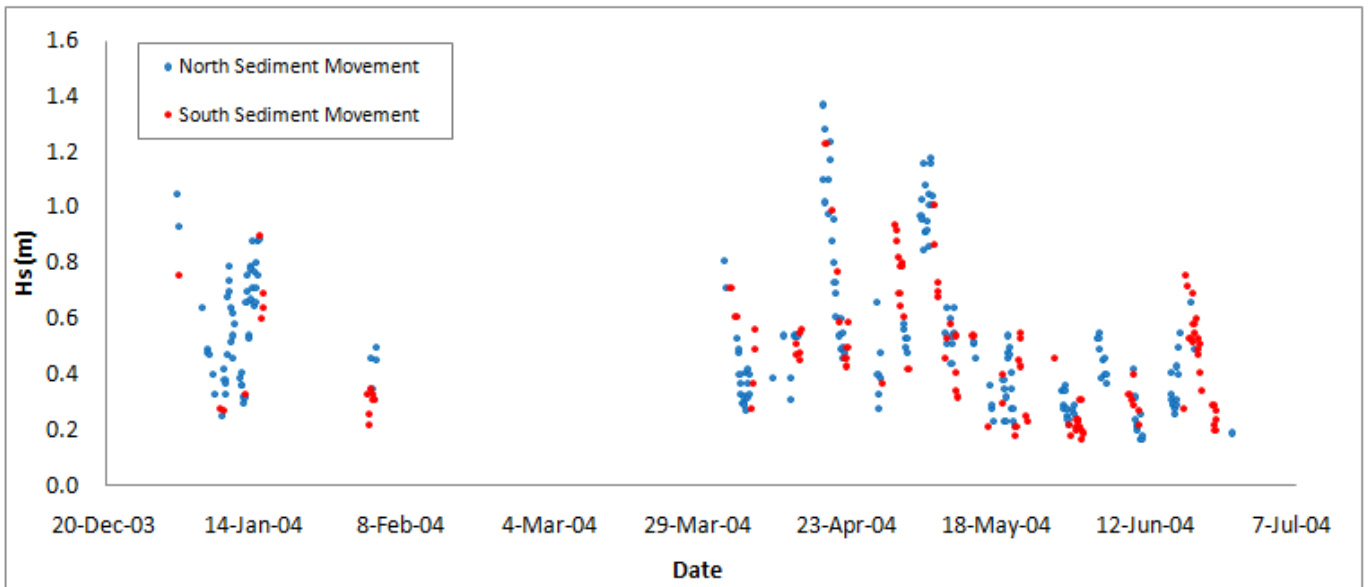


Figure 40 Wave condition during and shoreline effect at Canyelles, June 2004.

5.2.3 Lloret del Mar Beach

Lloret del Mar was considered a reflective beach with a linear configuration. The extension of the headland at both end is relative small on the order of 300meters, only affect a small area at the end where adopts a poorly curved form. The beach is oriented into the SSE (154°) with a length of 1100m.

Rotation Coefficient (RO)

Analysis of the rotation coefficient of the 17 coastlines demonstrates that Lloret del Mar was experience clockwise and an anticlockwise beach rotation. Positive values represented a clockwise rotation, the maximum value observed through the study (1986 to 2009) correspond to 3.8°, and a minimum value of -6.47°. The other values correspond to fluctuation rather than rotations. For example on May 2006, the entire embayment accretes about 10 meters (rotation coefficient of -3°).

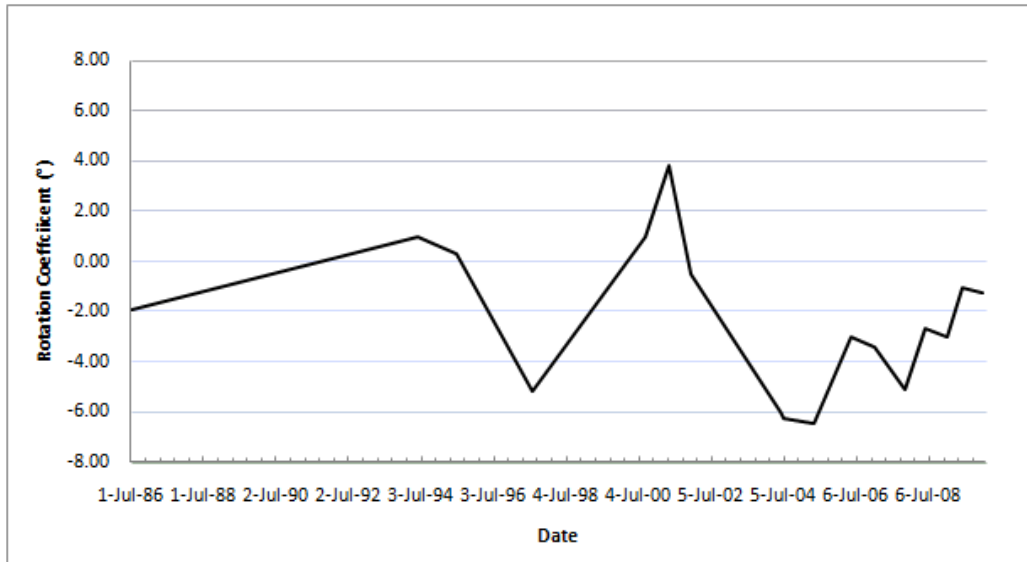


Figure 41 Evolution of the rotation coefficient, Lloret del Mar.

Theoretical Rotation Coefficient (RO_T)

From the 17 shoreline data three major configurations have been observed. Table 21 shows the values of the theoretical rotation coefficient and the percentage of occurrence during the study period.

The most common platform distribution was the configuration 1, which has been observed 4 times within the data. This configuration is characterized by a maximum width at the southern end on the order of 118 m that decrease progressive to the center and northern end 45 m to 15 m, correspondently. This was represented by the shoreline of April of 2005.

The second most common configuration is configuration 2; this platform distribution consisted in a more uniform beach width with values at the southern end of 72 m, at the center 45 m and at the southern end of 41 m. This configuration was shown in the shoreline of July 1986 and June 2008. But because we don't count with information from the wave condition of 2008 we cannot used in the analysis of wave forcing on the embayment presented below.

The last configuration corresponded to the configuration 3; this configuration has only been observed one time within the data. This corresponded to the beach leading to the north side. This distribution generates an increase in the beach width at the northern part on the order of 100 m, a retreat at the center of 15 meters and

at the southern end of 25m. Also increase the length of the beach 200m more at the northern end. This was observed in the shoreline of May 2001.



Figure 42 Theoretical Model of Lloret del Mar (Photo: Ortophotos 2008, ICC). Configuration 1, shoreline of April 27, 2004 (solid blue line), Configuration 2, shoreline of July 1st, 1986 (solid black line) and Configuration 3, shoreline May 1st, 2001 (solid red line).

Table 21 Theoretical Rotation Coefficient Lloret del Mar		
Configuration	Theoretical rotation coefficient	Number of observations *
C1	-5.0 to -6.7 ($r^2=0.90$ to 0.93)	4
C2	-1.9 to -2.7 ($r^2=0.92$ to 0.94)	3
C3	3.0 to 3.8 ($r^2=0.54$)	1

*From the 17 shorelines.

Waves Forcing on the Theoretical Model

Based on the theoretical model, the volume that needed to be exchange between configurations has been determined (e.g. from C1 to C2, C3 to C2, etc), the result are presented in table 22. The sub-aerial area that has been use to obtain the volumes correspond to the accretive area. Positive vales correspond to deposition at the north end; negative values correspond to deposition at the south end.

Table 22 Measured volume between configurations Lloret del Mar			
From To	ΔV_m [C1]	ΔV_m [C2]	ΔV_m [C3]
ΔV_m [C1]	-----	-128903	-315709
ΔV_m [C2]	125776	-----	-213247
ΔV_m [C3]	291144	182925	-----

The volumes were very similar (e.g. From C2 to C1 and backward). This implies that the system does not loose a significant amount of sand from this process, only redistributed along the beach.

Configuration C1

Four shorelines from the 17 shorelines presented a similar rotation coefficient to the one obtained from the theoretical model of the configuration 1 ($RO_T = -5.5$ to -5.8). Therefore, six combination of wave condition has been obtained. The bold values from the table correspond to the representative shoreline (April 2005).

Before the configuration 1, the beach could experience a configuration 2 or 3. For this reason, both alternatives were study. It has been observed that to achieve a configuration 1 coming from a configuration 2 or 3; SE and SSE directions (ranges from 124° to 168°) were needed. The cumulative mean of the longshore sediment rate presented a wider range of values; the higher values corresponded to $7286\text{m}^3/\text{yr}$, $7691\text{m}^3/\text{yr}$ and $8986\text{m}^3/\text{yr}$.

Table 23 Wave condition that generates configuration 1, Lloret del Mar					
From	Time (Days)	H_s Mean (m)	T Mean (s)	Φ Mean (°)	Q Cumulative Mean (m ³ /yr)
C2	14	0.30	4	144	-4121
	5	0.33	6	151	-3494
	9	0.67	7	160	-5418
C3	15	0.32	4	143	-8986
	5	0.34	6	143	-7691
	3	0.59	6	153	-7286

Figure 43 shows the wave condition for the representative shoreline date, it has been observed that three days before the 27 of April were needed to experienced a larger sediment movement to the south (cumulative mean wave condition: H_s 0.59m, T_s 6 s), while it required 9 days to achieve a less exchange volume (C2 to C1) and obtain a sediment movement directed to the south (cumulative mean wave condition: H_s 0.67m, T_s 7 s).

During this previous month there was only one significant event with a maximum significant wave height of 2.5m that generated a south directed sediment movement.

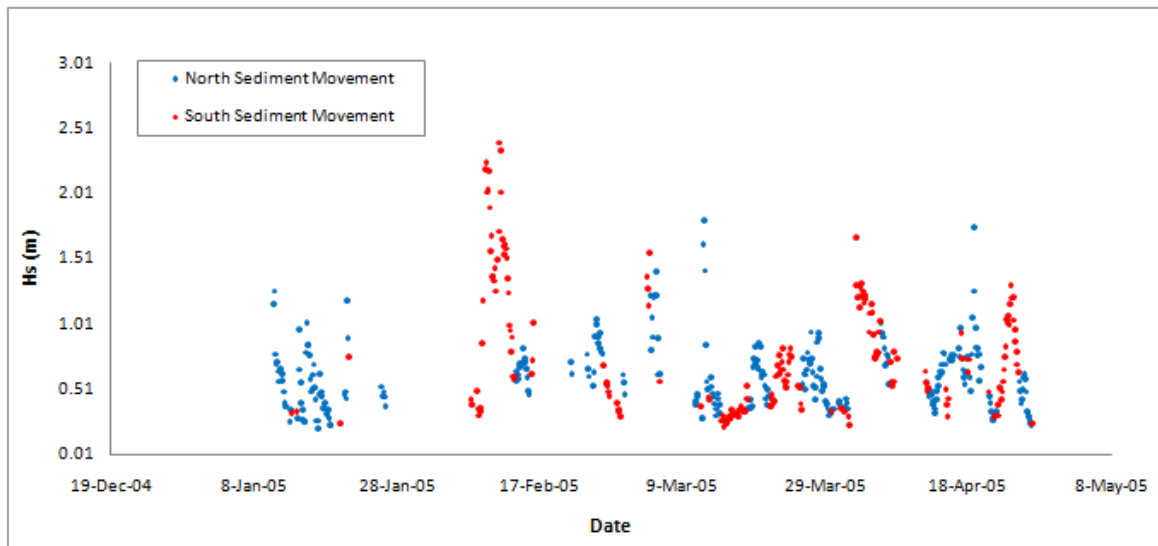


Figure 43 Wave condition during and shoreline effect at Lloret del Mar (Configuration 1), 1 April 2005.

Configuration C2

Only one wave conditions was obtained. This configuration corresponded to the more uniform platform distribution ($RO_T = -1.9$ to -2.7). In the same context, that the previous analysis we need to evaluate the relation between configuration 1 (C1) and 3 (C3) to configuration 2 (C2).

A persistent wave condition with a direction of 170° (S) will generate an exchange volume between configurations 1 to 2. While a persistent wave condition with a direction of 150° (SSE) will generate an exchange volume between configurations 3 to 2. The time required to obtain an exchange of volume between configurations 1 and 2 was higher, this was because they were a cluster of wave height that generate a longshore sediment movement directed to the south before the survey of 1 July 1986, therefore to achieve the same volume a wider period of time was needed to stabilize this effect.

Both mean wave heights are on the order of 0.34 to 0.38 m, with a same wave period of 4s.

Table 24 Wave condition that generates configuration 2, Lloret del Mar					
From	Time (Days)	H_s Mean (m)	T Mean (s)	Φ Mean ($^\circ$)	Q Cumulative Mean (m ³ /yr)
C1	46	0.38	4	170	2417
C3	24	0.34	4	151	-5416

Figure 44, shows that on February of 1986 there was an event that generated a longshore sediment transport directed to the south, with a maximum value of 2.51m.

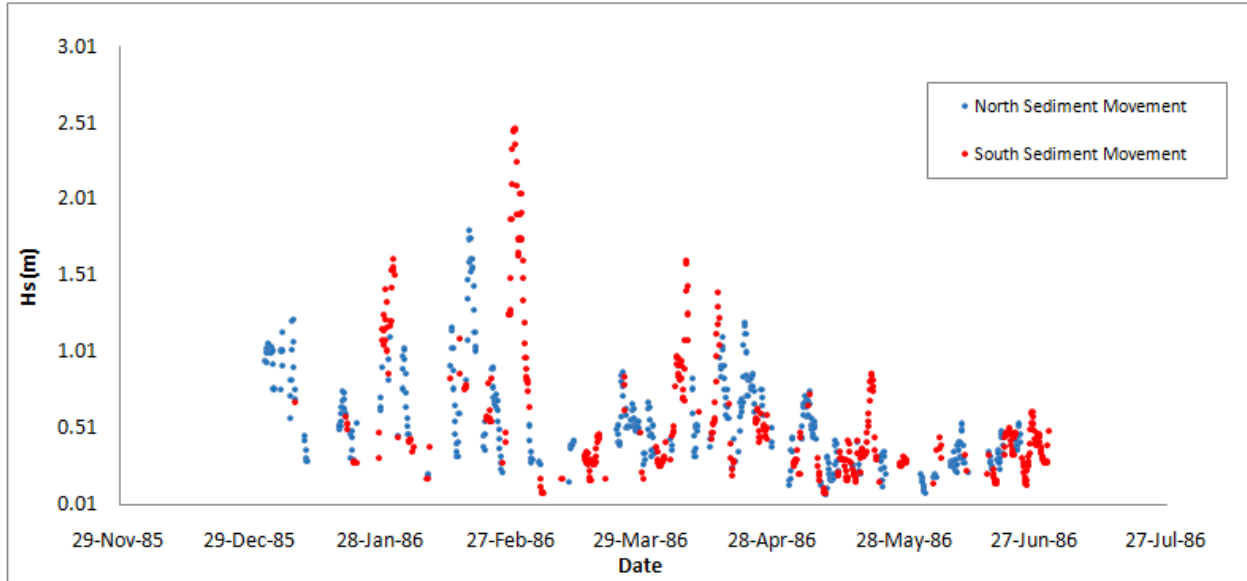


Figure 44 Wave condition during and shoreline effect at Lloret del Mar (Configuration 2), 1 July 1986.

Configuration C3

Finally, for configuration 3 ($RO_7=3.8$) the beach requires a wave condition coming from SW direction (ranges from 100° to 213°). A lower degree of direction was necessary to pass from C2 to C3, since the exchanged volume was lower than the one needed to pass from C1 to C3. The mean wave height corresponded to a value between 0.75 to 0.85m, with a period of 7 s. The cumulative longshore sediment rate varies between $6252 \text{ m}^3/\text{yr}$ and $6635 \text{ m}^3/\text{yr}$, the higher value corresponds to the second value, where the wave incident generate an angle of 44° between shoreline and the wave crest.

Table 25 Wave condition that generates configuration 3, Lloret del Mar

From	Time (Days)	H_s Mean (m)	T Mean (s)	Φ Mean ($^\circ$)	Q Cumulative Mean (m^3/yr)
C1	15	0.85	7	201	6252
C2	12	0.76	7	198	6635

Figure 45 shows a very different wave height condition during the previous months of the representative shoreline. During this period the beach experienced two events, the first event occurred on 26 of January with a wave maximum height of 2m and the second one occurred on March 1st with a maximum value of significant

wave height of 2.48m ($\varphi=205^\circ$). This differ from previous years on the direction, both events generate a sediment transport to the north.

Only a few wave conditions generate a sediment transport to the south. It was expected that an accumulation at the northern end occurred.

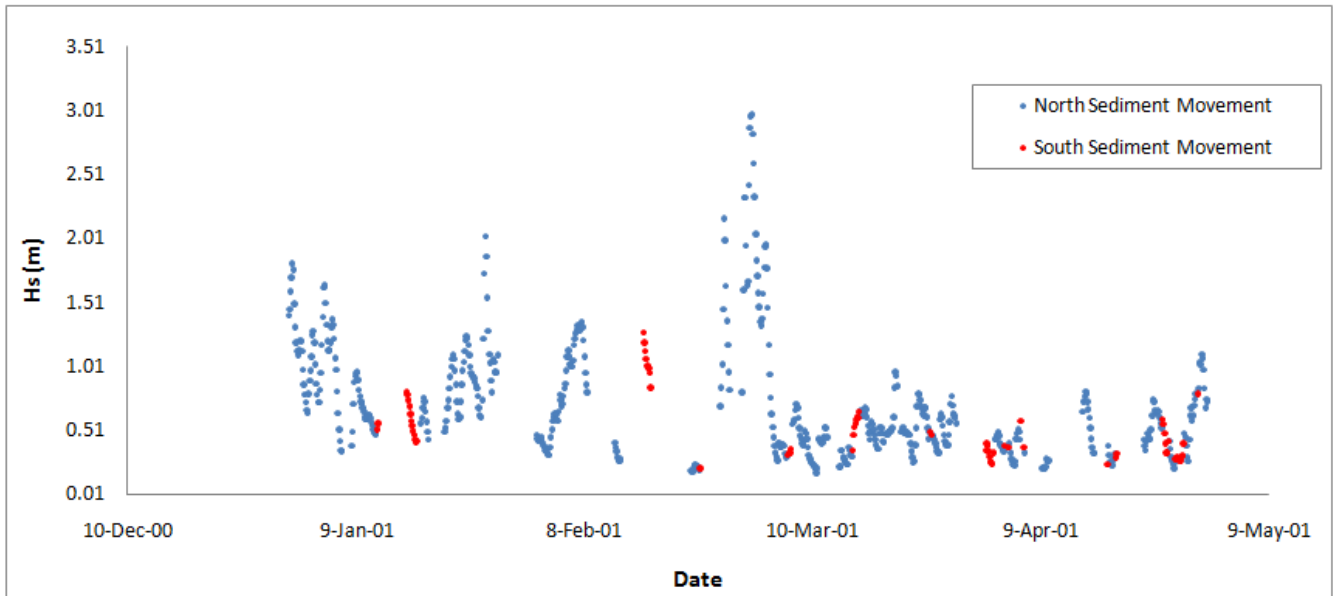


Figure 45 Wave condition and shoreline effect at Lloret del Mar (Configuration 3), 1May 2001.

5.2.4 Fenals Beach

Fenals was considered a reflective beach with a moderated curve platform distribution. The length of the beach is 731 m and is oriented towards the SSE (154°). The results for the analysis are presented below.

Rotation Coefficient (RO)

A data set of 17 coastlines has been used to analyze the evolution of the rotation coefficient. The results suggest that Fenals presented a high degree of rotation during the entire study period. The beach presented an anticlockwise rotation, negative values and a clockwise rotation, positive values of rotation coefficient.

The maximum clockwise rotation occurred two times during the 22 years of data on June 1994 and December of 2009 ($RO= 3.2$), while a maximum anticlockwise rotation only occurred one time on June 2004.

The evolution of the rotation coefficient was very similar to the one presented in Lloret del Mar, the only difference occur on August 1997, where Fenals presented a positive rotation coefficient and Lloret presented a negative rotation coefficient.

This could be attributed to the effect of the northern headland that attenuate direction from ENE and some of the E. While Lloret does not have this advantage since the length of the headland at the north is very small. Hence, the beach of Lloret del Mar response with an anticlockwise rotation and Fenals don't.

The values between these two extremes would correspond to fluctuation of the embayment, for example on July 1986 the entire embayment accretes at the southern end the beach width increase in 2 meters, while le northern part accretes 5 meters.



Figure 46 Evolution of the rotation coefficient, Fenals.

Theoretical Rotation Coefficient (RO_T)

During the study (22 years), three main configurations were differentiated. The first configuration corresponded to the beach tilted to the south, where the maximum width occurred on the order of 85 m, at the central part the beach width decreased to 48 m and at the southern end the lower value of beach width 28 m is presented.

This condition was observed 2 times during the study period and is represented by the shoreline of June 30, 2004.

The second configuration correspond a more uniform beach platform, this configuration occurred 3 times within the data. The configuration was characterized by a beach width of 57 meters at the southern and northern part, and at the central part a beach width of 48 meters.

Finally, the third configuration consisted in a beach rotating towards the north. At the southern end we observed a retreat of the shoreline resulting in a beach with of 46 m. Then there is a progressively increase of beach width of 50 m, 70 m and 75m while we moved to the northern end. The number of observations of this platform distribution was 3 times.

From the analysis we notice that configuration one was less frequent than the other two configurations, as mention before the headland at the northern end could generate this effect, since protect the beach from the most energetic direction (east), also in this area we observe that the most frequent direction correspond to the south.

The variation coefficient of the linear analysis of the RO_T presented a high correlation between the beach width and the alongshore location.

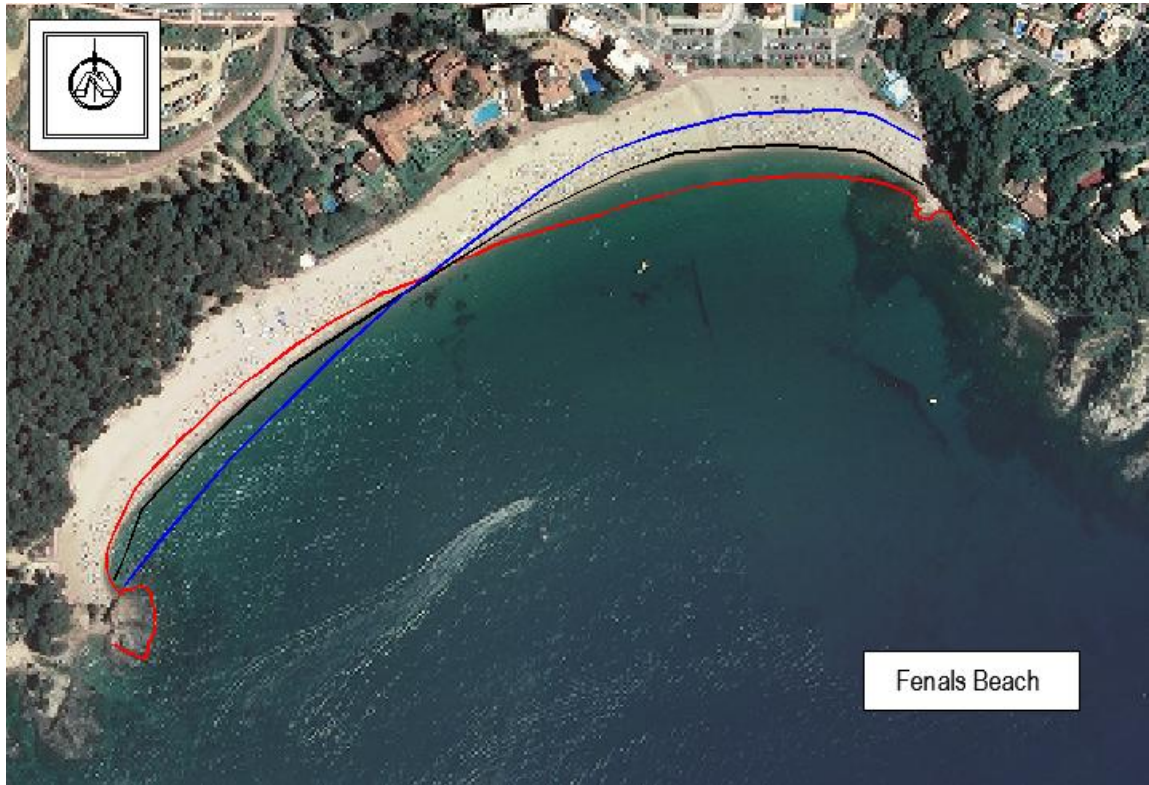


Figure 47 Theoretical Model of Fenals (Photo: Ortophotos 2008, ICC). Configuration 1, shoreline of June 30, 2008 (solid blue line), Configuration 2, shoreline of June 1st, 1995 (solid black line) and Configuration 3, shoreline July 1st, 1994 (solid red line).

Table 26 Theoretical Rotation Coefficient Fenals		
Configuration	Theoretical rotation coefficient	Number of observations*
C1	-5.0 to -6.5 ($r^2=0.87$ to 0.92)	2
C2	-0.4 to 0.6 ($r^2=0.40$)	3
C3	2.2 to 3.2 ($r^2=0.8$ to 0.9)	3

*From the 17 shorelines.

Waves Forcing on the Theoretical Model

Once the theoretical model has been identified, the calculation of the exchanged volume can be performed. Table 27 shows the result of the measured volume. There was a significant variation between volumes (e.g. between C1 to C3 and backwards). Headland bypassing might be occurring in this case since the southern headland does not have a sufficient length to accumulate the sediment.

From To	ΔV_m [C1]	ΔV_m [C2]	ΔV_m [C3]
ΔV_m [C1]	-----	-69947	-86253
ΔV_m [C2]	80507	-----	-20080
ΔV_m [C3]	134868	55354	-----

The results of the analysis are presented below.

Configuration C1

Similar to the analysis performed to Lloret del Mar, to study the wave condition required to achieve a beach setup with an anticlockwise rotation a RO_T of -5 to -6.5 (C1) we need to evaluate if the previous configuration correspond to a beach tilted to the north (C3) or to a more homogeneous platform (C2).

The bold numbers correspond to the values of representative shoreline June 2004. The result suggested that wave conditions coming from the SE to the SSE direction (range from 123° to 168°) generated a longshore sediment transport to the south. The mean wave height presented a value of 0.25 to 0.33m and the mean period vary from 5 to 6 s. More time was needed to observe a response in the beach from the lower wave height and period.

From	Time (Days)	H_s Mean (m)	T Mean (s)	Φ Mean ($^\circ$)	Q Cumulative Mean (m ³ /yr)
C2	5	0.32	6	150	-3412
	15	0.25	5	125	-2761
C3	5	0.33	6	150	-3412
	14	0.25	5	135	-2865

Figure 48 indicates that during the beginning of the year only one storm event occur. The maximum significant wave height was 4m and occurred on April of 2004. This storm generated a longshore sediment movement to the south, also consistent with the configuration 1. The storm presented an eastern direction ($\varphi=94^\circ$).

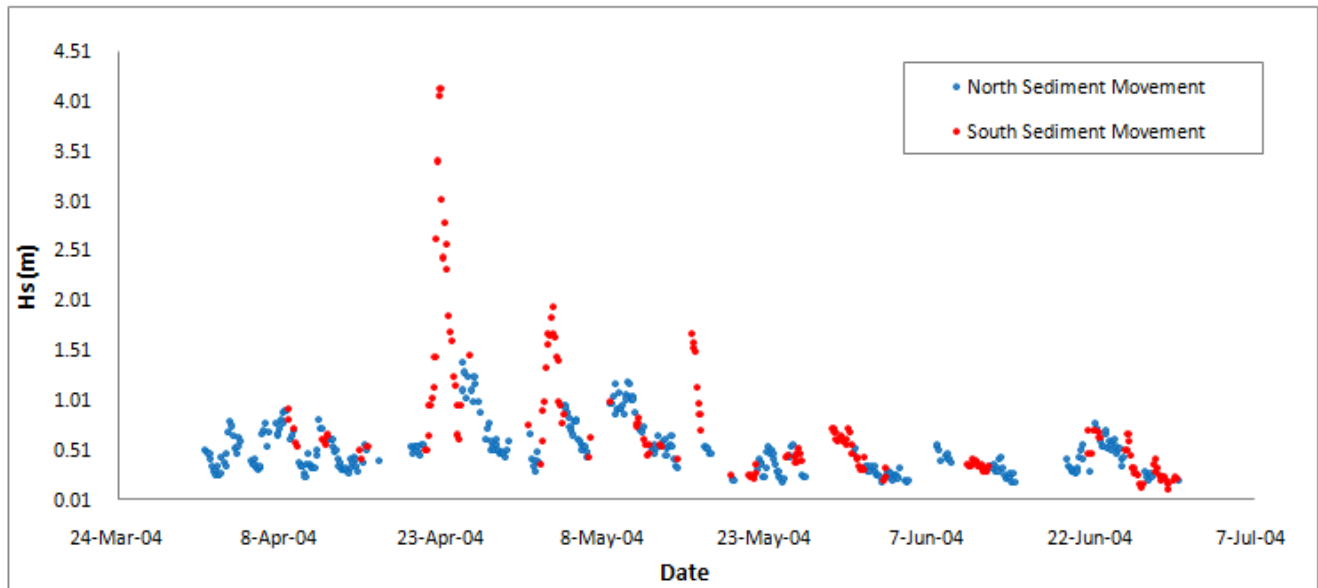


Figure 48 Wave condition and shoreline effect at Fenals (Configuration 1), 30 June 2004.

Configuration C2

Since there is a gap of wave data from 2006, the wave condition that will be presented correspond to the next representative shoreline for configuration 2, which is July 1 1995. The RO_T of this configuration varies from -0.4 to 0.6° .

For the second beach setup, we evaluated both extreme conditions a beach tilted to the north (C3) and tilted to the south (C1). To achieve configuration 2 from configuration 1, the beach required a wave condition coming from the SSE and SSW direction (range from 146° to 213°). While to obtain a configuration 2 from configuration 3 the directions of approach of the wave condition were from ESE to SSE (range from 101° to 146°).

The mean wave height and mean period presented a low variability between the different combinations ($H_s=0.30$ to 0.44 , $T=4s$). The first condition presented the higher time to achieve an exchange volume between C1 to C2, and presented a lower value of longshore sediment transport rate. This could be the effect of clusters

of wave condition that generated a south movement of sediment, so to achieve a north sediment movement it would required more time until a cluster of wave condition produced this sediment transport movement.

Another important aspect was the angle that was evaluated in the formula of sediment transport rate (difference between wave direction and the shoreline orientation, $\varphi-\theta$), if the value is around 40° and 45° the maximum longshore rate will be experienced. This was consistent with the sediment rate generated from the direction coming from 190° to 195° . But not with the one generated by the direction from 145° and 147° .

Table 29 Wave condition that generates configuration 2, Fenals					
From	Time (Days)	Hs _{Mean} (m)	T _{Mean} (s)	Φ _{Mean} (°)	Q _{Cumulative Mean} (m ³ /yr)
C1	37	0.35	4	162	4131
	6	0.30	4	193	14219
	5	0.32	4	194	50171
C3	6	0.32	4	142	-9231
	5	0.44	5	147	45973
	3	0.35	4	145	-15992

Five events occurred during January and July of 1995. Three of this five event generated a longshore sediment transport to the north, the first event took place on December 31, 1994 with a maximum wave height of 1.5m ($\varphi=199^\circ$), the second event happened on January, 17 1995 with a wave height of 1.87m ($\varphi=198^\circ$) and the third event occurred on March 7, 1995 with a wave height of 1.77m ($\varphi=195^\circ$). The other two events generated a sediment transport to the south, with a wave height of 2m on March 10, 1995 ($\varphi=121^\circ$) and 1.44m on June, 25 1995 ($\varphi=100^\circ$).

This appears to be consistent with the beach setup that has a more uniform behavior.

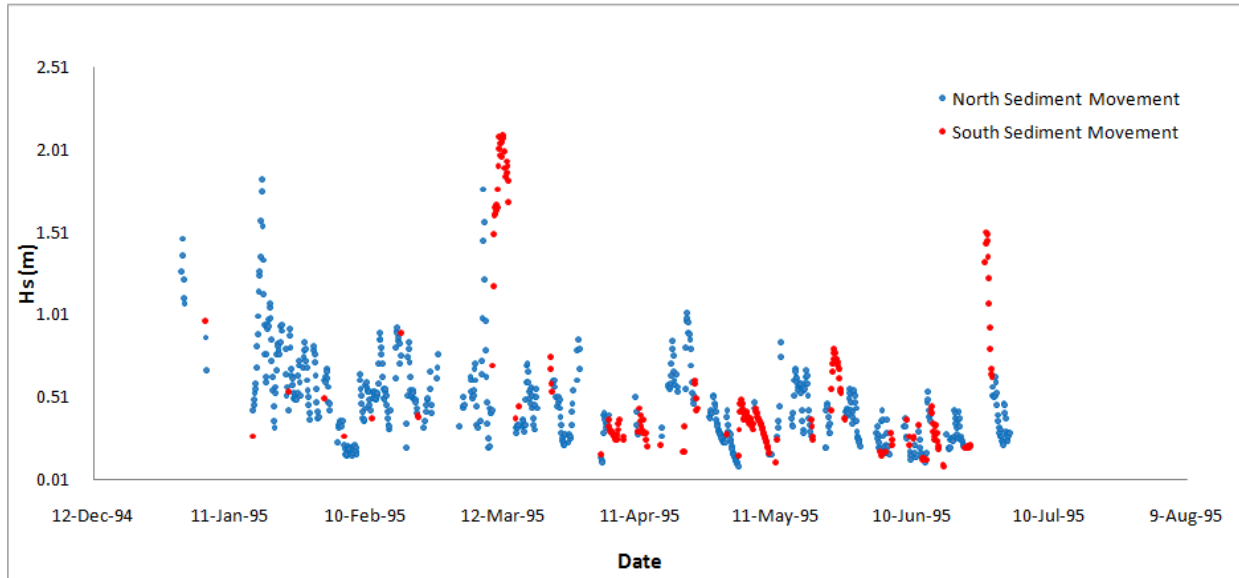


Figure 49 Wave condition and shoreline effect at Fenals (Configuration 2), 1 July 1995.

Configuration C3

The results for obtained a clockwise rotation ($RO_T=2.2$ to 3.2) of the shoreline (C3) suggested that S directions (ranges from 169° to 191°) were needed.

The mean wave height does not vary along the condition, either the mean wave period. The cumulative longshore sediment rate for all the conditions seems consistent with the time needed to achieve an exchange volume. The time of respond of the beach was very different, this was due to the wave distribution prior the date of the study shoreline.

Table 30 Wave condition that generates configuration 3, Fenals

From	Time (Days)	Hs _{Mean} (m)	T _{Mean} (s)	Φ _{Mean} (°)	Q _{Cumulative Mean} (m ³ /yr)
C1	14	0.36	4	178	26335
	20	0.37	5	163	10185
	8	0.38	4	166	4360
C2	12	0.35	4	168	20206
	19	0.20	4	179	7784
	7	0.38	4	177	3665

The wave condition during 1994, suggested that there was a tendency to generate an accumulation of material at the northern end of the beach. Three events occurred with the same tendency and with a wave height of 3m for the first storm ($\varphi=200^\circ$), 2m for the second ($\varphi=199^\circ$) and third storm ($\varphi=198^\circ$). The events took place before March 1994.

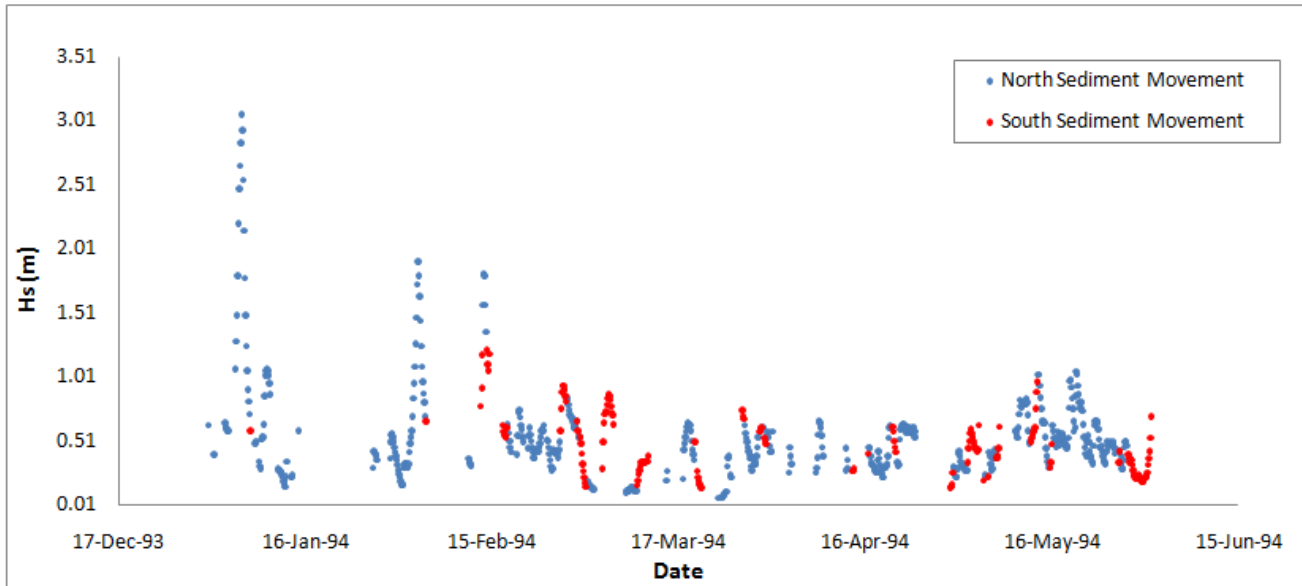


Figure 50 Wave condition and shoreline effect at Fenals (Configuration 3), 1 June 1994.

5.2.5 Bogatell Beach

Bogatell was considered an intermediate barred beach with a curved platform distribution. The beach is oriented towards the SE (130°) and has a length of 600m.

Rotation Coefficient (RO)

The analysis of the evolution of the rotation coefficient took place from 1994 to 2009 (18 coastlines). During this period it has been observed that Bogatell was experience anticlockwise/clockwise rotation (negative /positive slope of rotation coefficient). The beach presented the higher clockwise rotation on August 1, 2009 ($RO=4.3^\circ$) and the higher anticlockwise rotation on June 8, 2007 ($RO= -1.5^\circ$).

During the rest of the time the beach as experience oscillation with a RO of -0.3 to-0.6, for example of September 1, 2000 where the entire embayment erode between 2m and 6 m, at the northern and southern areas correspondently.

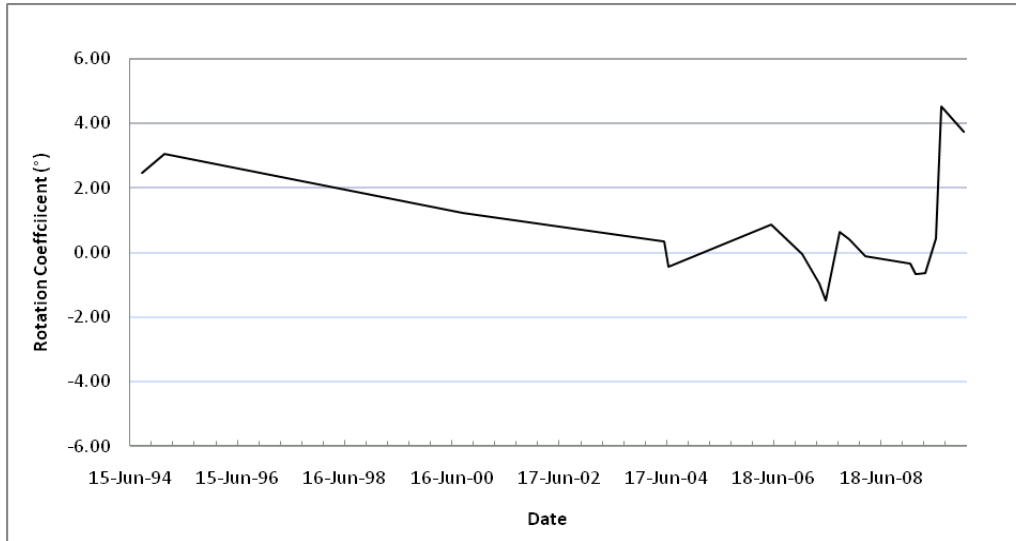


Figure 51 Evolution of the rotation coefficient, Bogatell. The rotation coefficient is illustrated in degrees. A positive slope indicates clockwise rotation.

Theoretical Rotation Coefficient (RO_T)

For this artificial beach three major configurations have distinguished. The three configurations have been observed 2 times within the data implying that this was a very dynamic beach.

The first configuration (RO_T=-0.9 to-1.4) that is represented by the shoreline of June 2007 was characterized by a beach width at the northern end of 25 m, at the center of 33m and at the southern end of 30 m. The second configuration (RO_T=0.3 to 0.6) corresponded to a more uniform shoreline distribution, similar to the presented for Lloret del Mar and Fenals. This configuration has a beach width at the northern end of 34m, at the center of 39m and at the southern end of 24m.

Finally, the third configuration corresponded to a clockwise rotation (RO_T=2.5 to 4.0). This beach setup has a width of 55m at the northern end, at the center of 48 m and at the southern en of 21m. This setup is represented by the shoreline of February, 1995.

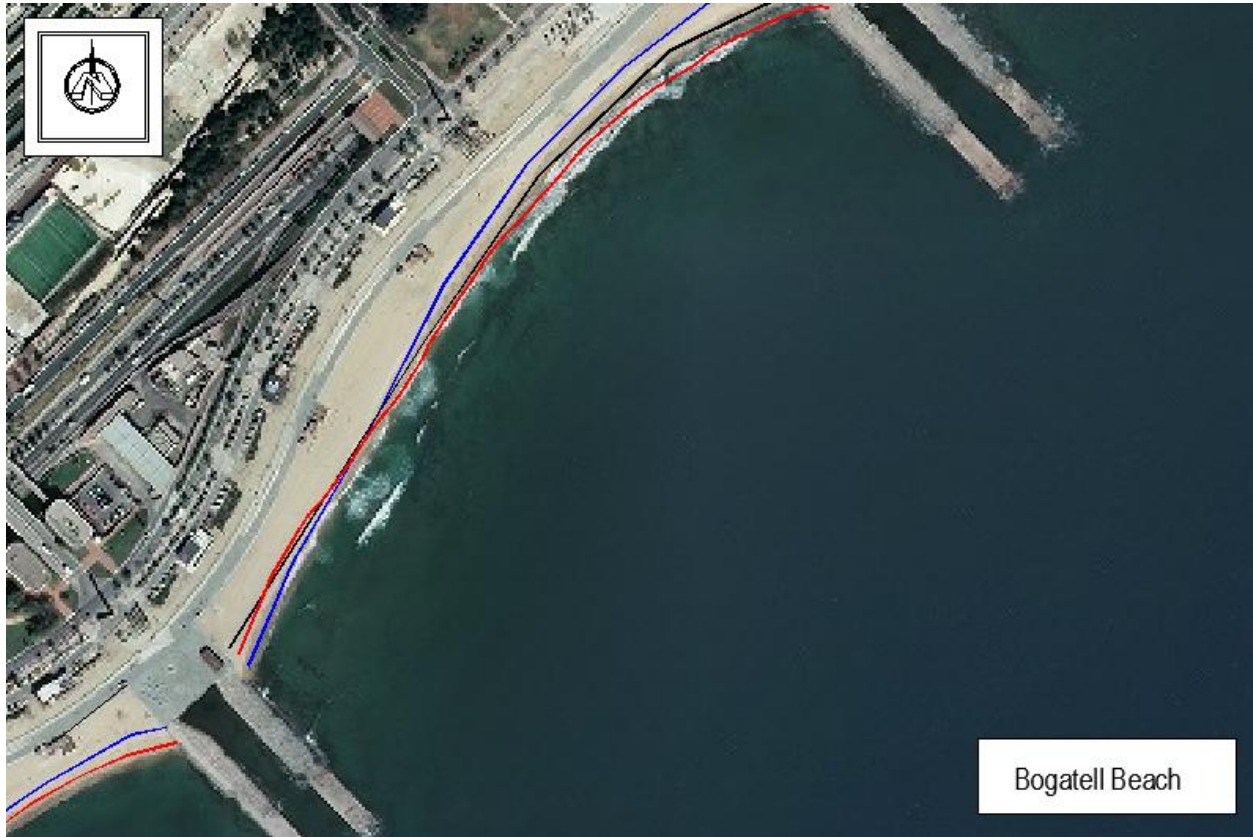


Figure 52 Theoretical Model of Bogatell (Photo: Ortophotos 2008, ICC). Configuration 1, shoreline of June 8, 2007 (solid blue line), Configuration 2, shoreline of November 15, 2007 (solid black line) and Configuration 3, shoreline February, 1995 (solid red line).

Table 31 Theoretical Rotation Coefficient Bogatell		
Configuration	Theoretical rotation coefficient	Number of observations *
C1	-0.9 to -1.4 ($r^2=0.2$ to 0.4)	2
C2	0.3 to 0.6 ($r^2=0.2$)	2
C3	2.5 to 4.0 ($r^2=0.6$)	2

*From the 18 shorelines.

Waves Forcing on the Theoretical Model

The following table presented the values of exchange volume for Bogatell beach. It was clear from figure 52 that the higher values of exchange volume occurred at the northern end. While at the southern end the volumes were lower.

As mention before Bogatell is a barred beach, therefore for this type of beach it was expected that wave energy were dissipated on the bar, the submerged sand bar can disturb the configuration of the shoreline

Table 32 Measured volume between configurations Bogatell

From To	ΔV_m [C1]	ΔV_m [C2]	ΔV_m [C3]
ΔV_m [C1]	-----	-15957	-11978
ΔV_m [C2]	13044	-----	-4149
ΔV_m [C3]	79678	64012	-----

Configuration C1

Result show that to obtain a configuration tilted to the south ($RO_T \sim -1.4$), the beach required waves approaching from the E and ESE direction (ranges from 79° to 123°). Bold number corresponds to values of the representative shoreline. Since configuration 2 and 3 move a very similar volume to configuration 1, it was expected to have also a similar wave condition. The mean wave condition corresponds to values between 0.35 to 0.45m with a cumulative mean period of 7 s. The combination of H_s , T and wave direction create a lower value of longshore sediment transport.

The wave condition during the previous moth of June 2007, reflect that four events occurs with a significant wave height higher than 2m of February, March and April. The events generate a southern directed longshore sediment transport, the storms correspond to Eastern events (see figure 53).

Table 33 Wave condition that generates configuration 1, Bogatell

From	Time (Days)	H_s Mean (m)	T Mean (s)	Φ Mean ($^\circ$)	Q Cumulative Mean (m3/yr)
C2 and C3	10	0.44	7	116	-11312
	6	0.35	7	119	-15438

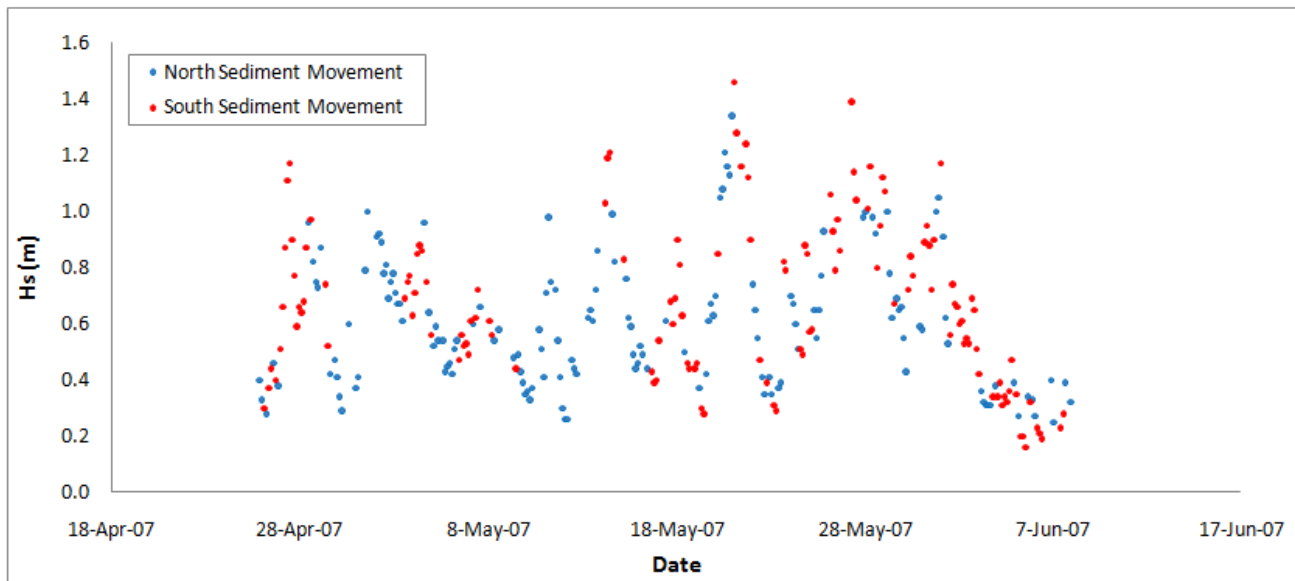


Figure 53 Wave condition and shoreline effect at Bogatell (Configuration 1), 8 June 2007.

Configuration C2

Form the analysis of the representative shorelines and those with similar configuration (e.g. theoretical rotation coefficient), the conditions required to move a volume of sand from the configuration C1 and C3 to C2 has been obtained. The wave information corresponds to mean wave climate.

Similar to other theoretical configuration, to obtain a RO_T of 0.3° to 0.6° , that characterize the configuration 2, the beach need to respond to waves coming from SE and SSE direction (ranges from 124° to 168°) if their previous configuration was C1. While, if the previous configuration was C3 the beach required waves coming from a lower direction ENE, E and ESE (ranges from 56° to 122°).

The combination of higher wave height (e.g. $H_s=0.6m$ and $0.4m$) and period (e.g. $T=6s$ and $8s$) also generate a higher longshore sediment transport ($Q=15034 m^3/yr$ and $-64308 m^3/yr$). Only one combination was generated (from C3 to C2) from the representative shoreline (bold values). The wave condition that generates this volume exchange presented the higher values, a mean wave height of $1.36m$ and period of $8s$. This condition also presented the maximum difference between the wave direction and the orientation of the shoreline around 43° . This implies that the sediment rate will be near the maximum.

Table 34 Wave condition that generates configuration 2, Bogatell					
From	Time (Days)	H _s Cumulative Mean (m)	T Cumulative Mean (s)	Φ Cumulative Mean (°)	Q Cumulative Mean (m ³ /yr)
C1	18	0.68	6	142	15034
	3	0.62	5	152	7180
C3	2	0.41	8	122	-64308
	1.5	0.31	5	116	-5484
	2	1.36	8	87	-687821

Figure 54 shows the condition and the shoreline effect of Bogatell during the previous months to November. The beach experienced several storms that generate longshore sediment transport to the south. The storm with higher values took place on August 27 ($H_s=2.07\text{m}$), on September 18 ($H_s=2.5\text{m}$) on October 20 ($H_s=3.1\text{m}$) and on October 24 ($H_s=2.3\text{m}$). All the storms presented an Easter direction.

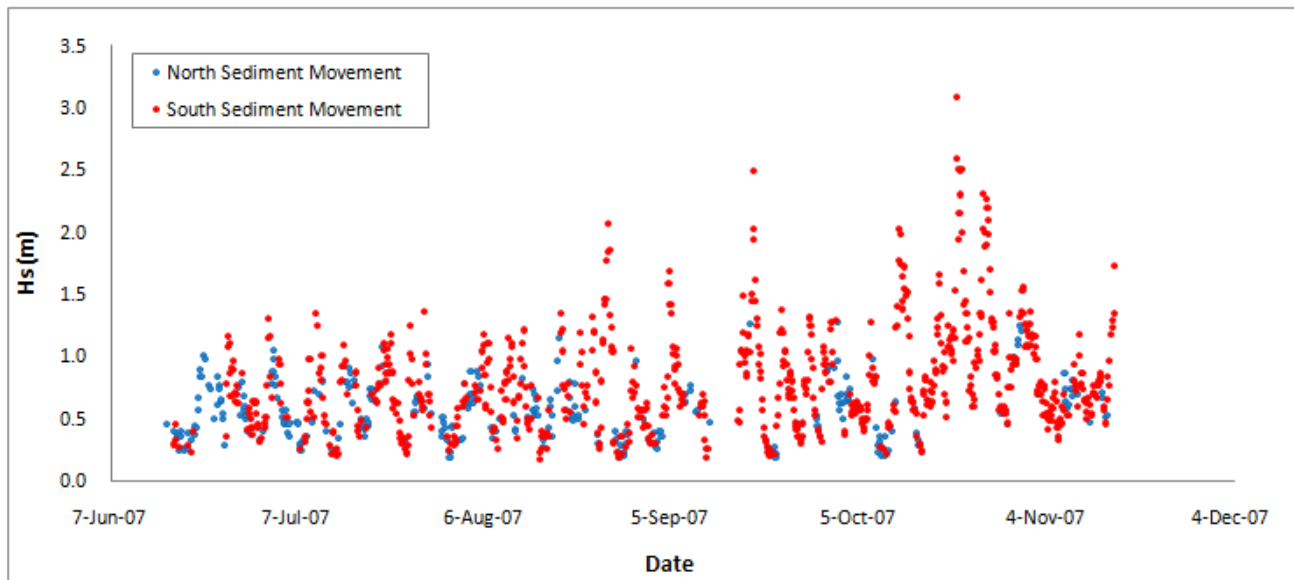


Figure 54 Wave condition and shoreline effect at Bogatell (Configuration 2), 15 November 2007.

Configuration C3

For the final configuration of Bogatell ($RO_T \sim 2^\circ$ to 4°), the results suggested that directions from SSE condition (ranges between 146° and 168°) will generate a sediment movement to the north, in response the shoreline will tilted to the north.

This direction corresponded to the specific wave condition, but direction coming from the SSE and SSW sector (ranges between 149° and 213°) will also generate a rotation of the beach.

Two different condition have been noticed, one with a lower mean wave height ($H_s=0.45m$) and the other with a higher value ($H_s=0.75m$) both with the same mean period of 6s. The sediment transport of the higher mean wave height differ from the lower mean wave heights, since during the previous months of that shoreline distribution the beach experience some waves coming from the East that generate a negative sediment transport and lower the cumulative value.

Table 35 Wave condition that generates configuration 3, Bogatell

From	Time (Days)	H_s Mean (m)	T Mean (s)	Φ Mean ($^\circ$)	Q Cumulative Mean (m ³ /yr)
C1	5	0.75	6	168	30377
	5	0.46	6	155	99359
C2	5	0.75	6	171	32645
	5	0.47	6	146	95218

Figure 55 exemplified the wave condition for the bold values. Before February 1, the beach experienced a cluster of wave state that generates a movement of sediment to the north. Only one event occurred with a value higher than 2 m on December 23, 1995 and presented an East direction.

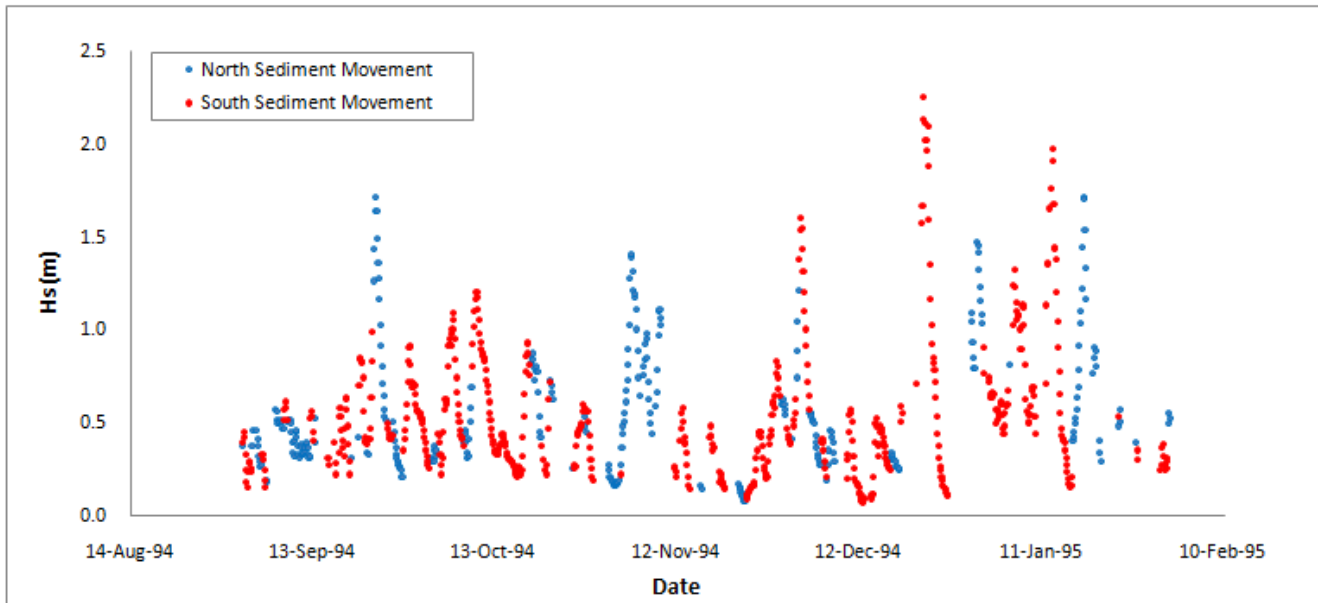


Figure 55 Wave condition and shoreline effect at Bogatell (Configuration 3), 1 February 1995.

5.2.6 Nova Icaria Beach

Nova Icaria is an artificial curved beach with a define shadow zone. This beach was defined in the previous chapter as an intermediate beach. The length of the beach is approximated 400m and is oriented towards the SE (136°).

Rotation Coefficient (RO)

A data set of 18 coastlines obtain from September of 1994 to December of 2009 has been used to analyze the presence of beach rotation at Nova Icaria beach. A rotation coefficient has been determined for the entire data set. Figure 56 show that Nova Icaria did not present a large degree of change; however there were rotation events at the end of the time series (2007 to 2008).

It is clear that the beach presented an anticlockwise rotation, since all the values of the RO are negative. A clockwise rotation was not observed during the study period.

This beach presented the higher values of rotation coefficient on the order of 10°. This was due to the existence of a promenade with a different alignment at the southern end, so in this area there were more sub-aerial beach

area (e.g. beach width), and generate a higher slope on the best fit line that it was use to fitted the shoreline (See figure 57).

The maximum value of an anticlockwise rotation corresponds to a RO of -9° , and the minimum value corresponds to a RO of -14° . Before 2007 and after 2008 relative flatter patter were observed, that indicate that beach oscillation was dominant and not beach rotation.

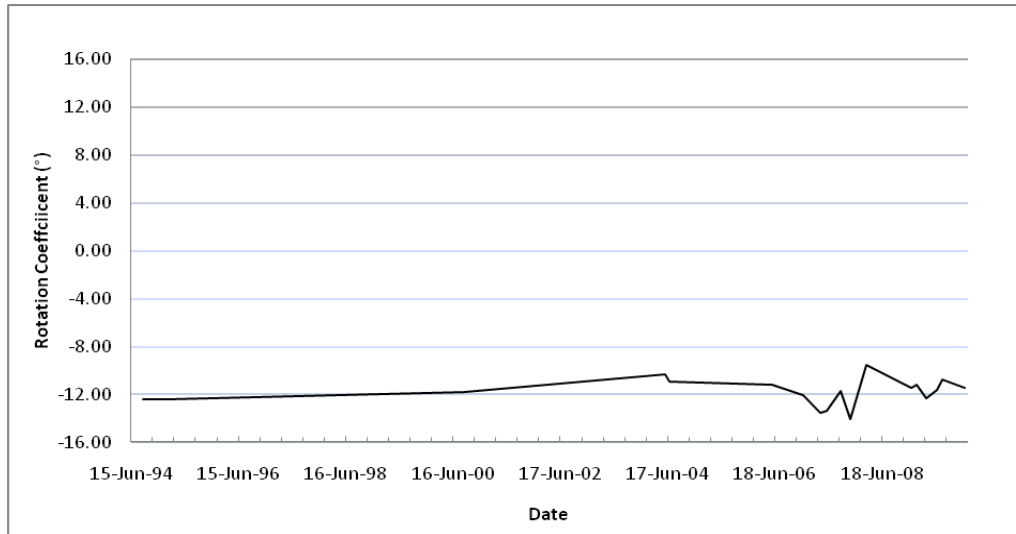


Figure 56 Evolution of the rotation coefficient, Nova Icaria. The rotation coefficient is illustrated in degrees. A positive slope indicates clockwise rotation.

Theoretical Rotation Coefficient (RO_T)

During the 8 years of shoreline data two main beach configurations were observed, this configuration will corresponded to the theoretical model of the beach.

The first configuration corresponded to the beach leaning to the south end (e.g. anticlockwise rotation, $RO_T = -13^\circ$ to -14°). The south section of the beach presented a maximum beach width of 98m, moving to the central part and northern part the beach width decrease and obtain a value of 55 m and 28m, correspondently. This configuration was presented three times during the study period and is represented by the shoreline of November 15, 2007.

The second configuration also corresponded to an anticlockwise rotation but with a lower RO_T coefficient on the order of -9.5° to 10° . For this beach setup the maximum beach width also corresponded to the southern sector

with a value of 88m, the central part maintain the same beach width of 55m and the northern part increase the beach width to obtain a final value of 38m. This distribution has been observed 2 times and the shoreline of March 1st, 2008 display the sub-aerial platform configuration.

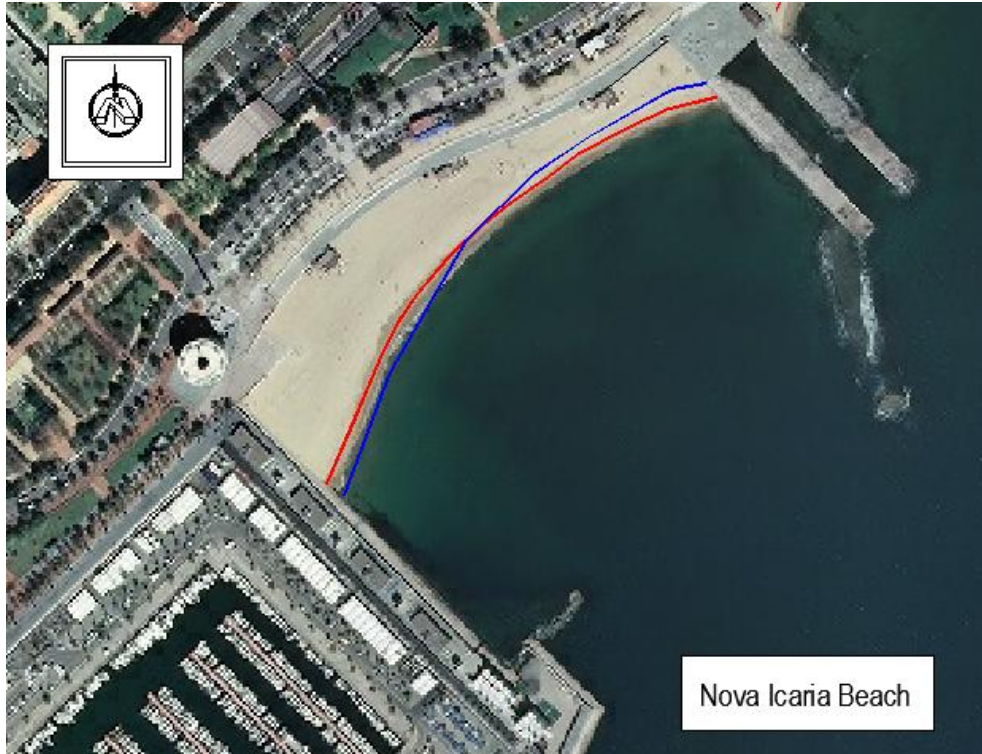


Figure 57 Theoretical Model of Bogatell (Photo: Ortophotos 2008, ICC) Configuration 1, shoreline of November 15, 2007 (solid blue line) and Configuration 2, shoreline of March 1st, 2008 (solid red line).

Table 36 Theoretical Rotation Coefficient Nova Icaria		
Configuration	Theoretical rotation coefficient	Number of observations *
C1	-13 to -14	3
C2	-9.5 to -10	2

*From the 18 shorelines.

Waves Forcing on the Theoretical Model

Based on the theoretical model of Nova Icaria, the volume exchange between configurations was calculated. Table 37 shows the result of the measured volume.

From To	ΔV_m [C1]	ΔV_m [C2]
ΔV_m [C1]	-----	-15020
ΔV_m [C2]	13595	-----

The differences between volumes were on the order of two thousand of cubic meters. The difference was associated with higher beach mobility at the southern end. While the northern end show lower beach mobility due to the effect of the protective structures located at the tip of the double dike.

Configuration C1

From the analysis of wave forces on the theoretical model, it has been determine that to achieve a higher anticlockwise rotation ($RO_T \sim -14^\circ$) the beach needs to experience a wave condition coming from the E to ESE (range from 79° to 132°).

The results suggest that a persistent wave condition within 4 to 5 days provides the optimum determination of beach response to the wave direction, and therefore a change in configuration. It was observed that the highest longshore sediment transport occurred to the representative shoreline (bold numbers); this data presented a significant wave height of 1.7m and presented the higher degree of direction approach (around 49°).

For the other conditions the values of mean wave height, mean wave period and direction approach were lower. This combination will generate a lower value of longshore sediment transport.

From	Time (Days)	H_s Mean (m)	T Mean (s)	Φ Mean ($^\circ$)	Q Cumulative Mean (m ³ /yr)
C2	4	0.41	6	137	-58535
	5	0.31	6	124	-18895
	5	1.31	7	87	-481345

Figure 58 shows the wave condition and its effects on the beach, it was clear that from September to November of 2007 the higher wave heights are presented, all approaching from the ENE and E.

During this period only a lower percentage of the waves generate a longshore sediment transport to the north.

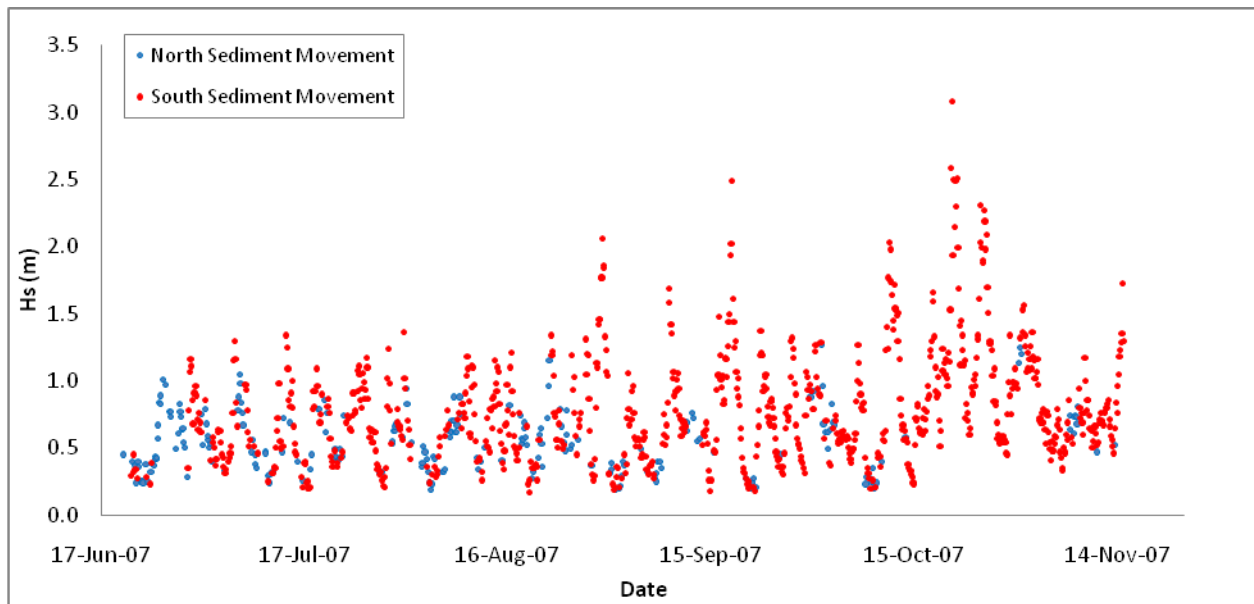


Figure 58 Wave condition and shoreline effect (Configuration 1) at Nova Icaria, 15 November 2007.

Configuration C2

The analysis has been performed to the shoreline of June 1st of 2004, since wave data from the period of 2008 to 2009 were not available. The shoreline of June 1st of 2004, presented a RO_T of -10° , this value fall in the classification of the theoretical model for configuration 2.

One combination have been determined, the time needed to achieve a lower anticlockwise rotation corresponded to 10 days, with a mean value of have height of 0.54m and period of 6s. The direction of approach was a 148° (SSE direction). The time needed generates a longshore sediment movement directed to the north of $64887\text{m}^3/\text{yr}$.

Table 39 Wave condition that generates configuration 2, Nova Icaria					
From	Time (Days)	Hs _{Mean} (m)	T _{Mean} (s)	Φ _{Mean} (°)	Q _{Cumulative Mean} (m3/yr)
C1	10	0.54	6	148	5278

Figure 59 presented the wave condition prior to June 1st of 2004. It was clear that the beach required 10 days to achieve exchange volume at their extremities. Just before the shoreline was measured there was a cluster of wave condition that generates a sediment movement to the south (8 days), on May 18 the wave condition generated a sediment movement to the north. This condition was the one that are reflected on table 39.

Six storm events occurred also during the previous months, with a wave height higher than 2 meters. Five of this storm presented a wave direction between 64° and 80°. One storm condition presented a wave direction of 200°.

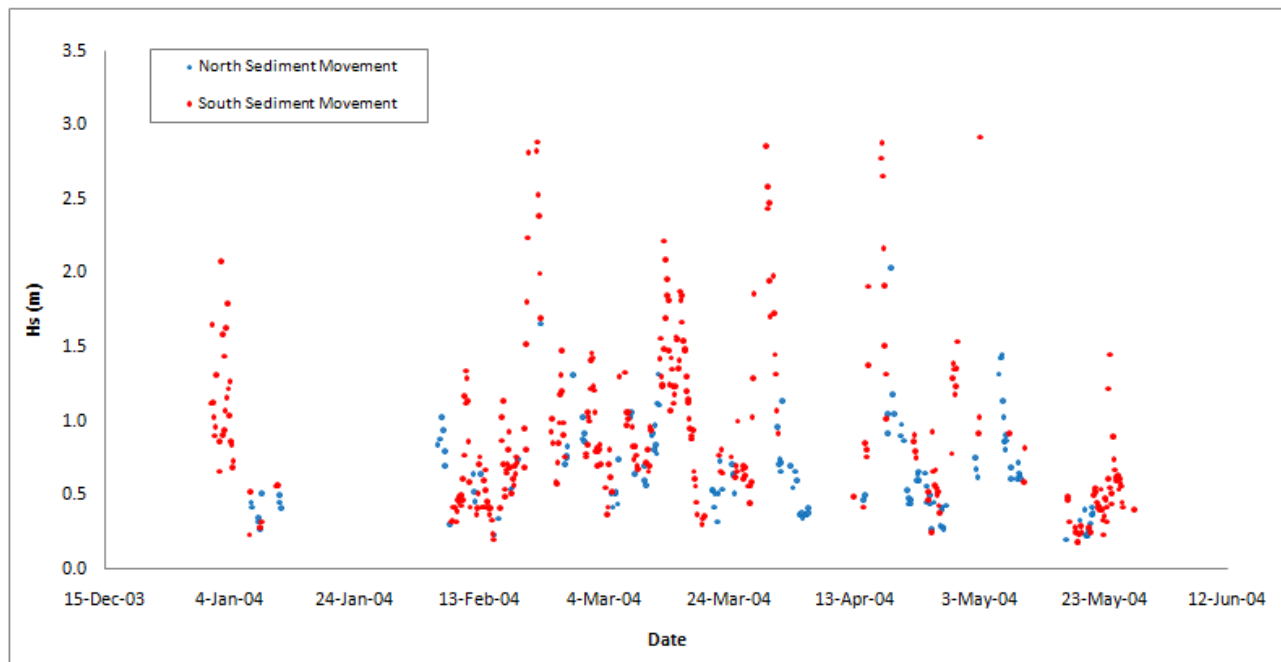


Figure 59 Wave condition and shoreline effect (Configuration 2) at Nova Icaria, 1 June 2004.

5.2.7 Barceloneta Beach

In a similar manner that the analysis of shoreline evolution was performed to Barceloneta, this analysis will be divided in two sections. The first section correspond to the configuration of the beach before 2006, when the beach as a length of 1.3km and was oriented toward the ESE (109°). The beach corresponds to a barred beach.

The second part of the analysis studies the configuration of the beach after 2006, where the effects of the offshore breakwater divide the beach in a north section and a south section. During this period the northern sector presented a length of 465m and the shoreline was oriented to the ESE (122°) and the southern sector presented a length of 924 m with and was oriented also to the ESE (104°).

A. Before 2006

Rotation Coefficient (RO)

Seven of the eighteen coast lines corresponded to the period before 2006. A rotation coefficient has been determined for each shoreline. The results are presented in figure 60, during this period a clockwise/anticlockwise rotation was occurring.

The maximum clockwise rotation generated a rotation coefficient of 1.8° and the minimum degree of rotation (anticlockwise) presented a value of -1.3°. The results showed that more negative values of rotation coefficient were observed than positive values. This suggests that the beach tend to accumulate more sediment to the southern end than the northern end. The lower values of RO, correspond to oscillation rather than rotation, for example on December of 2006 (RO=-0.85) the entire beach experience an accretive behavior with an increase of the beach width at the southern end of 40m and at the northern end of 7m.

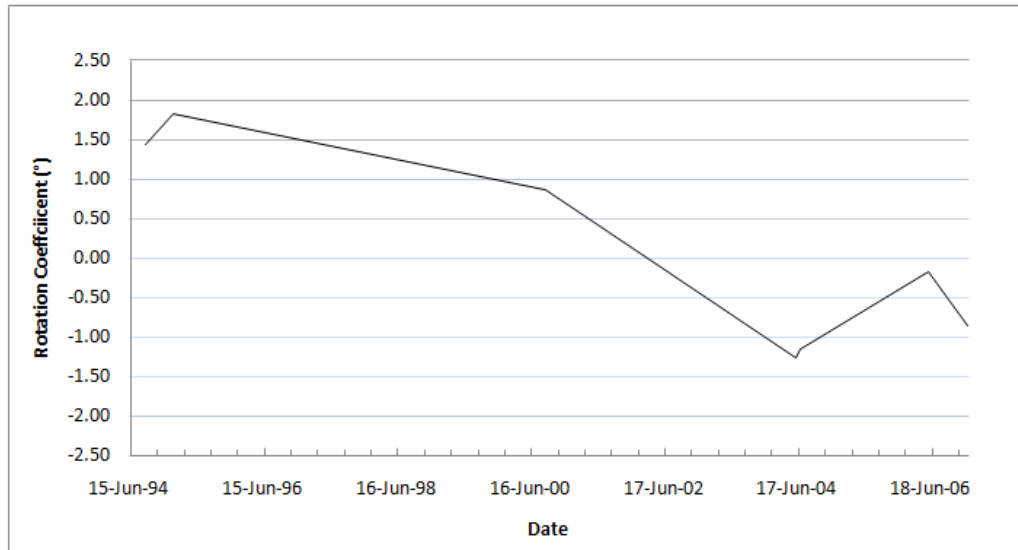


Figure 60 Evolution of the rotation coefficient, Barceloneta Before 2006. The rotation coefficient is illustrated in degrees. A positive slope indicates clockwise rotation.

Theoretical Rotation Coefficient (RO_T)

During this period a theoretical model has been identified. The model correspond to the three main configuration observed during 1994 to 2006.

The first configuration corresponded to an anticlockwise rotation ($RO_T = -1.3^\circ$), for this beach setup the maximum beach width correspond to the southern end with a value on the order of 46 m. In the central part values of 47m and 40m ($x=370$ m and 570m) has been observed, then the beach width decrease to obtain a width value of 25m and 14m ($x=800$ m and 900m).At the northern end the beach width as a value of 20 m. This configuration is represented by the shoreline of June 1st, 2004.

The second configuration corresponded to a more uniform beach distribution, this setup present a RO_T of 0.85° . It was characterized by a beach width at the northern end of 48m, and at the southern end of 17m. The central part located near the south present a beach width of 35m and 39m ($x=370$ m and 570m) and the one located near the north present a beach width of 31m and 28m ($x=800$ m and 900m). This shoreline distribution can be observed in figure 61 by a black line that correspond to the shoreline of September 1st, 2000.

The last configuration corresponded to a beach tilted to the north ($RO_T \sim 1.8^\circ$). This is represented by the shoreline of February 1st, 1995. The maximum beach width corresponded to the north end with a value of 67m; the southern end presented the lower beach width almost 2m. The locations of the center near the south had a beach width value of 51m and 48m ($x=370$ m and 570m) while the location located near the northern had lower value of 40m and 35m ($x=800$ m and 900m).

As mention before Barceloneta present a submerged bar morphology that was observe at the center locations near the south, this areas always presented a higher values of beach width. The effects of the bar reduce the H_b (wave breaking height) along this sector so the beach mobility was also reduced.



Figure 61 Theoretical Model of Barceloneta before 2006 (Photo: Ortophotos 2006, ICC) Configuration 1, shoreline of June 1st, 2004 (solid blue line), Configuration 2, shoreline of September 1st, 2000 (solid black line) and Configuration 3, shoreline February 1st, 1995 (solid red line).

The configurations 1 and 3 were observed 2 times within the shoreline data, while for configuration 2 was only observed 1 time. Higher correlations has been obtained from the relation of the beach width and the alongshore location for the theoretical model.

Table 40 Theoretical rotation coefficient Barceloneta Before 2006		
Configuration	Theoretical rotation coefficient	Numbers of Observations *
C1	-1.14 to -1.26 ($r^2=0.3$ to 0.4)	2
C2	0.85 ($r^2=0.3$)	1
C3	1.40 to 1.80 ($r^2=0.4$ to 0.5)	2

*From the 7 shorelines.

Waves Forcing on the Theoretical Model

The measured volumes were calculated for the theoretical model. Table 41 shows the values for all the configurations. The volume from C2 to C1, C3 to C2 and C3 to C1 corresponded to higher values, this was consistent with the fact that higher beach mobility occurs at the southern end. The sub-aerial area that was exposed between configurations is higher; hence a higher volume will be obtained.

Table 41 Measured volume between configurations Barceloneta Before 2006			
From To	ΔV_m [C1]	ΔV_m [C2]	ΔV_m [C3]
ΔV_m [C1]	-----	-75888	-81780
ΔV_m [C2]	45282	-----	-34466
ΔV_m [C3]	68407	12752	-----

Configuration C1

The result shows that to achieve a large degree of rotation ($RO_T \sim -1.3^\circ$); the beach should response to a wave climate coming from the E and ESE direction (range 79° to 113°).

The mean wave height and period correspond to values between 0.4m-0.5m with 5s -6s. The values suggest that 8 to 10 days are needed to observe a response in the coastline; regardless if the previous configuration was C2 or C3.

Table 42 Wave condition that generates configuration1, Barceloneta Before 2006					
From	Time (Days)	Hs _{Mean} (m)	T _{Mean} (s)	Φ _{Mean} (°)	Q _{Cumulative Mean} (m ³ /yr)
C2 and C3	10	0.53	6	113	-13894
	8	0.42	5	104	-56021

The longshore sediment transport rate for each condition was significant with a value on the order of 13390m³/yr for the 10 days and 56021m³/yr for the 8 days. Since the value corresponds to a cumulative sum it was expected that a longer time produced a lower rate, since both north and south directed condition are considered.

Figure 62 shows the shoreline effects from the wave conditions of the previous months to June, 2004. Before June, 2004 six storm events occurred during the first months of 2004. Five corresponded to direction from the East and one from the South.

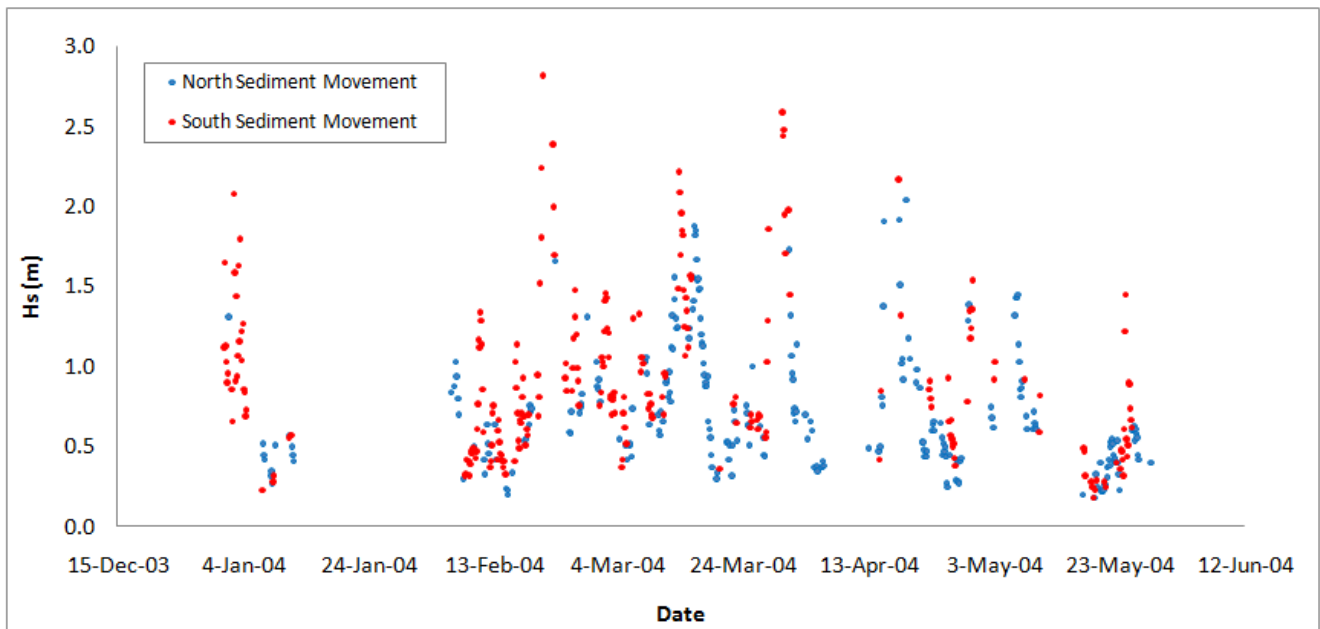


Figure 62 Wave condition and shoreline effect (Configuration 1) at Barceloneta before 2006, 1 June 2004.

Configuration C2

The results corresponded to the representative date of the shoreline. To achieve a more uniform configuration ($RO_T \sim 0.85^\circ$), the beach would have to experience two different wave conditions. If the platform distribution of the beach come from C1 (anticlockwise rotation) a mean wave condition with a H_s of 0.40m, T of 4s and a incoming direction from a 124° relative to the north (ESE) is required.

However, if the previous configuration of the beach was C3 (clockwise rotation), the mean wave condition needed will be a H_s of 0.35m, T of 4s and a incoming direction from a 95° relative to the north (E).

The result suggested that a longer time is needed to achieve configuration 2 from configuration 1 than from configuration 3. In this context, where the wave conditions are similar the effect of the direction on the longshore sediment transport is important. The maximum longshore sediment rate is achieved when the difference between the incoming wave and the shoreline orientation is near to 45° . This is consistent with the higher value obtained in the second condition (C3 to C2).

Table 43 Wave condition that generates Configuration 2, Barceloneta Before 2006

From	Time (Days)	H_s Mean (m)	T Mean (s)	Φ Mean ($^\circ$)	Q Cumulative Mean (m ³ /yr)
C1	20	0.40	4	120	3033
C3	4	0.35	4	95	-9265

Figure 63 shows that any storm with a value higher than 2m took place during the previous months to the configuration 2.

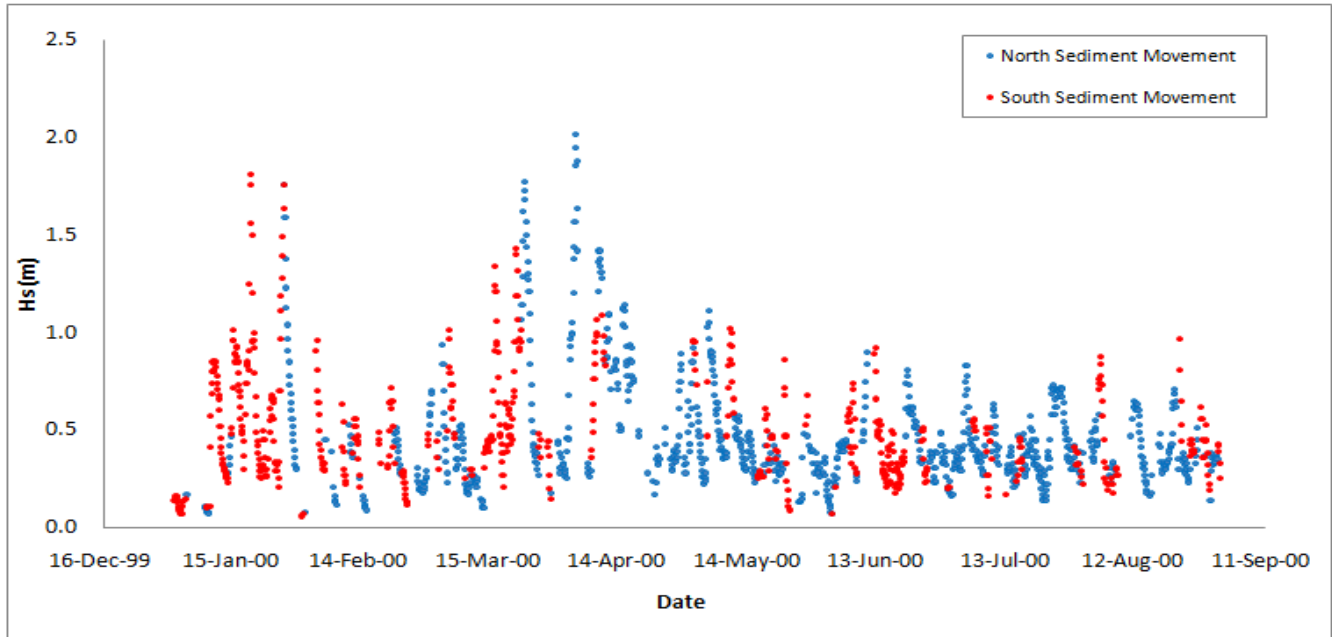


Figure 63 Wave condition and shoreline effect (Configuration 2) at Barceloneta before 2006, 1 September 2000.

Configuration C3

Four wave combinations have been obtained from the analysis of wave forcing on the embayment. The third configuration corresponded to the shoreline tilted to the north, so it is expected to observe in the resulting wave conditions direction that generates a longshore sediment transport to the north.

The outcome of the cumulative sum show that the mean direction to achieve a positive RO_T of 1.8° varies from 133° to 170° relative to the north (SE to S). The southern direction corresponded to the combinations of the configuration 1, since this require a larger volume exchange along the beach.

The maximum value of longshore sediment rate occurred on the first combination with H_s of 0.75m, T 6s and a difference between the incoming wave and the shoreline orientation of 44° , and the time needed for achieve the configuration 2 was of 11 day.

The lower value of longshore sediment rate occurred on the second combination with H_s of 0.55m, T 6s and a difference between the incoming wave and the shoreline orientation of 61° . The time needed in this case was 7 days.

Finally, for the last two combination that correspond to an exchanged volume between C2 to C3. The longshore sediment rate was similar, and also the mean wave height and period. The time in this case corresponded to 5 days.

Table 44 Wave condition that generates configuration 3, Barceloneta Before 2006					
From	Time (Days)	Hs _{Mean} (m)	T _{Mean} (s)	Φ _{Mean} (°)	Q _{Cumulative Mean} (m ³ /yr)
C1	11	0.75	6	153	31410
	7	0.55	6	170	23769
C2	5	0.73	6	140	26111
	5	0.41	6	133	25525

The bold values are represented in figure 64. Only one event occurred with a value higher than 2 m on December 23, 1995 and presented an East direction.

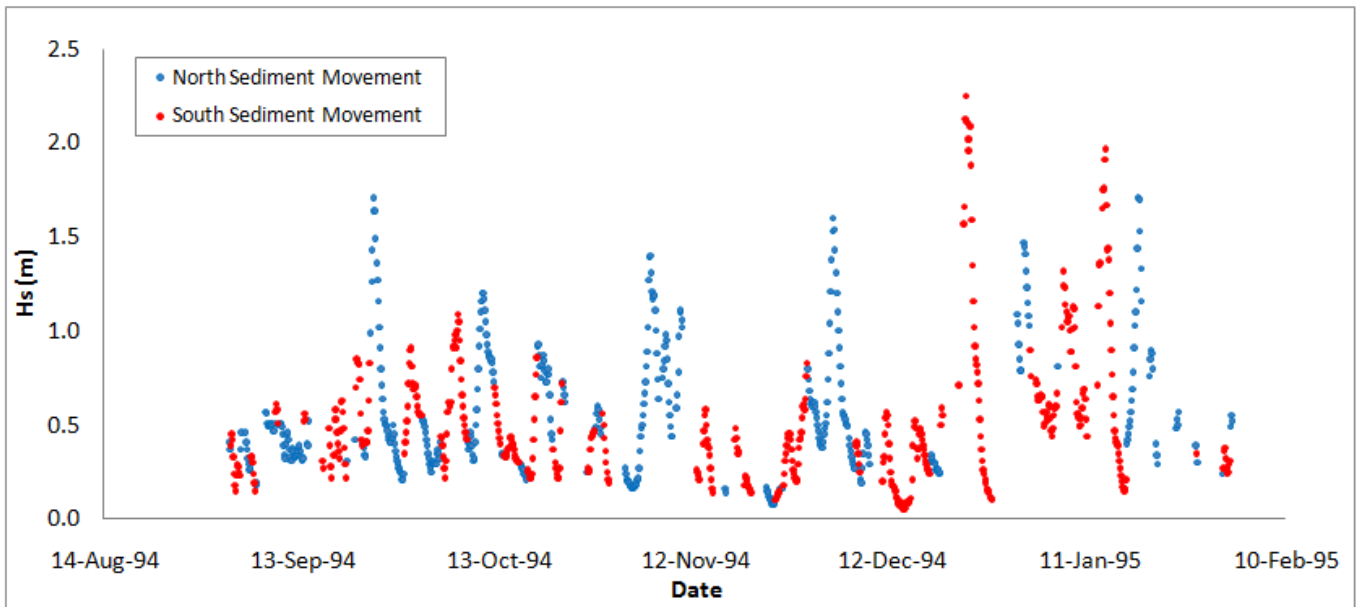


Figure 64 Wave condition and shoreline effect (Configuration 3) at Barceloneta before 2006, 1 February 1995.

B. After 2006

Rotation Coefficient (RO)

Eleven of the eighteen coast lines corresponded to the period after 2006. A rotation coefficient was determined for the shoreline data set. A significant different response was observed in the two section of the Barceloneta.

While the south section presented a clockwise rotation ($RO \sim 3.12^\circ$) on November 15, 2007 the northern part exhibits an anticlockwise rotation ($RO \sim -1.75^\circ$). This behavior was also observed on March, 2008 and on April 14, 2009. The different respond of the beach could be the effect generated by the submerged bars at the southern section. In figure 66, this bar morphology was prominent by white regions of wave breaking, while the north section shows no identification of waves breaking.

The maximum degree of rotation corresponded to a RO of 3.12° for the south section and 2.8° for the north section. The minimum degree of rotation for the northern section was -1.9° and for the south section -0.23° .

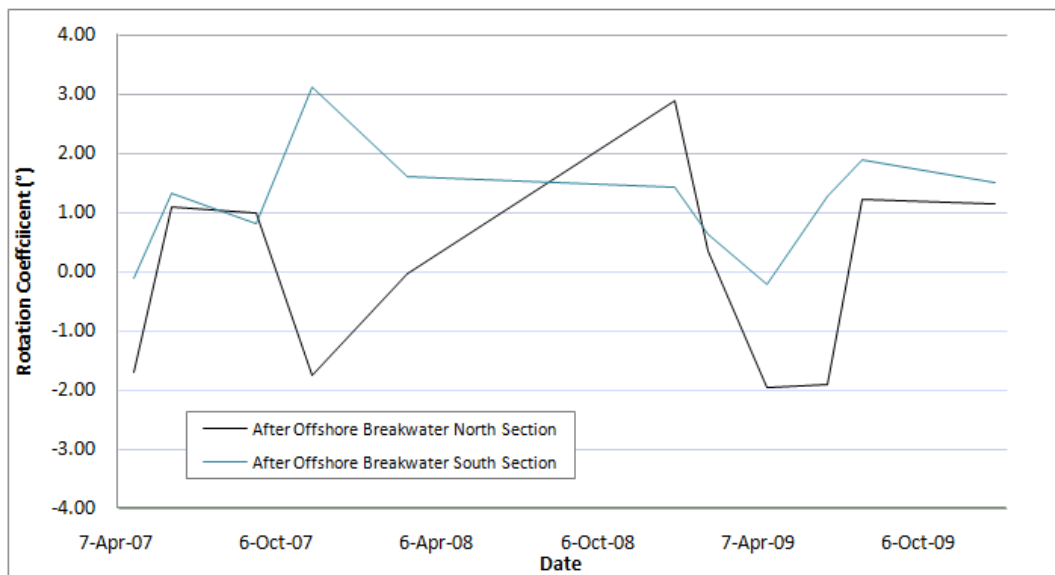


Figure 65 Evolution of the rotation coefficient, Barceloneta After 2006, north section (solid black line) and south section (solid blue line). The rotation coefficient is illustrated in degrees. A positive slope indicates clockwise rotation.

Theoretical Rotation Coefficient (RO_T)

Three main configurations were obtained from the analysis of the shoreline data set at each section of the Barceloneta. The results from the analysis are listed in table 45.

For the North section, the configuration 1 corresponded to a leaning shoreline to the south ($RO_T = -1.7^\circ$ to -1.9°), this was characterized by a beach width at the northern end (next to the Somorrostro dike) of 37m, at the center of 14m and at the southern end (next to the salient formation) of 46m.

The second configuration corresponded to a RO_T of $\approx 1.0^\circ$, for this setup the maximum beach width corresponded to 87m at the north, 52 at the center and 74m at the south. The third configuration presented a positive RO_T of $\approx 2.0^\circ$ to 2.8° , for this distribution the maximum beach width occur at the north with a value of 72 m, the lower value occurs at the center with 32m and at the south the beach width obtain a value of 56m.

For the South section, the first configuration also corresponded to an anticlockwise rotation but with a lower value of RO_T of $\approx -0.2^\circ$. This platform distribution presented the maximum beach width at the south (next to the Barcelona Harbor) on the order of 70m, which progressively decrease to the center until reach a value of 58m, and increase again to the south end (next to the salient formation) to obtain a value of 66m .

The second configuration is defined by a clockwise rotation with a RO_T of $\approx 1.2^\circ$ to 1.3° . In this configuration the northern end presented a beach width of 77m and the south end 55m. At the central area a beach width of 56m was observed. Finally for the third configuration that corresponded to the highest clockwise rotation (RO_T of $\approx 3.12^\circ$), the maximum beach width was observed at the north with a value of 97m, the central part and the south end presented the same width on the order of 40 m.

It is evident that the areas located next to the salient formation do not show a high degree of beach mobility since this sector will have a low wave activity and a reduced sediment transport capacity so the material will be deposited in the shadow zone rather than be carried away.



Figure 66 Theoretical Model of Barceloneta after 2006 (Photo: Ortophotos 2008, ICC) North Section: Configuration 1, shoreline of December 30, 2008 (solid blue line), Configuration 2, shoreline of December 31, 2009 (solid black line) and Configuration 3, shoreline June 23, 2009 (solid red line). South Section: Configuration 1, shoreline of November 15, 2007 (solid blue line), Configuration 2, shoreline of June 23, 2009 (solid black line) and Configuration 3, shoreline April 14, 2009 (solid red line).

Configuration 1 is the most common setup of the entire data set of the North section with a appearance of 4 times within the data, followed by configuration 2 with only 2 observations and configuration 3 presented the lower value, with only 1 observation. The variation coefficient of the RO_T of this section was not strong ($r^2=0.1$).

In the South section, configuration 1 and 2 were observed 2 times, whereas the configuration 3 was observed only 1 time. For this section the variation coefficient present a higher correlation than the north section ($r^2=0.1$ to 0.4).

Table 45 Theoretical rotation coefficient Barceloneta After 2006				
Configuration	Theoretical rotation coefficient		Numbers of observations *	
	North Section	South Section	North Section	South Section
C1	-1.7 to -1.9 ($r^2=0.10$)	-0.1 to -0.2 ($r^2=0.10$)	4	2
C2	0.90 to 1.2 ($r^2=0.10$)	1.2 to 1.3 ($r^2=0.2$)	2	2
C3	2.0 to 2.8 ($r^2=0.10$)	3.0 to 3.12 ($r^2=0.4$)	1	1

*From the 11 shorelines.

Wave Forcing on the Theoretical Model

Due to the lack of information from 2007 to 2009, the analysis for the North section has only been performed for the configuration 1 and 2. Configuration 3 has only been observed once on 2009. For the South section, the three configurations have been studied.

Table 46 shows the result of the measured exchange volume for both sections. Negative values corresponded to deposition at the southern end. For the North section we observed a similar exchange volume, while for the south section the higher values corresponded to a volume deposition at the southern end.

Table 46 Measured volume between configurations Barceloneta Before 2006						
To \ From	North Section			South Section		
	ΔV_m [C1]	ΔV_m [C2]	ΔV_m [C3]	ΔV_m [C1]	ΔV_m [C2]	ΔV_m [C3]
ΔV_m [C1]	-----	-16365	-26636	-----	-55594	-111899
ΔV_m [C2]	12861	-----	-13212	13974	-----	-52425
ΔV_m [C3]	22726	9259	-----	37132	29422	-----

North Section

Configuration C1

Two conditions have been obtained for the configuration 1. Results show that to obtain a negative RO_T (-1.7° to -1.9°), the beach need to respond to wave condition with an ESE incident direction (range between 101° and 123°), regardless in the previous configuration was C2 or C3.

The time obtained from the study suggested that the respond of the beach was in days (2 to 3), if the mean condition presented on table 46 persisted. Both condition had a similar longshore sediment rate, since presented very similar wave conditions ($H_s=0.87$ to $0.97m$ and $T=7s$).

Table 47 Wave condition that generates configuration 1, Barceloneta Before 2006 North Section					
From	Time (Days)	H_s Mean (m)	T Mean (s)	Φ Mean (°)	Q Cumulative Mean (m ³ /yr)
C2	2.5	0.97	7	110	-77450
C3	2.5	0.87	7	110	-77433

The wave conditions for the representative shoreline are illustrated on figure 67. It can be observed that most of the events with wave height higher than 2m generated a south directed movement of sand.

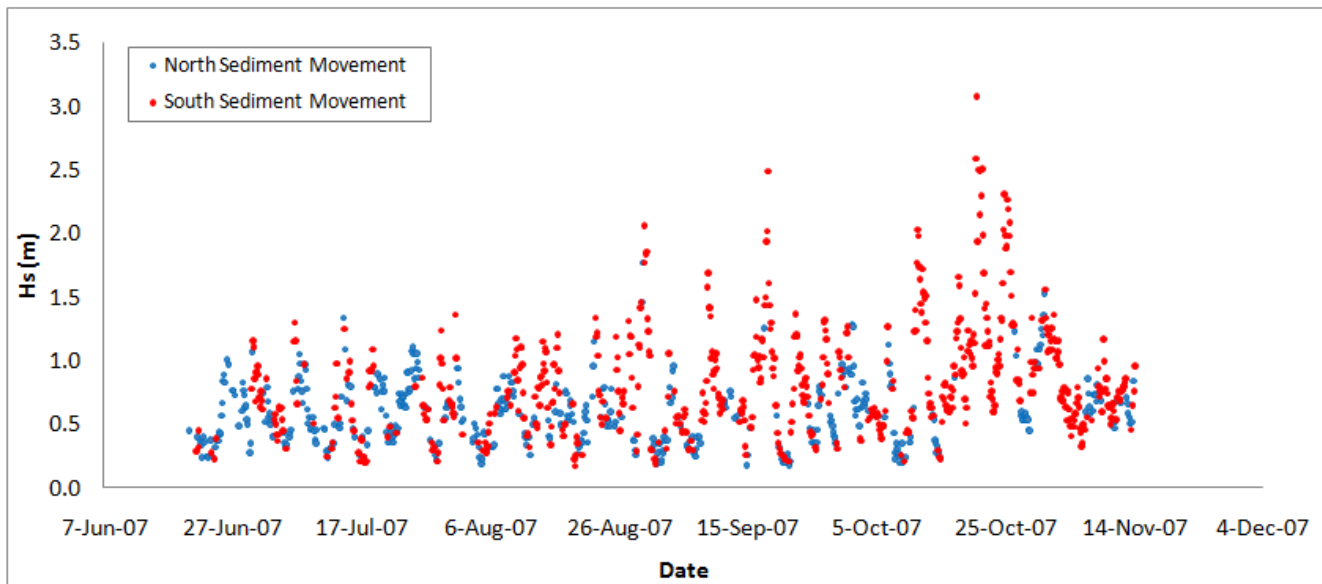


Figure 67 Wave condition and shoreline effect (Configuration 1) at Barceloneta after 2006 North Section, 15 November 2007.

Configuration C2

For the second configuration, the more uniform one ($RO_T=0.90^\circ$ to 1.2°) four conditions have been established. The bold values corresponded to the representative shoreline for this configuration, and figure 68 show the wave condition for the previous months before June 8, 2007.

Since the antecedent beach morphology could vary from C1 to C3. Both conditions were evaluated. If the previous configuration corresponded to C1 (anticlockwise rotation), the incident wave condition need to come from the SE direction (ranges between 123° to 146°). Meanwhile, if come from C3 (clockwise rotation), the incident wave should be from E to ESE direction (ranges between 79° to 123°).

Table 48 show the results of the mean wave height and period associated to each change between C1 to C2 and C3 to C2. The mean wave heights vary between 0.30 m to 0.6m, and the period between 5 and 7s. Most of the condition would achieve an exchange of volume in days.

Table 48 Wave condition that generates configuration 2, Barceloneta Before 2006 North Section					
From	Time (Days)	H_s Mean (m)	T Mean (s)	Φ Mean ($^\circ$)	Q Cumulative Mean (m ³ /yr)
C1	6.50	0.32	7	144	4135
	2	0.31	5	143	4365
C3	10	0.60	6	120	-3019
	3.5	0.34	5	104	-58957

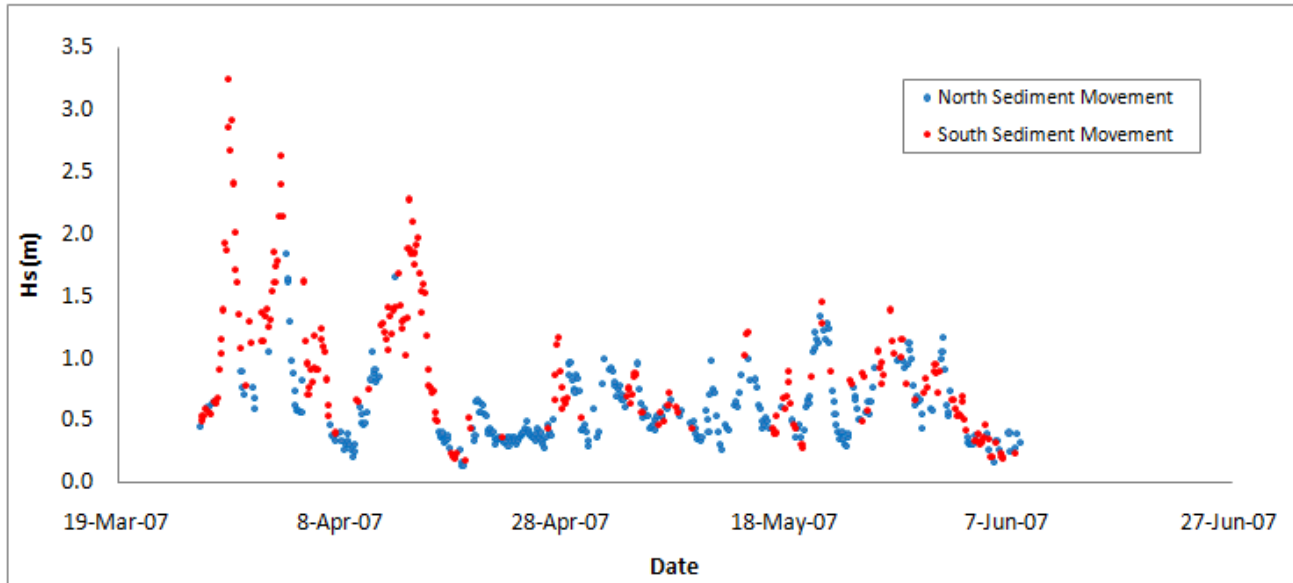


Figure 68 Wave condition and shoreline effect (Configuration 2) at Barceloneta after 2006 North Section, June 8, 2007.

South Section

Configuration C1

For the south section, in the analysis of configuration 1 only one combination was obtained. The result suggested that independently of which configuration the beach had before, a incident wave of 115° would generate a exchange of volume between the north and the south end.

The time needed for the beach to react to this change corresponds to 10 days, with a mean wave height of 0.45m and a period of 7s. Figure 69 show the wave condition for this period. It is important to observe that this wave condition in this section generate a lower anticlockwise rotation, $RO_\tau = -0.10^\circ$ to -0.2° , rather than a positive degree of rotation which occur in the south section of the Barceloneta.

Table 49 Wave condition that generates configuration 1, Barceloneta Before 2006 South Section					
From	Time (Days)	Hs _{Mean} (m)	T _{Mean} (s)	Φ _{Mean} (°)	Q _{Cumulative Mean} (m ³ /yr)
C2 and C3	10	0.45	7	115	-7304

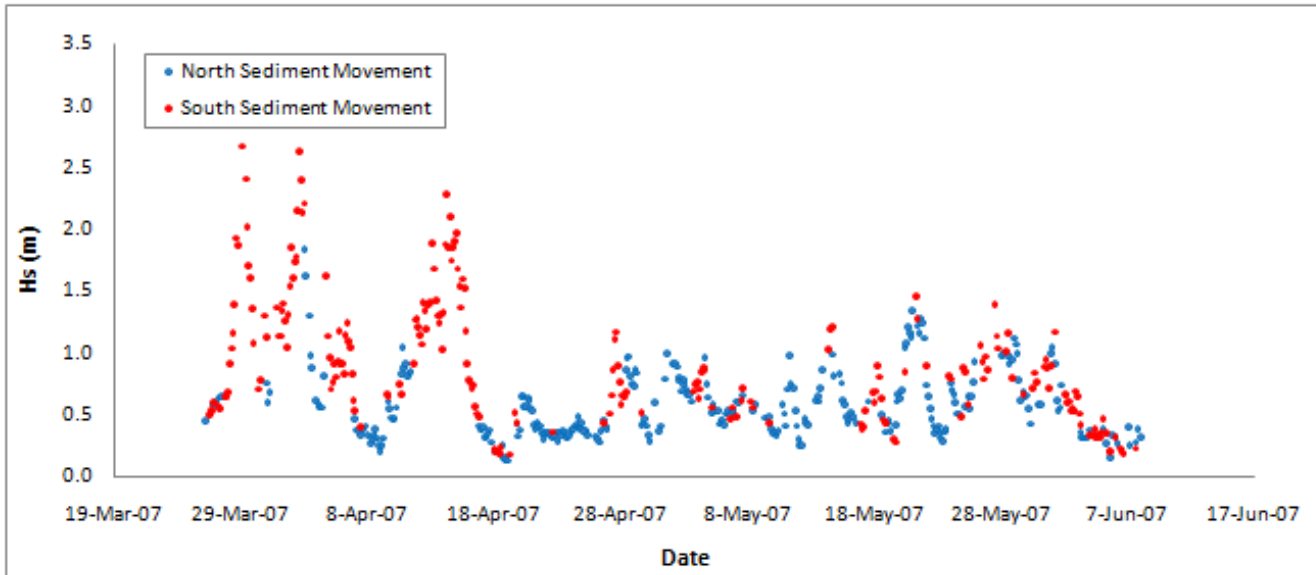


Figure 69 Wave condition and shoreline effect (Configuration 1) at Barceloneta after 2006 South Section, June 8, 2007.

Configuration C2

For the second configuration two conditions were obtained. This configuration presented a $RO_T=1.2^\circ$, similar to the one obtained for the configuration 2 at the North section. Therefore, wave conditions with the same characteristics are expected.

In the same context of the North section, we notice that to change an anticlockwise rotation to a more uniform platform, the direction of the wave approaching the beach should be around 140° , while to change an clockwise rotation to a more uniform platform, the direction should be around 116° .

The result show that more time is needed to achieve a change between C3 to C2. This was consistent to the result for configuration of the North Section.

Table 50 Wave condition that generates configuration 2, Barceloneta Before 2006 South Section					
From	Time (Days)	Hs _{Mean} (m)	T _{Mean} (s)	Φ _{Mean} (°)	Q _{Cumulative Mean} (m ³ /yr)
C1	4	0.32	7	145	7415
C3	5.5	0.37	6	116	-7952

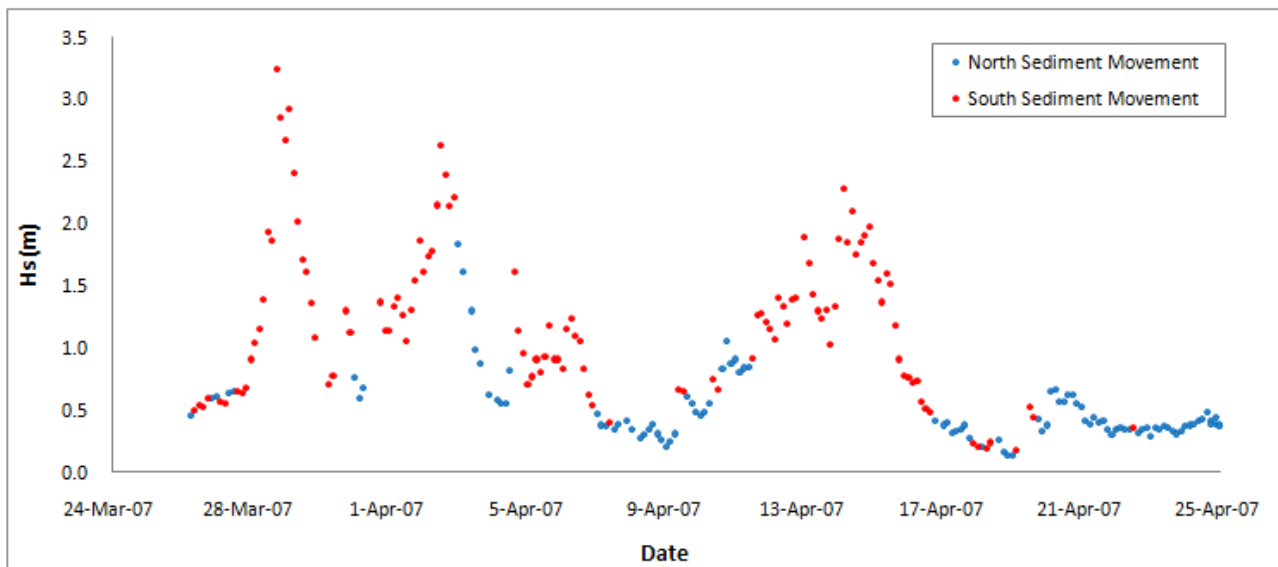


Figure 70 Wave condition and shoreline effect (Configuration 2) at Barceloneta after 2006 South Section, April 25, 2007.

Configuration C3

The final analysis for the Barceloneta beach corresponded to the configuration 3 of the South section, for this configuration one condition has been obtained. This configuration correspond to the clockwise rotation with the positive higher degree of rotation of the beach ($RO=3^\circ$).

The results show that to achieve a respond in the beach platform, the direction of the wave incident should be around 132° (SE), regardless if the previous distribution was C1 or C2. This was consistent with the fact that C1 presented a very low negative RO_r , so the change of configuration does not required a higher degree of wave direction. Figure 71 presented the wave conditions prior the date that the representative shoreline was obtain.

Table 51 Wave condition that generates configuration 3, Barceloneta Before 2006 South Section					
From	Time (Days)	Hs _{Mean} (m)	T _{Mean} (s)	Φ _{Mean} (°)	Q _{Cumulative Mean} (m ³ /yr)
C1 and C2	2	0.67	7	132	-6495

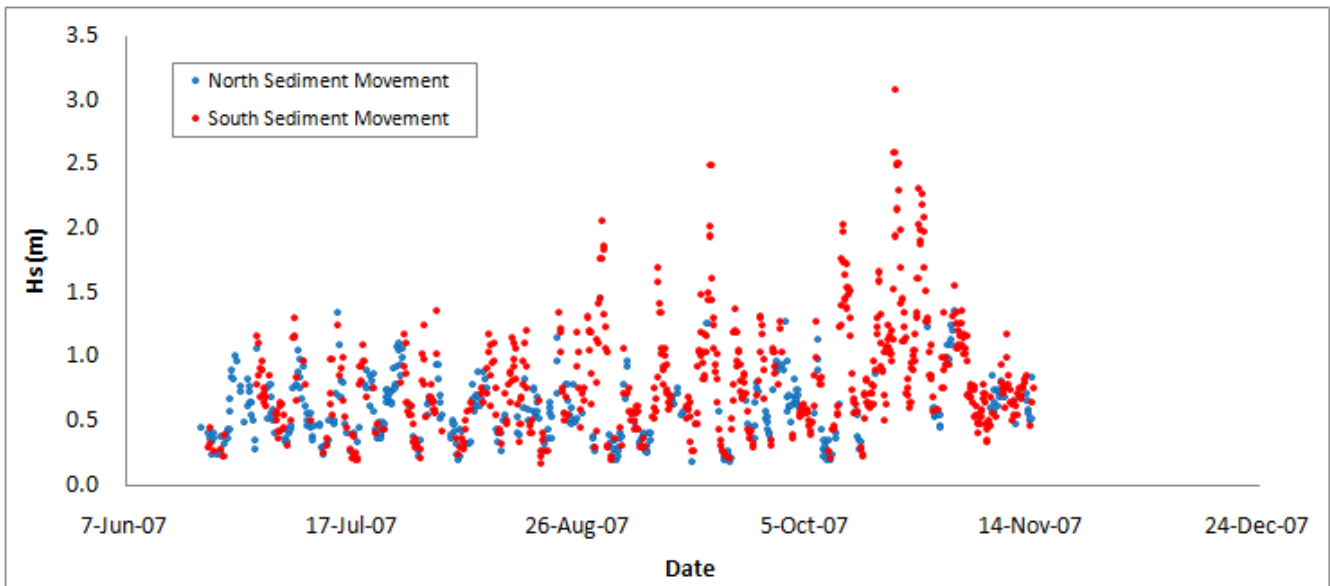


Figure 71 Wave condition and shoreline effect (Configuration 3) at Barceloneta after 2006 South Section, November 15, 2007.

5.2.8 Playa Larga Beach

Playa Larga was considered semi-exposed dissipative beach with a less curve platform. The length of the beach is approximately 640m and is oriented toward the SSW (206°).

Rotation Coefficient (RO)

A data set of 16 coastlines from February 1994 to December 2009 has been analysis, in order to determine if the beach is experience beach rotation. A rotation coefficient has been obtained for each shoreline position. Figure 72 illustrate the behavior of the rotation coefficient through the study period.

Negative values of rotation coefficient (RO) corresponded to an anticlockwise rotation of the beach. The results indicate that the beach is indeed experience an anticlockwise rotation, in a higher degree with a value of RO of -11.91° . Any clockwise rotation has been observed during this lapse of time.

The maximum value of RO -1.53° corresponded to May and June 2004, during this year we observed that the beach erode completely. So these values will not be considered as a representative rotation. The next maximum correspond to a RO around -4° , this correspond to a lower degree of anticlockwise rotation.

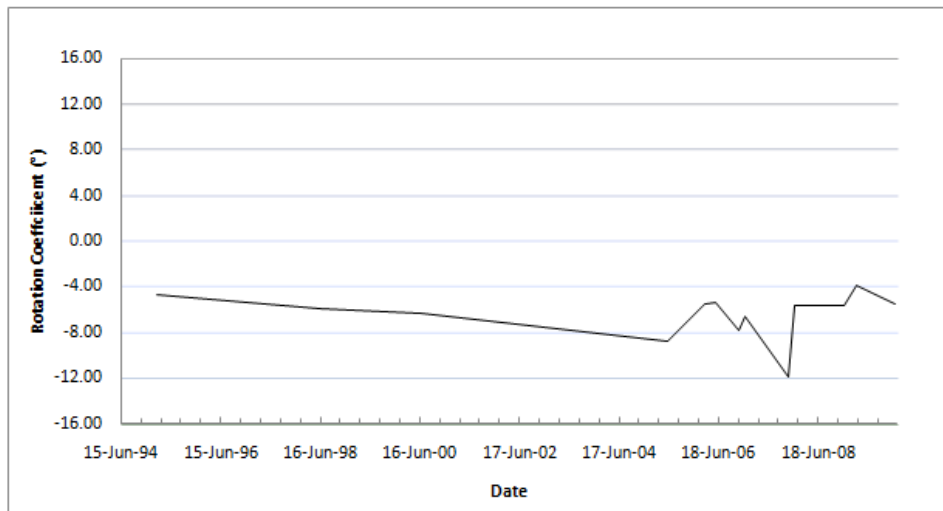


Figure 72 Evolution of the rotation coefficient, Playa Larga. The rotation coefficient is illustrated in degrees. A positive slope indicates clockwise rotation.

Theoretical Rotation Coefficient (RO_T)

During the study period, two major configurations has been notice at Playa Larga. The first configuration has been present 2 times. This setup is characterized by a shoreline leaning to the south (left hand side looking landward) with a RO_T= -8.8° to -11.8° . Accordingly with this setup, the maximum beach width was presented at the south part with a value of 104m, and then reduces gradually to the center to obtain a value of 26m and at

the north part achieve a value of 18m (right hand side looking landward). This is represented by the shoreline of November 11, 2007.

The second configuration occurs 1 time during the period analyze. This was characterized by a $RO_T = -4.6^\circ$. This corresponded to a more uniform platform (see figure 73), with a beach width at the south of 61m, at the center of 35m and at the north of 32m This was represented by the shoreline of March, 1995.

It is logical that a third configuration wasn't observed since this will correspond to a clockwise rotation. From the nearest wave node we notice that the presence of waves with a direction from the SSW are not that common (see figure 14), and the WSW or W direction will not have a sufficient energy since the fetch is not that large.



Figure 73 Theoretical Model of Playa Larga (Photo: Ortophotos 2008, ICC) Configuration 1, shoreline of November 11, 2007 (solid blue line), Configuration 2, shoreline of March 1st, 1995(solid red line).

The coefficient of variation of the relation between the beach width and the alongshore location, show a strong correlation for both configuration ($r^2=0.8$).

Table 52 Theoretical Rotation Coefficient Playa Larga		
Configuration	Theoretical rotation coefficient	Number of observations
C1	-8.8 to -11.9 ($r^2=0.8$)	2
C2	-4.6° ($r^2=$ to 0.8)	1

Wave Forcing on the Theoretical Model

Based on the theoretical model of Playa Larga, the exchanged volumes between configurations have been determined. Table 53 shows the obtained. Negative value corresponds to a deposition at the southern end (See figure 73). A higher volume is expected at the southern end since this zone presented the higher values of beach mobility.

Table 53 Measured volume between configurations Playa Larga		
From To	ΔV_m [C1]	ΔV_m [C2]
ΔV_m [C1]	-----	-58461
ΔV_m [C2]	38168	-----

The following sections show the wave conditions required to accomplish a volume exchange on the same order.

Configuration C1

To achieve a configuration with a $RO_T=-11.8^\circ$ (anticlockwise rotation), the beach need to experience waves coming from the SSE and S (range from 146° to 191°). Bold values correspond to the representative shoreline presented in figure 74.

It is suggest that the beach will respond to the wave condition in days. The difference in time is most likely to be attributed to the higher mean wave height, period and difference between the wave incident and the orientation of the beach. A value between $(\theta_{\text{Beach}} - \Phi_{\text{Wave incidents}})$ around 40° to 50° will generate the maximum longshore sediment transport.

Table 54 Wave condition that generates configuration 1, Playa Larga					
From	Time (Days)	Hs _{Mean} (m)	T _{Mean} (s)	Φ _{Mean} (°)	Q _{Cumulative Mean} (m ³ /yr)
C2	6	0.45	5	181	-47449
	3	0.67	7	155	-16644

Figure 74 showed the effects of the wave conditions on the coastline. Due to the orientation of the beach, we would expect a higher sand movement to the south than to the north.

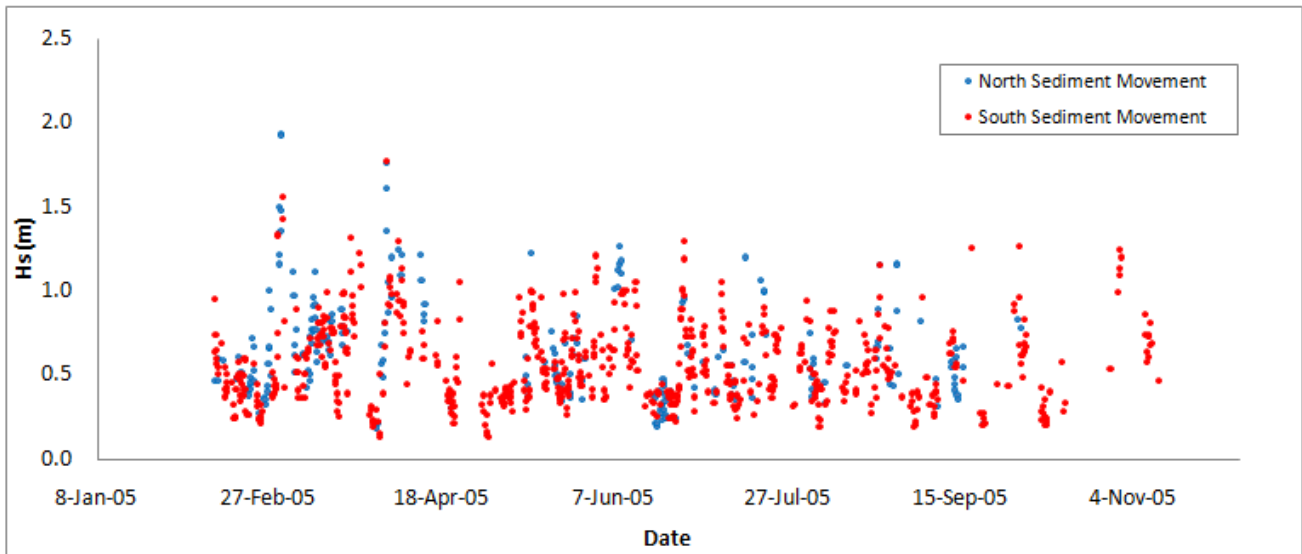


Figure 74 Wave condition and shoreline effect (Configuration 1) at Playa Larga, November 11, 2007.

Configuration C2

Only one combination was achieved for the configuration 2. To obtain a more uniform behavior with a $RO_T = -4.6^\circ$, beach need to experience an incoming wave direction from SW (ranges around 225°). Figure 75 showed that during the previous months to the date of the representative shoreline, wave conditions that generate a northern sand movement were rare to observe. This condition presented the lower values of mean wave height and period.

Table 55 Wave condition that generates configuration 2, Playa Larga

From	Time (Days)	Hs Mean (m)	T Mean (s)	Φ Mean (°)	Q Cumulative Mean (m3/yr)
C1	5	0.38	3	230	6262

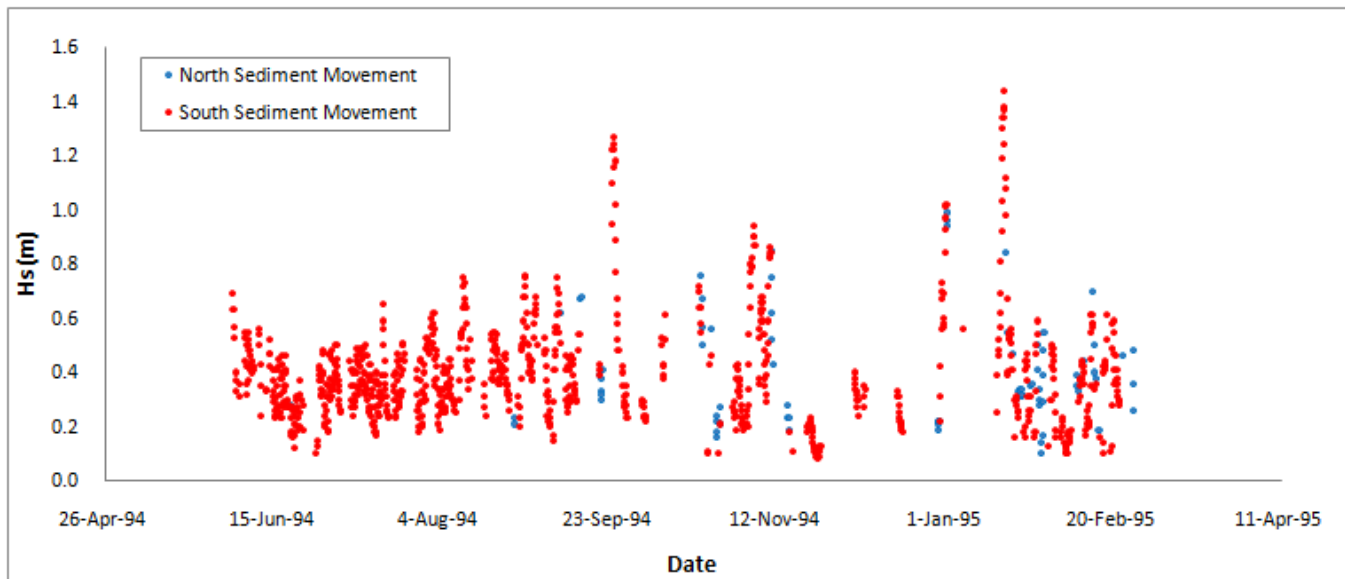


Figure 75 Wave condition and shoreline effect (Configuration 2) at Playa Larga, March 1st, 1995.

5.2.9 Salou Beach

The last beach of the study corresponds to Salou. Salou was considered semi-exposed dissipative beach with a platform with a lower degree of curvature. The length of the beach is approximately 1.2km and is oriented toward the SSW (199°).

Rotation Coefficient (RO)

Twenty coastlines from June 1957 to December of 2009 have been used to determine if the beach presented a higher degree of rotation. The evolution of the rotation coefficient is presented in the figure 76.

It is clear that Salou presented an anticlockwise behavior, similar to the one observed in Playa Larga. But any evidence of a clockwise rotation is observed. The higher negative degree of rotation corresponded to a RO of -3° and the lower negative degree corresponded to a RO of -0.4° .

The values between the two extremes corresponded to oscillations of the beach. For example the shoreline of January 1998 and December 2006 that presented a RO of -2° and during this period the entire beach move around 10-15 m seaward.

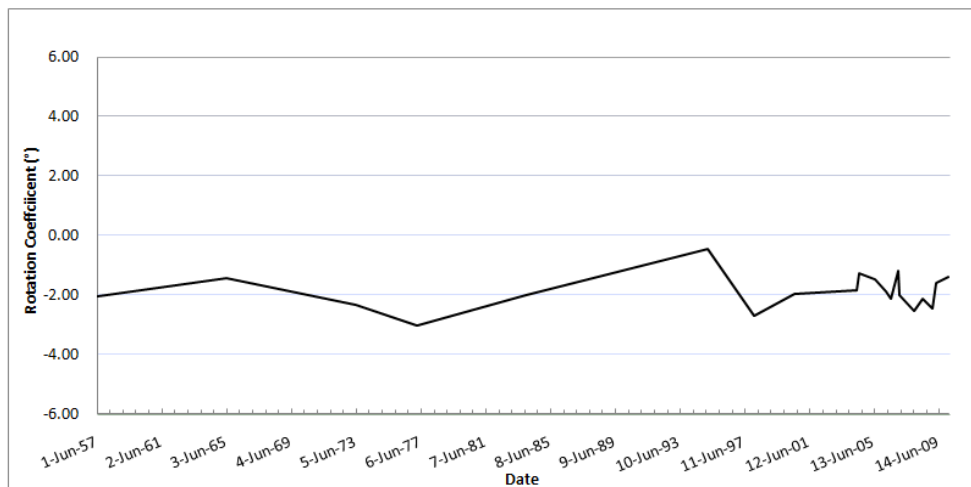


Figure 76 Evolution of the rotation coefficient, Salou. The rotation coefficient is illustrated in degrees. A positive slope indicates clockwise rotation.

Theoretical Rotation Coefficient (RO_T)

Two main configurations have been distinguished during these 14 years. The first configuration has been observed 3 times within the shoreline data. This setup presented the higher negative RO_T value of -2.5° to -3.8° . This configuration is illustrated in figure 77 by the shoreline of March 1st, 1997. The beach width at this beach setup corresponded to a maximum value of 94m at the south end (left hand side looking landward) and a minimum beach width of 41m at the southern end (right hand side looking landward). At the center the beach width is on the order of 69m.

The second configuration was presented only a 1 time during the study period. This configuration had a value of RO_T of -0.46° . This platform distribution was characterized by a beach width of 83m at the south end, 84 at the center and 72 at the north end. This corresponds to a more uniform setup and is illustrated in figure 77 by the shoreline of March 1st, 1995.

In the same context that Playa Larga the absence of a clockwise rotation (positive RO_T) is due to the less frequent waves with a direction from the SSW (see figure 22).



Figure 77 Theoretical Model of Playa Larga (Photo: Ortophotos 2008, ICC) Configuration 1, shoreline of March 1st, 1977 (solid blue line), Configuration 2, shoreline of March 1st, 1995 (solid red line).

The variation coefficient of the configuration 1 presented a strong relation of $r^2=0.92$ to 0.95 . The configuration 2 presented a less strong relation of $r^2=0.4$.

Table 56 Theoretical Rotation Coefficient Salou		
Configuration	Theoretical rotation coefficient	Number of observations*
C1	-2.5 to -3 ($r^2=0.92$ to 0.95)	3
C2	-0.4.6° ($r^2=$ to 0.4)	1

*From the 20 shoreline data set.

Waves Forcing on the Theoretical Model

From the theoretical model the volumes exchange between configurations has been obtained. Table 57 shows the volume values for Salou. As is expected the higher values correspond to the southern end since this zone presented the higher values of retreat and advance of the shoreline.

Table 57 Measured volume between configurations Salou		
From To	ΔV_m [C1]	ΔV_m [C2]
ΔV_m [C1]	-----	-40271
ΔV_m [C2]	17367	-----

The results from the waves forcing on the theoretical model are presented below.

Configuration C1

Three conditions were obtained for the configuration 1 the bold values corresponded to the representative shoreline. This configuration presented a $RO_T = -3^\circ$ (e.g. shoreline tilted to the south). The mean direction corresponded to S directions (range from 169° to 191°).

The mean wave heights presented values from 0.30m to 0.60m with a period of 4 to 5s. The lower mean cumulative longshore sediment transport rate corresponded to the lower wave height and period.

Table 58 Wave condition that generates configuration 1, Salou					
From	Time (Days)	$H_{s \text{ Mean}}$ (m)	T_{Mean} (s)	Φ_{Mean} ($^\circ$)	$Q_{\text{Cumulative Mean}}$ (m ³ /yr)
C2	6	0.34	5	182	-53346
	6	0.28	4	178	-38712
	3	0.61	4	175	-40084

Figure 78 presents the wave condition for the previous months to March 1st, 1995. During this period any storm event have been identified ($H_s=2\text{m}$).

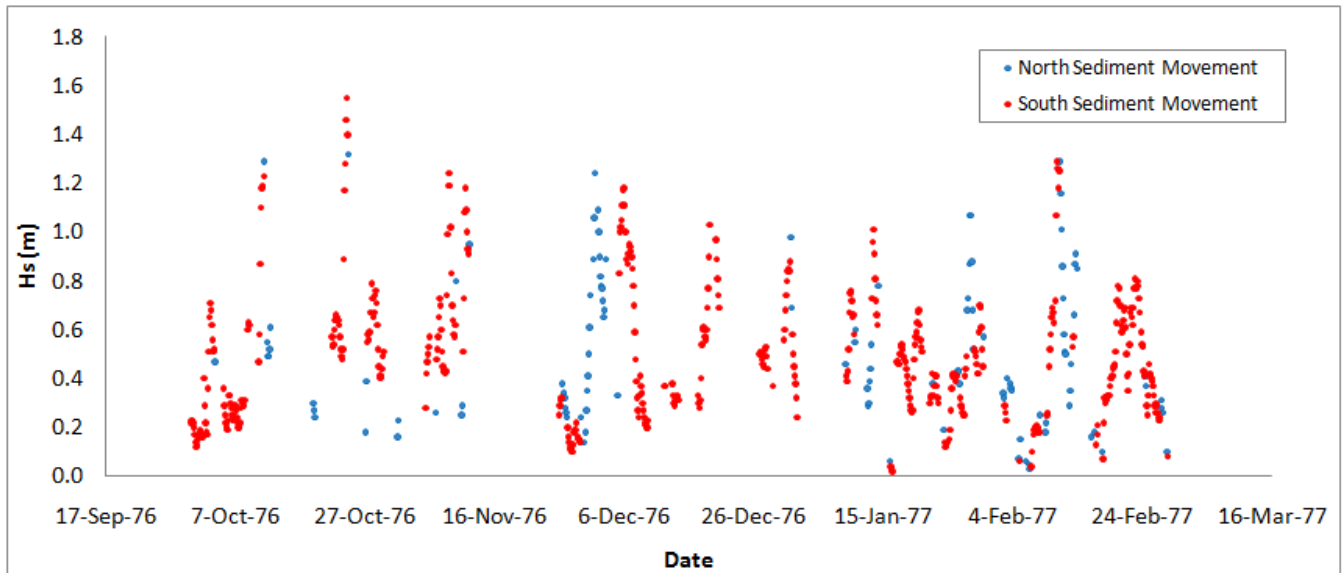


Figure 78 Wave condition and shoreline effect (Configuration 1) at Salou, March 1st, 1977.

Configuration C2

For the configuration 2 only one condition has been obtain from the analysis, since only one shoreline presented this platform distribution.

It has been observed that to achieve an exchanged volume between configurations 1 to 2, the beach need to respond to a wave incident direction of 229° (SW sector). Similar to the configuration 2 of Playa Larga this condition presented the lower value of mean period. The cumulative mean of the sediment transport rate was around 20213 m³/yr. Figure 79 shows the wave condition before March 1st 1995, we notice that most of the wave condition during that period generated a movement of sand to the south, only a few conditions generated a movement to the north.

Table 59 Wave condition that generates configuration 2, Salou

From	Time (Days)	Hs Mean (m)	T Mean (s)	Φ Mean (°)	Q Cumulative Mean (m3/yr)
C1	3.00	0.4	3	229	20213

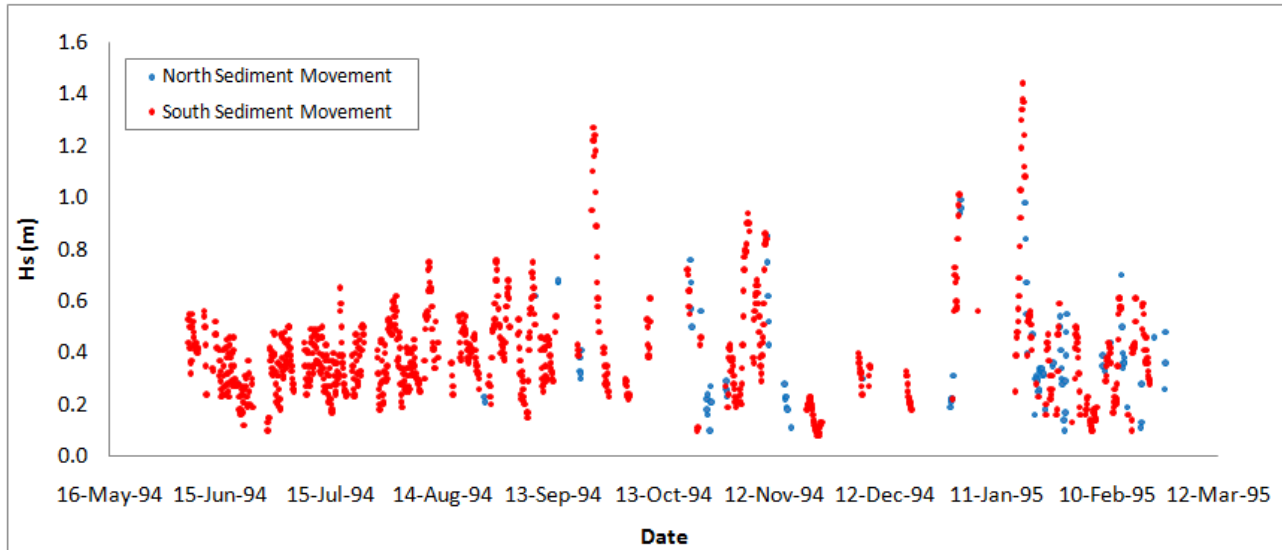


Figure 79 Wave condition and shoreline effect (Configuration 2) at Salou, March 1st, 1995.

5.3 Discussion

Results showed that beach rotation occurred on embayed beach along the Catalan coast which is accord with other studies of embayed beaches (e.g. Ojeda and Guillen, 2008 and Garcia et.al 2008). However, the degree of rotation was not uniform across all the embayment. For example the most exposed beaches, the ones oriented towards the SSE to SE (e.g. shorelines oriented 19° to 54° relative to the north) presented a wider degree of rotation (anticlockwise, uniform and clockwise rotation), with the exception of Salou and Nova Icaria. The semi exposed beaches oriented towards the SSW (e.g. shorelines oriented 102° to 116° relative to the north) only presented an anticlockwise rotation.

Literature on beach rotation has suggested that beaches with similar platform morphology and hydrodynamic characteristic would exhibit similar beach rotation behavior, and that this behavior can differ significantly between reflective, intermediate and dissipative beaches (Klein et.al 2002, Short et.al 2000). In this study, beaches with the same morphology has experience a similar beach rotation.

Based on the theoretical model of the different embayment, it has been observed that the reflective exposed beaches as Lloret del Mar and Fenals, presented the higher degree of rotation (anticlockwise/clockwise rotation) with a minimum theoretical rotation coefficient of -6.47° for both beaches (e.g. anticlockwise rotation), a mean RO_T of -1.8° for Lloret and 0.2° for Fenals and a maximum theoretical rotation coefficient of 3.84° and 3.15° , respectively (e.g. clockwise rotation). Intermediate exposed beaches presented the second higher rotation (Bogatell and Barceloneta before and after 2006), with a maximum theoretical coefficient between 1° to 3° , a mean RO_T of 0.4° to 1.8° and a minimum value between 0.9° to 1.76° . The semi-exposed dissipative beaches (Playa Larga and Salou)only presented an anticlockwise degree of rotation with a value between -3° to -8° and a minimum RO_T of -0.45° to -4.6° . For the semi-exposed reflective and intermediate beaches (Canyelles, Sant Pol and Nova Icaria) only an anticlockwise degree of rotation was identified with maximum value of RO_T of -3° , -0.6 and -10° , and a minimum value of RO_T of -5.6° , -1.8° and to -13° , respectively.

Nevertheless, there were at least some years where the rotation behavior was the opposite between beaches with the same morphology. For example on reflective beaches in August, 1997 Lloret del Mar presented an anticlockwise rotation while Fenals presented a clockwise rotation. This behavior can be attributed to the sheltered nature of Fenals to the ENE and E directions, so the beach will not experience the same rotation within the same period of time. On Intermediate beaches the same contradiction was observed at the North and South sections of Barceloneta during November 15, 2007, March 2008, and April of 2009 where the North section presented a clockwise rotation the South section presented an anticlockwise rotation. This effect can also be attributed to the degree of protection of the North section to ENE and E directions and the presence of megacusps observed at the South section of Barceloneta.

In the analysis of wave forcing on the theoretical model, an attempted to identify the forcing mechanisms (mean wave conditions) that act on a configuration was made. Over the years the study of beach forcing mechanism imply that wave direction was the primary forcing mechanism of beach rotation, since this process results from a change in the longshore sediment transport direction between headlands extremities on the embayed beaches (Short and Masselink, 1999; Klein et al 2002; Ranashinge et al 2004). However the respond of the beach may also depend on the degree of protection, the orientation of the shoreline and the previous morphodynamics configuration (Ojeda and Guillen 2008, Harley 2009).

The analysis of forcing mechanisms proposed in this thesis was performed for each individual beach, based on the specific theoretical model. As mention before the most exposed beaches presented three major configurations (anticlockwise rotation, uniform and a clockwise rotation) while the semi-exposed beaches only presented two major configurations (anticlockwise rotation and uniform distribution).

For the exposed beaches that were oriented toward the SSE (Lloret del Mar and Fenals), the results of wave forcing on the embayment suggest that SE to SSE waves resulted in an anticlockwise rotation and that S to SSW waves resulted in a clockwise rotation of the embayment. The results of the exposed beaches that are oriented toward the ESE (Bogatell, Barceloneta before and after 2006), indicate that E to ESE/ SE to S waves resulted in an anticlockwise /clockwise rotation.

For the semi-exposed beaches oriented to the SSE (Sant Pol), the result show that SE/S wave generated a higher anticlockwise rotation/ lower anticlockwise rotation. Nova Icaria that was considered a semi-exposed beach and is oriented to the ESE, the higher degree of anticlockwise rotation was presented in E to ESE waves, while SSE waves generated a lower anticlockwise rotation.

Finally for the semi-exposed beaches oriented to the SSW (Canyelles, Playa Larga and Salou), a higher anticlockwise rotation was presented for the SSE to S waves; the lower degree of anticlockwise rotation was generated by SSW to SW waves.

In terms of time, wave height (H_s from 0.20m to 1.3m) and period (T 3 to 8s) a wide range of combinations has been encountered for all the study beaches, but any indication of an individual relationship between these variables and an anticlockwise or clockwise behavior. Instead, the results suggested that a combination of wave height, period and direction was the responsible of the response time of the beach to changes in the configuration. Wave height influences the magnitude of the longshore sediment rate, but is the wave period in combination with the wave direction that affected the direction of the longshore sediment rate. These two parameters affect the refraction patter of the wave and determine the final degree of wave approach to the shoreline, therefore modify the gradient in the longshore sediment transport and the final shoreline configuration.

Overall, the study presented sufficient information to create a theoretical model for each beach. The analysis of beach rotation and wave forcing on the embayment generate a better understanding of the respond of the beach to mean wave conditions.

5.4 Summary

The following conclusion can be drawn from the analysis of beach rotation and oscillation along the Catalan coast.

- Beach rotation was evident in all the study beaches. A theoretical model for each beach base on the rotation coefficient has been developed.
- The study beaches presented a wide degree of rotation. Exposed beaches to easterly wave condition presented an anticlockwise/clockwise rotation behavior, while semi-exposed beaches presented only an anticlockwise rotation.
- The beach type (e.g. beach slope and grain size) also influences the degree of rotation. The exposed reflective beaches presented the higher degree of rotation (anticlockwise/clockwise); the exposed intermediate presented the second higher degree of rotation (anticlockwise/clockwise). The lower degrees of rotation were presented in the dissipative beaches (only anticlockwise rotation).
- Wave direction was the primary forcing mechanism observed on the analysis. The combination of wave height, period and direction where the responsible of the response time of the beach to a new configuration.
- Wave height influences the magnitude of the longshore sediment rate, but is the wave period in combination with the wave direction that affects the direction of the longshore sediment rate.
- Exposed beaches oriented to the SSE presented an anticlockwise/clockwise rotation to SE-SSE/S-SSW waves and exposed beaches oriented to the ESE presented an anticlockwise/clockwise rotation to E-ESE/ SE-S waves.
- Semi-exposed beaches oriented to the SSE responded to SE/S wave in a higher anticlockwise rotation/ lower anticlockwise rotation. While the ones oriented to ESE responded in the same matter to E-ESE/SSE waves. Finally the beaches oriented to the SSW reacted to SSE-S waves with a higher anticlockwise rotation, than to SSW waves that generate a lower anticlockwise rotation.

6. Wave Condition and the Theoretical Model Respond: 2001- 2007

Coastal environment has been extensively used for activities as fishing, tourism, transport of good, water treatment and housing. Approximately three billion people (half of the world population) live and work within a couple of hundred kilometers of a coastline, in spite of the vulnerability of coastal areas to erosion and flooding. Due to the high population densities and extensive infrastructure and property develop; disasters will have major consequences (Bosboom and Stive, 2010).

According with the DPTOP (2006) 48% of the population of Catalonia is concentrated in the 7% of the territory, a 500m wide strip along the coast. Without considering the touristic season that can double or triple the density (Mendoza, 2008).

Shorelines, especially sandy beaches are highly dynamic environments, and changes in the beach configuration can jeopardize the functions of the beach. The assessment of 38 municipalities along the Catalan coast of Ariza et al, 2007, has show that two thirds of these local authorities (20 municipalities) reported erosion problems on some of the beaches. The main concern of the manager in these areas was related to sediment management. Since the loss of sub-aerial beach area is a critical issue in the recreational use of the beach, in addition affects the protective function of the beaches by reducing the available surface for dissipating wave energy during storm.

Local managers have to deal with the “unexpected” results of shoreline fluctuation, such as promenade reconstruction and reconstruction of minor infrastructure. However, if the prior configuration of the beach is known and determine as a risk configuration for the incoming event, different managing option can be undertaken (Ariza et al, 2007).

The objective of this chapter is determining the frequency of occurrence of the different configuration of the theoretical model presented in the previous chapter. Based on the mean wave condition obtained in the analysis of beach rotation and oscillation, an evaluation on how many times during the last 7 year of available wave data (2001 to 2007) the same conditions were observed. The chapter consisted in four sections. The following section describe the methodology uses to accomplish the objective. Section 6.2 shows the results of the analysis, in section 6.3 and 6.4 the discussion and the summary is presented.

6.1 Methodology

The analysis of the frequent wave conditions was based on the wave data of the XIOM buoys located along the Catalonia coast. As mention in chapter 3, each beach has been associated to the nearest buoy. The description of the buoys, the beach affected by the wave data and the effective direction previously define in section 3.4.3 is show in table 60.

Table 60 Table Buoy description and beach associated to it.				
Name	Longitud E	Latitud N	Beach affected	Effective Range of Direction
Tordera	2 48.93	41 38.81	Sant Pol	E-SW
			Canyelles	SSE-WSW
			Lloret del Mar Fenals	E-SW
Llobregat	2 08.48	41 16.69	Bogatell Nova Icaria Barceloneta	NE-SSW
			Playa Larga	SE-WSW
			Tortosa	00 58.89

To accomplish the objective the effective range of direction has been divided in sectors of 22.5° centered in the north (see figure 80). The grey sector correspond to directions that not affect the morphodynamics of the beach e.g. directions coming from the land and parallel direction to the shoreline.

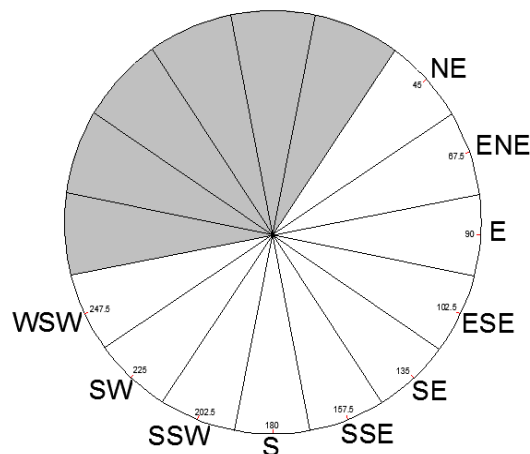


Figure 80 Sectors of wave conditions.

For each sector a join distribution of significant wave height and peak period has been obtained. The period has been classified in interval of 2 seconds, and the wave height has been classified in intervals of 0.1 meters until a wave height of 1 m is obtained, then the intervals varies to 0.5m until reach a value of 4m. A frequency of occurrence for each set par (e.g. H_s , T_p , φ) has been obtained per sector.

$$Frequency[H, T, \varphi]_i = \frac{no\ of\ waves[H, T, \varphi]_i}{no\ of\ waves\ in\ the\ sector}$$

(Eq. 12)

Finally for each wave buoy, we obtain a data set in the form of (H_s , T_p , φ) and the frequency of occurrence for the study period (7 years). Using this frequency of occurrence we can determine how many days per year the specific wave conditions obtain in the chapter 5 occurred. Since the main forcing mechanisms were determined by the longshore sediment transport, the parameters that would be analyzed are the ones that affect this behavior. The wave period and wave direction influence the refraction patter of the wave, and influence the final wave direction approach in respect with the shoreline, resulting in a positive or negative longshore sediment transport. The wave height influences the magnitude of this rate, but does not influence the direction (e.g. gradient). Therefore, any distinction will be made for the specific wave height; all the combination of wave height with a specific wave period and direction will be considered.

Each beach has been study separately, but they are base on the information of the correspondent wave buoy. The figures show the join distribution per direction sector, the color range represents a percentage of occurrences.

6.2 Results

6.2.1 Tordera Buoy

Figure 81 show the result of the analysis of frequency of occurrence for the Tordera buoy. Only the effective directions are represented in the figure. The higher percentage corresponded to the SSW direction with a 19%, the second higher percentage corresponded to the E, SE and S direction with a 9% each followed by the ESE and S direction with an 7% each.

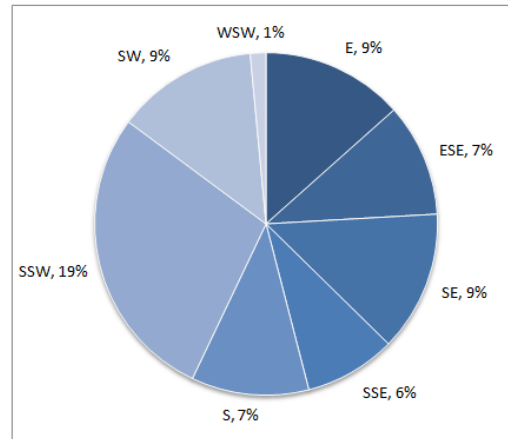


Figure 81 Frequency of occurrence per year, Tordera Buoy.

Figures 82 and 83 presented the joint frequency distribution of significant wave height and peak period per the specific direction sectors. It is clear that the condition with a wave height of 1m and with periods between 7 and 8s corresponded to the most frequent condition for the E and ESE directions. For the SE and SSE directions the most frequent conditions corresponded to a wave height lower than 0.5m with a peak period of 4s.

The SSW and SW direction also presented a significant contribution for conditions with a wave height higher than 1 m but a lower peak period of 6s, finally for the S and WSW direction the most frequent conditions corresponded to a wave height lower than 0.5m and a peak period of 4s.

For storms condition the longer waves correspond to the Easterly directions while the shorter waves correspond to the Southerly directions.

The wave conditions of four beaches (Sant Pol, Canyelles, Lloret del Mar and Fenals) are represented by the Tordera Buoy. Each beach was studied separately, since they have a different effective range of direction. The analysis of the frequency of the wave conditions describe in Chapter 5 is presented below. The shading cell of the tables corresponded to the wave condition that generated a uniform and clockwise behavior from an anticlockwise rotation; the clear cells corresponded to the wave condition that generated an anticlockwise rotation from the more uniform and clockwise distribution.

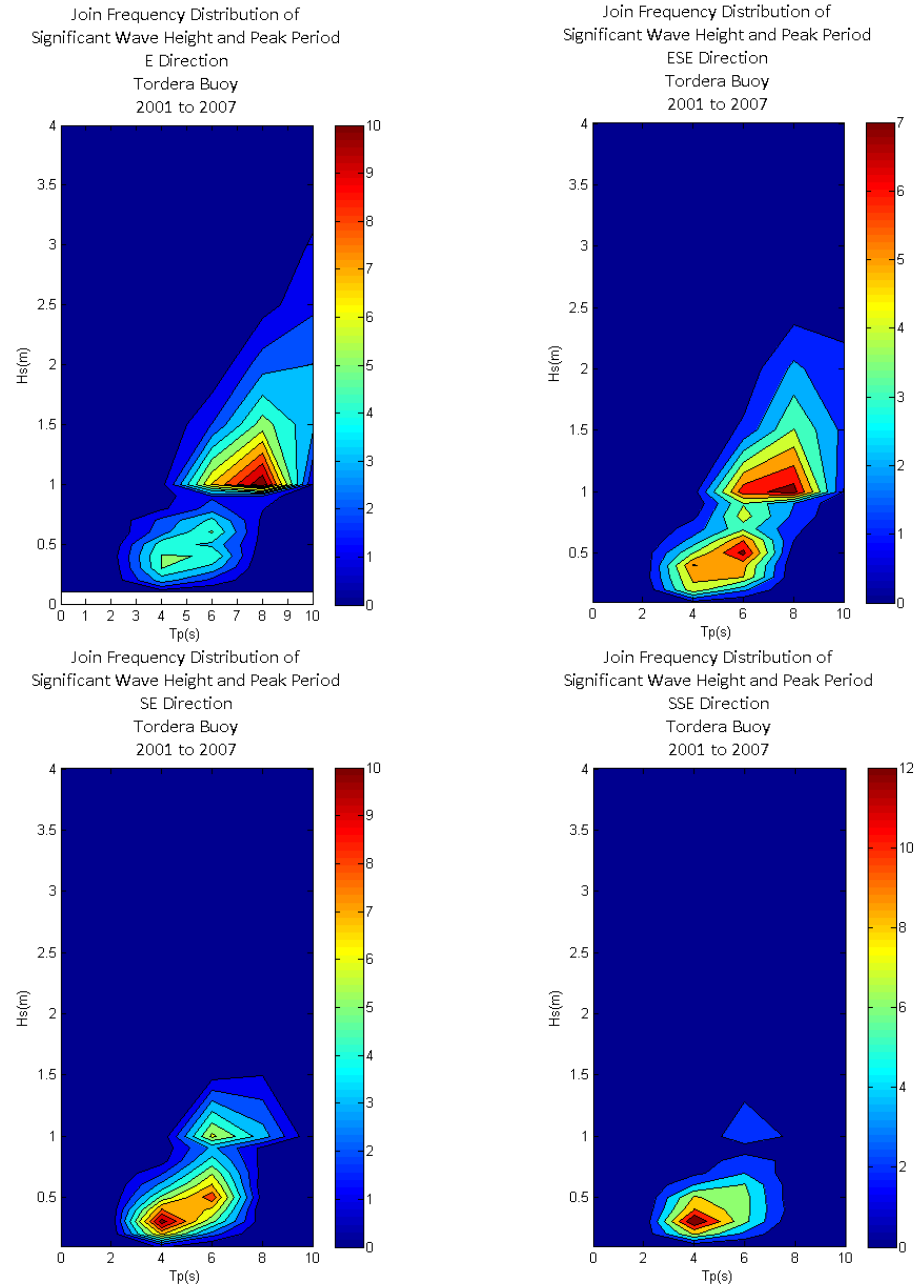


Figure 82 Join Frequency Distribution Significant Wave Height and Peak Period a) E Directions, b) ESE Directions, c) SE Directions and d) SSE Direction. The color bars illustrate the frequency of the data. The wave direction is the direction the waves come from.

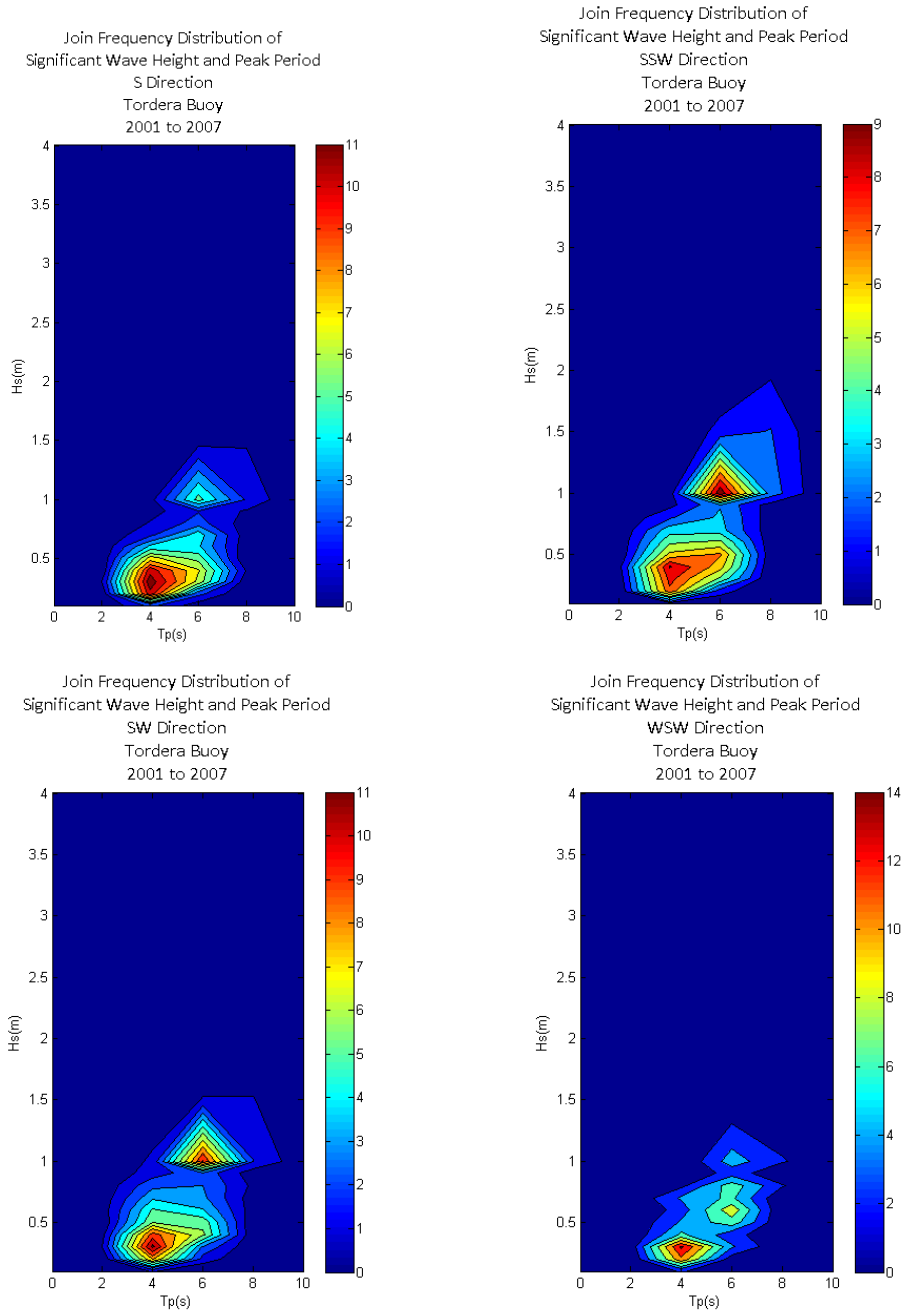


Figure 83 Joint Frequency Distribution Significant Wave Height and Peak Period e) S Directions, f) SSW Directions, g) SW Directions and h) WSW Direction. The color bars illustrate the frequency of the data. The wave direction is the direction the waves come from.

6.2.1.1 Sant Pol Beach

The effective range of direction of Sant Pol corresponded to E to SW directions. The result of the previous chapter show that to achieve a higher negative degree of rotation (anticlockwise rotation), the beach need to experience a direction from the SE to the E direction. It has been observed that this direction collectively corresponded to a 25% of the mean wave climate. The specific wave condition with a period of 8s corresponds to a 8% of the SE sector (13 day per year), but it is clear from figure 82.c that lower wave heights with lower period corresponded to the most common conditions for the SE sector (e.g. H_s 0.3m to 0.6m with T_p 4s to 8s).

The percentage of occurrence of the directions (S to SW direction) that generates a lower degree of rotation ($RO_T \sim -0.50^\circ$ to -0.70°) in the beach corresponded to a 35%. The percentage of occurrence for the specific wave conditions with a period between 3 to 6s (S sector) that generated this lower degree of rotation corresponded to 53%. These conditions are presented 69 days per year.

This is consistent with the number of observation for the second configuration within the shoreline data set (see table 13). Figure 82 and 83, show that the higher wave conditions (e.g. Storm threshold $H_s > 2m$) corresponded to the E, ESE, SSW and SW directions. Due to the sheltered nature of the beach, the energetic waves from the E direction would be diffracted and the wave height that arrived to the beach would be lower.

Table 61 Frequency of Occurrence of the Specific Wave Condition Sant Pol

RO_T (°)	T (s)	Dir (°)	Sector	Percentage of Occurrence (%)	Days per year
-1.80	8	136	SE	8	13
-0.69	3	187	S	2	3
-0.57	4	172	S	51	65
-0.50	6	168	S	51	65

6.2.1.2 Canyelles Beach

The effective range that affects Canyelles beach corresponded to SSE to WSW direction. The wave directions (SSE to S sectors) that generate the higher anticlockwise rotation in the beach ($RO_T \sim -5.4^\circ$ to -5.8°) have a percentage of occurrence 13% of the mean wave climate. The specific wave conditions with a period of 5s (S sector) found in the previous chapter presented a percentage of occurrences between 51% around 65 days per year each.

The wave directions (SSW to WSW sectors) that generated the lower anticlockwise rotation in the beach ($RO_T \sim -3.51^\circ$) have a percentage of occurrences 29%. The specific wave condition with a period of 6s corresponded to the SSW sector, and has a percentage of occurrences of 46% (150 days per year).

Due to the orientation of the beach (oriented 102° relative to the north), events with a wave height higher than 2m from the ESE sector would not have a significant effect in the morphodynamics of the beach. The events from the SSW sector affect the beach in a more normal direction; therefore the longshore sediment gradient generated by this direction would be lower than for other direction. Consequently, the most frequent configuration would be the beach tilted to the south; this is consistent with the number of times that this specific setup was observed.

Table 62 Frequency of Occurrence of the Specific Wave Condition Canyelles

RO_T ($^\circ$)	T (s)	Dir ($^\circ$)	Sector	Percentage of Occurrence (%)	Days per year
-5.49	5	188	S	51	65
-5.83	5	192	S	51	65
-3.51	6	195	SSW	46	150

6.2.1.3 Lloret del Mar Beach

The effective range of direction of Lloret corresponded to the E to SW sectors. Based on the theoretical model, the wave conditions that generated a beach set up leaning to the south ($RO_T \sim -5.1^\circ$ to -6.5°) corresponded to the directions from the SE to SSE sector, which represent the 31% of the mean wave climate.

The specific wave conditions determined before correspond to the SE and SSE sectors, wave conditions that presented a period between 4 and 6s had the higher percentage within the sector 30-51%, which represent about 42 to 78 days per year. The wave conditions with a T_p of 6 to 8s have a percentage between 9% and 42%, around 13 to 42 days per year.

The directions that generate a beach set up leaning to the north ($RO_T \sim 3.84^\circ$) corresponded to the S to SSW sector; these represented the 35% of the mean wave climate. The specific wave conditions ($T \sim 4s-7s$) to achieve this configuration show a percentage of occurrences within the SSW sector of 46%-51%, around 65 to 150 days per year.

To achieve a more uniform configuration ($RO_T \sim -2^\circ$), it would depend on the previous setting of the beach. So a specific direction cannot be established.

Figures 82 and 83, shows that waves that potentially produce an accumulation towards the north are more frequent (S-SW directions), however the higher values ($H_s > 2m$) of wave height and peak period are presented in the E and ESE direction. The SSW and SW sector presented lower values of wave height in storm conditions ($H_s \sim 1$ to $1.5m$). The linear configuration of the beach and the absence of an adequate protected feature at the north end resulted in a beach easily affected by the higher wave condition, which can be interpreted as a tendency to be tilted towards the south.

The wave conditions found in the analysis of beach rotation corresponded to the most frequent condition within each sector of direction, the theoretical model appear to be a good representation of the behavior of the beach during the study period.

Table 63 Frequency of Occurrence of the Specific Wave Condition Lloret del Mar

RO_T (°)	T (s)	Dir (°)	Section	Percentage of Occurrence (%)	Days per year
-5.14	4	144	SE	38	59
-5.96	6	151	SSE	42	42
-6.47	7	160	SSE	42	42
-5.10	8	137	SE	9	13
-5.14	4	143	SE	30	59
-5.96	6	143	SE	51	78
-6.47	6	153	SSE	42	42
-5.10	7	135	SSE	42	42
-1.89	4	151	SSE	48	48
-1.89	4	170	S	51	65
3.84	7	201	SSW	46	150
3.84	7	198	SSW	46	150

6.2.1.4 Fenals Beach

Fenals presented the same range of direction that Lloret del Mar (E to SW). The shading cells from the table show the wave conditions to achieve a clockwise configuration and a more uniform configuration coming from an anticlockwise setup.

Result from the previous chapter show that SE to SSE directions generated an anticlockwise rotation of the beach ($RO_T \sim -5.50^\circ$ to -6.5°), which corresponded to the 31% of the mean wave climate. The four specific wave conditions with a period between 4s-5s that generate this behavior from the SE sector presented a percentage of occurrences within the sector of 38% (52 to 59 days per year each). These conditions are a good representation of the most frequent condition within the SE sector.

The conditions from the SSE sector ($T \sim 5s-6s$) presented a percentage of occurrences of a 42% to 48% around 42 to 48 days per year each.

The percentages of occurrence of the direction (S to SSW) that generated a clockwise rotation ($RO_T \sim 2^\circ$ to 3.15°) corresponded to a 35% of the mean wave climate. The condition with a period of 4s from the S sector presented a percentage of occurrences around 51% (65 days per year each), and the condition with a period of 4s from the SSW sector presented a 43% of occurrence around 142 days per year.

The result shows that the theoretical model is consistent with the wave climate that affected the beach. Since Fenals is protected from the E and ESE sectors (energetic wave conditions), the behavior of the beach would be determine by the second most frequent direction (S to SSW) that produce an accumulation toward the north section.

Table 64 Frequency of Occurrence of the Specific Wave Condition Fenals

RO_T (°)	T (s)	Dir (°)	Section	Percentage of Occurrence (%)	Days per year
-5.56	6	150	SSE	42	42
-6.47	5	125	SE	38	59
-6.47	5	135	SE	38	52
0.17	5	142	SE	38	52
0.69	5	147	SSE	48	48
-0.06	4	145	SE	38	59
0.17	4	162	SSE	48	48
0.69	4	193	SSW	43	142
-0.06	4	194	SSW	43	142
3.15	4	178	S	51	65
3.15	4	168	S	51	65
2.01	4	179	S	51	65
2.23	4	177	S	51	65

6.2.2 Llobregat Buoy

Figure 84 show the result of the analysis of frequency of occurrence for the Llobregat buoy. Only the effective directions are represented in the figure. The higher percentage corresponded to the E direction with an 18%, the second higher percentage corresponded to the SSW with a 17%, followed by the ESE, SE and ENE direction with a 13%, 12% and 11% correspondently.

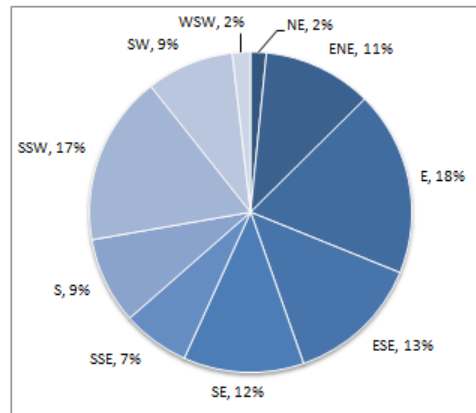


Figure 84 Frequency of occurrence per year, Tordera Buoy.

Figures 85, 86 and 87 presented the joint frequency distribution of significant wave height and peak period per the specific direction sectors. The ENE, E and ESE sector presented the higher wave conditions with $H_s > 1.5\text{m}$ and a T_p around 8 to 10s.

The S and SW sectors presented the lower wave conditions with $H_s < 1.0\text{m}$ and a T_p around 4 to 8s. The S, SSW, SW and WSW sectors also presented a significant contribution of wave condition with $H_s > 1.5\text{m}$ and a T_p around 8 to 10s. It is clear from the figures below that the most common storms events come from the E and the SSW sector.

The wave conditions of four beaches (Bogatell, Nova Icaria, Barceloneta and Playa Larga) are represented by the Llobregat Buoy. The analysis is performed separately for each beach, since the effective range of direction differ in each beach system. The shading cell of the tables corresponded to the wave condition that generated a uniform and clockwise behavior from an anticlockwise rotation; the clear cells corresponded to the wave condition that generated an anticlockwise rotation from the more uniform and clockwise distribution.

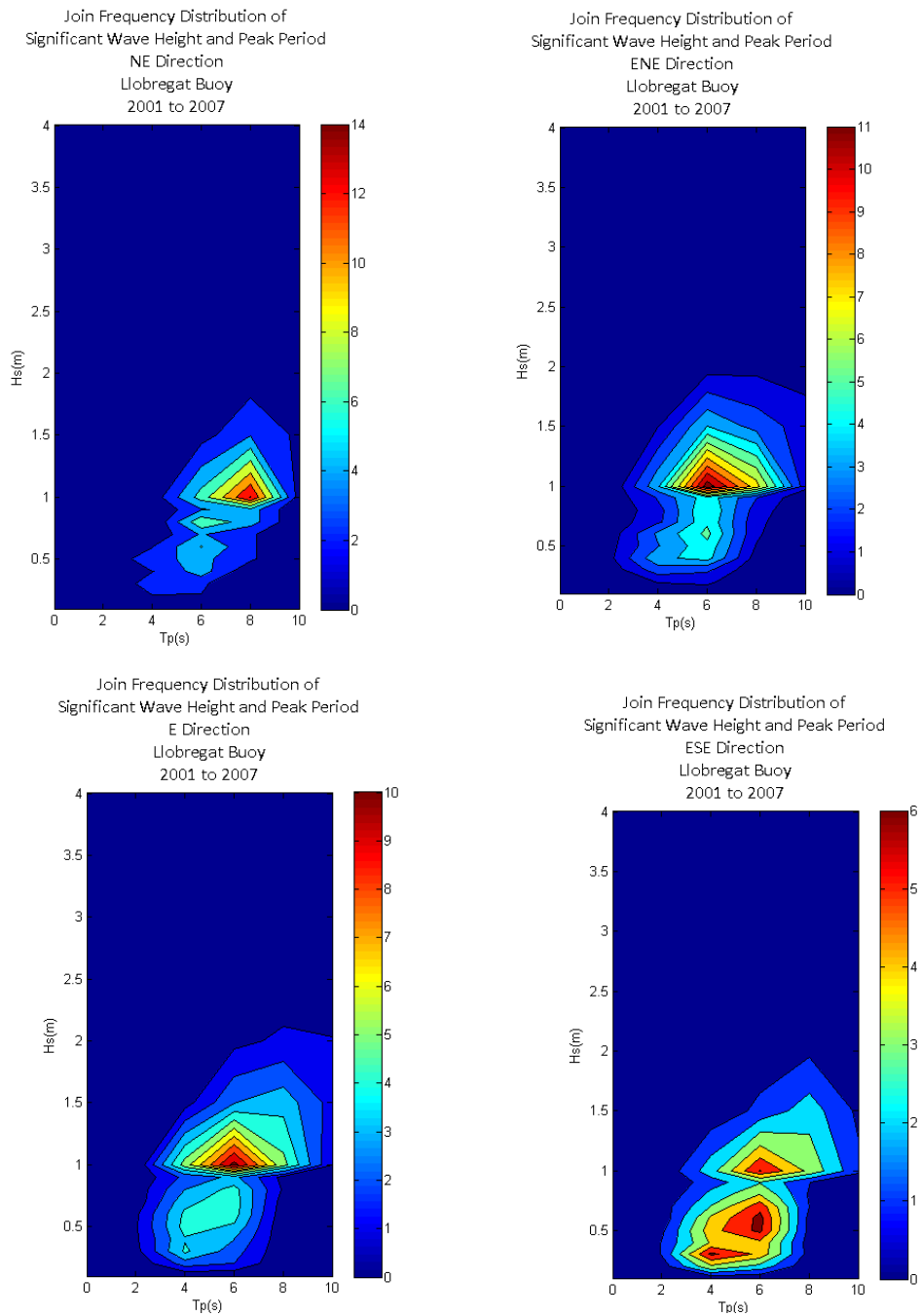


Figure 85 Join Frequency Distribution Significant Wave Height and Peak Period a) NE Directions, b) ENE Directions, c) E Directions and d) ESE Direction. The color bars illustrate the frequency of the data. The wave direction is the direction the waves come from.

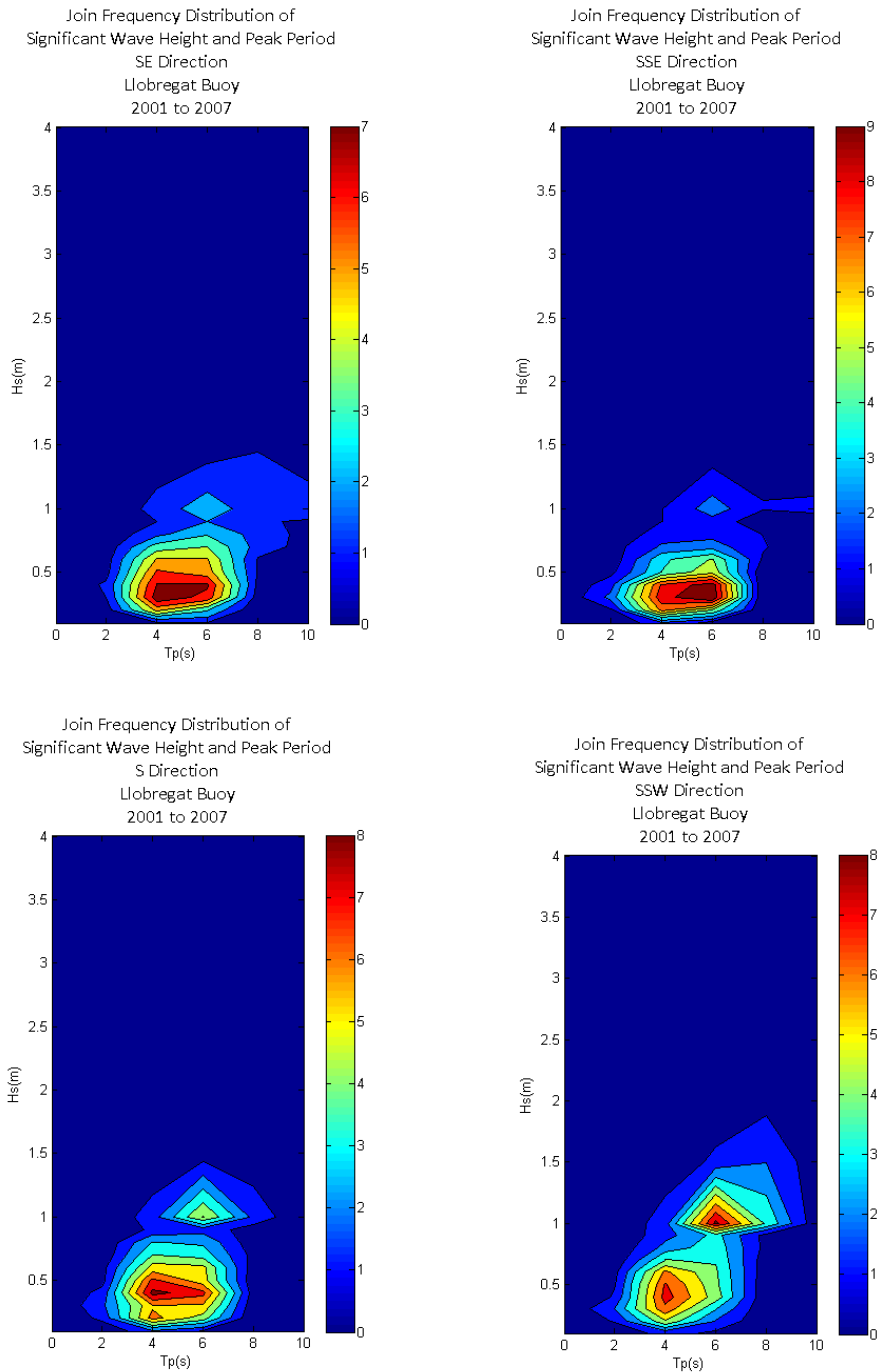


Figure 86 Join Frequency Distribution Significant Wave Height and Peak Period e) SE Directions, f) SSE Directions, g) S Directions and h) SSW Direction. The color bars illustrate the frequency of the data. The wave direction is the direction the waves come from.

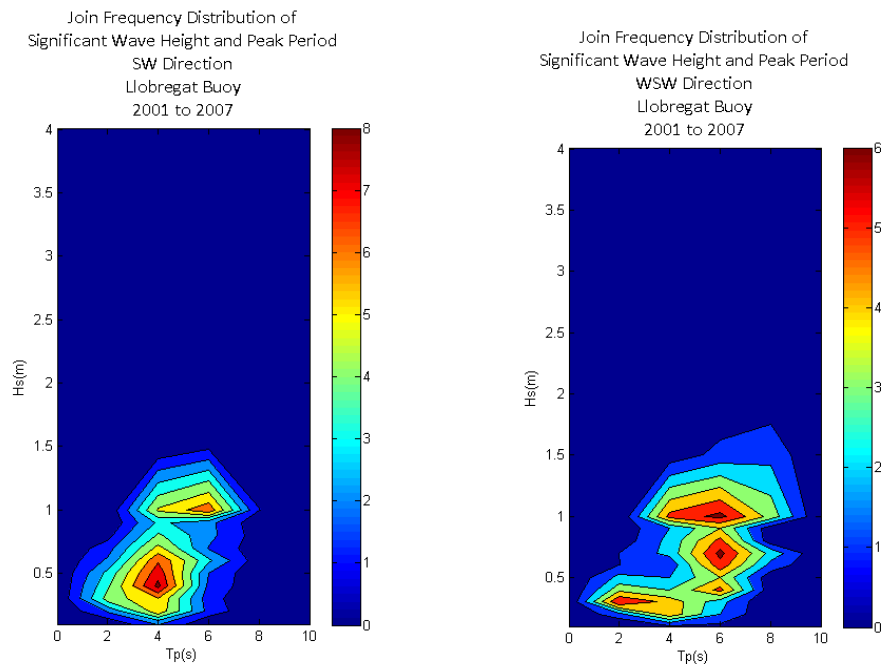


Figure 87 Join Frequency Distribution Significant Wave Height and Peak Period i) SW Directions and j) WSW Direction. The color bars illustrate the frequency of the data. The wave direction is the direction the waves come from.

6.2.2.1 Bogatell Beach

The effective range of direction for Bogatell corresponded to the NE to SSW sectors. Result showed that to achieve an anticlockwise behavior ($RO_T \sim -1$ to -1.5) the beach has to respond to the E-ESE directions which represented the 32% of the wave climate. However, the ENE direction can also affect the beach increasing the range of directions that generate that response, the percentage of occurrence increase to 42%.

The specific wave condition were also analyzed, conditions with a $T_p \sim 5s$ to $7s$ presented the higher percentage of occurrence within the ESE sector around 13% and 45% (13 to 126 days per year). While the condition from the SE sector with a $T_p \sim 8s$ presented the lower percentage of occurrence 10% (25 days per year). This is consistent with the behavior of the join distribution within the each sector.

The SE to S sectors that generated a positive rotation of $RO_T \sim 2.5^\circ$ to 3° (clockwise) presented a 27% of occurrence, but due to the orientation of the beach the SSW condition can also generate this rotation so the

percentage of occurrence taking into account this direction corresponded to a 44%. The specific condition presented the same tendency (SSE direction), table 65 show the percentage of occurrence for this condition (shading cells). The higher percentage of occurrence corresponded to the wave conditions with a T_p of 6s (44%), the condition is presented 63 days per year. The lower percentage of occurrence corresponded to the wave conditions with a T_p of 5s (39%); this corresponded to 55 days per year.

No distinction has been made to the uniform configuration ($RO_T \sim 0.3^\circ$ to 0.6°) since to achieve this platform distribution it would depend in the previous shoreline setup. In the previous chapter the three main configurations were observed 2 times over the shoreline data set, this is consistent with the wave condition from the past 7 years.

Table 65 Frequency of Occurrence of the Specific Wave Condition Bogatell

RO_T (°)	T (s)	Dir (°)	Section	Percentage of Occurrence (%)	Days per year
-0.97	7	116	ESE	45	126
-1.49	6	119	ESE	45	126
0.34	8	122	ESE	13	36
0.63	5	116	ESE	33	92
0.40	8	87	SE	10	25
0.34	6	142	SSE	44	63
0.63	5	152	SSE	39	55
2.46	6	168	SSE	44	63
3.03	6	155	SSE	44	63
2.46	6	171	SSE	44	63
3.03	6	146	SSE	44	63

6.2.2.2 Nova Icaria Beach

Nova Icaria presented the same effective range of direction that Bogatell, this beach differ from the other in the semi-exposed curve shape. Results have showed that to achieve a higher anticlockwise degree of rotation ($RO_T \sim -13^\circ$ to -14°) the beach needs to experience E and ESE directions. These directions corresponded to 32% of the wave climate.

The specific wave conditions with a T_p of 6s correspond to the 45% of the ESE sector (126 days per year). The condition from the E sector presented a percentage of occurrences of 42% (163 days per year). This is consistent with the joint distribution of wave height and peak period of that sector.

The wave condition that presented the lower anticlockwise rotation ($RO_T \sim -10^\circ$), presented a lower occurrence within the sector of 44% about 62 days per year.

The shelter nature of this beach reduced the range of direction that can affect it. The wave conditions during the past 7 years are consisted with the behavior of the theoretical model of the beach.

Table 66 Frequency of Occurrence of the Specific Wave Condition Nova Icaria					
RO_T (°)	T (s)	Dir (°)	Section	Percentage of Occurrence (%)	Days per year
-13.58	6	137	ESE	45	126
-13.35	6	124	ESE	45	126
-14.09	7	87	E	42	163
-10.80	6	148	SSE	44	62

6.2.2.3 Barceloneta Beach

Barceloneta presented the same effective range of direction that Bogatell and Nova Icaria. The analysis of the beach before and after 2006 suggested that E to ESE direction generated a negative RO_T (clear cells from table 67, 68 and 69). This sector corresponded to a 42% of the mean wave climate. Meanwhile, the SE to SSW direction that generated a positive RO_T (shading cells) corresponded to a 44% of the mean wave climate.

No distinction has been made to the uniform configuration. If uniform configuration come from an anticlockwise rotation will required a wave condition from the E and ESE, while if it come from a clockwise rotation it will required direction from the SSE to S sectors.

Before 2006, the wave condition that characterized the beach configuration presented the following percentage of occurrence. The wave conditions from the ESE sector were characterized by a T_p between 4s and 6s, with a percentage of occurrences of 33% to 45% (92 to 122 days per year). The wave condition ($T_{p=4s}$) from the E sector presented an occurrence of 34%; this condition was presented 132 days per year. The wave distribution is consistent with the frequency of the theoretical model during the study period (see table 40). The wave conditions with a period of 6 s from the SE, SSE and S sector presented a percentage of occurrences between

40% and 44%, conditions with this period and these directions would be observed between 62 to 101 days per year.

Table 67 Frequency of Occurrence of the Specific Wave Condition Barceloneta Before 2006

RO _T (°)	T (s)	Dir (°)	Section	Percentage of Occurrence (%)	Days per year
-1.26	6	113	ESE	45	126
-1.24	5	104	ESE	33	92
0.86	4	95	E	34	132
0.86	4	120	ESE	33	92
1.43	6	153	SSE	44	62
1.83	6	170	S	43	76
1.43	6	140	SE	40	101
1.83	6	133	SE	40	101

After 2006, the same range of directions affects the beach. In the north sector, the wave condition with a period between 6s and 7s of the ESE sector presented a percentage of occurrences of 45% (126 days per year). And the ones with a period of 5s presented a 33% of occurrence, around 92 days per year.

The wave condition with a period of 5s within the SE sector presented a percentage of occurrences of 40% (99 days per year), and the ones with a period of 7s presented a 33% of occurrence around 92 days per year. It is clear that the environments that generated an anticlockwise and a uniform distribution from the clockwise condition are more frequent. This is also accorded with the theoretical model of the beach.

Table 68 Frequency of Occurrence of the Specific Wave Condition Barceloneta After 2006 North Section

RO _T (°)	T (s)	Dir (°)	Section	Percentage of Occurrence (%)	Days per year
-1.76	7	110	ESE	45	126
-1.76	7	110	ESE	45	126
1.08	6	120	ESE	45	126
0.99	5	104	ESE	33	92
1.08	7	144	SE	40	101
0.99	5	143	SE	40	99

In the South section, the percentage of occurrence of the ESE sector (e.g. wave conditions with a T_p between 6s and 7s) corresponded to a 45% (126 days per year). For the SE sector (e.g. wave conditions with a T_p of 7s) the percentage was 40% within the sector; the presence of this wave condition is lower about 101 days per year. Both conditions presented a similar occurrence during the year, which agree with the behavior of the shoreline. Both configurations (tilted to the south and to the north) have the same occurrence during the 2006 to 2009.

RO_T (°)	T (s)	Dir (°)	Section	Percentage of Occurrence (%)	Days per year
-0.11	7	115	ESE	45	126
1.31	6	116	ESE	45	126
1.31	7	145	SE	40	101
3.12	7	132	SE	40	101

The theoretical model of Barceloneta (before and after 2006) is consistent with the joint distribution of the wave height and peak period for each sector, and also with the direction itself. The beach is protected from waves coming from the northern sectors, but is affected by the easterly sector that corresponded to the most energetic direction. However, the southern direction also presented significant events with wave height greater than 1.5m.

6.2.2.4 Playa Larga Beach

Playa Larga is the only beach from the Llobregat buoy that presented a different effective range of direction, due to the orientation of the beach (116° relative to the north). The effective range of direction corresponded to SE to the SSW direction.

Result indicated that to achieve a higher anticlockwise rotation the beach need to experience waves from the SE and S direction (clear cells). The percentage of occurrence of these directions corresponded to 27%. The specific wave condition with a period of 5s for the S sector presented a percentage of occurrences of 45% which represent 80 days per year. The SSE condition (wave period of 7s) presented a 44% of occurrence around 62 days per year. Both conditions corresponded to the most common condition within the sectors.

The directions needed to achieve a lower degree of anticlockwise rotation ($RO_T \sim 5^\circ$) corresponded to the SSW and SW sector; that represented a 25% of the wave climate. The specific wave condition with a period of 4s presented a 54% of occurrence within the sector (99 days per year).

The result suggested that wave conditions that generate a higher anticlockwise rotation are more frequent than those that generate a lower rotation, also consistent with the theoretical model of the beach.

Table 70 Frequency of Occurrence of the Specific Wave Condition Playa Larga					
RO_T (°)	T (s)	Dir (°)	Section	Percentage of Occurrence (%)	Days per year
-8.82	5	181	S	45	80
-11.91	7	155	SSE	44	62
-4.68	4	230	SW	54	99

6.2.3 Tortosa Buoy

Figure 88 shows the result of the analysis of frequency of occurrence for the Tortosa buoy. Only the effective directions are represented in the figure. The higher percentage corresponded to the S direction with a 15%, the second higher percentage corresponded to the SSE with a 9%, followed by the SE direction with an 8%.

Only one beach is represented by the Tortosa buoy (Salou). Figures 89 and 90 presented the joint distribution of the significant wave height and peak period per sectors. Figures illustrate that the majority of the sector presented a lower wave height and peak period. Only the S and SSW sector presented wave condition with $H_s > 1.0m$.

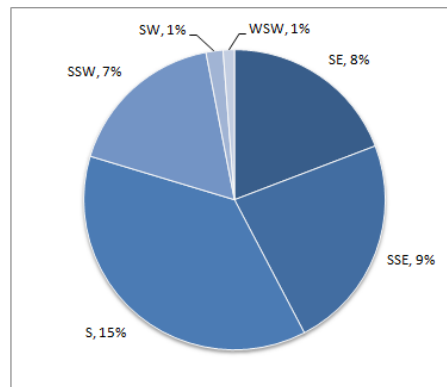


Figure 88 Frequency of occurrence per year; Tortosa Buoy.

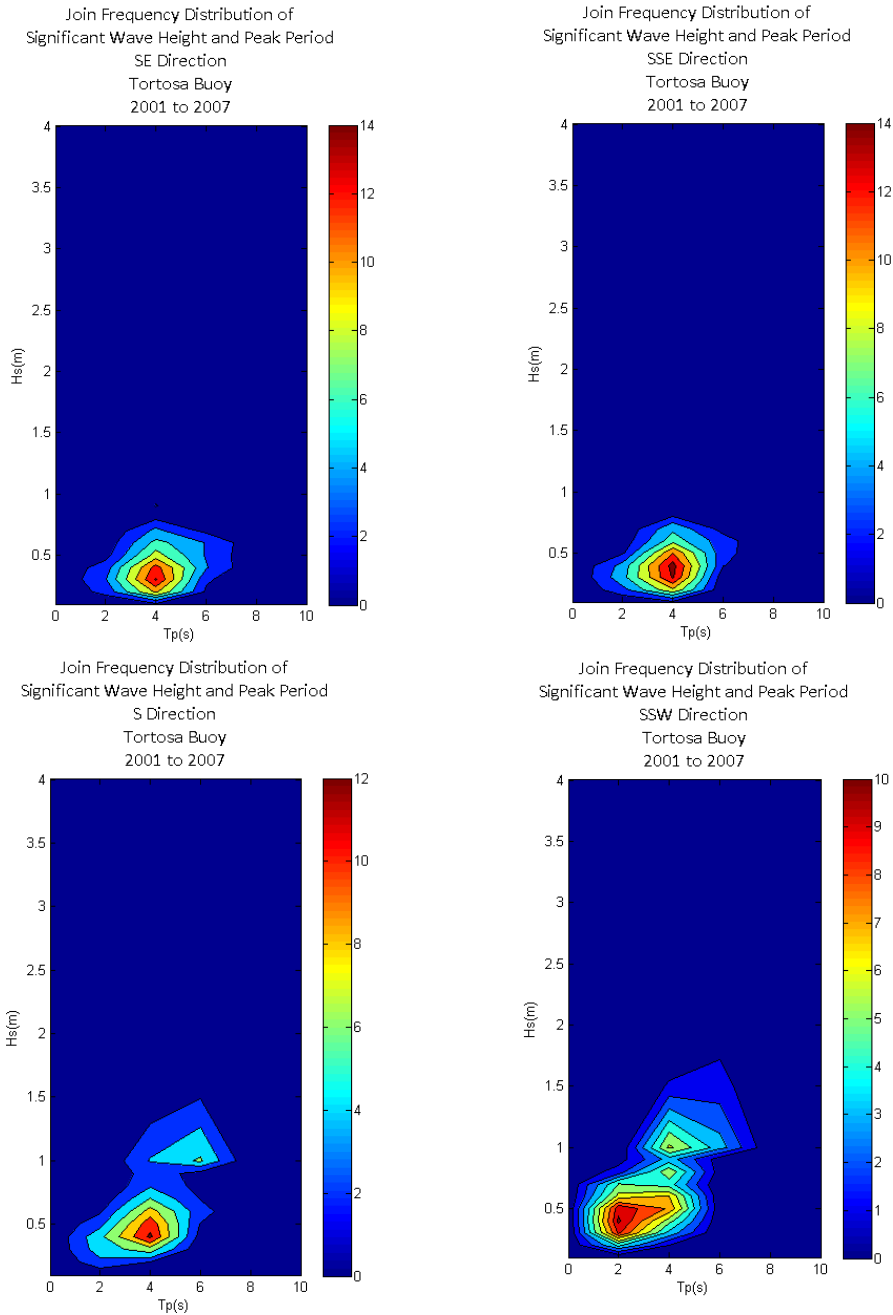


Figure 89 Joint Frequency Distribution Significant Wave Height and Peak Period a) SE Directions, b) SSE Directions, c) S Directions and d) SSW Direction. The color bars illustrate the frequency of the data. The wave direction is the direction the waves come from.

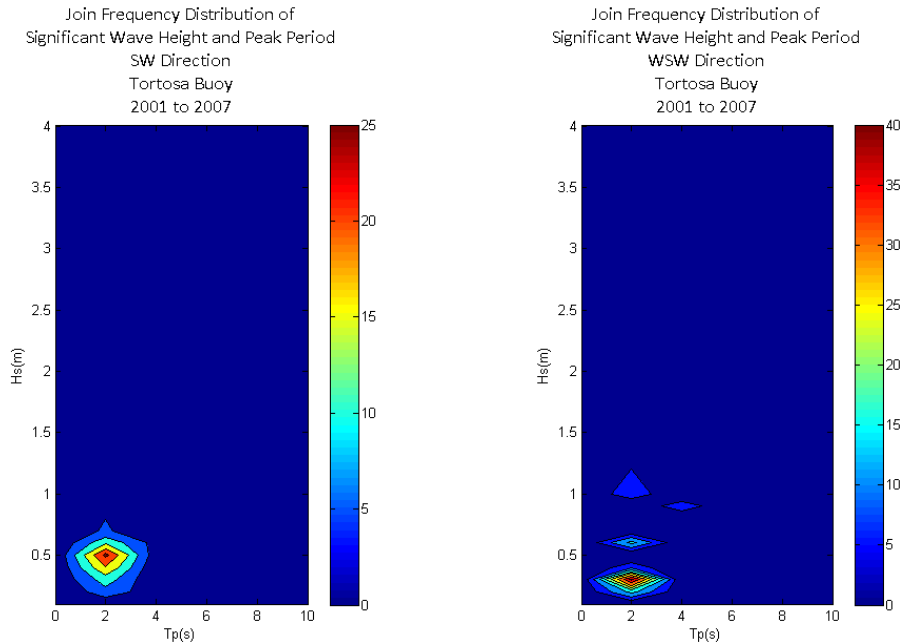


Figure 90 Join Frequency Distribution Significant Wave Height and Peak Period e) SW Directions and f) WSW Direction. The color bars illustrate the frequency of the data. The wave direction is the direction the waves come from.

6.2.3.1 Salou Beach

The effective range of directions for Salou corresponded to the SE to SSW sectors. The results from the previous chapter indicate that to obtain a higher inclination to the south ($RO_T \sim -3^\circ$) the beach need to be exposed to direction from the SE to S sector (33%). Within the S sector, the conditions with a wave period between 5s and 4s presented a percentage of occurrences of 59% around 162 days per year.

The directions that generated a lower degree of rotation ($RO_T \sim -0.5^\circ$) corresponded to the SSW to the WSW (8%). The specific wave condition presented the lower wave period in the order of 3s; this condition presented a 94% of occurrence around 12 days per year.

It is evident that the beach is more exposed to waves that generated a higher anticlockwise rotation. The wave condition determined before are a good representation of the wave climate, therefore the theoretical model is also consisted with the results.

Table 71 Frequency of Occurrence of the Specific Wave Condition Salou					
RO _T (°)	T (s)	Dir (°)	Section	Percentage of Occurrence (%)	Days per year
-3.03	5	182	S	59	162
-2.69	4	178	S	59	162
-2.50	4	175	S	59	162
-0.45	3	229	SW	94	12

It is important to observe that only the specific wave conditions were evaluated by means of the wave period and direction, since the wave height only determine the magnitude of the sediment budget and not the direction towards where this sediment would move.

6.3 Discussion

The results presented above indicate that the frequency of theoretical model is consistent with the wave climate of the beach. Changes in beach configuration are highly related with the wave direction and the antecedent beach conditions (Short and Masselink, 1999; Harley, 2008).

Two different frequencies were established to analyze the theoretical model, the first one that corresponded to the frequency of each directional sector and the second one that relate the wave peak period and the direction. Only the effective range of direction of each beach has been study. None distinction has been made between the uniform configuration and the two extremes, the frequency will depend if the configuration come from a rotation to the south or to the north.

The analysis of Sant Pol beach show that the 25% of the mean wave climate corresponded to direction from the E to the SSE that generate a higher degree of anticlockwise rotation of the beach. And 35% corresponded to direction from the S to the SW that generated a lower anticlockwise rotation of the beach. The specific wave conditions found in the previous chapter corresponded to the most common condition per sectors and indeed represented the behavior of the beach. In terms of days, specific conditions ($T_p \sim 3s-6s$) that generated a lower degree of rotation are present 69 days per year while conditions ($T_p \sim 8s$) that generated a higher degree are presented only 13 days per year.

The frequency of occurrence of wave directions (SSE to S) that generated an higher anticlockwise rotation in Canyelles beach corresponded to 13%, while the directions (S to WSW) that generated a lower antiilockwise

rotation of the beach corresponded to 29%. The specific wave conditions ($T_p \sim 5s-6s$) are present 130 to 150 days per years for both situations. The wave conditions are not consistent with the number of times a specific configuration was observed during the shoreline data set. A logical hypothesis would suggest that due to the orientation of the beach (102°) the waves from the SSW sector does not generate a larger longshore sediment transport component, than other direction.

The result of the analysis for Lloret showed that the direction that generated a beach setup leaning to the south (E to SSE) corresponded to a 31%, whereas direction that generated a beach set up leaning to the north (S to SW) corresponded to a 35%. The specific wave conditions ($T_p \sim 5s-8s$) that generated an anticlockwise rotation occurred around 170 days per year (rotation to the south coming from a beach set up leaning to the north or a more uniform platform). And the wave conditions ($T_p \sim 7s$) that generate the opposite behavior occurred around 150 days per year. The orientation and linear character of the beach made it susceptible to the more energetic wave conditions (E storms), rather than the more frequent. The theoretical model of the beach is consistent with the wave frequency.

For Fenals the same percentage of occurrence per direction sector was obtained. The difference between this beach and Lloret rely in the length of the natural outcrops that protected from the most energetic storm events (E), therefore the beach will experience in a larger degree the effects of the South storms than the East storms. The specific wave conditions found before corresponded to the most frequent conditions within each sectors. The results show that 159 days per year the beach experience wave conditions ($T_p \sim 4s-6s$) that define an anticlockwise rotation from a clockwise setup and 148 days per year the opposite behavior ($T_p \sim 4s$).

The analysis of the Barcelona city beaches, indicate that 42% corresponded to directions that generated an anticlockwise rotation (NE to ESE), and 44% corresponded to directions that generated a clockwise rotation (SSE to SSW). The specific wave conditions found for each beach is also consistent with the most frequent conditions in the join distribution of wave height and peak period per sector. Difference would be attributed to the morphology of the beach (e.g. bar conditions in the South Section of the Barceloneta and Bogatell) and the protective structure outside Nova Icaria.

Results showed that in these three beaches the specific wave conditions ($T_p \sim 4s-8s$) that generated a anticlockwise rotation/higher anticlockwise rotation were presented around 126 days per year, while to achieve a clockwise rotation/lower anticlockwise rotation the specific wave conditions ($T_p \sim 6s-8s$) were presented around 63 to 100 days per year.

At Playa Larga the result showed that 27% of the wave directions (SE to S) generate the higher anticlockwise rotation and a 25% (SSW to WSW) would generate a lower anticlockwise behavior; which agrees with the theoretical model observed within the 16 studied shorelines. The specific wave conditions ($T_p \sim 4s-7s$) found in

the previous chapter was presented 142 day per year for a higher anticlockwise rotation and 99 days per year for the lower anticlockwise behavior.

Finally Salou presented a higher percentage of occurrences for the higher anticlockwise rotation 33% (SE to S) and only an 8% for the SSW to WSW direction (lower anticlockwise rotation). The specific wave conditions of these two last beaches were also consistent with the distribution per sector. In terms of days, the specific wave conditions ($T_p \sim 4s-5s$) that produce the higher beach set up tilted to the south were presented around 162 days per year. And the wave conditions with a T_p of 3s that generate a lower anticlockwise rotation were only presented 13 days per year

The results of the analysis indicate that the theoretical model is a good representation of the behavior of the beach and showed the tendency of the beaches towards one configuration or another.

6.4 Summary

The following conclusion can be drawn from the analysis of wave condition and the theoretical model respond.

- Changes in beach configuration are highly related with the wave direction, wave period, beach exposure and the antecedent beach conditions.
- The theoretical model is a good representation of the wave conditions acting on the beach.
- The theoretical model response to the percentage of occurrence of the direction sectors indicates that some beaches have tendency towards one configuration, most of the cases to a higher anticlockwise rotation.
- Differences between beaches can be attributed to the shelter nature of the beach, the orientation and the effect of the natural or man made headland.
- The specific wave condition (e.g. T_p) obtained in the previous chapter corresponded to the most common conditions within each sector.
- The most energetic conditions corresponded to the East sector, however higher wave height are also found in the South sector.
- The mean wave conditions were the one that has been studied, but the effect of a storm can lead to reproduce the theoretical model in a short time.

7. Conclusions and Recommendation

The main objective of this study was to analyze the behavior of the embayed beaches along the Catalan Coast in order to quantify the morphological variability of these bounded systems. This was undertaken by analyzing a unique shoreline dataset and wave climate of nine embayed beaches along the coast. From this main objective, three sub-objectives were proposed in section 1.2. The outcomes from this aims are presented below.

1. Study of the shoreline evolution base on the analysis of historical aerial photographs of embayed beaches in the Catalan coast.

The shoreline evolution analysis showed that most of the beaches are experiencing a similar stable mode. The stability tests have revealed that the stability curve of the study beaches is shifted from the curve proposed by Hsu, 1989. This implied that the beaches presented a stable mode, since beaches with the same morphology follow a same trend.

The variability of the beaches was dependent of the degree of curvature, their exposure to wave conditions and the intertidal slope and the grain size. In particular the following behavior was exhibit:

- The study beaches presented a wide range of indentation. Girona and Barcelona presented the moderate to high indented beaches, while Tarragona presented the less indented beaches.
- Beach mobility (e.g. beach width) along the beaches presented a high degree of variability and is function of the degree of curvature of the beach and their exposure to wave conditions.
- Most of the beaches do not present any trends in the emerged beach area, characteristic of the conservative environments.
- Reflective beaches had the greatest variation on the sub-aerial beach, and were characterized by beaches with moderate to less curvature.
- Intermediate beaches had the smaller variation on the sub-aerial beach, and were characterized by beaches with a moderate curvature.
- The dissipative beaches of the study presented a different behavior with each other.

Since only the sub-aerial beach behavior has been study, it is logical to observe that the reflective beaches are the one that present a higher variability. But, intermediate beaches has been known to exist in a grater range of

beach state, therefore an specific study of beach profile should be perform in order to observe what is the behavior of this specific beach types.

2. *Determine the presence of medium term oscillation and variation of the Catalan Coast and identify the conditions require that accomplish a change in the shoreline position using a theoretical model.*

Beach rotation was prominent on the embayment beaches on the Catalan coast. Of our interesting; the degree of rotation were related to the exposure of the more energetic wave condition and the beach type. The exposed reflective beaches presented the higher degree of rotation (anticlockwise/clockwise); the exposed intermediate presented the second higher degree of rotation (anticlockwise/clockwise). The lower degrees of rotation were presented in the dissipative beaches and the semi-exposed reflective and intermediate beaches (only anticlockwise rotation).

Based on the theoretical model developed for each beach, the following conclusions were obtained:

- Wave direction was the primary forcing mechanism observed on the analysis. The combination of wave height, period and direction where the responsible of the response time of the beach to a new configuration.
- Wave height influences the magnitude of the longshore sediment rate, but is the wave period in combination with the wave direction that affects the direction of the longshore sediment rate. Therefore, the changes in configuration.
- Exposed beaches oriented to the SSE presented an anticlockwise/clockwise rotation to SE-SSE/S-SSW waves and exposed beaches oriented to the ESE presented an anticlockwise/clockwise rotation to E-ESE/ SE-S waves.
- Semi-exposed beaches oriented to the SSE respond to SE/S wave in a higher anticlockwise rotation/ lower anticlockwise rotation. While the ones oriented to ESE respond in the same matter to E-ESE/SSE waves. Finally the beaches oriented to the SSW react to SSE-S waves with a higher anticlockwise rotation, than to SSW waves that generate a lower anticlockwise rotation.

3. *Determine the frequency of occurrence of the wave conditions that produce a change in the theoretical model over 2001 to 2007.*

The theoretical model was a good representation of the wave conditions acting on the beach. Changes in beach configuration are highly related with the wave direction, beach exposure and the antecedent beach conditions.

The percentage of occurrence of the wave climate during 2001 to 2007 suggested that some beaches have tendency towards one configuration, in most cases to a higher anticlockwise rotation. Differences between beaches can be attributed to the shelter nature of the beach, the orientation and the effect of the natural or man made headland.

The frequency of the specific wave condition (e.g. T_p) obtained in the previous objective corresponded to the most common conditions within each sector, implied that they represent the behavior of the wave climate within the directional sector. The most energetic conditions corresponded to the East sector, however higher wave height are also found in the South sector.

Finally, the results presented in this thesis show that the embayed beaches along the Catalan coast presented a wide degree of variation. The result corresponded to a general overview of the morphological process within the embayment. Further detail research should be realize in each beach by using beach profile surveys , in order to determine seasonal variation that couldn't be obtain in this study. Also a monitoring campaign along the beaches should be performed with the objective of increase the amount of information of the data set to future research studies in the subject.

8. References

- Ariza, E., Jimenez, J.A, Sarda, R., 2008 “A critical assessment of beach management on the Catalan coast”, *Ocean & Coastal Management* 51 (2008) 141–160.
- Ashton, A.D. and Murray, A. B., 2006 “High- angle wave instability and emergent shoreline shapes: Wave climate analysis and comparison to nature”. *Journal of Geophysical Research* vol III, F04012.
- Bowman, D., Guillen, J., Lopez, L., Pellegrino, V., 2009 “Planview Geometry and morphological characteristics of pocket beaches on the Catalan coast (Spain)”, *Geomorphology* 18, p 191-199.
- Bosboom, J. and Stive, M.J.F., 2010 “Coastal Dynamics I and II”, Delft University of Technology.
- Casas-Prat, M., Sierra, J.P., 2010 “Trend analysis of the wave storminess: the wave direction”. *European Geosciences Union*. p. 89-92.
- Garcia, V., Valdemoro, H., Mendoza, T., Sánchez-Arcilla, A., Jiménez, J.A. 2008 “Coastal protection issues in bayed beaches. The importance of shoreline tilting ”.
- Harley, M. 2009 “Daily to decadal embayed beach response to wave and climate forcing”, The University of New South Wales. PhD thesis.
- Harley, M., Turner, I., Short, A., Ranasinghe, R., 2008 “Rotation and Oscillation of an Embayed Beach”. *Coastal Engineering*, p 865-864.
- Hart, D.E and Bryan, K.R., 2008 “New Zealand coastal system boundaries, connections and management”. *New Zealand Geographer* 64, p 129-143.
- Hsu, J.R., Yu M.J., Lee, F.C. Benedet, L., 2009 “Static bay beach concept for scientists and engineers: A review”. *Coastal Engineering* 57, p 76-91.
- Jiménez, J. A. 2007, “Playas encajadas-Bahía de equilibrio”. *Universitat Politècnica de Catalunya*.
- Kamphuis J.W., Davies, M.H., Nairn, R.B., Sayao, O.J., 1986 *Coastal Engineering* 10, p 1-21.
- Klein, A.H.F., Menezes, J.T., 2001 “Morphodynamics and Profile Sequence for a Headland Bay”. *Journal of Coastal Research*, 17(4), p. 812-835.
- Klein, A.H.F., Benedet, L., Schumacher, D.H., 2002b “Short-term beach rotation process in distinct headland bay beach systems”. *Journal Coastal Research* 18, p 442-458.

- Klein, A.H.F., Ferreira, O., Dias, J. A. M., Tessler, M.G.,Silveira, L.F., Benedet, L., Menezes, J.T., Abreu, J.G.N., 2009 “Morphodynamics of structurally controlled headland-bay beaches in southeastern Brazil”, Coastal Engineer 57, p 98-111.
- Lewis, W.V. 1938 “The evolution of shoreline curves” .
- Martins, C.C., Michaelovitch de Mahiques, M., Alveirinho J., 2010 “Daily morphological changes determined by high-energy events on an embayed beach: qualitative model”. Earth surface process and landforms 35, p 487-495.
- Masselink, G., Pattiaratchi, C.B. “Seasonal changes in beach morphology along the sheltered coastline of Perth, Western Australia”. Marine Geology 172, p243-263.
- Mendoza Ponce, E. T., 2008 “Coastal vulnerability to storms in the Catalan coast”. PhD Thesis.
- Ministerio de Fomento; Puertos del Estado. “Conjunto de datos SIMAR-44, Proyecto HIPOCAS”, July 2008.
- Ojeda, E., Guillen, J., 2008 “Shoreline position and beach rotation of artificial embayed beaches”. Marine Geology, p. 51-62.
- Olijslagers, F.J.H, 2003 “Pocket perched beaches”. MSc Thesis.
- Pinto, C.A., Taborda, R., Andrade, C., Teixeira, S.B., 2009 “Seasonal and Meso-scale Variation at Embayed Beach (Armacao de Pera, Portugal)”. Journal of Coastal Research 56, p 118-122.
- Ranashinge, R., Rodney, McL., Short, A., Graham, S., 2004 “The Southern Oscillation Index, wave climate and beach rotation”. Marine Geology, p 273-287.
- Short A.D. and Wright L.D. 1984 “Morphodynamics variability of surf zone and beaches: A synthesis”. Marine Geology 56, p 93-118.
- Short, A.D. and Masselink, G., 1999 “Embayed and structurally controlled beaches”. In: Short, A.D. (Ed.), Handbook of Beach and Shoreface Morphodynamics. Wiley, New York, pp 230-249.
- Silvester, R., Hsu, J.R.C., 1997”Coastal stabilization”. Advances series on Ocean Engineering, Vol. 14. World Scientific, Singapore, p 578.
- Small, C., Nicholls, R. J., 2003. “A global analysis of human settlement in coastal zones”. Journal of Coastal Research 19, p 584-599.

- Stive, M.J.F., Aarninkhof, S.G.J., Hamm, L., Hanson, H., Larson, M., Wijnberg, W., Nicholls, R.J., Capobianco, M., 2002 "Variability of shore and shoreline evolution". Coastal engineering 47, p 211-235.
- Sweers, K.B., 1999 "Equilibrium bays". MSc thesis.
- Vintém G.; M.P. Freitas; J.T. Menezes and A. H. Klein, 2006 "Beach Rotation Processes: 35 Month Survey of Embayed Beaches of Santa Catarina Brazil", Proceedings of the 8th International Coastal Symposium, p 1752-1755.
- Wood, A., 2010 "Episodic, seasonal and long term morphological changes on Coromandel beaches". MSc Thesis.

Appendix A: General Classification of the Embayed Beaches along the Catalan Coast

This appendix contained the following information from the shoreline data set of each beach:

- Date
- Type of shoreline
- Length of the embayment
- Length of the control line (R_o)
- Orientation of the Control line
- Indentation (a)
- Indentation criteria (a/R_o)
- Wave obliquity (β)
- Beach orientation (θ)
- Beach area
- Beach width
- Normalized Beach width
- Rotation Coefficient (RO)

General Classification Sant Pol

Date (m/d/y)	Type	Length (m)	Ro (m)	Length/Ro	Orientation	Indentation a	a/Ro	β	Beach	
					Ro (°)	(m)			orientation	Beach area
1-Jul-95	MMA	884	739	1.20	280	299	0.40	51	74	2.52
1-Sep-00	ICC	872	750	1.16	286	283	0.38	54	73	2.75
1-Jun-04	ICC	883	722	1.22	289	343	0.48	47	74	2.88
30-Jun-04	Google	891	725	1.23	299	347	0.48	52	73	2.81
1-May-06	ICC ORTO	867	700	1.24	280	282	0.40	54	73	2.35
31-Dec-06	Google	871	717	1.21	282	302	0.42	51	73	3.11
11-Nov-07	Google	856	723	1.18	279	305	0.42	55	74	4.08
1-Jun-08	ICC ORTO	864	749	1.15	282	312	0.42	55	73	2.50
31-Dec-08	Google	867	759	1.14	284	324	0.43	53	74	2.85
1-Jun-09	ICC ORTO	857	803	1.07	281	342	0.43	46	73	2.50
31-Dec-09	Google	846	726	1.17	282	305	0.42	55	72	2.69
Average		869	738	1.18	284	313	0.42	52	73	2.82

Date (m/d/y)	Linear Rotation Coefic	Linear Rotation Coefic	R2
1-Jul-95	-0.01	-0.69	0.31
1-Sep-00	-0.01	-0.57	0.09
1-Jun-04	-0.01	-0.53	0.14
30-Jun-04	-0.02	-0.97	0.29
1-May-06	-0.01	-0.49	0.12
31-Dec-06	-0.03	-1.46	0.34
11-Nov-07	-0.03	-1.84	0.40
1-Jun-08	-0.02	-1.15	0.33
31-Dec-08	-0.03	-1.64	0.41
1-Jun-09	-0.02	-1.00	0.18
31-Dec-09	-0.02	-1.15	0.26

Date (m/d/y)	Beach width (m)					Normalized Beach width (m)				
	P1 (100m)	P2 (250m)	P3 (450m)	P4 (650m)	P5 (800m)	P1	P2	P3	P4	P5
1-Jul-95	33.63	28.54	41.07	28.70	22.21	1.91	-4.53	-3.64	-1.72	5.30
1-Sep-00	28.44	29.37	45.75	30.03	20.98	-3.27	-3.70	1.04	-0.40	4.07
1-Jun-04	32.61	36.13	47.73	32.84	26.07	0.90	3.06	3.02	2.41	9.16
30-Jun-04	33.38	38.54	46.00	30.76	22.00	1.67	5.47	1.29	0.33	5.09
1-May-06	22.65	23.23	37.20	26.32	13.43	-9.06	-9.84	-7.51	-4.11	-3.48
31-Dec-06	34.42	39.98	47.70	34.06	15.02	2.71	6.91	2.99	3.63	-1.89
11-Nov-07	43.40	47.14	55.77	41.46	18.06	11.69	14.07	11.06	11.03	1.15
1-Jun-08	30.54	26.12	40.55	24.96	12.74	-1.18	-6.95	-4.16	-5.47	-4.17
31-Dec-08	35.45	35.23	48.41	27.68	14.13	3.74	2.16	3.70	-2.75	-2.78
1-Jun-09	25.32	26.99	40.55	26.50	10.18	-6.39	-6.09	-4.16	-3.93	-6.73
31-Dec-09	28.99	32.53	41.07	31.41	11.20	-2.72	-0.54	-3.64	0.98	-5.71
Average	31.71	33.07	44.71	30.43	16.91					

General Classification Canyelles

Date (m/d/y)	Type	Length (m)	Ro (m)	Length/Ro	Orientation Ro (°)	Indentation a (m)	a/Ro	β	Beach orientation	Beach area
1-Jul-86	ICC	415	335	1.24	315.00	97	0.29	34	102	1.94
1-Jun-94	ICC	406	328	1.24	318.00	92	0.28	33	103	1.90
1-Jul-95	MMA	465	359	1.29	314.00	110	0.31	34	102	1.64
1-Jul-00	ICC	485	353	1.37	316.00	103	0.29	31	101	1.55
1-Jun-04	ICC	490	368	1.33	313.00	113	0.31	38	102	1.53
30-Jun-04	Google	407	328	1.24	314.00	110	0.33	33	102	1.50
May-06	ORTO ICC	398	333	1.20	318.00	107	0.32	37	102	1.64
31-Dec-06	Google	413	376	1.10	313.00	114	0.30	39	102	1.35
11-Nov-07	Google	398	347	1.15	315.00	111	0.32	35	103	1.46
1-Jun-08	ORTO ICC	457	347	1.32	316.00	99	0.28	32	102	1.73
31-Dec-08	Google	399	345	1.16	318.00	98	0.28	33	102	1.47
1-Aug-09	ORTO ICC	443	360	1.23	314.00	112	0.31	39	103	1.51
31-Dec-09	Google	470	347	1.35	317.00	103	0.30	33	103	1.57
Average		434	348	1.25	315	105	0.30	35	102	1.60

Date (m/d/y)	Linear Rotation Coefic	Linear Rotation Coefic (°)	R2
1-Jul-86	-0.08	-4.79	0.62
1-Jun-94	-0.08	-4.41	0.55
1-Jul-95	-0.10	-5.49	0.60
1-Jul-00	-0.07	-4.22	0.52
1-Jun-04	-0.10	-5.83	0.68
30-Jun-04	-0.06	-3.51	0.42
May-06	-0.08	-4.41	0.55
31-Dec-06	-0.09	-4.98	0.61
11-Nov-07	-0.07	-4.29	0.52
1-Jun-08	-0.08	-4.78	0.58
31-Dec-08	-0.08	-4.37	0.47
1-Aug-09	-0.10	-5.59	0.69
31-Dec-09	-0.09	-4.92	0.57

Date (m/d/y)	Beach width (m)					Normalized Beach width (m)				
	P1 (30m)	P2 (100m)	P3 (170m)	P4 (270m)	P5 (370m)	P1	P2	P3	P4	P5
1-Jul-86	57.67	58.70	36.13	49.98	27.25	5.75	11.17	12.69	9.71	6.43
1-Jun-94	57.17	54.13	32.60	49.90	27.07	5.25	-0.93	1.48	3.42	-4.15
1-Jul-95	55.34	46.60	24.92	43.69	16.67	3.42	-5.36	-0.45	0.81	-3.52
1-Jul-00	47.67	42.17	22.99	41.08	17.30	-4.25	-5.36	-0.45	0.81	-3.52
1-Jun-04	53.66	45.40	20.94	35.86	15.83	1.74	-2.13	-2.50	-4.41	-4.99
30-Jun-04	46.78	46.02	19.81	37.50	25.01	-5.14	-1.51	-3.63	-2.77	4.19
May-06	53.21	49.05	24.36	41.41	24.59	1.29	1.52	0.92	1.14	3.77
31-Dec-06	48.87	43.33	16.47	31.08	18.33	-3.06	-4.20	-6.97	-9.19	-2.49
11-Nov-07	47.93	45.59	18.88	35.87	21.19	-3.99	-1.94	-4.56	-4.40	0.37
1-Jun-08	56.33	48.99	25.96	43.20	24.15	4.40	1.46	2.52	2.93	3.33
31-Dec-08	50.25	44.46	18.08	38.82	20.74	-1.68	-3.07	-5.36	-1.45	-0.08
1-Aug-09	49.78	47.17	22.71	35.97	14.70	-2.14	-0.36	-0.73	-4.30	-6.12
31-Dec-09	50.33	46.25	20.89	39.19	17.79	-1.60	-1.28	-2.55	-1.08	-3.03
Average	51.92	47.53	23.44	40.27	20.82					

General Classification Lloret del Mar

Date (m/d/y)	Type	Beach		Beach area
		Length (m)	orientation	
1-Jul-86	ICC	1084	65	5.34
1-Jun-94	ICC	1087	67	5.57
1-Jul-95	MMA	1082	64	5.42
1-Aug-97	ICC	1053	67	6.13
1-Sep-00	ICC	1090	69	4.95
1-May-01	ICC	1227	73	5.38
1-Dec-01	MMA	1074	65	5.20
1-Jun-04	ICC	1138	60	5.27
30-Jun-04	Google	1048	60	5.51
27-Apr-05	Google	1039	58	5.34
1-May-06	ORTO ICC	1115	65	6.25
31-Dec-06	Google	1114	65	6.02
11-Nov-07	Google	1063	60	6.06
1-Jun-08	ORTO ICC	1104	64	5.80
31-Dec-08	Google	1070	62	5.78
1-Jun-09	ORTO ICC	1127	67	5.09
31-Dec-09	Google	1104	65	5.38
Average		1095	64	5.56

Date (m/d/y)	Linear	Linear	R2
	Rotation	Rotation	
	Coefic	Coefic (°)	
1-Jul-86	-0.03	-1.89	0.92
1-Jun-94	0.02	0.97	0.34
1-Jul-95	0.01	0.29	0.04
1-Aug-97	-0.09	-5.14	0.10
1-Sep-00	0.02	0.97	0.23
1-May-01	0.07	3.84	0.55
1-Dec-01	-0.01	-0.50	0.14
1-Jun-04	-0.10	-5.96	0.95
30-Jun-04	-0.11	-6.25	0.94
27-Apr-05	-0.11	-6.47	0.94
1-May-06	-0.05	-3.04	0.95
31-Dec-06	-0.06	-3.44	0.96
11-Nov-07	-0.09	-5.10	0.97
1-Jun-08	-0.05	-2.64	0.95
31-Dec-08	-0.05	-2.98	0.94
1-Jun-09	-0.02	-1.03	0.30
31-Dec-09	-0.02	-1.26	0.49

Date (m/d/y)	Beach width (m)					Normalized Beach width (m)				
	P1 (100m)	P2 (300m)	P3 (500m)	P4 (700m)	P5 (900m)	P1	P2	P3	P4	P5
1-Jul-86	72.00	54.79	45.80	38.93	40.63	-9.80	-4.26	0.85	1.96	-5.12
1-Jun-94	51.88	41.10	52.32	49.32	73.28	-29.92	-17.95	7.37	12.35	27.53
1-Jul-95	58.59	41.10	42.03	52.04	63.98	-23.21	-17.95	-2.92	15.07	18.23
1-Aug-97	110.00	81.00	57.11	31.34	25.30	28.20	21.95	12.16	-5.63	-20.45
1-Sep-00	48.36	30.67	34.19	49.04	66.16	-33.44	-28.38	-10.76	12.07	20.41
1-May-01	25.55	15.34	17.09	51.97	100.00	-56.25	-43.71	-27.86	15.00	54.25
1-Dec-01	64.92	48.70	35.00	44.10	60.97	-16.88	-10.35	-9.95	7.13	15.22
1-Jun-04	110.03	78.21	42.59	13.38	14.94	28.23	19.16	-2.36	-23.59	-30.81
30-Jun-04	115.52	82.53	48.24	12.51	17.77	33.72	23.48	3.29	-24.46	-27.98
27-Apr-05	118.14	82.01	46.10	11.05	15.26	36.34	22.96	1.15	-25.92	-30.49
1-May-06	93.52	71.60	54.69	43.50	43.58	11.72	12.55	9.74	6.53	-2.17
31-Dec-06	96.05	70.24	54.06	39.40	39.25	14.25	11.19	9.11	2.43	-6.50
11-Nov-07	110.81	81.00	54.06	31.34	26.88	29.01	21.95	9.11	-5.63	-18.87
1-Jun-08	86.42	65.21	51.00	43.27	42.61	4.62	6.16	6.05	6.30	-3.14
31-Dec-08	89.49	68.53	51.00	40.44	41.35	7.69	9.48	6.05	3.47	-4.40
1-Jun-09	68.50	43.03	37.27	36.69	53.76	-13.30	-16.02	-7.68	-0.28	8.01
31-Dec-09	70.76	48.71	41.57	40.13	52.08	-11.04	-10.34	-3.38	3.16	6.33
Average	81.80	59.05	44.95	36.97	45.75					

General Classification Fenals

Date (m/d/y)	Type	Length (m)	Ro (m)	Length/Ro	Orientation Ro (°)	Indentation a (m)	a/Ro	β	Beach orientation	Beach area
1-Jul-86	ICC	743.54	619.45	1.20	274.00	185.84	0.68	38.00	65.00	4.19
1-Jun-94	ICC	742.86	625.42	1.19	274.00	165.72	0.60	31.00	66.00	4.22
1-Jul-95	MMA	726.25	577.86	1.26	277.00	171.76	0.62	34.00	65.00	4.02
1-Aug-97	ICC	753.81	580.67	1.30	276.00	163.97	0.59	39.00	65.00	4.49
1-Sep-00	ICC	757.22	609.38	1.24	278.00	172.56	0.62	36.00	66.00	3.86
1-Dec-01	MMA	721.85	613.59	1.18	274.00	178.43	0.65	36.00	64.00	4.02
1-Jun-04	ICC	739.38	619.56	1.19	271.00	219.71	0.81	47.00	63.00	3.74
30-Jun-04	Google	724.95	605.04	1.20	271.00	225.99	0.83	48.00	62.00	3.69
27-Apr-05	Google	727.96	619.04	1.18	272.00	203.43	0.75	44.00	64.00	3.99
1-May-06	ORTO ICC	725.13	658.10	1.10	270.00	204.75	0.76	35.00	63.00	3.81
31-Dec-06	Google	722.96	669.94	1.08	268.00	212.36	0.79	41.00	64.00	3.95
11-Nov-07	Google	707.50	670.49	1.06	267.00	218.29	0.82	41.00	64.00	3.97
1-Jun-08	ORTO ICC	723.79	689.88	1.05	268.00	211.52	0.79	40.00	65.00	3.76
31-Dec-08	Google	727.07	690.86	1.05	268.00	215.78	0.81	37.00	64.00	3.87
1-Jun-09	ORTO ICC	716.62	605.00	1.18	266.00	160.00	0.60	32.00	65.00	3.60
31-Dec-09	Google	734.35	603.00	1.22	270.00	168.00	0.62	32.00	65.00	3.70
Average		730.95	628.58	1.17	271.50	192.38	0.71	38.00	64.00	3.93

Date (m/d/y)	Linear Rotation Coefic	Linear Rotation Coefic (°)	R2
1-Jul-86	0.00	0.17	0.38
1-Jun-94	0.06	3.15	0.89
1-Jul-95	0.01	0.69	0.44
1-Aug-97	0.04	2.01	0.81
1-Sep-00	0.04	2.23	0.91
1-Dec-01	0.00	-0.06	0.40
1-Jun-04	-0.10	-5.56	0.87
30-Jun-04	-0.11	-6.47	0.92
27-Apr-05	-0.05	-2.75	0.72
1-May-06	-0.01	-0.40	0.07
31-Dec-06	-0.02	-1.03	0.48
11-Nov-07	-0.05	-2.86	0.66
1-Jun-08	0.01	0.34	0.14
31-Dec-08	0.00	-0.17	0.11
1-Jun-09	0.05	2.92	0.86
31-Dec-09	0.06	3.27	0.92

Date (m/d/y)	Beach width (m)					Normalized Beach width (m)				
	P1 (110m)	P2 (250m)	P3 (380m)	P4 (520m)	P5 (650m)	P1	P2	P3	P4	P5
1-Jul-86	59.65	60.06	48.58	58.59	62.79	1.47	2.40	-0.98	7.07	4.98
1-Jun-94	46.28	49.49	52.07	70.59	75.18	-11.89	-8.16	2.51	19.06	17.36
1-Jul-95	53.68	54.75	53.76	63.30	57.95	-4.49	-2.90	4.20	11.77	0.13
1-Aug-97	54.04	56.36	55.58	70.62	71.80	-4.14	-1.30	6.03	19.09	13.98
1-Sep-00	44.93	47.60	49.71	62.43	65.65	-13.24	-10.06	0.16	10.91	7.84
1-Dec-01	63.69	54.26	48.10	53.23	63.37	5.51	-3.39	-1.45	1.70	5.55
1-Jun-04	83.20	72.14	46.52	28.80	35.70	25.03	14.49	-3.04	-22.73	-22.12
30-Jun-04	84.75	77.58	47.75	28.80	28.54	26.57	19.93	-1.80	-22.73	-29.28
27-Apr-05	69.61	67.44	51.05	39.68	49.26	11.44	9.79	1.49	-11.85	-8.55
1-May-06	56.32	57.57	48.22	45.34	57.50	-1.86	-0.08	-1.34	-6.19	-0.31
31-Dec-06	60.66	60.16	51.65	46.27	54.37	2.48	2.50	2.09	-5.26	-3.45
11-Nov-07	72.66	69.12	48.25	40.27	51.42	14.48	11.46	-1.30	-11.25	-6.39
1-Jun-08	50.47	55.66	49.93	49.69	58.11	-7.70	-1.99	0.38	-1.83	0.29
31-Dec-08	53.40	56.52	53.20	50.87	54.12	-4.78	-1.13	3.64	-0.66	-3.69
1-Jun-09	39.86	41.53	43.38	56.63	69.29	-18.32	-16.12	-6.18	5.11	11.47
31-Dec-09	37.62	42.22	45.14	59.33	70.00	-20.55	-15.43	-4.41	7.81	12.18
Average	58.18	57.65	49.55	51.53	57.82					

General Classification Bogatell

Date	Type	Length (m)	Ro (m)	L/Ro	Orientation		Indentation		β	Beach	
					Ro (°)	a (m)	a/Ro	orientation		Beach area	
1-Sep-94	ICC	614	407	1.51	243	174	0.43	39	43	3.09	
1-Feb-95	MMA	594	448	1.33	243	169	0.38	40	44	3.19	
1-Sep-00	ICC	610	511	1.19	244	200	0.39	39	42	1.93	
1-Jun-04	ICC	627	509	1.23	244	204	0.40	37	39	1.94	
30-Jun-04	Google	622	490	1.27	244	201	0.41	40	38	1.97	
1-Jun-06	ICC Ortofoto	623	485	1.28	245	195	0.40	38	42	2.22	
31-Dec-06	Google	600	525	1.14	245	205	0.39	36	40	1.98	
25-Apr-07	Google	623	472	1.32	244	199	0.42	46	39	1.84	
8-Jun-07	Google	617	495	1.25	242	209	0.42	45	38	1.87	
11-Sep-07	Google	618	495	1.25	243	201	0.41	39	41	1.95	
15-Nov-07	Google	585	497	1.18	243	200	0.40	40	40	1.96	
1-Mar-08	ICC Ortofoto	621	468	1.33	241	189	0.40	39	39	2.40	
31-Dec-08	Google	609	464	1.31	240	189	0.41	41	38	2.14	
7-Feb-09	Google	616	492	1.25	243	186	0.38	38	38	2.20	
14-Apr-09	Google	622	449	1.39	240	185	0.41	45	39	2.15	
23-Jun-09	Google	607	458	1.33	242	189	0.41	44	39	1.45	
1-Aug-09	ICC Ortofoto	611	455	1.34	244	169	0.37	38	43	2.40	
31-Dec-09	Google	612	437	1.40	243	163	0.37	37	42	2.51	
Average		612.91	475.39	1.29	242.94	190.39	0.40	40.06	40.22	2.18	

Date	Linear		R2
	Rotation Coefic	Linear Rotation Coefic (°)	
1-Sep-94	0.04	2.46	0.60
1-Feb-95	0.05	3.04	0.65
1-Sep-00	0.02	1.20	0.26
1-Jun-04	0.01	0.34	0.20
30-Jun-04	-0.01	-0.46	0.10
1-Jun-06	0.02	0.86	0.12
31-Dec-06	0.00	-0.06	0.10
25-Apr-07	-0.02	-0.97	0.23
8-Jun-07	-0.03	-1.49	0.60
11-Sep-07	0.01	0.63	0.21
15-Nov-07	0.01	0.40	0.10
1-Mar-08	0.00	-0.11	0.10
31-Dec-08	-0.01	-0.34	0.10
7-Feb-09	-0.01	-0.69	0.13
14-Apr-09	-0.01	-0.63	0.10
23-Jun-09	0.01	0.42	0.10
1-Aug-09	0.08	4.53	0.85
31-Dec-09	0.07	3.72	0.71

Date	Beach width (m)					Normalized Beach width (m)				
	P1 (50m)	P2 (170m)	P3 (300m)	P4 (420m)	P5 (550m)	P1	P2	P3	P4	P5
1-Sep-94	23.02	38.82	46.27	35.77	51.68	-1.42	3.40	5.59	10.41	14.15
1-Feb-95	21.10	39.51	47.82	37.55	55.51	-3.34	4.09	7.14	12.19	17.98
1-Sep-00	18.29	33.02	38.01	24.39	36.55	-6.15	-2.40	-2.67	-0.97	-0.98
1-Jun-04	20.98	34.03	37.77	22.97	30.93	-3.46	-1.39	-2.91	-2.39	-6.60
30-Jun-04	26.29	36.72	39.73	21.62	28.72	1.85	1.30	-0.95	-3.74	-8.81
1-Jun-06	22.32	40.04	42.08	26.65	39.36	-2.12	4.62	1.40	1.29	1.83
31-Dec-06	24.73	35.10	40.02	21.58	31.08	0.29	-0.32	-0.66	-3.78	-6.45
25-Apr-07	28.98	33.91	36.47	18.07	26.24	4.54	-1.51	-4.21	-7.29	-11.29
8-Jun-07	30.89	38.72	33.55	17.68	25.00	6.45	3.30	-7.13	-7.68	-12.53
11-Sep-07	18.77	34.44	40.77	20.32	33.34	-5.67	-0.98	0.09	-5.04	-4.19
15-Nov-07	23.53	34.70	39.11	24.04	33.67	-0.91	-0.72	-1.57	-1.32	-3.86
1-Mar-08	33.24	42.25	45.01	27.38	39.76	8.80	6.83	4.33	2.02	2.23
31-Dec-08	33.33	37.15	40.36	21.88	37.55	8.89	1.73	-0.32	-3.48	0.02
7-Feb-09	35.87	38.05	42.00	23.90	35.55	11.43	2.63	1.32	-1.46	-1.98
14-Apr-09	34.53	40.93	37.74	21.89	37.45	10.09	5.51	-2.94	-3.47	-0.08
23-Jun-09	17.12	23.31	29.57	13.21	26.99	-7.32	-12.11	-11.11	-12.15	-10.54
1-Aug-09	9.88	26.21	45.02	39.71	52.23	-14.56	-9.21	4.34	14.35	14.70
31-Dec-09	17.12	30.59	50.93	37.87	53.98	-7.32	-4.83	10.25	12.51	16.45
Average	24.44	35.42	40.68	25.36	37.53					

General Classification Nova Icaria

Date	Type	Length (m)	Ro (m)	L/Ro	Orientation		a/Ro	β	Beach	
					Ro (°)	a (m)			orientation	Beach area
1-Sep-94	ICC	395	350	1.13	261	183	0.52	66	45	2.51
1-Feb-95	MMA	402	348	1.14	261	182	0.52	68	44	2.55
1-Sep-00	ICC	391	352	1.08	264	187	0.53	65	46	2.15
1-Jun-04	ICC	402	361	1.11	259	186	0.52	65	47	2.06
30-Jun-04	Google	392	356	1.10	261	183	0.51	63	44	2.16
1-Jun-06	ICC Ortofoto	408	355	1.15	264	184	0.52	65	49	2.29
31-Dec-06	Google	404	360	1.12	265	191	0.53	62	48	2.25
25-Apr-07	Google	401	353	1.14	260	190	0.54	72	45	2.26
8-Jun-07	Google	403	358	1.13	259	187	0.52	69	44	2.17
11-Sep-07	Google	401	356	1.13	259	186	0.52	67	45	2.18
15-Nov-07	Google	400	361	1.11	259	202	0.56	65	46	2.22
1-Mar-08	ICC Ortofoto	406	356	1.14	258	182	0.51	66	46	2.25
31-Dec-08	Google	407	368	1.11	260	200	0.54	61	45	2.26
7-Feb-09	Google	401	355	1.13	260	187	0.53	66	47	1.92
14-Apr-09	Google	403	357	1.13	260	198	0.55	68	46	2.07
23-Jun-09	Google	399	373	1.07	259	202	0.54	62	45	1.90
1-Aug-09	ICC Ortofoto	400	362	1.11	260	194	0.54	64	46	2.25
31-Dec-09	Google	395	357	1.11	258	193	0.54	63	47	2.07
Average		400.58	357.67	1.12	260.39	189.86	0.53	65.39	45.83	2.20

Date	Linear		R2
	Rotation Coefic	Rotation Coefic (°)	
1-Sep-94	-0.22	-12.43	0.96
1-Feb-95	-0.22	-12.43	0.98
1-Sep-00	-0.21	-11.80	0.95
1-Jun-04	-0.18	-10.31	0.96
30-Jun-04	-0.19	-10.94	0.97
1-Jun-06	-0.20	-11.23	0.93
31-Dec-06	-0.21	-12.09	0.97
25-Apr-07	-0.24	-13.58	0.95
8-Jun-07	-0.23	-13.35	0.95
11-Sep-07	-0.21	-11.75	0.94
15-Nov-07	-0.25	-14.09	0.97
1-Mar-08	-0.17	-9.57	0.94
31-Dec-08	-0.20	-11.46	0.96
7-Feb-09	-0.20	-11.23	0.98
14-Apr-09	-0.22	-12.38	0.96
23-Jun-09	-0.20	-11.69	0.96
1-Aug-09	-0.19	-10.77	0.96
31-Dec-09	-0.20	-11.46	0.96

Date	Beach width (m)					Normalized Beach width (m)				
	P1 (50m)	P2 (100m)	P3 (200m)	P4 (300m)	P5 (350m)	P1	P2	P3	P4	P5
1-Sep-94	94.24	71.78	55.10	32.44	30.13	2.47	-0.71	1.61	-1.58	-1.58
1-Feb-95	93.78	72.88	58.48	35.82	28.71	2.01	0.39	4.99	1.80	-3.00
1-Sep-00	92.92	72.65	54.68	33.59	33.20	1.15	0.16	1.19	-0.43	1.49
1-Jun-04	86.91	66.61	50.78	34.92	31.58	-4.86	-5.88	-2.71	0.90	-0.13
30-Jun-04	89.17	73.59	55.50	36.83	34.14	-2.60	1.10	2.01	2.81	2.43
1-Jun-06	95.71	74.19	54.88	38.17	38.13	3.94	1.70	1.39	4.15	6.42
31-Dec-06	95.25	73.95	55.17	37.70	32.08	3.48	1.46	1.68	3.68	0.37
25-Apr-07	100.97	78.37	52.75	33.71	31.85	9.20	5.88	-0.74	-0.31	0.14
8-Jun-07	96.99	75.46	52.06	33.55	31.92	5.22	2.97	-1.43	-0.47	0.21
11-Sep-07	94.86	71.88	51.38	35.28	34.12	3.09	-0.61	-2.11	1.26	2.41
15-Nov-07	98.69	81.65	55.25	32.23	28.70	6.92	9.16	1.76	-1.79	-3.01
1-Mar-08	87.87	68.87	55.32	38.70	38.42	-3.90	-3.62	1.83	4.68	6.71
31-Dec-08	94.20	75.89	55.38	38.32	35.88	2.43	3.40	1.89	4.30	4.17
7-Feb-09	85.10	70.71	53.47	32.51	28.85	-6.67	-1.78	-0.02	-1.51	-2.86
14-Apr-09	88.12	76.20	54.07	29.55	28.58	-3.65	3.71	0.58	-4.47	-3.13
23-Jun-09	85.17	65.00	48.05	26.84	25.83	-6.60	-7.49	-5.44	-7.18	-5.88
1-Aug-09	85.81	66.36	49.18	32.69	30.10	-5.96	-6.13	-4.31	-1.33	-1.61
31-Dec-09	86.06	68.83	51.26	29.55	28.58	-5.71	-3.66	-2.23	-4.47	-3.13
Average	91.77	72.49	53.49	34.02	31.71					

General Classification Barceloneta

Date	Type	Length (m)	Ro (m)	L/Ro	Orientation Ro (°)	Indentation a (m)	a/Ro	β	Beach orientation	Beach area
1-Sep-94	ICC	1319.15	802.30	1.64	212.00	185.44	0.23	20.00	23.00	4.39
1-Feb-95	MMA	1305.88	702.50	1.86	210.00	170.88	0.24	24.00	24.00	5.05
1-Sep-00	ICC	1361.09	784.88	1.73	214.00	195.74	0.25	22.00	20.00	3.87
1-Jun-04	ICC	1381.84	738.29	1.87	213.00	211.51	0.29	30.00	17.00	3.51
30-Jun-04	Google	1383.78	710.00	1.95	213.00	204.96	0.29	30.00	16.00	4.40
Jun-06	ICC Ortofoto	1392.73	732.55	1.90	211.00	198.59	0.27	26.00	18.00	3.56
31-Dec-06	Google	1382.49	700.61	1.97	212.00	182.32	0.26	24.00	17.00	6.59
Average		1360.99	738.73	1.85	212.14	192.77	0.26	25.14	19.29	4.48
After Offshore Breakwater North Section										
25-Apr-07	Google	467.80	395.85	1.18	236.00	145.28	0.37	43.00	24.00	3.37
8-Jun-07	Google	476.01	402.91	1.18	235.00	134.85	0.33	35.00	26.00	3.32
11-Sep-07	Google	473.54	368.49	1.29	237.00	132.18	0.36	40.00	26.00	3.47
15-Nov-07	Google	479.33	381.61	1.26	242.00	149.00	0.39	46.00	24.00	2.33
Mar-08	ICC Ortofoto	463.72	394.25	1.18	242.00	138.40	0.35	44.00	24.00	2.45
31-Dec-08	Google	471.64	380.53	1.24	245.00	142.72	0.38	40.00	23.00	2.32
7-Feb-09	Google	488.16	404.16	1.21	245.00	154.29	0.38	44.00	23.00	1.48
14-Apr-09	Google	476.97	398.98	1.20	243.00	169.05	0.42	45.00	22.00	1.70
23-Jun-09	Google	467.53	388.82	1.20	241.00	160.17	0.41	45.00	24.00	2.43
01-Aug-09	ICC Ortofoto	473.21	398.27	1.19	243.00	145.37	0.37	40.00	25.00	1.93
31-Dec-09	Google	482.83	369.76	1.31	245.00	124.52	0.34	42.00	26.00	2.64
Average		474.61	390.68	1.22	243.43	147.79	0.38	42.86	23.86	2.14
After Offshore Breakwater South Section										
25-Apr-07	Google	922.75	561.15	1.64	219.00	174.32	0.31	21.00	14.00	5.34
8-Jun-07	Google	941.70	608.40	1.55	218.00	169.86	0.28	23.00	12.00	4.54
11-Sep-07	Google	909.98	555.03	1.64	219.00	158.82	0.29	24.00	15.00	5.31
15-Nov-07	Google	902.15	579.06	1.56	220.00	165.86	0.29	22.00	16.00	3.71
Mar-08	ICC Ortofoto	909.72	561.50	1.62	219.00	173.14	0.31	20.00	16.00	4.70
31-Dec-08	Google	922.98	624.29	1.48	217.00	160.12	0.26	21.00	14.00	5.01
7-Feb-09	Google	917.01	567.64	1.62	220.00	174.76	0.31	25.00	14.00	4.20
14-Apr-09	Google	921.20	552.28	1.67	220.00	176.84	0.32	26.00	13.00	4.84
23-Jun-09	Google	927.67	611.17	1.52	218.00	182.97	0.30	22.00	14.00	4.14
01-Aug-09	ICC Ortofoto	944.19	638.21	1.48	219.00	191.56	0.30	22.00	15.00	2.44
31-Dec-09	Google	944.77	575.31	1.64	220.00	168.09	0.29	27.00	14.00	4.44
Average		924.01	590.06	1.57	219.00	175.35	0.30	23.29	14.29	4.25

Before Offshore Breakwater	Beach width (m)								
	P1 (100m)	P2 (230m)	P3 (370m)	P4 (570m)	P5 (700m)	P6 (800m)	P7 (900m)	P8 (1150m)	P9 (130m)
1-Sep-94	-13.73	24.45	47.47	43.90	40.36	34.90	29.26	26.09	53.55
1-Feb-95	-9.28	21.80	51.56	48.98	44.14	40.69	35.47	31.55	67.30
1-Sep-00	17.13	9.53	35.32	39.21	37.27	31.14	28.06	22.53	47.74
1-Jun-04	46.51	12.33	47.33	40.97	26.60	25.77	14.03	4.61	21.07
30-Jun-04	45.69	26.18	48.96	44.25	37.40	28.76	17.32	15.51	26.81
Jun-06	34.79	17.27	36.30	33.59	23.94	26.33	20.44	15.53	38.46
31-Dec-06	60.57	43.52	64.23	58.23	51.45	46.73	39.63	30.14	49.83
Average	20.19	18.59	44.49	41.82	34.95	31.26	24.09	19.30	42.49

	Beach width (m)								
	P1	P2	P3	P4	P5	P6	P7	P8	P9
1-Sep-94	-33.91	5.86	2.98	2.09	5.41	3.64	5.16	6.79	11.06
1-Feb-95	-29.47	3.21	7.07	7.17	9.19	9.43	11.37	12.24	24.81
1-Sep-00	-3.06	-9.06	-9.17	-2.61	2.32	-0.13	3.96	3.23	5.25
1-Jun-04	26.33	-6.27	2.84	-0.85	-8.35	-5.50	-10.07	-14.69	-21.42
30-Jun-04	25.51	7.58	4.47	2.43	2.45	-2.51	-6.77	-3.79	-15.68
Jun-06	14.61	-1.32	-8.19	-8.23	-11.01	-4.93	-3.65	-3.77	-4.03
31-Dec-06	40.38	24.93	19.74	16.41	16.50	15.46	15.53	10.83	7.34

After Offshore Breakwater North Section	Beach width (m)					Normalized Beach width (m)				
	P1 (80m)	P2 (160m)	P3 (240m)	P4 (320m)	P5 (410m)	P1	P2	P3	P4	P5
25-Apr-07	86.02	64.00	56.00	59.00	77.00	24.13	24.85	22.69	19.94	14.91
8-Jun-07	74.50	56.13	52.42	56.22	83.07	12.61	16.98	19.11	17.16	20.98
11-Sep-07	79.92	59.06	52.58	61.93	86.44	18.03	19.91	19.27	22.87	24.35
15-Nov-07	63.03	38.34	30.84	38.47	50.79	1.14	-0.81	-2.47	-0.59	-11.30
Mar-08	63.81	36.33	32.62	33.24	65.94	1.92	-2.82	-0.69	-5.82	3.85
31-Dec-08	56.15	32.81	31.32	44.73	72.02	-5.74	-6.34	-1.99	5.67	9.93
7-Feb-09	38.89	13.38	7.30	16.87	40.51	-23.00	-25.77	-26.01	-22.19	-21.58
14-Apr-09	46.46	24.34	14.60	15.90	37.12	1.80	4.40	3.81	-2.55	-8.18
23-Jun-09	63.69	43.55	37.12	36.51	53.91	-15.45	-15.55	-14.99	-11.36	-7.95
01-Aug-09	46.44	23.60	18.32	27.70	54.14	-2.49	-1.62	2.44	1.89	4.71
31-Dec-09	59.40	37.53	35.75	40.95	66.80	-2.49	-1.62	2.44	1.89	4.71
	61.89	39.15	33.31	39.06	62.09					

After Offshore Breakwater South Section	Beach width (m)						Normalized Beach width (m)					
	P1 (100m)	P2 (230m)	P3 (370m)	P4 (570m)	P5 (700m)	P6 (780m)	P1	P2	P3	P4	P5	P6
25-Apr-07	79.56	42.07	67.03	63.80	52.98	72.81	21.07	7.51	16.58	18.51	7.75	-4.60
8-Jun-07	55.60	31.92	56.40	46.30	44.54	77.32	-2.89	-2.64	5.95	1.02	-0.70	-0.09
11-Sep-07	73.58	46.13	58.59	53.00	52.45	89.45	15.09	11.57	8.14	7.71	7.21	12.03
15-Nov-07	41.51	25.61	39.27	34.91	36.55	97.39	-16.99	-8.95	-11.18	-10.38	-8.68	19.98
Mar-08	54.78	42.96	50.69	48.77	52.41	81.55	-3.71	8.40	0.24	3.49	7.17	4.14
31-Dec-08	69.20	40.75	51.22	45.53	55.08	92.24	10.71	6.19	0.77	0.24	9.85	14.83
7-Feb-09	58.12	35.39	47.27	39.36	43.88	68.56	-0.38	0.82	-3.18	-5.92	-1.36	-8.85
14-Apr-09	70.04	44.47	58.79	53.87	45.56	66.70	11.54	9.90	8.34	8.59	0.32	-10.72
23-Jun-09	53.88	27.17	47.68	43.99	44.18	70.29	-4.62	-7.39	-2.77	-1.30	-1.06	-7.13
01-Aug-09	28.67	9.14	27.56	23.31	24.74	57.82	-29.83	-25.43	-22.88	-21.98	-20.50	-19.59
31-Dec-09	56.86	33.27	46.24	39.31	47.68	80.35	-1.63	-1.29	-4.20	-5.97	2.45	2.94
	58.49	34.56	50.45	45.28	45.23	77.41						

Date	Linear Rotation Coefic	Linear Rotation Coefic (°)	R2
1-Sep-94	0.03	1.43	0.30
1-Feb-95	0.03	1.83	0.40
1-Sep-00	0.02	0.86	0.29
1-Jun-04	-0.02	-1.26	0.37
30-Jun-04	-0.02	-1.15	0.47
Jun-06	0.00	-0.17	0.10
31-Dec-06	-0.02	-0.86	0.37

After Offshore Breakwater North Section	Linear Rotation Coefic	Linear Rotation Coefic (°)	R2
25-Apr-07	-0.03	-1.72	0.10
8-Jun-07	0.02	1.08	0.10
11-Sep-07	0.02	0.99	0.10
15-Nov-07	-0.03	-1.76	0.10
Mar-08	0.00	-0.05	0.10
31-Dec-08	0.05	2.88	0.10
7-Feb-09	0.01	0.34	0.10
14-Apr-09	-0.03	-1.96	0.11
23-Jun-09	-0.03	-1.91	0.14
01-Aug-09	0.02	1.22	0.10
31-Dec-09	0.02	1.14	0.10

After Offshore Breakwater South Section	Linear Rotation Coefic	Linear Rotation Coefic (°)	R2
39197.00	0.00	-0.11	0.10
39241.00	0.02	1.32	0.20
39336.00	0.01	0.80	0.10
39401.00	0.05	3.12	0.37
39508.00	0.03	1.60	0.36
39813.00	0.03	1.43	0.15
39851.00	0.01	0.63	0.10
39917.00	0.00	-0.23	0.10
39987.00	0.02	1.26	0.21
40026.00	0.03	1.89	0.36
40178.00	0.03	1.49	0.21

General Classification Playa Larga

Date	Type	Length (m)	Ro (m)	Length/Ro	Orientation	Indentation	a/Ro	β	Beach	
					Ro (°)	a (m)			orientation	Beach area
1-Mar-95	MMA	650.46	691.00	0.94	208.00	227.62	0.33	29.00	117	1.36
20-Jun-98	MMA	655.06	689.00	0.95	317.00	216.00	0.31	32.00	115	2.43
1-Jul-00	ICC	642.82	709.00	0.91	317.00	214.00	0.30	35.00	115	2.20
1-May-04	ICC	688.38	707.30	0.97	321.00	215.69	0.30	35.00	118	0.74
30-Jun-04	Google	607.00	665.28	0.91	322.00	191.41	0.29	35.00	119	0.61
7-Jun-05	Google	657.19	678.11	0.97	315.00	228.77	0.34	48.00	112	2.21
12-Mar-06	Google	611.59	675.55	0.91	319.00	223.93	0.33	36.00	116	1.33
1-Jun-06	ORTO ICC	640.94	661.91	0.97	316.00	213.35	0.32	39.00	114	1.47
14-Nov-06	Google	610.44	699.47	0.87	318.00	234.25	0.33	37.00	114	1.79
31-Dec-06	Google	653.83	679.36	0.96	316.00	217.98	0.32	42.00	115	1.85
11-Nov-07	Google	693.89	706.21	0.98	310.00	241.37	0.34	46.00	109	3.16
1-Jan-08	ORTO ICC	645.54	682.49	0.95	317.00	211.80	0.31	32.00	116	1.63
31-Dec-08	Google	649.86	694.04	0.94	317.00	205.38	0.30	36.00	116	1.89
1-Apr-09	ORTO ICC	606.30	713.80	0.85	320.00	208.95	0.29	33.00	118	1.39
31-Dec-09	Google	619.04	670.50	0.92	320.00	221.39	0.33	32.00	119	1.99
Average		642.16	688.20	0.93	310.20	218.13	0.32	36.47	115.53	1.74

Date	Linear	Linear	R2
	Rotation	Rotation	
	Coefic	Coefic (°)	
1-Mar-95	-0.08	-4.68	0.83
20-Jun-98	-0.10	-5.96	0.74
1-Jul-00	-0.11	-6.36	0.95
1-May-04	-0.04	-2.11	0.69
30-Jun-04	-0.03	-1.53	0.68
7-Jun-05	-0.15	-8.82	0.83
12-Mar-06	-0.10	-5.53	0.84
1-Jun-06	-0.09	-5.36	0.63
14-Nov-06	-0.14	-7.84	0.92
31-Dec-06	-0.12	-6.61	0.72
11-Nov-07	-0.21	-11.91	0.88
1-Jan-08	-0.10	-5.61	0.80
31-Dec-08	-0.10	-5.63	0.88
1-Apr-09	-0.07	-3.84	0.71
31-Dec-09	-0.10	-5.50	0.88

Date	Beach width (m)					Normalized Beach width (m)				
	P1 (100m)	P2 (200m)	P3 (350m)	P4 (500m)	P5 (600m)	P1	P2	P3	P4	P5
1-Mar-95	61.01	61.62	35.04	33.42	31.65	5.36	17.75	16.23	19.80	14.44
20-Jun-98	66.45	53.44	18.99	25.79	25.68	10.80	9.57	0.18	12.17	8.47
1-Jul-00	60.46	51.65	29.02	19.99	16.98	4.81	7.78	10.21	6.37	-0.23
1-May-04	26.57	21.50	17.30	6.32	14.97	-29.08	-22.37	-1.51	-7.30	-2.24
30-Jun-04	22.96	18.23	18.72	8.39	13.76	-32.69	-25.64	-0.09	-5.23	-3.45
7-Jun-05	77.58	51.08	14.53	12.87	15.59	21.93	7.21	-4.28	-0.75	-1.62
12-Mar-06	46.10	36.37	10.80	6.21	10.33	-9.55	-7.50	-8.01	-7.41	-6.88
1-Jun-06	53.33	37.81	7.11	7.53	20.14	-2.32	-6.06	-11.70	-6.09	2.93
14-Nov-06	60.91	40.84	19.25	2.80	7.40	5.26	-3.03	0.44	-10.82	-9.81
31-Dec-06	64.24	44.23	11.76	10.36	21.14	8.59	0.36	-7.05	-3.26	3.93
11-Nov-07	104.13	67.46	26.64	17.87	18.98	48.48	23.59	7.83	4.25	1.77
1-Jan-08	52.11	40.10	14.69	8.21	16.79	-3.54	-3.77	-4.12	-5.41	-0.42
31-Dec-08	54.94	43.98	20.18	15.39	17.33	-0.71	0.11	1.37	1.77	0.12
1-Apr-09	36.23	38.13	12.75	9.80	15.22	-19.42	-5.74	-6.06	-3.82	-1.99
31-Dec-09	47.73	51.62	25.31	19.32	12.15	-7.92	7.75	6.50	5.70	-5.06
Average	55.65	43.87	18.81	13.62	17.21					

General Classification Salou

Date	Type	Length (m)	Ro (m)	Length/Ro	Orientation		Indentation a (m)	a/Ro	β	Beach	
					Ro (°)					orientation	Beach area
1-Jun-57	MMA	1187.49	669.34	1.77	311.00	192.66	0.29	31.00	109.00	7.77	
1-Jun-65	MMA	1171.72	653.76	1.79	317.00	192.68	0.29	30.00	108.00	6.80	
1-Jun-73	MMA	1325.36	609.79	2.17	314.00	190.21	0.31	36.00	108.00	8.46	
1-Mar-77	MMA	1439.02	683.05	2.11	313.00	203.65	0.30	35.00	108.00	7.87	
1-Dec-83	MMA	1196.49	672.80	1.78	312.00	205.12	0.30	32.00	110.00	7.08	
1-Mar-95	MMA	1158.95	636.95	1.82	312.00	170.94	0.27	25.00	109.00	8.87	
1-Jan-98	MMA	1187.05	644.55	1.84	316.00	181.38	0.28	32.00	109.00	10.10	
1-Jul-00	ICC	1163.31	677.43	1.72	311.00	201.23	0.30	29.00	108.00	7.59	
1-May-04	ICC	1161.22	617.58	1.88	315.00	182.65	0.30	30.00	108.00	8.67	
30-Jun-04	Google	1184.66	624.17	1.90	313.00	189.88	0.30	29.00	110.00	7.76	
7-Jun-05	Google	1155.29	667.00	1.73	312.00	172.16	0.26	26.00	109.00	10.01	
12-Feb-06	Google	1155.66	710.81	1.63	308.00	188.51	0.27	27.00	109.00	9.49	
1-Jun-06	ORTO ICC	1180.44	639.83	1.84	312.00	200.53	0.31	34.00	109.00	7.64	
14-Nov-06	Google	1152.96	719.35	1.60	308.00	197.69	0.27	27.00	109.00	8.47	
31-Dec-06	Google	1177.71	616.46	1.91	313.00	186.24	0.30	33.00	109.00	8.65	
11-Nov-07	Google	1124.07	590.44	1.90	313.00	171.00	0.29	32.00	109.00	10.37	
1-Jun-08	ORTO ICC	1176.69	689.26	1.71	310.00	203.23	0.29	29.00	109.00	7.76	
31-Dec-08	Google	1180.19	687.51	1.72	312.00	209.92	0.31	33.00	108.00	7.32	
1-Apr-09	ORTO ICC	1192.02	660.72	1.80	315.00	191.68	0.29	29.00	110.00	7.27	
31-Dec-09	Google	1190.51	620.70	1.92	313.00	193.67	0.31	30.00	110.00	7.82	
Average		1193.04	653.52	1.79	312.20	189.38	0.29	29.67	109.00	8.52	

Date	Linear Rotation Coefic	Linear Rotation Coefic (°)	R2
1-Jun-57	-0.04	-2.06	0.85
1-Jun-65	-0.03	-1.43	0.83
1-Jun-73	-0.04	-2.35	0.97
1-Mar-77	-0.05	-3.04	0.96
1-Dec-83	-0.04	-2.01	0.94
1-Mar-95	-0.01	-0.46	0.37
1-Jan-98	-0.05	-2.69	0.93
1-Jul-00	-0.03	-1.95	0.93
1-May-04	-0.03	-1.83	0.91
30-Jun-04	-0.02	-1.26	0.88
7-Jun-05	-0.03	-1.49	0.95
12-Feb-06	-0.03	-1.89	0.93
1-Jun-06	-0.04	-2.12	0.97
14-Nov-06	-0.02	-1.20	0.85
31-Dec-06	-0.04	-2.01	0.96
11-Nov-07	-0.04	-2.52	0.93
1-Jun-08	-0.04	-2.12	0.97
31-Dec-08	-0.04	-2.46	0.98
1-Apr-09	-0.03	-1.60	0.95
31-Dec-09	-0.02	-1.38	0.95

Date	Beach width (m)					Normalized Beach width (m)				
	P1 (100m)	P2 (300m)	P3 (500m)	P4 (750m)	P5 (1000m)	P1	P2	P3	P4	P5
1-Jun-57	93.56	70.13	67.46	60.96	54.63	1.40	-8.49	-8.68	-5.95	-4.07
1-Jun-65	77.62	60.65	61.50	55.77	50.42	-14.54	-17.97	-14.64	-11.14	-8.28
1-Jun-73	99.54	85.02	73.79	68.20	59.10	7.38	6.40	-2.35	1.29	0.40
1-Mar-77	93.68	84.52	69.17	64.12	41.26	1.52	5.90	-6.97	-2.79	-17.44
1-Dec-83	83.58	67.77	67.36	56.77	47.01	-8.58	-10.85	-8.78	-10.14	-11.69
1-Mar-95	83.30	78.86	84.62	81.84	72.43	-8.86	0.24	8.48	14.93	13.73
1-Jan-98	113.02	99.47	95.69	71.97	72.00	20.86	20.85	19.55	5.06	13.30
1-Jul-00	85.60	70.81	71.45	60.27	50.97	-6.56	-7.81	-4.69	-6.64	-7.73
1-May-04	97.98	80.14	79.75	71.22	63.97	5.82	1.52	3.61	4.31	5.27
30-Jun-04	81.91	70.34	73.00	64.96	58.38	-10.25	-8.28	-3.14	-1.95	-0.32
7-Jun-05	104.98	94.26	91.92	82.00	79.71	12.82	15.64	15.78	15.09	21.01
12-Feb-06	105.28	88.86	84.70	78.04	71.60	13.12	10.24	8.56	11.13	12.90
1-Jun-06	86.28	73.97	70.78	60.64	49.13	-5.88	-4.65	-5.36	-6.27	-9.57
14-Nov-06	83.33	78.98	81.09	67.85	63.49	-8.83	0.36	4.95	0.94	4.79
31-Dec-06	97.49	82.62	76.88	71.43	61.24	5.33	4.00	0.74	4.52	2.54
11-Nov-07	117.50	96.35	94.50	80.45	73.33	25.34	17.73	18.36	13.54	14.63
1-Jun-08	88.53	75.44	71.41	62.49	50.98	-3.63	-3.18	-4.73	-4.42	-7.72
31-Dec-08	87.83	73.03	67.34	56.40	44.91	-4.33	-5.59	-8.80	-10.51	-13.79
1-Apr-09	79.71	67.68	67.28	57.66	51.97	-12.45	-10.94	-8.86	-9.25	-6.73
31-Dec-09	82.45	73.56	73.04	65.11	57.55	-9.71	-5.06	-3.10	-1.80	-1.15
	92.16	78.62	76.14	66.91	58.70					